

RPSEA

Evaluation of Electrodialysis for the Desalinization of Shale Gas Flowback Water Report No. 08122-05.12

Barnett and Appalachian Shale Water Management and Reuse Technologies

Contract 08122-05

March 16, 2012

Principal Investigator
Blaine F. Severin, Ph.D., P.E.
Senior Process Engineer
Environmental Process
Dynamics, Inc.
4117 Spinnaker Ln.
Okemos, MI

Principal Investigator
Tom Hayes, Ph.D.
Coordinator, Environmental
Engineering Solutions
Gas Technology Institute
1700 S. Mount Prospect Rd.
Des Plaines, IL

LEGAL NOTICE

This report was prepared by the Gas Technology Institute as an account of work sponsored by the Research Partnership to Secure Energy for America, RPSEA. Neither RPSEA members of RPSEA, the National Energy Technology Laboratory, the U.S. Department of Energy, nor any person acting on behalf of any of the entities:

- a. MAKES ANY WARRANTY OR REPRESENTATION, EXPRESS OR IMPLIED WITH RESPECT TO ACCURACY, COMPLETENESS, OR USEFULNESS OF THE INFORMATION CONTAINED IN THIS DOCUMENT, OR THAT THE USE OF ANY INFORMATION, APPARATUS, METHOD, OR PROCESS DISCLOSED IN THIS DOCUMENT MAY NOT INFRINGE PRIVATELY OWNED RIGHTS, OR**
- b. ASSUMES ANY LIABILITY WITH RESPECT TO THE USE OF, OR FOR ANY AND ALL DAMAGES RESULTING FROM THE USE OF, ANY INFORMATION, APPARATUS, METHOD, OR PROCESS DISCLOSED IN THIS DOCUMENT.**

THIS IS AN INTERIM REPORT. THEREFORE, ANY DATA, CALCULATIONS, OR CONCLUSIONS REPORTED HEREIN SHOULD BE TREATED AS PRELIMINARY.

REFERENCE TO TRADE NAMES OR SPECIFIC COMMERCIAL PRODUCTS, COMMODITIES, OR SERVICES IN THIS REPORT DOES NOT REPRESENT OR CONSTITUTE AND ENDORSEMENT, RECOMMENDATION, OR FAVORING BY RPSEA OR ITS CONTRACTORS OF THE SPECIFIC COMMERCIAL PRODUCT, COMMODITY, OR SERVICE.

THIS PAGE INTENTIONALLY LEFT BLANK

Table of Contents

Table of Contents	i
LIST OF FIGURES	iii
LIST OF TABLES	vi
1 Abstract	1
2 Executive Summary	4
3 Introduction	7
3.1 Problem Statement	7
3.2 Water Management (Life Cycle Analysis)	9
3.3 Electrodialysis as a Treatment Option	11
3.4 Objectives	14
3.5 Approach	14
4 Background	16
4.1 Standard Description of Electrodialysis	16
4.2 Electrodialysis Concepts for Concentrated Brines	18
4.3 Scale-up	19
5 Methods	22
5.1 Standard Configuration of the Electrodialysis Pilot Plant	22
5.2 Non-Standard Configurations of the Pilot Plant	25
5.3 5.3 Data Collection	25
5.4 Data Analysis	26
5.4.1 Presentation of “In-Tank” Concentration	26
5.4.2 Mass Transfer Data	26
5.4.3 Energy use	27
5.4.4 Energy Efficiency	27
6 Theoretical Development	28
6.1 Computer Model of the Eurodia Pilot Plant	28
6.1.1 Current Efficiency and Limiting Current:	28
6.1.2 Components of the Total Stack Voltage and Total Current	29
6.1.3 Boundary Layer Dynamics, Ion Flux and Water Splitting	30
6.1.4 Osmotic Potential	31
6.1.5 Fluid conductivity	31
6.1.6 Membrane Resistance	32
6.1.7 Electrode Resistance and Overvoltage	32
6.1.8 Model Logic	32
6.1.9 Example Model Run	32
6.2 Implications of the Model Solution	33
6.2.1 Meeting the Initial Energy Goals	34
6.2.2 Improvements for Extremely Concentrated Salt Solutions	36
6.3 Adaptation of Arrhenius Equation for Electrodialysis	40
6.3.1 Nomenclature	41
7 Results	43
7.1 Range of Operation	47
7.2 Electrolyte Chemistry	47
7.2.1 Effect of electrolyte concentration	47
7.2.2 Electrolyte pH	48

7.2.3	Disodium Phosphate (Na_2HPO_4) as an Electrolyte.....	54
7.3	Effect of Calcium on Electrodialysis	56
7.4	Mitigation of the Calcium Problem with Cathode Protection	64
7.5	Mechanism of Calcium Interference.....	72
7.6	Effect of Multivalent Cations.....	79
7.7	Clean-in-Place Pulsed Pole Reversal	84
7.8	Samples from the Barnett and the Marcellus	89
7.9	Treatment of Field Samples; with and without CIP-PR	91
7.9.1	Taylor Dooley from the Barnett.....	92
7.9.2	Maggie Spain from the Barnett.....	95
7.9.3	Unlabeled Sample from the Marcellus	103
7.9.4	Mcadoo Labeled Sample from the Marcellus	106
7.10	Effect of Temperature	109
7.10.1	Series 1	109
7.10.2	Series 2.....	113
7.11	Estimated Capital and Operational Costs	114
8	8. Discussion	121
8.1	Defining a Range of Operation	121
8.2	Electrolyte Chemistry	122
8.3	Mitigation of the Effects of Calcium with Cathode Protection	123
8.4	Interference from Multivalent Cations.....	126
8.5	Fate of Multivalent Cations	130
8.6	Mechanism of Interference by Multivalent Cations	133
8.6.1	Type I Fouling.....	133
8.6.2	Type II Fouling	134
8.6.3	Type III Fouling.....	134
8.7	Development of Clean-in-Place Pole Reversal.....	135
8.8	Field Waters from the Barnett and the Marcellus.....	137
8.8.1	Effect of Temperature	138
8.9	Process Improvements for the Field	139
8.10	Economic and Design Considerations	140
9	9 Conclusions.....	142
9.1	Preliminary Clean-in-Place	143
9.2	Field waters from the Barnett and the Marcellus.....	143
9.2.1	Effect of Temperature	144
9.2.2	Process Recommendations:	144
10	10 References.....	145
11	11 Acknowledgements.....	146

LIST OF FIGURES

1	Examples of Flowback Waters from the Marcellus: Percent of Flowback Water with Less than Stated	9
2	Cumulative Fracture and Process Water Recovery vs Projected Reuse Capacity in a 19,200 Fracture Play	11
3	Conceptual Placement of Electrodialysis (Concentrating Membrane System) in a Water Treatment Process	12
4	Ion Flow in an Electrodialysis Stack	17
5	Photograph of the Eurodia Pilot ED Skid	22
6	Flow Diagram for the Eurodia Industrie, S.A., Ameridia Eur2B-10 Electrodialysis Pilot Plant	24
7	Model Simulation of the Pilot ED Performance with 3% NaCl	34
8	Predicted Power Requirements per Pound NaCl Removed with 100% Current Efficiency	36
9	Model Simulation: Relative Voltage Drop for Initial Conditions At Start of run (Concentrate = Diluate) at 5000 mg/l NaCl	37
10	Model Simulation of the Relative Potential Drop At 80% Transfer (Concentrate 1,000; Diluate = 9,000) with Initial = 5,000 mg/l NaCl	38
11	Model Simulation of the Relative Potential Drop At Start (Concentrate = Diluate) with 50,000 mg/l NaCl	39
12	Figure 15: Model Simulation of the Relative Potential Drop At 80% Transfer (Concentrate 10,000; Diluate = 90,000); Initial = 50,000	10
13	Effect of Electrolyte Concentration on Initial Current Density in 3% NaCl	48
14	Effect of Sodium Hydroxide Addition on Electrolyte Performance	49
15	3% NaCl with 90 g/l Disodium Sulfate Electrolyte	51
16	3% NaCl with 90 g/l Disodium Sulfate Electrolyte	51
17	3% NaCl with 90 g/l Disodium Sulfate + 1 g/l NaOH in the Electrolyte	52
18	Amperage Profile for Electrolyte Chemistry Improvements	53
19	Performance Enhancements through Chemical Adjustment of the Electrolyte	53
20	Disodium Phosphate as an Electrolyte	54
21	Disodium Phosphate as an electrolyte Test Run E	55
22	Test A: Reference Test for 3% NaCl	56
23	Test G with 3% NaCl + 1000 mg/l Ca++	57
24	Test F, 3% NaCl with 4000 mg/l Ca++	58
25	Summary of Current Density Profiles Figures 25,26, and 27 Showing Effect of Calcium Addition with Conventional Membrane at the Cathode	59
26	Recovery of Current Density by Acidification of the Electrolyte after Calcium Poisoning	60
27	Figure 30: Test I; Baseline 6% NaCl	61
28	Test H, 6% NaCl with Calcium Poisoning	62
29	Comparison of Test H and I Showing poisoning of the Current Density with 4,000 mg/l Ca++ in the Feed Stock	63
30	Recovery of Current Density by Electrolyte Acidification after Calcium Poisoning of the Electrolyte Test H.	64
31	Test J, Standard 3% NaCl Test with the CMX-S Multivalent Exclusionary Membrane at the Cathode Boundary.	65
32	Comparison of Current Density with Cathode Protective Membrane (Test J) Compared to Standard Reference (Test A)	66

33	Test K, 3% NaCl Challenged with 4,000 mg/l Ca++ with CMX-S protective Membrane at the Cathode Boundary	66
34	Effect of Cathode Protection by Multivalent Cation Exclusionary Membrane	67
35	Test L with 6% NaCl with 4000 mg/l Ca++	68
36	Effect of Calcium on Protected and Un-Protected Cathode with 6% NaCl	69
37	Cathode Protective Membrane Accounts for 66-73% Rejection of Calcium Flux to the Electrolyte	72
38	Test M; Effect of Adding Calcium (400 mg/l) to the Electrolyte, Followed by Acidification of the Electrolyte	74
39	Test N, Effect of Soluble Calcium in Electrolyte	76
40	Test O: Effect of Adding Carbonate and Bicarbonate to Precipitate the Calcium in the Electrolyte	77
41	Unexpected Benefits of Cathode Protection from Calcium	79
42	Test Q: Effect of Magnesium on ED performance	80
43	Test R, Effect of Calcium, Barium, and Magnesium	81
44	Test S, Loss of Current Density by addition of 44 mg/l Fe	82
45	Test S with precipitated iron in Test Water	83
46	Test T, Full Salt Test Repeat of Test S	84
47	Summary Effects of Various Cation Blends on Current Density	85
48	Mixed Salt Test U, Baseline without Clean-in-Place Pole Reversal	86
49	Immediate Loss of Current by Addition of Complex Salts to NaCl, Test X	87
50	Test X: Mixed Salt Test with Clean-in-Place Pole Reversal	88
51	Taylor Dooley Barnett Shale Sample, no CIP	93
52	Taylor Dooley Barnett Shale Sample, with CIP	94
53	Maggie Spain Field Sample Test without Pulsed Pole Reversal	95
54	Field Sample Test with Pulsed Pole Reversal, Maggie Spain	96
55	Maggie Spain Field Sample (diluted 1:1) without CIP Pole Reversal	98
56	Maggie Spain Field Sample (diluted) with CIP Pole Reversal	99
57	Maggie Spain CIP Regime 2; 10 V for 15 seconds every ½ hour	101
58	Example 3D, Ability of the Proposed CIP-PR to Restore the Electrodes to an Initial Condition.	103
59	Marcellus UL Field Test Sample with no CIP	104
60	Marcellus UL Field Test Water with Complex CIP Pole Reversal	106
61	Mcadoo Sample from the Marcellus, No-CIP	107
62	Sample Mcadoo from the Marcellus, with CIP-PR	108
63	Example Volt-Amp Profiles with 3% NaCl and 90 g/l Disodium Sulfate Electrolyte over a Range of Temperature Conditions	111
64	Arrhenius Plot of Data from Tables 49 and 50	112
65	Data from Table 51 with Varied Water and Electrolyte Temperatures Versus Prediction from Equation 11a.	113
66	Arrhenius Plot of Data from Table 52 (Points) and Prediction (Line) from Equation 11b.	114
67	Conversion Chart, BBL/day Treated Water vs Pounds Salt Removed/day as a Function of the PPM Salt Removed.	115
68	Capital Costs as a Function of Daily Salt Removal	117
69	Operating Costs as a Function of Salt Removal	118

70	Breakdown of Operating Costs (\$/1000 lb salt) as a Function of Daily Salt Removal	119
71	Amortized Capital Normalized (\$/1000 Lb Salt Treated) versus Daily Treatment.	120
72	Summary of All ED Runs, Energy Utilization (Work) Required Per Pound of TDS Transferred	122
73	Effect of Calcium Addition to Test Waters with Unprotected Cathode Barrier	124
74	Improved Performance in Solutions of Calcium with Cathode Protective Membrane installed at the Cathode Boundary	124
75	Loss of Sodium Transport Capacity as a Function of the Concentration of the Multivalent Cations	127
76	Fate of the Cations; Relative Flux from the Diluate to the Concentrate; Normalized to Sodium	132
77	Fate of the Cations; Relative Flux from the Diluate to the Concentrate; Normalized to Sodium	133
78	Control Chart for Operation of the Pilot ED Unit (at 5 Volts) as a Basis for Implementation of a CIP-Pole Reversal.	136
79	Summary of Potential Process Improvements	140

LIST OF TABLES

1	Recovered Flow-back Water Inventory (After Hayes, 2009)	8
2	Chemical Characteristic; 19 Marcellus Wells: Day 5 After Fracture	13
3	Metals Data for Flowback Waters 5 Days after Fracture	13
4	Example Scale-up	21
5	List of Model Variables and Parameters	29
6	Conditions for Example ED Model Run	33
7	Summary of 15 Electrodialysis Runs with Sodium and Calcium Chloride	45
8	Summary of 7 Electrodialysis Runs with Complex Salts	45
9	Summary of 11 Electrodialysis Runs with Field Samples from Barnett and Marcellus	46
10	Summary of Nine Electrodialysis Runs Demonstrating Target Efficiency	47
11	Summary of Effects of Electrolyte Chemistry Improvements	52
12	Chemical Analyses: Tests with Unprotected Cathode	70
13	Chemical Analyses, Tests with Protected Cathode	71
14	Rejection of Calcium in Cathode Protected Membrane	72
15	Test M, Effect of Precipitated and Soluble Calcium in Electrolyte: Test for Transport of Calcium from Electrolyte into Concentrate	73
16	Test N: Effect of Soluble Calcium in Electrolyte: Test for Transport of Soluble Calcium from Diluate to Electrolyte and from Electrolyte to Concentrate	75
17	Test O: Effect of Bicarbonate and Carbonate on the Electrolyte Solution	78
18	Chemical Analyses, Tests with Protected Cathode Test Q Magnesium	80
19	Test R with Protected Cathode ; Magnesium, Barium and Calcium	80
20	Test S with Protected Cathode ; Magnesium, Barium, Calcium and Iron	81
21	Test T with Protected Cathode ; Magnesium, Barium, Calcium and Iron	82
22	Test U with Protected Cathode ; Magnesium, Barium, Calcium and Iron	83
23	CIP Regime for Test X: Mixed Salts Test	86
24	Test X with CIP-PR ; Magnesium, Barium, Calcium and Iron	88
25	Summary of CIP Improvements with Lab Examples U and X	89
26	Initial Treatment of Samples from the Barnett	89
27	Initial Treatment of Samples from the Marcellus	90
28	Test TD without CIP-PR ; Magnesium, Barium, Calcium and Iron, Taylor Dooley	91
29	Pole Reversal Regime for Taylor Dooley with CIP-PR	92
30	Test TD with CIP-PR ; Magnesium, Barium, Calcium and Iron, Taylor Dooley	93
31	Summary of CIP-PR with Taylor Dooley Samples	94
32	Test MS without CIP-PR ; Magnesium, Barium, Calcium and Iron, Maggie Spain	94
33	CIP Regime for the Maggie Spain	96
34	Test MS with CIP-PR ; Magnesium, Barium, Calcium and Iron, Maggie Spain	97
35	Summary of CIP-PR Improvements with Maggie Spain Water	97
36	Test Maggie Spain Diluted, without CIP; Mg, Ba, Ca and Fe	97
37	CIP Regime for the Maggie Spain Diluted Regime 1	99
38	Test Maggie Spain Diluted, with CIP Regime 1; Mg, Ba, Ca and Fe	99
39	CIP Regime for Maggie Spain Run 3	100
40	Test Maggie Spain Diluted, with CIP Regime 1; Mg, Ba, Ca and Fe	100
41	Summary of CIP-PR Improvements with Maggie Spain Diluted	101
42	Accumulation of Multivalent Cations in the Electrolyte During MSD Runs 1-3	102
43	Marcellus Unlabeled without CIP, Mg, Ba, Ca and Fe	104

44	Marcellus UL CIP Regime	105
45	Marcellus Unlabeled with CIP-PR, Mg, Ba, Ca and Fe	105
46	Summary of CIP-PR Improvements with Marcellus Unlabeled Sample	105
47	Mcadoo Sample from Marcellus without CIP-PR, Mg, Ba, Ca and Fe	107
48	Sample Mcadoo CIP Regime	108
49	Mcadoo Sample from Marcellus with CIP-PR, Mg, Ba, Ca and Fe	108
50	Summary of CIP-PR Improvements with Sample Mcadoo	109
51	Data Series 1A, Cool Water; Varied Electrolyte Temperature	110
52	Series 1B; Warm Electrolyte; Varied Water Temperature	110
53	Data Series 1C; Varied Electrolyte and Varied Water Temperatures	110
54	Series 2, Electrolyte and Water Temperature $\pm 1^{\circ}\text{C}$	114
55	Test Cases for Economic Analysis	115
56	Economic Data Provided by Eurodia	115
57	Additional Economic Assumptions	116
58	Capital Costs on a Case-by-Case Basis	116
59	Daily Operating Costs on a Case-by-Case Basis	116
60	Operating Costs Cost Basis \$/Thousand Pounds Salt Removed	116
61	Summary of Initial Cation Concentrations in Tests with Complex Salts and Field Samples	126
62	Fate of the Cations; Transport From the Diluate to the Concentrate	131
63	Perceived Mechanism of Fouling Presented by the Various Multivalent Cations	132
64	Summary of CIP-PR Improvements	135
65	Potential Improvements with Operation at Elevated Temperatures	136
66	Reverse Engineering of the Economic Data to Conventional Design parameters	141
67	Comparison of Typical Pilot Run vs Typical Economic Case (by Eurodia)	142

1 ABSTRACT

This project was a portion of a larger investigation into the quantity and quality of the flowback water and process alternatives available to 1) maximize the reuse of recovered water, 2) minimize the volume of deep well disposal, and 3) reduce the cost and environmental impact of disposal of flowback water. This report represents the first laboratory published investigation of the potential of electrodialysis as an alternative desalination process for flowback water, culminating in the treatment of field water from the Marcellus and from the Barnett.

Electrodialysis is an electrochemically driven membrane separation technology. A pair of electrode cells generates a potential across a number of cell pairs designed to segregate ions into a diluate stream and a concentrate stream. This process has historically been successfully used for water containing several thousand mg/l (roughly parts per million) TDS down to several hundred mg/l. The range of TDS expected in flowback water is several tens of thousands mg/l, and includes ranges of divalent cations in the thousands of mg/l.

Eight full electrodialysis runs were performed with pure sodium chloride. Seven runs were dedicated to understanding the effect of calcium to the electrodialysis process. An additional seven runs addressed the added complexity of treating water in the presence of calcium, barium, magnesium, and iron. Eleven tests were performed with waters from the Marcellus and the Barnett.

During the test period, a number of problems were encountered. Literature suggests that these problems historically impeded development of electrodialysis for complex solutions of concentrated divalent cations. As these problems were encountered in this project, they were addressed by making a number of improvements to the electrodialysis process specific to this laboratory unit. Some of these improvements represent potentially scalable means for cost savings. Others of these improvements represent critical changes needed to keep the electrodialysis unit operational.

Range of Operation: An arbitrary energy utilization limit (0.1 to 0.15 kWh/lb TDS removed) was established to keep the electrical costs of electrodialysis at less than \$0.18 per barrel of flowback water treated. Energy utilization was calculated for 33 electrodialysis runs. The average energy expended was 0.12 kWh/lb TDS with a range from 0.1 to 0.148 kWh/lb. The field waters performed within the range of results expected from laboratory tests. Design considerations indicate that there is a trade-off between low power costs and higher initial capital costs.

Chemistry of the Electrolyte: The chemistry of the electrolyte solution was investigated as a means of improving the rate of salt transfer at the desired stack potential. Increasing the electrolyte concentration to an ionic strength similar, or exceeding that of the feed water improved the process by as much as 24%. Lowering the overvoltage of the electrodes by operation of the electrolyte at a pH greater than about pH 11 can yield an additional 15% improvement. However, pH control of the electrolyte becomes problematic if there is incursion of multivalent cations into the electrolyte. The relative process improvements decrease as the number of cell pairs increases.

Mitigating the Effects of Calcium: Calcium concentrations greater than several hundred mg/l have traditionally been a problem with electrodialysis. Flowback water usually has calcium at levels exceeding several thousand mg/l. Initial tests with lab generated samples showed that high rates of calcium incursion into the electrolyte were encountered. The apparent calcium fouling (in and around) the electrode cells was indicated by a rapid degradation of process efficiency. The single cathode boundary membrane was replaced with a membrane that

selected against multivalent cations. Calcium flux into the electrolyte was reduced by 66-73%, with an improvement in ion flux of about 40% compared to the baseline observations.

Interference and Fate of Multivalent Cations: Flowback water contains a variety of multivalent cations, in addition to calcium, that can potentially adversely affect electrodialysis. Iron caused an immediate loss of process efficiency, likely by precipitation at all membrane surfaces. Calcium, barium, and magnesium caused a slower degradation of ion flux. Barium, iron, magnesium, and calcium were preferentially transported from the diluate to the concentrate. Calcium and magnesium were transported slowly into the electrolyte. Barium and iron were either not readily transported, or not readily measured in the electrolyte.

Clean-in-Place: Loss of process efficiency was observed when calcium, iron, and barium were present in the test water. To overcome this problem, a rapid clean-in-place regime was developed. Short pulses (15 seconds to one minute duration at intervals of 15 minutes to one hour) of pole reversal (cathode to anode) at elevated voltages (5-15 V) improved total ion flux. Tests were conducted with mixed salt solutions and field waters from the Barnett and Marcellus. Flux improvements of up to 37% were measured for waters treated using a CIP regime.

Field waters from the Barnett and the Marcellus: Samples were received from two field sites in each the Barnett and the Marcellus (total four field samples). Pretreatment consisting of pH adjustment to neutrality, aeration, and filtration with a 5 μ cartridge filter, was sufficient to create treatable waters. In three of four cases, the water was deemed beyond the concentration suitable for effective electrodialysis (150,000 – 270,000 mg/l TDS), and likely represented water collected from late in the flowback periods at these sites. These waters were diluted with tap water for the tests with ED.

Effect of Temperature: The design of the electrodialysis process creates two co-dependent, rate limiting reaction sites; the electrode cell reactions, and the transport of ions within the membrane stack. The Arrhenius equation for temperature dependency was modified for two co-dependent rates over a temperature range of 8°C to 33°C. Independent temperature coefficients for the electrode cells and the stack were obtained. These tests predict that field operation can be improved with increased operating temperature. Partial, yet significant improvements (15-50%) may be made by increasing only the electrolyte bath temperature.

Process Recommendations: Iron should be aggressively removed in pre-treatment. Increased concentration of electrolyte can improve the process by around 24%. If the level of calcium and iron is fairly low, then the pH of the electrolyte can be increased to pH 11 for an additional 15% improvement in the rate of the process. With high concentrations of calcium, protection of the cathode barrier membrane with a multivalent cation exclusionary membrane is imperative. Improvements of 40% are possible. Clean-in-place technology will be needed to keep the ED unit operational. For very little expenditure, 35% process improvement can be realized using a simple pulsed pole reversal. The use of waste heat to increase the temperature of the electrolyte, the water, or both, can improve the rate of the process by at least 15%.

Process Economics: Eurodia provided a set of capital and operational parameters for specific design examples. The design parameters were converted, with additional assumptions, into cost estimates. A typical design case resulted in an operational cost of about \$35-40/ 1000 lb salt removed. The majority of the operational cost (75%) was determined to be electric power to operate the electrodes. Power costs were estimated at \$0.10/kWh. Membrane replacement and labor accounted equally for 20-25% of the costs. Pumping costs and chemical cleaning agents were nominal, compared to the other operational costs. Capital costs were amortized for 7 years and 7% interest to estimate a capital cost per 1000 pounds salt removed. A typical design case resulted in a capital cost of \$30-45/1000 lb salt transferred. Capital costs were

dominated (>80%) by the process equipment for the electrodialysis unit. Placeholder costs estimates for generators and construction (building and site preparation) accounted for about 20% of the required capital. A further comparison between the process data in this report and the estimates from Eurodia suggests increased capital costs (dominated by the cost of the electrodialysis equipment), can be offset by lower operating costs (dominated by energy requirements).

2 EXECUTIVE SUMMARY

This project was a portion of a larger investigation into the nature (quantity and quality) of the flowback water and process alternatives available to 1) maximize the reuse of recovered water, 2) minimize the volume of deep well disposal, and 3) reduce the cost and environmental impact of disposal of flowback water.

Electrodialysis is an electrochemically driven membrane separation technology that has been successfully used for water containing several thousand mg/l (roughly parts per million) TDS down to several hundred mg/l. The range of TDS expected in flowback water is several tens of thousands mg/l. A number of problems were encountered that were systematically addressed as the project proceeded from the treatment of water containing pure sodium chloride (30,000-60,000 mg/l) to the treatment of solutions with sodium, calcium (up to 4,000 mg/l), barium (up to 400 mg/l), iron (up to 50 mg/l), and magnesium (up to 600 mg/l). The project culminated in the treatment of field samples from the Barnett and the Marcellus.

Operation of ED under the high salt conditions places the process in a regime of relatively low voltage and high amperage compared to the normal range of operation. This has led to an understanding of the relation between ion flux and applied voltage that allowed for a number of process improvements for operation in this regime. Another challenge to the desalinization of the shale flowback water is the potential for process poisoning by soluble calcium and other multivalent cations. This challenge was addressed by other process improvements aimed at mitigating the effects of divalent cations on the electrolyte cell.

Eight full electrodialysis runs were performed with pure sodium chloride. Seven runs were dedicated to understanding the relation of calcium to the electrodialysis process. An additional seven runs addressed the complexity of calcium, barium, magnesium, and iron. Eleven tests were performed with water from the Marcellus and the Barnett. Analysis of these results yielded the following observations and recommendations.

During the test period, a number of problems were encountered. Literature suggests that these problems historically impeded development of electrodialysis for complex solutions of concentrated divalent cations. As these problems were encountered in this project, they were addressed by making a number of improvements to the electrodialysis process specific to this laboratory unit. Some of these improvements represent potentially scalable means for cost savings. Others of these improvements represent critical changes needed to keep the electrodialysis unit operational.

Range of Operation: An arbitrary energy utilization limit (0.1 to 0.15 kWh/lb TDS) was established to keep the electrical costs of electrodialysis at less than \$0.18 per barrel of flowback water treated. This limit was based on the projected recovery of 67% of the volume from each barrel (42 gallon/barrel) and taking the diluate stream from 50,000 mg/l TDS to 10,000 mg/l TDS. The cost of electricity was assumed to be \$0.10/kWh. Theoretical calculations for this ED skid suggested that the goal could be achieved by maintaining a low stack potential of 5 volts (nominally 0.5 volts/membrane pair). Energy utilization was calculated for 33 electrodialysis runs. The average energy expended was 0.12 kWh/lb TDS with a range from 0.1 to 0.148 kWh/lb. Design considerations indicate that there is a trade-off between low power costs and higher initial capital costs.

Chemistry of the Electrolyte: The chemistry of the electrolyte solution was investigated as a means of improving the rate of salt transfer at the desired stack potential. Theoretical calculations showed that at high concentrations of brine, there would be significant resistance to ion flux within the electrode cells. Increasing the electrolyte concentration to an ionic strength similar to the water being treated increases ion flux for a given stack potential. Improvements

may also be made by lowering the overvoltage of the electrodes by operation of the electrolyte at a pH greater than about pH 11. However, pH control of the electrolyte becomes problematic if there is incursion of multivalent cations into the electrolyte. The relative process improvements decrease as the number of cell pairs increases.

Mitigating the Effects of Calcium: A generic cation selective membrane was installed at the boundary to the cathode cell. High rates of calcium incursion into the electrolyte were encountered, causing calcium fouling of the electrode cells. The cathode boundary membrane was replaced with a membrane that selected against multivalent cations. Calcium flux into the electrolyte was reduced by 70%. An apparent added benefit was that calcium deliberately introduced into the electrolyte, both as free ions or as a precipitate, no longer interfered with ion flux. This indicated that the initial calcium poisoning was at the surfaces of the cathode boundary.

Interference and Fate of Multivalent Cations: The adverse role of calcium (eg. multivalent cations) on the duration of a process run were expected, and demonstrated. The effect of multivalent cation incursion into the electrolyte was mitigated with a more optimum cathode boundary membrane. Iron caused an immediate loss of process efficiency, likely by precipitation at all membrane surfaces. Calcium, barium, and magnesium caused a slower degradation of ion flux. The fate of the multivalent cations was investigated. Barium, iron, magnesium, and calcium were readily transported from the diluate to the concentrate. These ions were preferentially transported to the concentrate. Calcium and magnesium were transported slowly into the electrolyte. Barium and iron were either not readily transported, or not readily measured in the electrolyte.

Clean-in-Place: A concept for maintaining consistent operation was investigated. Loss of process efficiency was observed when calcium, iron, and barium were present in the test water. A possible mechanism is the establishment of a stagnant charge layer at the cathode boundary membrane. Short pulses (15 seconds to one minute duration at intervals of 15 minutes to one hour) of pole reversal (cathode to anode) at elevated voltages (5-15 V) improved total ion flux. Tests were conducted with mixed salt solutions and field waters from the Barnett and Marcellus. Flux improvements of up to 37% were measured for waters treated using a CIP regime.

Field waters from the Barnett and the Marcellus: Four samples were received; two from Barnett and two from the Marcellus. Simple pretreatment consisting of pH adjustment to neutrality, aeration, and filtration with a 5 μ cartridge filter was sufficient to create treatable waters. In three of four cases, the water was deemed beyond the concentration suitable for effective electrodialysis (150,000 – 270,000 mg/l TDS), and likely represented water collected from late in the flowback periods at these sites. These waters were diluted with tap water for the tests with ED. Eleven tests were performed with the field waters, including five tests with the clean-in-place pole reversal technology. Overall rates of treatment with ED were slow, as expected from the high levels of multivalent cations in the samples. Iron seemed to be the worst component in these samples.

Effect of Temperature: The electrodialysis process poses a unique opportunity to take advantage of improved current capacity with increased operating temperature. The design of the electrodialysis process creates two co-dependent, rate limiting reaction sites; the electrode cell reactions, and the transport of ions within the membrane stack. The Arrhenius equation for temperature dependency was modified for two co-dependent rates over a temperature range of 8°C to 33°C. Independent temperature coefficients for the electrode cells and the stack were obtained. These relations predicted operation over range of other temperatures. These tests predict that field operation can be improved with increased operating temperature. Partial, yet significant improvements (15-50%) may be made by increasing only the electrolyte bath

temperature. As such, the full water stream does not need to be temperature controlled. Waste heat added to the electrolyte will improve performance.

Process Recommendations: The following recommendations are made for the operation of ED with complex brine solutions. Some of these improvements represent potentially scalable means for cost savings. Others of these improvements represent critical changes needed to keep the electrodialysis unit operational.

- Iron appears to be the most likely cation to cause fouling of the ED process. Iron should be aggressively removed in pre-treatment.
- Increase the concentration of electrolyte to reduce resistance at the electrodes. This can improve rate of the ED process by around 24%.
- If the level of calcium and iron is fairly low, then the pH of the electrolyte can be increased to pH 11. This reduces the overvoltage applied to the anode and can account for an additional 15% improvement in the rate of the process.
- With high concentrations of calcium, protection of the cathode barrier membrane with a multivalent cation exclusionary membrane is imperative. Improvements of 40% are possible.
- Clean-in-place technology will be needed to keep the ED unit operational. For very little expenditure, 35% process improvement in ion flux can be realized using a simple pulsed pole reversal.
- The use of waste heat to increase the temperature of the electrolyte, the water, or both, can improve the rate of the process by at least 15%.

Process Economics: Eurodia provided a set of capital and operational parameters for specific design examples. The design parameters were converted, with additional assumptions, into cost estimates. A typical design case resulted in an operational cost of about \$35-40/ 1000 lb salt removed. The majority of the operational cost (75%) was determined to be electric power to operate the electrodes. Power costs were estimated at \$0.10/kWh. Membrane replacement and labor accounted equally for 20-25% of the operating costs. Pumping costs and chemical cleaning agents were nominal, compared to the other operational costs. Capital costs were amortized for 7 years and 7% interest to estimate a capital cost per 1000 pounds salt removed. A typical design case resulted in a capital cost of \$30-45/1000 lb salt removed. Capital costs were dominated (>80%) by the process equipment for the electrodialysis unit. Placeholder costs estimates for generators and construction (building and site preparation) accounted for about 20% of the required capital. A further comparison between the process data in this report and the estimates from Eurodia suggests increased capital costs (dominated by the cost of the electrodialysis equipment), can be offset by lower operating costs (dominated by energy requirements).

3 INTRODUCTION

3.1 Problem Statement

The hydraulic fracture of shale formations for the capture of natural gas is a relatively new technology. Work on North American shale formations, such as the Barnett and the Marcellus, has demonstrated the potential to capture trillions of cubic feet of high value gas. Other shale formations on other continents have the potential for development, therefore, potentially revolutionizing energy economies on a worldwide basis.

During the fracture process, between 1 and 4 million gallons of water and sand is expended “down hole” into each extraction well to aide in the fracture. A portion of this water is recovered during the initial extraction of the gas. The recovered fluid can contain high concentrations of dissolved salt, plus trace concentrations of residual anti-oxidants and lubrication fluids. Therefore, recovered flowback water presents a disposal problem, as well as a financial burden on the operation of the well.

The nature of the chemistry and dynamics of recovered water is of vital interest for effective environmental stewardship of a gas field. This project is part of a larger effort to define flowback water chemistry, dynamics of recovery, and engineering solutions to lower the cost of water handling. Electrodialysis is examined as one potential piece of an engineering solution for water management. To investigate the use of electrodialysis for flowback waters, it is first important to understand the flow and salt profiles of the recovered water.

Hayes (2009) presented data collected on flow and salt profiles of flowback water from the Marcellus formation (see also Hayes and Severin, 2012 A). Salt (TDS) concentrations from the influent to the storage reservoirs and the total volume of water collected on 1, 5, 14, and 90 days after the fracture event were collected from 19 wells (Table 1).

Three important conclusions may be immediately discovered from these data.

- The ultimate recovery of water is less than 35% of the initial charge on a weighted basis of flow from all wells.
- The flow rate from the wells decreases rapidly with time, such that most of the water (80%) is collected within the first 14 days after fracture. Less than 20% recovery occurs between days 15 and 90.
- The concentration of salt increases as a function of time after fracture. Four data sets show salt concentrations at 14 and 90 days. The 90 day concentrations are 50% greater than the 14 day concentrations.

Twelve of these data sets contain sufficient information to develop empirical correlation of flow versus time and salt concentration versus time for the individual events. These two correlations, when analyzed together, yield a third correlation between total salt recovered versus total flow recovered for each event. Surprisingly, eight of twelve events showed remarkably similar total salt versus total volume profiles. Figure 1 is a summary plot showing the percent of flowback water having less than the stated salt concentration during the first 90 days after fracture. The three lines represent the median Marcellus event, a high salt event (Site F), and a low salt event (Site E).

Table 1 Recovered Flow-back Water Inventory (After Hayes, 2009)

	Total Used bbls	Barrels Recovered by Days After Fracture				%Barrels Recover- ed	Input Frac Fluid mg/l	Well Stream Concentration (mg/l) Days After Fracture			
		1	5	14	90			1	5	14	90
A	40,046	3,950	10,456	15,023		38	990	15,400	54,800	105,000	216,000
B	94,216	1,095	10,782	13,718	17,890	19	27,800	22,400	87,800	112,000	194,000
C	146,226	3,308	9,652	15,991		11	719	24,700	61,900	110,000	267,000
D	21,144	2,854	8,077	9,938	11,185	53	1,410	9,020	40,700		155,000
E	53,500	8,560	20,330	24,610	25,680	48	5,910	2,890	55,100	124,000	
F	77,995	3,272	10,830	12,331	17,413	22	462	61,200	116,000	157,000	
G	123,921	1,219	7,493	12,471	31,735	26	1,920	74,600	125,000	169,000	
H	36,035	3,988	16,369	21,282		59	7,080	19,200	150,000	206,000	345,000
I							265	122,000	238,000	261,000	
J							4,840	5,090	48,700	19,100	
K	70,774	5,751	8,016	9,473		13	804	18,600	39,400	3,010	
L							221	20,400	72,700	109,000	
M	99,195	16,419	17,935	19,723		20	371			228,000	
N	11,435	2,432	2,759	3,043	3,535	31	735	31,800	116,000		
O							2,670	17,400	125,000	186,000	
P							401	11,600	78,600	63,900	
Q	23,593	1,315	3,577	5,090		22	311	16,600	38,500	120,000	
R							481	15,100	46,900	20,900	
S	16,460	2,094	7,832	9,345	10,723	65	280	680	58,300	124,000	

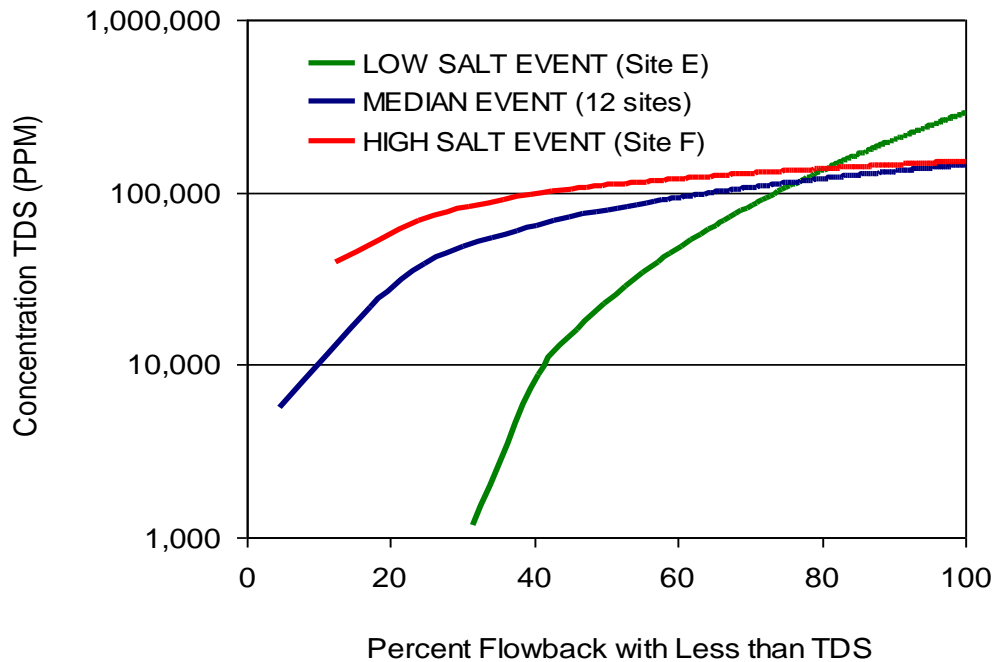


*Figure 1: Examples of Flowback Waters from the Marcellus:
Percent of Flowback Water with Less than Stated*

3.2 Water Management (Life Cycle Analysis)

The short term water management issues (at a single well field, or between several local well fields) suggest that segregation of early flowback water from late term flowback is feasible and beneficial (Galusky 2001A, 2001B). Small, regional treatment systems can be established to handle a range of water qualities. For example, relatively salt free water can be reused with minimal pretreatment. Water with mid-range concentrations, e.g. 10,000-60,000 mg/l TDS can be treated with membrane desalination systems, such as reverse osmosis (Li et al., 2010 and Huang et al., 2011) and/or electrodialysis (Severin and Hayes 2011). Extremely salty water, representing late flowback and/or produced water, may be desalinated using distillation methods, such as mechanical vapor recompression (Hayes and Severin, 2012 B).

A preliminary life cycle model was developed (Hayes and Severin, 2012 C) to examine a hypothetical shale gas region over a 45 year period based on a presumed median Marcellus flowback event. The hypothetical play was based on 48% coverage of a 25 x 25 mile area, including 300 fields with 16 wells per field for a total of 4,800 wells. A baseline recovery of 7 barrels per day of recovered water was assumed after completion of the immediate flowback recovery (180 days).

A current practice in the Marcellus is to use as much of the recovered flowback water, as possible, as part of the feed water for the next fracture. A common fracture event requires about 4 million gallons, or about 95,000 barrels of water. A typical recovery of flowback water is 1 million gallons, or about 24,000 barrels. Each subsequent fracture would require 3 million gallons fresh water plus the 1 million gallons collected from the previous fracture. Therefore, if

19,200 fractures are planned in a 300 field play, then each fractures represents 25% of 4 million gallons, for a total planned reuse capacity of $19,200 \times 24,000 = 461,000,000$ barrels of reuse capacity. As each fracture occurs, the reuse capacity of that fracture is used-up. It is a matter of book-keeping to compare the total planned reuse capacity of 19,200 fractures versus the total of the flowback water plus produced water collected.

Figure 2 is an example of a 19,200 fracture Marcellus play assuming that an even larger percent reuse (33%) than described above is assigned to each fracture. The red line represents the planned reuse capacity. The blue represents the recovered flowback plus produced water. The green line represents the average concentration of the recovered water. The planned capacity curve crosses the recovered water line at about 11.5 years into the life of the play. The significance of the cross-over point is that it demarks the transition between a young play and a middle aged play. In the years up to the cross-over, the axiom holds that “all the recovered water can be sent back down-hole”. At year 11.5, however there remains less reuse capacity available than the projected future recovery. At year 11.5 it becomes difficult to schedule enough reuse to keep up with the recovery. In a sense, the business changes from the business of gas production to the business of water management. Figure 2 also implies that as the recovered water quality and quantity changes throughout the years, the treatment needs for water conservation are also time dependent. For example, the treatment needs for years 1-10 might be simple treatment, such as coagulation and settling. By year 15, however, the average concentration is slowly increasing. This makes advanced treatment, such as membrane desalination necessary. By year 20, aggressive desalination such as MVR distillation may be needed.

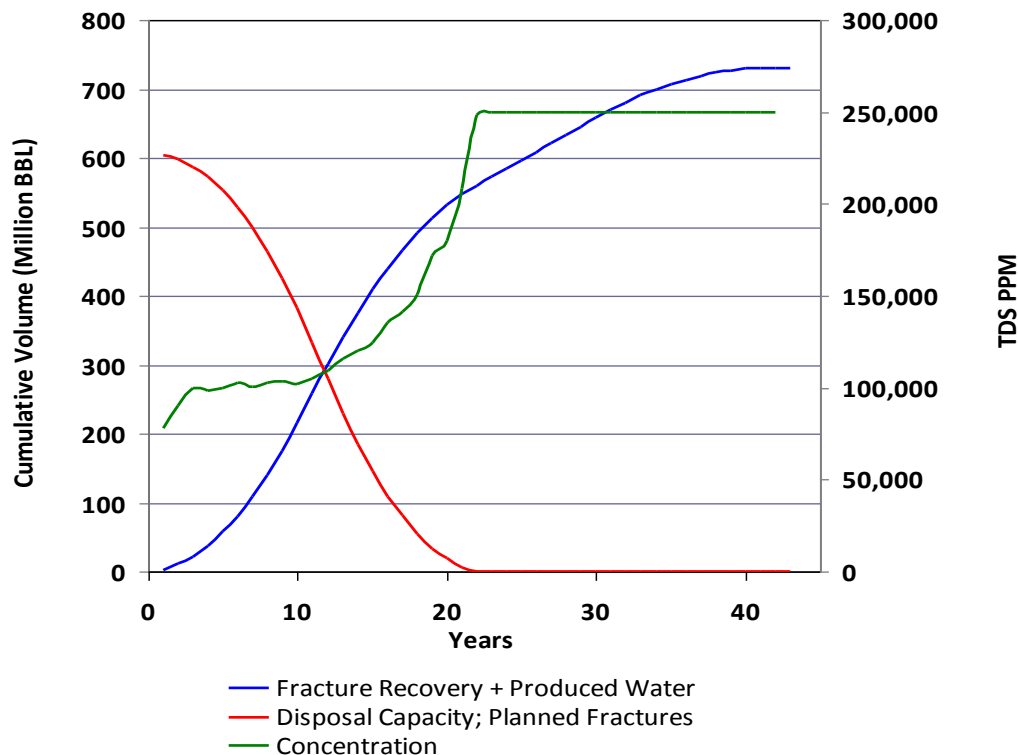


*Figure 2 Cumulative Fracture and Process Water Recovery vs Projected Reuse Capacity in a 19,200 Fracture Play
Assuming 33% Blend of Recovered Water in Each Fracture*

3.3 Electrodialysis as a Treatment Option

The objective of this project is to evaluate the efficacy of electrodialysis in the treatment of flowback waters. It is therefore necessary to develop a rationale in which electrodialysis makes engineering sense within a treatment train. As discussed in Section 1.B., the quantity and nature of the flowback water varies with the ability to classify and segregate the flows, the scale of the regional treatment plan, and the timing within the life cycle of the play. The desirability of electrodialysis in a treatment scheme is, therefore, nuanced by perceived need for treatment at any scale of process or timing within the life cycle of the play.

Figure 3 shows the placement of a concentrating membrane system, such as electrodialysis or reverse osmosis, within a treatment scheme. Moderately concentrated waters of 3% to 5% TDS could be treated on the membrane unit to make a diluate stream for reuse. A concentrated stream would be sent to an evaporator. The concentrate from the evaporator could be deep well injected.

Conventional use of electrodialysis is on water with less than several thousand mg/l TDS and less than several hundred mg/l calcium. The water generated in the flowback from shale gas hydraulic fracture is tens of thousands mg/l TDS with several thousand mg/l calcium. Additionally, hundreds of mg/l barium, and tens of mg/l of iron and other multivalent cations are present in the water. Hayes (2009) presented chemical data on water from 19 sites in the Marcellus (Table 1). These data are reproduced in Tables 2 and 3.

The challenges faced in this project were:

1. Define an operating range to keep the power requirements (kWh/lb salt removed) less than 0.15 kWh/lb .
2. Optimize the current draw while keeping the current efficiency approaching 100%.
3. Demonstrate that the multivalent cations are moving to the concentrate.
4. Demonstrate that the multivalent cations are rejected from the electrolyte.

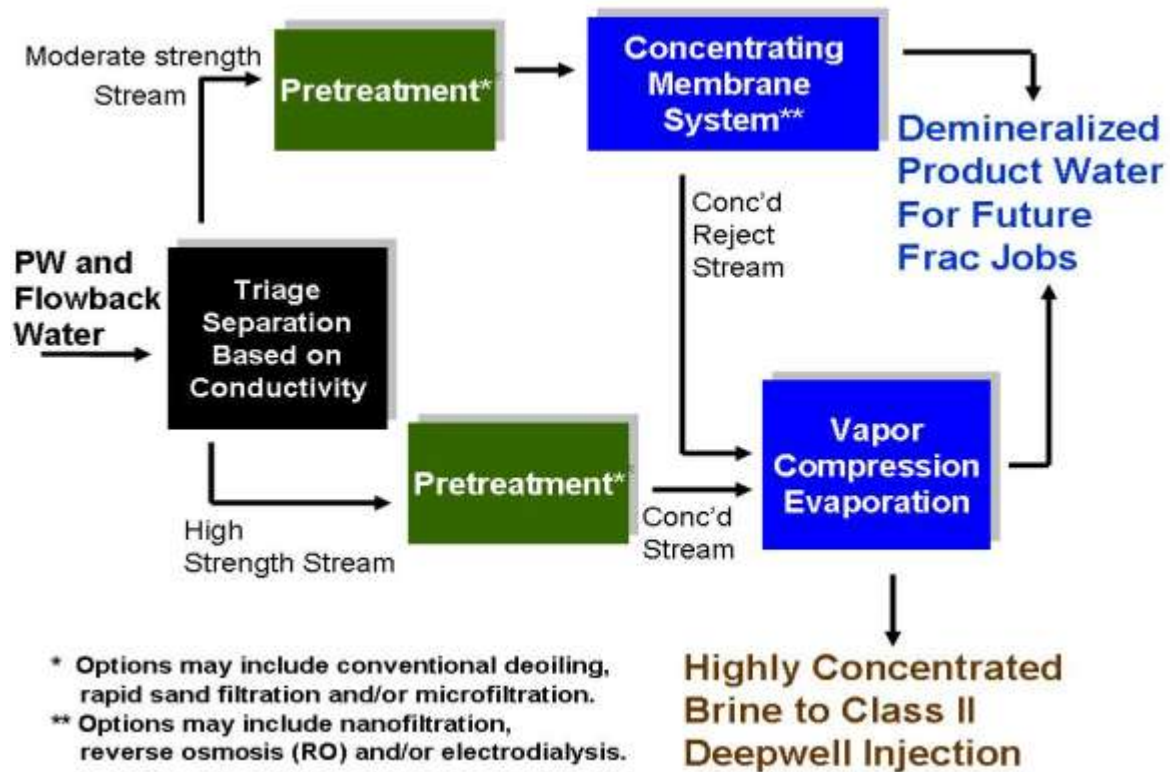


Figure 3: Conceptual Placement of Electrodes (Concentrating Membrane System) in a Water Treatment Process

Table 2: Chemical Characteristic; 19 Marcellus Wells: Day 5 After Fracture (Hayes, 2009)			
	Range	Median	Units
pH	4.9 - 7.2	6.8	pH Units
Total Alkalinity as CaCO ₃	48.8 - 266	122	mg/l
Hardness as CaCO ₃	4,000 – 55,000	17,700	mg/l
Total Suspended Solids	10.8 – 3,220	99	mg/l
Turbidity	2.3 - 786	80	mg/l
Chloride	26,400 -14,8000	41,850	mg/l
Total Dissolved Solids	20,900 – 238,000	67,300	mg/l
Total Kjeldahl Nitrogen	30.5 - 204	86	mg/l
Ammonia-N	15 - 242	82	mg/l
Biochemical Oxygen Demand	6.2 – 1,950	138	mg/l
Chemical Oxygen Demand	195 – 17,700	4,870	mg/l
Total Organic Carbon	3.7 - 323	63	mg/l
Dissolved Organic Carbon	30.7 - 343	114	mg/l
Oil and Grease	<0.5 - 350	5	mg/l
Cyanide, Total	<1.7 - 72.1	<1.7	mg/l
Bromide	113 – 1,190	445	mg/l
Sulfate	<0.031 - 106	26	mg/l

Table 3: Metals Data for Flowback Waters 5 Days after Fracture (Hayes, 2009)			
Parameter	Range	Median	Units
Aluminum	ND - 47,200	360	ug/L
Antimony	ND - 47.2	17.3	ug/L
Arsenic	ND - 124	28.8	ug/L
Barium	21,400 - 13,900,000	686,000	ug/L
Boron	3,140 - 97,900	12,200	ug/L
Calcium	1,440,000 - 23,500,000	4,950,000	ug/L
Chromium	ND - 152	15.1	ug/L
Chromium (III)	ND - 92.4	7.5	ug/L
Copper	ND - 4,150	ND	ug/L
Iron	10,800 - 180,000	39,000	ug/L
Lithium	10,600 - 153,000	41,800	ug/L
Magnesium	135,000 - 1,550,000	559,000	ug/L
Manganese	881 - 7,040	2,630	ug/L
Molybdenum	ND - 147	30.6	ug/L
Potassium	48,900 - 2,430,000	301,000	ug/L
Sodium	10,700,000 - 65,100,000	18,000,000	ug/L
Strontium	345,000 – 4,830,000	1,080,000	ug/L
Zinc	67.6 – 2,930	156	ug/L
Beryllium, Cadmium, cobalt, Copper, Mercury. Nickel, Selenium, Tin, Titanium, and Thallium below			

3.4 Objectives

1. Determine the technical feasibility of using electrodialysis (ED) to demineralize Barnett shale flowback water; specifically:
 - Design/construct an integrated laboratory treatment system based on treatment needed to meet specifications consistent with the recommendations of the BSWCMC Hydraulic Fracturing Expert Panel to be made available from GTI.
 - Perform treatment tests on the integrated system including pretreatment, a laboratory scale ED unit, and post-treatment conditioning (if needed) to achieve a partially demineralized water product suitable for reuse in frac jobs in the Barnett and Appalachian Shale Regions.
 - Determine the baseline performance of conventional ED and electrodialysis reversal (EDR) membranes, process configurations, and operating conditions in the partial demineralization of flowback waters to meet water reuse specs for frac jobs.
2. Evaluate the Potential of Advanced Electrodialysis
 - Membranes to Improve ED and EDR Demineralization of Flowback Water
 - Select advanced candidate membranes suitable for the treatment of high-salinity, chloride-based, flowback waters
 - Determine the operating conditions needed to demineralize flowback waters to salinity conditions that meet ASWCMC and BSWCMC specs for reuse in the performance of frac jobs, including membrane type.

3.5 Approach

The timeline for Task 8 covered approximately 24 months with initial goals developed for each of the two years. The complexity of the project, however, required a technical approach that could rapidly move from basic theoretical understanding to creating innovative strategies for optimization. The approach for Year 1 was to:

- Provide theoretical modeling specific to the pilot ED unit sufficient to guide the direction of the initial experiments. Predetermine the operating conditions to meet an aggressively low energy demand (0.1-0.15 kWh/lb TDS removed) for a range 30,000 – 60,000 mg/l sodium chloride.
- Confirm the ability of the pilot ED unit to treat 30,000 – 60,000 mg/l sodium chloride within the desired range of energy demand.
- Investigate the role of electrolyte chemistry in improving ion flux for a set stack voltage.
- Determine the influence of extreme concentrations of soluble calcium (1000-4000 mg/l) as surrogate for barium and magnesium and other multivalent cations on the electrodialysis process.
- Mitigate the influence of extreme concentrations of soluble calcium on the electrodialysis process.

The projected approach for Year 2 was:

- Confirm the ability to treat recovered flowback water in the range of 30,000-60,000 mg/l TDS under laboratory conditions.
- Determine advanced pretreatment needs specific to the water chemistry expected for recovered flowback water (example, filtration)
- Continue ED process developments, such as membrane selection, advanced process chemistry, or process hydraulics to optimize economics and/or stabilize operation specific to the demineralization of flowback water.
- Provide systems modeling for guidance in the optimum placement of ED within a treatment train.

4 BACKGROUND

4.1 *Standard Description of Electrodialysis*

Electrodialysis is a membrane separation technology containing four distinct components;

1. Multiple pairs of cation and ion selective membrane are collectively called the stack.
2. A series of hydraulic paths to collect demineralized water (the diluate stream) and the concentrated water (the concentrate stream).
3. A pair of electrode cells; one containing the anode and the second containing the cathode.
4. An electrolyte reservoir and hydraulic paths to provide anolyte and catholyte.

A generic depiction of the electrodialysis process is presented in Figure 4. As shown here, the cathode is to the right and the anode to the left. Therefore, the cations move toward the right while anions move toward the left.

Proceeding left to right, the anode is bounded by a cation selective membrane. This membrane provides hydraulic separation of the anolyte from the concentrate stream. An integral part of the process is the free transport of cations (viz. sodium) from the anolyte into the concentrate, which is allowed by the boundary membrane at the cathode. Just as importantly, anions from the concentrate stream cannot be transported into the anolyte due to rejection of the cation selective boundary and by the electronic attraction of the anode.

The neighboring membrane to the immediate right of the anode boundary membrane is an anion selective membrane. This membrane pair collectively forms the first compartment of the concentrate hydraulic pathway. This pair of membranes naturally causes ion concentration. Cations entering the compartment from the anolyte cannot pass further to the right due to the restriction caused by the anion selective membrane. Likewise, anions crossing from right to left, compelled by anode potential, cannot pass further to the left due to the cation selective membrane.

Continuing to the right, a cation selective membrane to the right of the first anion selective membrane constitutes the first component of the diluate pathway. Water in this cell naturally loses anions to the left through the anion selective membrane and loses cations to the right through the cation selective membrane.

The pattern of alternating cation and anion selective membrane creates a pattern of alternating concentrate and diluate streams. The concentrate streams are manifolded together and the diluate streams are manifolded together to form two separate hydraulic pathways.

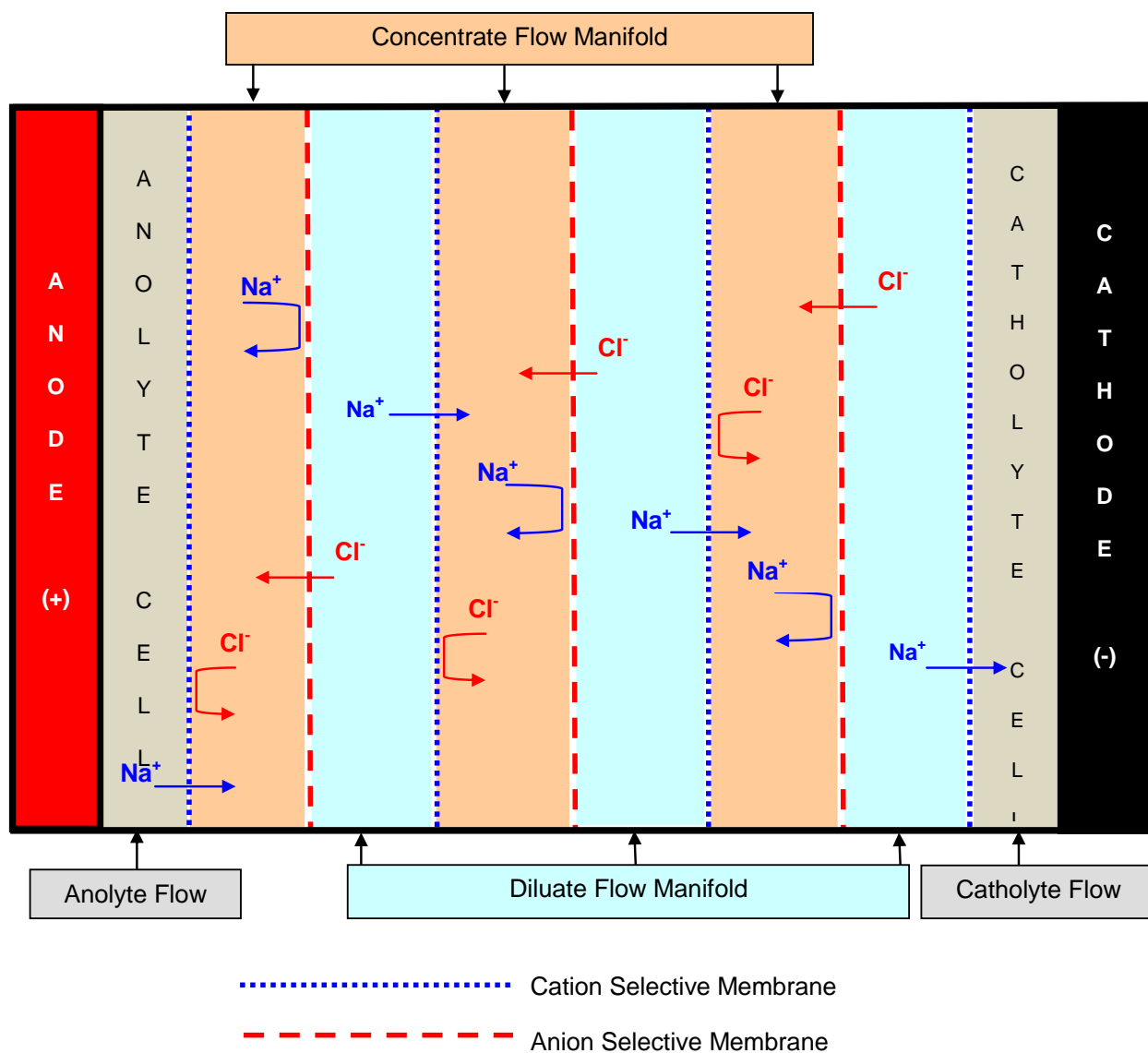
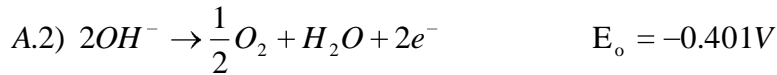
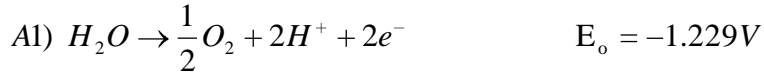


Figure 4: Ion Flow in an Electrodialysis Stack

The final membrane on the right hand side is also a cation selective membrane and forms the boundary of the cathode cell. This membrane, and the anion selective membrane, immediately to the left, forms the last final diluate path. Cations from the diluate stream are compelled to pass into the catholyte, whereas, anions freely pass from the diluate through the anion selective membrane to the left.

It is germane to this project that the desired cation exchange across the cation selective membrane at the cathode boundary is sodium ion. Much of the project effort, as will be seen in the subsequent sections, is aimed at minimized the flux of multivalent cations across the cathode cell boundary.

The passage of ions from the diluate into the concentrate is driven by the electrochemistry that occurs at the electrodes. The following pair of chemical reactions is often presented as examples of likely reaction at the anode (A1 or A2) and at the cathode (C1).



The reactions are driven by a direct current power source. The oxidation of water to oxygen at the anode provides electrons. The reduction of water to hydrogen at the cathode provides the electron sink. Resistance to these reactions in the electrode cells is reduced by using a conductive electrolyte, such as disodium sulfate.

Electronic neutrality must be maintained in the catholyte and in the anolyte. The production of hydronium ion (or destruction of hydroxide) in the catholyte compels a cation (viz. sodium) to cross the anode cell boundary membrane into the first concentrate cell. The production of hydroxide at the cathode compels a cation (viz. sodium) to leave the final diluate cell into the catholyte. These boundary ionic balancing reactions cascade throughout the membrane stack, as depicted in Figure 4.

A final outcome, evident from the above discussion, is the observation that the anolyte will become acidic and sodium poor. Likewise, the catholyte will become basic and sodium rich. It is imperative, both for pH control and sodium balance, that the anolyte and catholyte are remixed into a single electrolyte solution. This is usually done after the catholyte and anolyte are allowed a modest time for degassing (hydrogen and oxygen, respectively).

4.2 Electrodialysis Concepts for Concentrated Brines

Electrodialysis can be considered as a completed electronic circuit in which an applied potential (voltage) causes current (amperage viz. Ion flux) across a series of resistors. The resistances can be itemized:

- Boundary diffusion resistance at all membrane surfaces
- Resistance to current transmittal in all solutions
- Osmotic pressure between dilute and concentrate streams
- Voltage drop across each membrane
- Reaction initiation and transfer of ions at the electrodes.

Conventional treatment with ED is typically with waters at a concentration less than seawater (between several thousand and 500 mg/l TDS). In these designs, the process usually has a high voltage and a low amperage. It is beneficial from a standpoint of energy efficiency to run a high amperage at as low a voltage as possible when treating extremely highly concentrated waters (30,000-60,000 mg/l TDS) Under these two operating regimes (high volts, low amps; vs. low volts, high amps) it is expected that the various resistances will have different influences within the process.

A specific case-in-point is a design criterion known as “limiting current”. The concept of “Limiting current” originates from the estimation of the concentration gradients that form at diffusion boundaries at the various membranes. If D is the diffusion coefficient (L^2T^{-1}), δ (L) is the diffusion boundary established between the bulk solution and the membrane, and A (L^2) is the area of a single membrane, then the flow (moles/time) of an ion, such as sodium (Na^+), passing a selective membrane is a function of the concentration gradient (mole L^{-3}) established in the bulk and at the surface of the membrane.

$$\frac{\Delta Na^{+} \text{ moles}}{\Delta T} = \frac{DA}{\delta} \left(Na^{+}_{bulk} - Na^{+}_{membrane} \right)$$

Using the definition of amp (i) = coulomb/sec and Faraday (F) = 96,500 coulomb/ mole, then the amperage needed to cause the ion flow is:

$$i = F \frac{\Delta Na^{+} \text{ moles}}{\Delta T} = F \frac{DA}{\delta} \left(Na^{+}_{bulk} - Na^{+}_{membrane} \right)$$

The limiting current, i_{lim} occurs as the concentration of the ion at the membrane surface approaches a concentration of zero.

$$i_{lim} \cong F \frac{DA}{\delta} Na^{+}_{bulk}$$

If too high a voltage is applied, an ion imbalance can form that causes the water near the membrane to polarize or “split” into its conjugate acid proton and caustic hydroxide ions. This allows hydrogen ion (instead of sodium ion) to cross the cation selective membranes; and hydroxide ion (instead of chloride ion) to cross the anion selective membranes. This is inefficient from an energy standpoint and can also be detrimental to the life of the membranes.

If the diffusion coefficient ,D, for sodium chloride is taken as about $1.5 \times 10^{-5} \text{ cm}^2\text{sec}^{-1}$ (CRC Handbook of Chemistry and Physics, 54th edition, 1973) and δ is on the order of 0.01 cm (Leibovitz, Mass Transport and Acid-Base Generation in Solution/Membrane Systems, Ph.D. thesis, UC Berkley, 1977.), then for the pilot system tested in this project ($A= 200 \text{ cm}^2$) the limiting current can be estimated.

- For 1 g/L NaCl, the limiting current is just under 0.5 amps.
- For 10 g/L NaCl, the limiting current is just under 5 amps
- For 30 g/L NaCl, the limiting current is just under 15 amps.
- For 60 g/L NaCl, the limiting current is just under 30 amps.

This suggests that for normal operation of the electrodialysis process, the limiting current is from 0.5 to 5 amps. Much effort is taken to keep the voltage well below that which can cause current inefficiency.

In treating highly concentrated brines, the operational area of interest for this project, the limiting current may be as high as 5-30 amps (as specific to this pilot plant). An entirely different set of resistances to ion flow resistances are encountered. Specifically, a major resistance to ion flow occurs at or near the electrode surfaces rather in addition to those at the membrane surfaces.

4.3 Scale-up

There are four issues to be considered for scale-up of the electrodialysis process:

1. Stack voltage (V_s), volts per cell pair (V_{cp}), and electrode/overvoltage (E)
2. Total amps (I_T), surface area per single membrane (A_{cp}), and amp flux (j) per single membrane
3. Ion transfer capacity (q = charge equivalents/sec) and transfer efficiency (f)

4. Number of cell pairs (N_{cp}).

The scale factor for voltage is:

$$V_{CP} = \frac{V_S - V_E}{N_{CP}}$$

The scale factors for ion transfer capacity (where F = Faraday = 96,000 coulomb/charge equivalent) are:

$$I_T = jA_{CP}$$
$$q = \frac{fN_{CP}I_T}{F}$$

The pilot data are analyzed as follows:

1. Determine the volume of diluate treated
2. Determine the time to treat the diluate
3. Calculate the effective total amperage from total charge equivalents treated per second
4. Calculate the transfer efficiency from the effective total amperage and the measured average amperage
5. Determine the volts per cell using the pilot stack voltage and electrode voltage
6. Calculate the amps per unit area of a cell (one membrane in a pair)

A full scale unit with the same performance (amps/unit area of a cell) and volts/cell pair treating a larger volume of similar water to a similar end point is calculated as follows:

1. Determine the volume to be treated
2. Determine the time allowed to treat the water
3. Calculate the total amperage and effective amperage
4. Postulate an area per cell (one membrane) to be used
5. Postulate a number of cell pairs
6. Calculate the amps/area of a cell (one membrane)
7. Compare the amps/area calculated against the amps/area of the pilot unit.
8. Change the number of cell pairs until the amps/area of the full scale unit equals the amps/area of the pilot unit.
9. Calculate the stack voltage of the full-scale unit using the volts/cell from the pilot data.

Table 4 shows an example scale-up for treatment of 3% NaCl down to 1% NaCl. Typical pilot results were used to build the parameters. Treatment of 100 barrels per day would require about 80 cell pairs of 1 m² per single membrane and operate at a stack voltage of 22 volts and 80 amps. This is a trial and error method and other combinations of unit area and total cells can also be found that would meet the criteria.

Table 4: Example Scale-up						
Pilot System				Full Scale		
Volume		0.066	Barrel	Volume	100	Barrel
Volume		10.5	Liter	Volume	15890	Liter
Time		6	Hours	Time	24	Hours
Initial		3	% NaCl	Initial	3	% NaCl
Final		1	% NaCl	Final	1	% NaCl
equivalent wt.		58.5	g/eq.	equivalent wt.	58.5	g/eq.
ion capacity	q	0.000166	Eq./sec	ion capacity	0.0629	Eq./sec
current eff.	f	0.99		current eff.	0.99	
cell pairs	N _{CP}	10		cell pairs	76	
stack voltage	V _s	5	volts	stack voltage	20.8	volts
overvoltage	V _E	2	volts	overvoltage	2	volts
volts/cell	V _{CP}	0.3	volts	volts/cell	0.3	volts
area/cell	A _{CP}	0.02	m ²	area/cell	1	m ²
amp/area	j	80	amps/m ²	amp/area	79.7	amps/m ²
Total amps	I _T	1.6	amps	Total amps	79.7	amps

5 METHODS

5.1 Standard Configuration of the Electrodialysis Pilot Plant

This project was performed using an Eurodia Industrie, S.A (Rungis, France) Ameridia Eur2B-10 electrodialysis unit (Figure 5). A flow chart is presented in Figure 6. The main component is the Eur2B-10 Electrodialysis Dialysis Stack (10) that consists of twenty-one alternating cationic and anionic selective membranes, beginning and ending with cationic selective membranes. All anionic selective membranes were provided by the vendor. In the first portion of this project, all cationic selective membranes were standard, generic selectivity. In the final portion of this project, the single cation selective membrane at the cathode boundary was replaced with a cation selective, multi-valent exclusionary membrane. Individual membranes have an area of 200 cm².



Figure 5: Photograph of the Eurodia Pilot ED Skid

The diluate is collected in a diluate tank (T300). A pump (P301), a control valve (CV301), and a rotometer (FI 301) are used to deliver and control the flow of diluate to the diluate manifold within the stack. A diluate tube returns the diluate to the diluate tank. The volume of the diluate tank (T300) is approximately 10L. The nominal volume of diluate within the rotometer (FI301), pump (P301), and various pipes, tubes, and manifolded cell pairs associated with the diluate flow loop is about 0.5L. The recommended flow of diluate through the manifold is about 1.0-1.5 L/minute.

The concentrate is collected in a concentrate tank (T200). A pump (P201), a control valve (CV201), and a rotometer (FI 201) are used to deliver and control the flow of concentrate to the concentrate manifold within the stack. A tube returns the concentrate to the tank. The volume of the concentrate tank (T200) is approximately 10L. The nominal volume of concentrate within the rotometer (FI201), pump (P201), and various pipes, tubes, and manifolded cell pairs associated with the concentrate flow loop is about 0.5L. The recommended flow of concentrate through the manifold is about 1.0-1.5 L/minute.

The electrolyte that has passed through the anode cell is collected in the anolyte tank (T100a). Likewise the electrolyte that has passed through the cathode cell is collected in the catholyte tank (T100c). The production of oxygen at the anode and hydrogen at the cathode requires that these two tanks be isolated from each other for degassing. In the Eur2B-10 Electrodialysis Pilot Plant, the feed of electrolyte to the electrode cells is provided by a single electrolyte pump (P101) that captures electrolyte from both the anolyte and catholyte tanks in roughly the same proportions. This single pump feeds a pair of control valves (CV 101 and CV 102) and flow indicators (FI101 and FI 102) that provide electrolyte separately to the cathode and anode.

The anode and cathode electrodes are connected to a Power Supply (11) which supplies from 0-40 volts DC at a maximum of 25 amps. The recommended maximum potential for this Eur2B-10 is 1.5 volts per cell pair, or 15 volts.

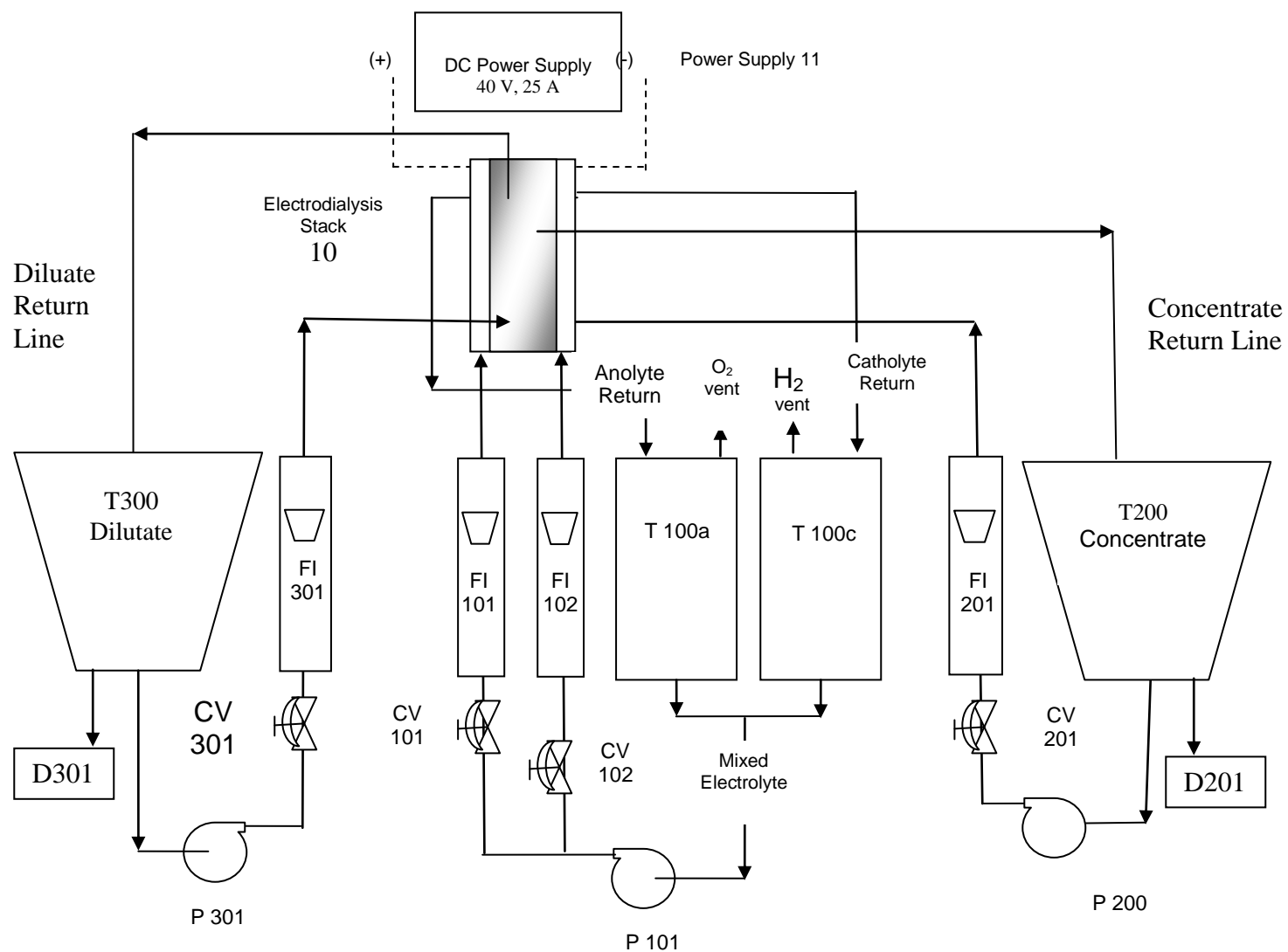


Figure 6: Flow Diagram for the Eurodia Industrie, S.A., Ameridia Eur2B-10 Electrodialysis Pilot Plant

5.2 Non-Standard Configurations of the Pilot Plant

Cathode Protected Mode: All anionic selective membranes were provided by the ED vendor. In the first portion of this project, all cationic selective membranes were of generic selectivity. In the final portion of this project, the single cation selective membrane at the cathode boundary was replaced with a cation selective, multi-valent exclusionary membrane..

Constant Feed Configuration: To provide a constant source of feed waters, especially during the temperature studies, the diluate tank T300 and the concentrate tank T200 were cross-connected by diluate return line to the concentrate tank and the diluate return line to the concentrate tank. Hydraulic stability was achieved by connecting a hose between the diluate tank drain D301 and the concentrate tank drain D201.

Pulsed Pole Reversal Clean-in-Place Mode: Pole reversal was accomplished by switching the plug connections between the power supply and the anode and cathode on the electrodialysis stack terminals.

5.3 Data Collection

Two types of tests were conducted, 1) volt-amp profile or 2) continuous run. The Volt-amp profile was performed by quickly ramping the power source down, in increments, from 15 to 3 volts; 2.5 volts and 2 volts. The amperage was recorded at each voltage and provided a snap shot view of the ED process under the extant conditions. The VA profile was taken at the start and end of each continuous run, or during a run if of interest. VA profile data were hand recorded.

Continuous run tests were performed by filling the diluate and concentrate tank each with about 10.5 liters of the desired feed water. The electrolyte tank was filled with 10.5 liters (in all cases except test N59 where the volume was 3.5 L) of the desired electrolyte. When in continuous-mode, the instruments were polled once every minute by data collection software. The master software was Labview (National Instruments) written as a local program by a GTI engineer.

Two or three Oakton Instruments Con 110 meters were used to continuously measure conductivity and temperature in the diluate tank (always), the concentrate tank (always) and in the anolyte tank (occasionally). The conductivity meters were calibrated by setting all meters to a 12.50 mS/cm (milli-Semens per centimeter) standard (Oakton Instruments). Subsequently, a series of sodium chloride solutions ranging from 120,000 mg/l to about 8000 mg/l NaCl were prepared. Calibration equations were thus generated for each conductivity meter. Calibrations were regenerated each week of testing and spot checked against a single solution daily during a week of testing. Temperature changed throughout each test run, usually increasing with test duration. The conductivity probes were sensitive to temperature (the higher the temperature, the lower the reading for a given salt solution), so an Arrhenius relation was developed to correct for minor changes in temperature.

Three Oakton Instruments pH 110 meters were occasionally used to measure the pH of the diluate, the concentrate, and the electrolyte. The pH probes (when used) were calibrated to pH7.

The power source was equipped with a computer interface. The volts and amperage were polled every minute by the Labview software.

Many of the tests that used calcium were monitored by chemical tests. These samples were sent to an outside contractor (STAT Analysis Corporation, Chicago, IL). The samples were

tested by ion chromatography for sodium, barium, chloride, sulfate, and calcium and total dissolved solids.

5.4 Data Analysis

Continuous run data were analyzed with the following interpretations:

5.4.1 Presentation of “In-Tank” Concentration

Conductivity data from the diluate and the concentrate were transposed into concentration (mg/l as NaCl) using calibration curves as described above. The concentration data were then corrected for temperature influences using an Arrhenius interpolation. These data represent the “in-tank” concentrations presented in the graphs.

5.4.2 Mass Transfer Data

As each run progressed, there was a net increase in volume in the concentrate tank, and a net decrease in volume in the diluate tank. The observed final volume transferred from the diluate to the concentrate was between about 500 and 1000 ml depending on the duration of the test and the initial salt concentration in the feed stock. It is thought that there are two contributions to this volume change; 1) osmotic drift of water across the membranes and 2) a change in the specific volume of the diluate and the concentrate with the change in salt concentration. In general, the osmotic drift accounted for about 90% of the volume shift, whereas, the change in specific volume accounted for 10% of the volume shift based on the following mathematical corrections.

The total mass of salt in the diluate and concentrate tanks was first established at the start of the test; $M(0) = C_d(0)V_d(0) + C_c(0)V_c(0)$. At each subsequent time interval (i), the mass of salt was calculated as $M(i) = C_d(i)V_d(i-1) + C_c(i)V_c(i-1)$ based on the presumed volume of the diluate $V_d(i-1)$ and the volume of the concentrate $V_c(i-1)$ during the previous time interval (i-1). The concentrations of the diluate, $C_d(i)$, and the concentrate, $C_c(i)$ were transposed from the conductivity measurements, as previously described. If the total mass, $M(i)$, was less than the initial mass, $M(0)$, then an incremental volume, ΔV was subtracted from the volume of the diluate and added to the volume of the concentrate. consistent with this mathematical treatment.

At each time element, the total salt transferred (M_{total}) is the average of the change in mass of the diluate and the change in the mass in the concentrate.

The effective salt transfer, M_e , was calculated by the below process:

1. Estimate the total salt transfer $M(i=final)$:
2. Calculate the ratio ($R = V_d(i=final)/V_d(0)$) of the final volume in the diluate tank to initial volume in the diluate tank, for a first approximation. The value of R was usually around 1.1)
3. Calculate the ratio, S, as the specific volume (volume/g salt) of the final concentrate divided by the specific volume of the initial concentrate. Specific volumes were calculated from the concentration data based on correlations in CRC (1973). This accounts for volumetric changes due the volume occupied by the salt. The value of S was usually around 0.98.
4. Estimate the effective salt transfer, $M_e = M_{total}/(RS)$

5.4.3 Energy use

The energy used during each test was calculated by summing the product of the volts and amps recorded at each time interval and converted to kWh.

5.4.4 Energy Efficiency

The effectiveness of energy utilization is presented as the energy utilized to transport one pound of salt removed from the diluate (kWh/lb salt removed). This was calculated on a point by point basis, as well as the overall average. Most results in this report represent the overall average.

6 THEORETICAL DEVELOPMENT

6.1 *Computer Model of the Eurodia Pilot Plant*

A simplified series resistance model was developed gain an initial understanding of the Eurodia pilot plant under high salt concentrations prior to the initiation of the experimental work. The model included:

- Boundary diffusion resistance at all membrane surfaces
- Resistance to current transmittal in the diluate solution
- Resistance to current transmittal in the concentrate solution
- Resistance to current transmittal in the electrolyte solution
- Osmotic pressure between dilute and concentrate streams
- Potential drop across each membrane
- Reaction initiation (overvoltage + electrode potential).

6.1.1 *Current Efficiency and Limiting Current:*

For this simplified model, the current is considered to be carried by the flux of cations; near to and across the various membrane and electrode surfaces. As defined in an earlier section, each electrode is bounded by a cation selective membrane. It is necessary for cations to move from the anode cell to the concentrate stream; and likewise, it is necessary for cations to be transported from the diluate stream into the cathode cell. Therefore, cation transport can be used as a common basis for development of a model for the behavior of the entire process.. For further simplicity, the use of the term “cation” will be used synonymously with the charge carried by the sodium ion or the hydronium ion.

Most literature concerning electrodialysis introduces the concept of “limiting current”. This is a simplistic evaluation of the condition where a diffusion boundary becomes depleted of sodium such that the current must be carried by water split into hydronum ion at the membrane surface. This condition may also be called the “polarized” condition. From a practical standpoint, this condition is caused by excessively overdriving the current by applying too high a voltage. Since there is always some hydronium present in water, it is better to assume that there is always a competition between sodium ion and hydronium ion transport.

Another commonly used term, “current efficiency”, is used to define the ratio of target cation (sodium) transport to total transport (sodium plus hydronium). In this model, the current efficiency is defined by as the ratio the current carried by sodium ion to the total of current carried by the sodium ion plus hydronium ion. At the limiting current, the current efficiency rapidly diminishes. A more realistic modeling method is to assume that the splitting of water always occurs; and is in competition with the diffusion of the sodium ion. Therefore, the total current is found from treating the competing currents across parallel resistances. It is noteworthy that in this research, TDS levels of 0.5-6% insure that sodium ion is always present under any reasonable set of conditions within the diffusion boundaries. Therefore, water splitting at the membrane surfaces is minimal compared to current transported by sodium.

Table 5: List of Model Variables and Parameters		
D_C	diffusion coefficient	cm^2/sec
A	Area of a single membrane	cm^2
F	Faraday	96,500 coulomb/g-
C_{DB}	Cation concentration of the diluate in the bulk solution	$\text{g-mole}/\text{cm}^3$
C_{DM}	Cation concentration of the diluate at the cation selective membrane	$\text{g-mole}/\text{cm}^3$
δ	Depth of diffusion boundary	cm
i_C	Current carried by the cation	Amp = coulomb/sec
i_{WS}	Current carried by water splitting	Amp
F	Faraday	96,500 coulomb/g-
i_T	Total current	
OH_{DM}	Hydroxide concentration at the diluate membrane	$\text{g-mole}/\text{cm}^3$
OH_{DB}	Hydroxide concentration in the bulk diluate stream	$\text{g-mole}/\text{cm}^3$
H_{CB}	Hydronium concentration of the concentrate in the bulk solution	$\text{g-mole}/\text{cm}^3$
H_{CM}	Hydronium concentration of the concentrate at the cation selective membrane	$\text{g-mole}/\text{cm}^3$
C_{CB}	Cation concentration of the concentrate in the bulk solution	$\text{g-mole}/\text{cm}^3$
C_{CM}	Cation concentration of the concentrate at the cation selective membrane	$\text{g-mole}/\text{cm}^3$
V_T	Voltage total all contributions (stack potential)	Joules/coulomb
V_E	Electrochemical voltage at the electrodes	Joules/coulomb
V_M	Voltage contribution by resistance across the structured membranes	Joules/coulomb
V_δ	Boundary layer resistance	Joules/coulomb
V_S	Voltage contribution by solution resistance across the electrolyte	Joules/coulomb
V_D	Voltage contribution by solution resistance across the diluate	Joules/coulomb
V_C	Voltage contribution by solution resistance across the concentrate	Joules/coulomb
V_O	Overvoltage (excess potential needed to initiate the electrode reactions)	Joules/coulomb
V_P	Voltage contribution by osmotic backpressure between the diluate and the	Joules/coulomb
W	Width of a cell pair	cm
W_E	Width of an electrode cell	cm
γ	Solution Conductivity	mS/cm
R	Universal Gas Law Constant	8.314 Joule/(°K g-
T	Temperature	°Kelvin
N_E	Number of electrode cells =2	dimensionless
N_{CP}	Number of membrane cell pairs	dimensionless

6.1.2 Components of the Total Stack Voltage and Total Current

The electrodialysis process removes salt from the diluate and transports it to the concentrate. For this purpose, the operator applies a potential that causes a DC current across a series of resistances. A relevant model must relate these outside observations, a total current and a potential across the stack, to a rate of salt transfer and the efficiency of salt transport. The development of the model begins by assigning the division of the total stack voltage (V_T) across all the resistances.

$$i_T \Omega_T = i_T (\Omega_E + \Omega_S + \Omega_D + \Omega_C + \Omega_\delta + \Omega_P + \Omega_O)$$

$$V_T = V_E + V_S + V_D + V_C + V_\delta + V_P + V_O$$

These potentials are required to

overcome the resistances associated with the chemical potential of the electrode reactions (V_E), the resistivity (inverse of conductivity) of the electrolyte solution (V_S), the resistivity of the diluate (V_D), the resistivity of the concentrate (V_C), the establishment of the diffusion gradients at the membrane surfaces (V_δ), the osmotic pressure gradient between the diluate and the concentrate (V_P), and the overvoltage (V_O). The overvoltage is included to account for difference in the minimum voltage required for initiation compared to the standard potential of the chemical reactions at the electrodes. All the associated resistances can be treated as a series resistance law. The derivation of the various voltages follows.

6.1.3 Boundary Layer Dynamics, Ion Flux and Water Splitting

Consider the diffusion of a monovalent cation (other than hydronium ion) near the cation selective membrane. The cation is forced to move from the diluate to the concentrate. On the diluate side, the diffusion gradient is written as the difference between the cation concentration in the bulk minus the concentration at the membrane ($C_{DB} - C_{DM}$) divided by the depth of the diffusion boundary, δ . On the concentrate side, the diffusion gradient ($C_{CM} - C_{CB}$) is written as the difference between the cation concentration at the membrane surface minus the cation concentration in the concentrate divided by the depth of the diffusion boundary. These two gradients must be equal in order to maintain equivalent ion flux across the membrane. By assuming that the depths of the boundary layer are equivalent on either side of the membrane, the ion flux can be related to the current (carried by the target cation).

$$i_C = \frac{D_C a}{\delta} F (C_{DB} - C_{DM}) = \frac{D_C a}{\delta} F (C_{CM} - C_{CB})$$

The membrane is indiscriminate to the passage hydronium ion along with the other monovalent cation. If the voltage is excessive, then water splits to form hydronium ion along the diluate side of the membrane. The bookkeeping for hydronium becomes complex. However, if hydronium ion is formed, then hydroxide also forms. The hydroxide must diffuse from the diluate side of the cation selective membrane back to the diluate stream. Therefore, the current carried by water splitting can be estimated based on the back diffusion of hydroxide. On the concentrate side, the transported hydronium ion must diffuse away from the membrane into the concentrate stream.

$$i_{WS} = \frac{D_{OH} a}{\delta} F (OH_{DM} - OH_{DB}) = \frac{D_H a}{\delta} F (H_{CM} - H_{CB})$$

The total current across the membrane is the sum of the current carried by water splitting and the target cation.

$$i_T = i_{WS} + i_C$$

The potential expended to maintain the gradient at the diluate side cationic membrane is

$$V_\delta = \frac{RT}{F} \ln \left(\frac{C_{DB}}{C_{DM}} \right) = \frac{RT}{F} \ln \left(\frac{OH_{DM}}{OH_{DB}} \right)$$

The potential expended to maintain the gradient at the concentrate side of the cationic selective membrane is

$$V_{\delta D} = \frac{RT}{F} \ln \left(\frac{C_{CM}}{C_{CB}} \right) = \frac{RT}{F} \ln \left(\frac{H_{CM}}{H_{CB}} \right)$$

Subject to the constraints imposed by charge neutrality:

$$C_{DM} = OH_{DM} + A_{DM}$$

$$C_{CM} + H_{CM} = A_{CM}$$

The total voltage expended across all the boundary layers is approximately equal to the twice the number of membranes in the system times the voltage at one boundary.

$$V_{\delta} = 4N_{CP}V_{\delta D}$$

6.1.4 Osmotic Potential

As the concentrations of ions in the diluate and the concentrate streams diverge, the net osmotic pressure creates a potential that must be overcome:

$$V_P = \frac{RT}{F} \ln \left(\frac{C_{CM}}{C_{DM}} \right)$$

6.1.5 Fluid conductivity

Conductivity is the ability of a fluid to transmit current and is conceptually the inverse of the fluid resistivity. In this study, conductivity (γ) is presented in milli-Siemen/cm (Note the term (1000) in the following equations corrects to Siemens/cm). There are three fluids of interest, the electrolyte (γ_E), the diluate (γ_D), and the concentrate (γ_C).

$$V_S = N_S \left(\frac{1000 W_E}{\gamma_S a} \right) i_T$$

$$V_D = N_{CP} \left(\frac{1000 W_{CP}}{\gamma_D 2a} \right) i_T$$

$$V_C = N_{CP} \left(\frac{1000 W_{CP}}{\gamma_C 2a} \right) i_T$$

Where W is the width of a membrane cell pair cell, W_E is the width of the electrode cell, N_S is the number of electrode cells =2, and N_{CP} is the number of membrane cell pairs.

6.1.6 Membrane Resistance

The membrane resistance (r) is supplied by the manufacturer as being about 2.5 ohm- cm². The voltage required to overcome the membrane resistance is:

$$V_M = \eta N_{CP} + 1 \frac{-\Omega_M}{a}$$

6.1.7 Electrode Resistance and Overvoltage

The present model uses a single value entry for the initiation voltage (see equations A1 and C1). This is set at 1.2 V in the model. Recent improvements in electrolyte chemistry provide an opportunity to improve this section of the model so that it may be predictive rather than the single value. An improvement to this section of the model is on-going and will be reported in Year 2 results. The overvoltage is used to calibrate the model.

$$V_e = 1.2$$

6.1.8 Model Logic

The model is initiated by assuming a voltage across a single diffusion boundary layer on a dilute side of a cationic selective membrane ($V_{\delta D}$). From this voltage, it is possible to estimate the boundary layer concentration of hydroxide ion and sodium ion. The boundary layer concentrations yields a calculation of the amperage attributed to water splitting and that attributed to sodium transport. The total amperage is then used to estimate the overall stack voltage. In this study, as will be seen in later sections, a total stack voltage is targeted to be 5V. The initial single boundary voltage is adjusted until the total stack voltage equals the desired set point. The amperage is then used to estimate the ion flux across all membranes. The nominal time period is ten seconds, which yields an estimate of the salt removed during the time increment. This salt mass is mathematically added to the concentrate volume and removed from the dilute volume.

The dilute and concentrate concentrations are then used to recalculate the amperage across the single boundary condition. This yields a voltage calculation across the boundary. A total stack voltage is recalculated. If the stack voltage is sufficiently deviant from the set point, an incrementally small change in the boundary voltage is made. This is equivalent to a constant voltage run.

6.1.9 Example Model Run

The following model inputs (Table 6) were used to generate an estimate for a 5V run with 10L of water at 3% initial NaCl concentration. The results are presented in Figure 7. These results represent a calibrated run based on observations of lab results.

Similar model runs were made prior to any lab data collection and represented a significant benefit to isolating various effects as either artifacts of the model, or artifacts of the operation of the ED stack. Most significantly, the energy efficiency (kWh/lb NaCl removed) was identified as a guiding factor in experimental design with a target to not exceed 0.1 kWh/lb NaCl. As seen in Figure 8, this goal was achieved by keeping the stack voltage of the pilot unit at 5V for a 3% NaCl simulation.

Another achievement attributed to the model development was the discovery of the sensitivity of the pilot ED stack to electrolyte chemistry. The model developed to the present

state represents a fair approximation of the art for treatment of low salt concentrations. As such, there was not any initial attempt to reflect electrolyte chemistry in the model. This allowed the development team to identify electrolyte chemistry as a fruitful area of research to garner improvements in process efficiency for high salt concentrations.

Table 6: Conditions for Example ED Model Run		
NaCl starting solution	3	%
pH diffusion coefficient salt	7	units
DNa diffusion coefficient hydroxide	2.00E-05	cm ² /sec
DOH diffusion coefficient hydroxide	8.00E-05	cm ² /sec
T Temperature of solution	25	°C
δ Boundary Layer estimate	0.0075	
a single membrane area	200	cm
N _p Number of stacks	10	cm ²
W Width of a cell pair (cm)	1.05	cm
electrode distance to membrane (cm)	0.5	cm
Volume Reservoir Dilute Side (L)	10	L
Volume Reservoir Concentrate (L)	10	L
low rate Dilute Side	50	cm ³ /sec
Flow rate Feed pump Dilute Side	50	cm ³ /sec
electrolyte conductivity	54	mS/cm
Resistivity of membrane	2	Ohm/cm2

6.2 Implications of the Model Solution

There are two challenges to the operation of electrodialysis for the desalinization of flowback water. One is the economic performance at extremely high salt conditions. The second is the high concentrations of calcium and other multivalent cations expected in the flowback water. The present discussion will focus on the first of these topics.

The electrodialysis process can be understood as a series of reactions, as described above. An applied voltage across an electrode pair causes an electrochemical reaction in the electrode cells. The chemical imbalance caused by the anode and cathode reactions drives ion flux across a series of membranes. The membranes are barriers that cause separation of a diluate stream from a concentrate stream. The flux of cations from the diluate stream to the cathode and from the anode into the concentrate stream; and the transfer of anions from the diluate to the concentrate; act as the electrochemical conduit required to continue the electrochemical reaction at the electrodes. More simply, the process can be described as an induced electrical current impeded by a series of resistances.

These concepts, as they apply to the pilot electrodialysis unit used in this study, were developed into a mathematical model. Model results will be used to illustrate salient points of experimental direction and process needs in the presence of extreme concentrations of sodium and divalent cations.

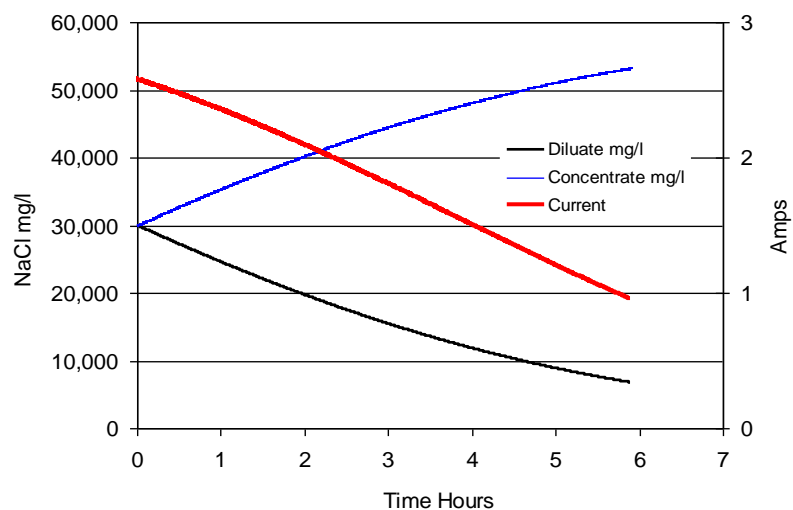


Figure 7: Simulated Pilot Performance for 3% NaCl

6.2.1 Meeting the Initial Energy Goals

The initial goal was to demonstrate that the electrodialysis process could work satisfactorily at a power utilization rate of between about 0.1 and 0.15 kWhr/lb salt transferred. For a first approximation, the computer simulation at 3% NaCl until the low end of the imposed limit was satisfied. These results demonstrated that if we operated the ED pilot unit at 5 V, then we would demand 1.04 kWhr/ lb NaCl. The following derivation from fundamental Faraday law interpretation is presented, herein, for completeness of the discussion.

Define:

$$\text{amp} = \frac{\text{coulomb}}{\text{sec}}$$

$$\text{Volt} = \frac{\text{Joule}}{\text{coulomb}}$$

$$\text{Faraday}(F) = \frac{96,500 \text{ Coulomb}}{\text{g - mole}}$$

$$\text{MW} = \frac{\text{g}}{\text{g - mole}} = 58.5 \text{ for NaCl}$$

$$\text{area} = \frac{200 \text{ cm}^2}{\text{cell pair}} \text{ for this pilot unit}$$

$$N_{CP} = 10 \text{ cell pairs for this pilot unit}$$

$$\text{kW} = \frac{\text{Volt} \times \left(\frac{\text{amp}}{\text{area}} \right) \times \text{area}}{1000 \left(\frac{\text{W}}{\text{kW}} \right)}$$

$$\frac{\text{lb NaCl}}{\text{hr}} = \frac{\frac{\text{amp}}{\text{area}} \times \text{area}}{F} \times \text{MW} \frac{\text{lb}}{454\text{g}} \times \frac{3600\text{sec}}{\text{hr}} \times N_{CP}$$

$$\frac{\text{kWhr}}{\text{lb NaCl}} = \frac{\text{Volt}}{1000} \left(\frac{96,500}{58.5} \right) \left(\frac{454}{3600} \right) \left(\frac{1}{10} \right) = 0.0208 \text{ Volt}$$

This derivation suggests this pilot plant should be operated at a stack potential of 5 V to approach 100% current efficiency and 0.104 kWh/lb NaCl transferred. The corollary to this proposition is that if more energy is required, then operation is < 100% current efficiency. Figure 8 shows the model prediction for the power requirements per mass salt removed 100% current efficiency versus applied voltage.

If a current efficiency is below 100%, this is usually blamed on the phenomenon of water splitting. However, the present operating conditions are far from salt concentrations that reflect the limiting current. Therefore, other reasons for loss of current efficiency must be investigated. One likely factor is the loss of water from the diluate to the concentrate caused by osmotic pressure. Other areas of interest may be interference by multivalent cations, or loss of electrode efficiency through electrode fouling.

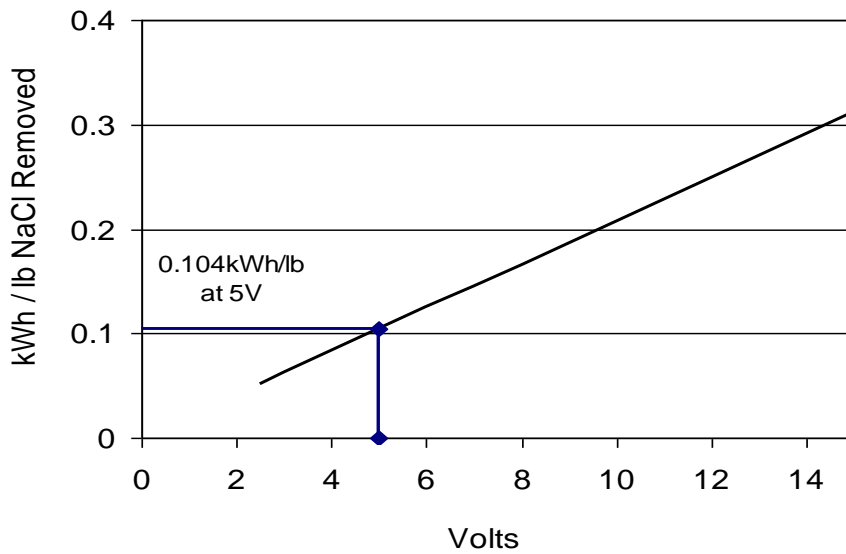


Figure 8: Predicted Power Requirements per Pound NaCl Removed with 100% Current Efficiency

6.2.2 Improvements for Extremely Concentrated Salt Solutions

In typical operation of electrodialysis, the process encounters salt concentrations of several thousand mg/l TDS with the treatment goal to about 500 mg/l. In the flowback water, the expected median concentration (on day 5 from the fracture) to be in the range of 60,000 – 70,000 mg/l, with the need to treat to about 10,000 mg/l. This represents water 10-15 times as concentrated as normally used in the ED process. This would suggest that the various resistances encountered in the ED process will be shifted, compared to conventional usage. Examination of these resistances should yield some interesting areas for process improvement.

The following four figures (Figures 9-12) are computer simulations of the relative resistance expected within the pilot plant stack under various conditions. These demonstrate that the relative resistances within the stack are constantly changing between the initial conditions and the final process. These also demonstrate that the relative resistances encountered under low salt conditions are different than encountered with extremely concentrated salt.

Figure 9 shows the relative voltage drops expected for initial conditions at 5,000 mg/l NaCl, where the diluate and the concentrate concentrations are equal. Under these conditions, there is no resistance due to osmotic pressure between the concentrate and the diluate. The resistance due to the concentrate stream and the diluate stream are equal. It is likely that at the conditions described, the unit would be driven at 10-15 Volts in an effort to increase ion flux. At these conditions; the major resistances are: concentrate solution = diluate solution > overvoltage/electrode > diffusion boundary > membrane > electrolyte solution.

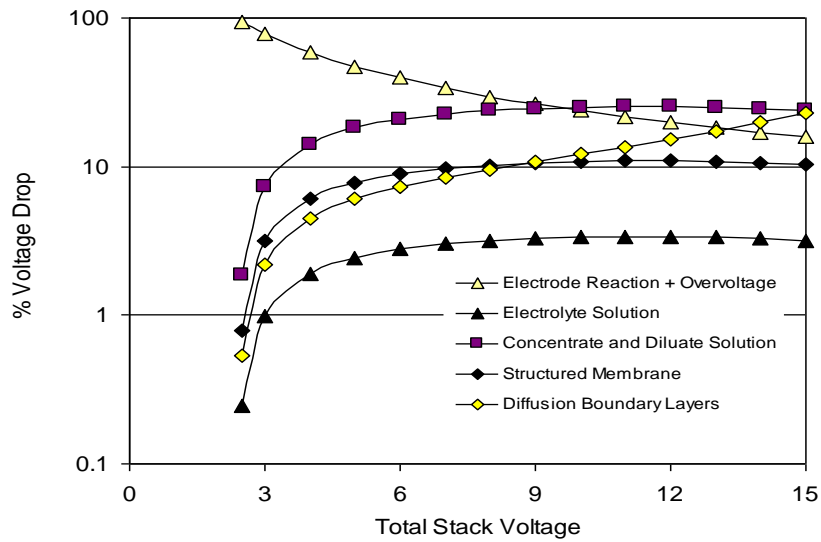


Figure 9: Model Simulation: Relative Voltage Drop for Initial Conditions At Start of run (Concentrate = Diluate) at 5000 mg/l NaCl

Figure 10 shows the relative voltage drops expected at the point where 80% of the salt has been transferred from the diluate to the concentrate for initial conditions at 5,000 mg/l NaCl. There is considerable resistance due to osmotic pressure between the concentrate and the diluate. The resistance due to the concentrate stream and the diluate stream are unequal. Note that the unit is virtually un-operable at less than about 3.5 Volts. It is likely that at the conditions described, the unit would be driven at 10-15 Volts in an effort to increase ion flux. At these conditions; the major resistances are: diffusion boundary > diluate solution > overvoltage/electrode > osmotic pressure > concentrate > membrane resistance > electrolyte solution. Compared to Figure 9, Figure 10 demonstrates that toward the end of the process, the importance of the various resistances has changed.

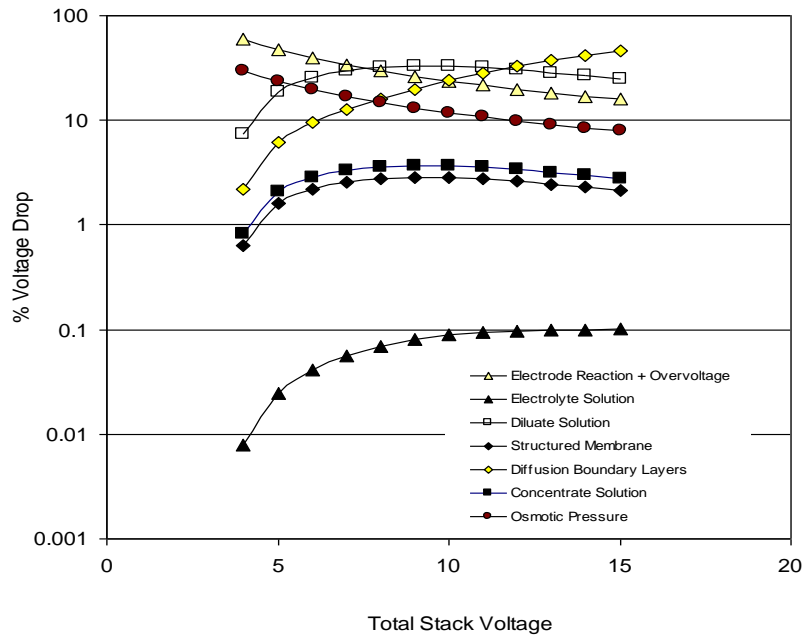


Figure 10: Model Simulation of the Relative Potential Drop At 80% Transfer

(Concentrate 1,000; Diluate = 9,000) with Initial = 5,000 mg/l NaCl

Figure 11 is a computer simulation of the relative stack resistances under extremely high initial salt concentrations at 50,000 mg/l NaCl. At the start of the process, the diluate and the concentrate concentrations are equal. Under these conditions, there is no resistance due to osmotic pressure between the concentrate and the diluate. The resistance due to the concentrate stream and the diluate stream are equal. It is likely that at the conditions described, the unit would be driven at 5 Volts in an effort to minimize the power. At these conditions; the major resistances are: overvoltage/electrode > membrane > electrolyte > concentrate solution = diluate solution > diffusion boundaries. It is telling the resistance from the electrolyte represents 10-11% of the overall resistance at high salt concentrations (Figure 11), but only 3% of the overall resistance at low salt concentrations (Figure 9).

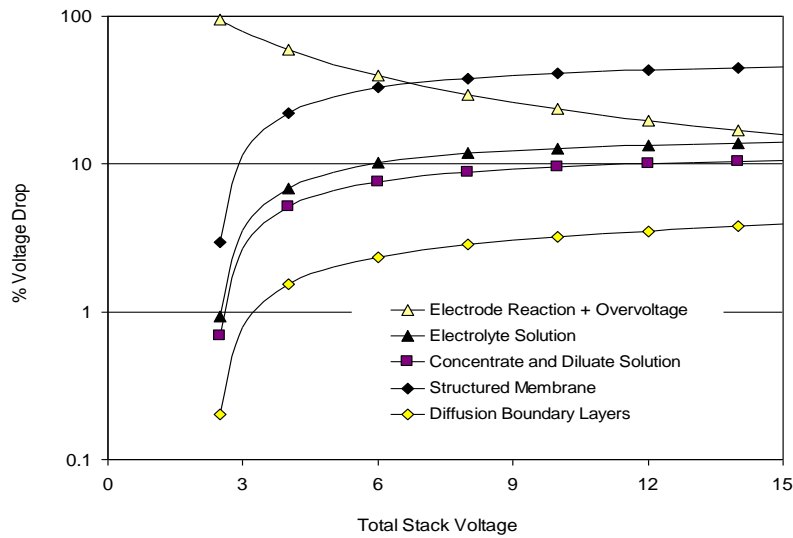


Figure 11: Model Simulation of the Relative Potential Drop

At Start (Concentrate = Diluate) with 50,000 mg/l NaCl

Figure 12 shows the relative voltage drops expected at the point where 80% of the salt has been transferred from the diluate to the concentrate for initial conditions at 50,000 mg/l NaCl. There is considerable resistance due to osmotic pressure between the concentrate and the diluate. The resistance due to the concentrate stream and the diluate stream are unequal. Note that the unit is virtually un-operable at less than about 3.0 Volts. It is likely that at the conditions described, the unit would be driven at 5 Volts in an effort to optimize the mass of salt transferred per kilowatt expended. At these conditions; the major resistances are: overvoltage/electrode > osmotic pressure > diluate solution > membrane > osmotic pressure > diffusion boundary > electrolyte solution > concentrate solution. Compared to Figure 12, Figure 9 once again demonstrates that toward the end of the process, the importance of the various resistances has changed.

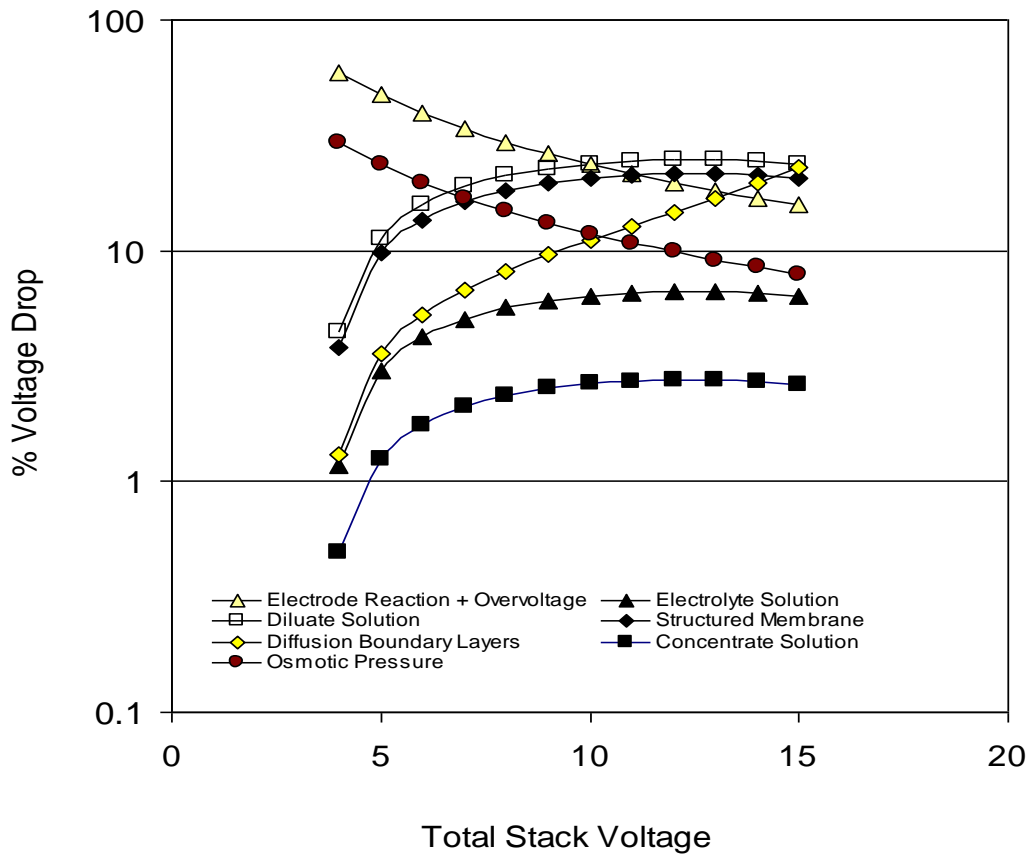


Figure 12: Model Simulation of the Relative Potential Drop At 80% Transfer (Concentrate 10,000; Diluate = 90,000); Initial = 50,000 mg/l NaCl

In summary of these four figures, it is evident that the influences of the various resistances to ion flux are different magnitudes and relative orders that with low salt concentrations. Given that the mechanical structure pilot unit is fixed, there is a limited range of opportunity to improve the process short of improvements to the chemistry of the electrolyte. However, since we are operating in such a different performance landscape, it is little wonder that there is little supportive literature for guidance on treating highly concentrated brines with electrodialysis. For example, a recent review of 64 current articles on the state of the art for ED processes (Xu and Huang, 2008) does not mention any examples of work on electrolyte chemistry.

6.3 Adaptation of Arrhenius Equation for Electrodialysis

Electrodialysis presents an unique situation where the ion flux from a diluate stream to a concentrate stream, is controlled by reactions or diffusion occurring at two different temperatures. With pure salt water i.e. NaCl, and with pure electrolyte, ie Na₂SO₄, the ion flux is directly proportional to the amperage. When the water concentration is elevated, and the stack is operated at voltages less than the limiting current, then the current efficiency approaches 100% and the ion flux can be calculated from the amperage.

6.3.1 Nomenclature

T_w = temperature of the salt water, °K

T_e = temperature of the electrolyte, °K

i_{Tw} = amperage when water temperature varies, electrolyte temperature constant

i_{Te} = amperage when electrolyte temperature varies, water temperature varies

i = amperage when electrolyte and water temperature have any temperature

E_w = Activation energy for the salt diffusion in the water solution

E_e = Activation energy for the electrolyte reaction

E = Activation energy for the overall reaction

R = universal gas law constant

C_{303} = Arrhenius coefficient, electrolyte held constant $T_e = 303^\circ\text{K}$ (amps)

B_{281} = Arrhenius coefficient, water held constant $T_w = 281^\circ\text{K}$ (amps)

A = Arrhenius coefficient (amps)

Equations 1, 2 and 3 define the general format for the Arrhenius temperature dependency for the general condition, a specific case where the temperature of the water is constant at 281 °K, and a second specific case where the temperature of the electrolyte is constant at 303 °K.

$$1) i = Ae^{-E/RT}$$

$$2) i_{T_w=281} = B_{281} e^{-E_e/RT_e}$$

$$3) i_{T_e=303} = C_{303} e^{-E_w/RT_w}$$

Equation 4, 5, and 6 expresses the logarithmic transform of Equation 1, 2, and 3. Arrhenius temperature dependency is demonstrated as a linear relation between natural logarithm of the reaction rate (vis. Amperage) versus the inverse temperature.

$$4) \ln(i) = \ln(A) - \frac{E}{RT}$$

$$5) \ln(i_{T_w=281}) = \ln(B_{281}) - \frac{E_{T_e}}{RT_e}$$

$$6) \ln(i_{T_e=303}) = \ln(C_{303}) - \frac{E_{T_w}}{RT_w}$$

As will be seen in the results section, Arrhenius linearity for equations 4, 5, and 6 can be verified experimentally. It is inferred from the results that values of B would differ if the temperature of the water was held constant at some other value than 281°K; likewise values of C would differ if the temperature of the electrolyte was held constant at some other temperature than 303 °K. More general temperature dependencies for the electrode and the stack are developed in Equations 7 and 8, where B_{Te} and C_{Tw} are temperature dependent.

$$7) i_{T_w} = B_{T_e} e^{-E_w/RT_w}$$

$$8) i_{T_e} = C_{T_w} e^{-E_e/RT_e}$$

In these experiments, the amperage is solely a function of the temperatures in the electrolyte and in the water. The temperature dependency of C_{T_w} is, therefore, deduced from Equation 2. Likewise, the temperature dependency of B_{T_e} is deduced from Equation 3. The constants C^* and B^* are introduced as temperature independent constants.

$$9) C_{T_e} = C^* e^{-E_e / RT_e}$$

$$10) B_{T_w} = B^* e^{-E_w / RT_w}$$

Equations 11 and 12 show the general cases

$$11) i_{T_w, T_e} = B^* e^{-E_w / RT_w} e^{-E_e / RT_e}$$

$$12) i_{(T_w, T_e)} = C^* e^{-E_e / RT_e} e^{-E_w / RT_w}$$

By definition, B^* and C^* are temperature independent. By virtue of the specific case, defined, by Equation 1, where $T_w = T_e$, it follows that an identity exists in which:

$$13) B^* = C^* = A$$

7 RESULTS

During the test period, a number of problems were encountered. Literature suggests that these problems historically impeded development of electrodialysis for complex solutions of concentrated divalent cations. As these problems were encountered in this project, they were addressed by making a number of improvements to the electrodialysis process specific to this laboratory unit. Some of these improvements represent potentially scalable means for cost savings. Others of these improvements represent critical changes needed to keep the electrodialysis unit operational.

Range of Operation: In an effort to control the electrical costs of the process, an arbitrary limit of 0.1-0.15 kWhr/lb was imposed. Tests with sodium chloride confirmed the limit could be achieved.

Electrolyte Chemistry: The chemistry of the electrolyte solution was investigated as a means of improving the rate of salt transfer at the desired energy limit. Improvements yield increases in process rate.

Effects of Calcium on Electrodialysis: The adverse role of calcium on duration of a process run were expected, and demonstrated.

Mitigation of the Effects of Calcium with Cathode Protection: The effect of a single membrane change at the cathode barrier was investigated as a means to mitigate the effects of calcium.

1. **Mechanism of Calcium Interference:** The protected cathode had surprising resilience to deliberate calcium additions.
2. **Effect of Multivalent Cations:** The effect of barium, magnesium, and iron were investigated.

Clean-in-Place Pulsed Pole Reversal (CIP-PR): A concept for cleaning residual multivalent cations from the electrolyte on a pulsed basis was investigated.

Samples from the Barnett and the Marcellus: Raw samples from the field, two each from the Barnett and the Marcellus, were pretreated for trial on the electrodialysis unit.

Treatment of Field Samples; with and without CIP-PR: Eleven tests with water from the field sample were performed. CIP-PR was shown to increase the rate of the process.

Effect of Temperature: The electrodialysis process poses a unique opportunity to take advantage of improved current capacity with increased operating temperature.

Estimated Capital and Operational Costs: Eurodia provided a set of economic projections for specific treatment objectives representing a range of potential field conditions.

Electrodialysis runs (Test-A-E, I, J, and M) were performed with sodium chloride (Table 7). Tests F-H define the problems associated with soluble calcium in the test water in tests with sodium and calcium chloride. These tests were performed with the original membrane at the cathode barrier. Tests J-O represent the operation of the unit with the cathode barrier membrane changed to a multivalent selective membrane change designed to mitigate the effect of calcium incursion into the catholyte. Tests were also performed with a range of electrolyte formulas, as indicated in the table.

Table 8 is a summary of the full electrodialysis runs with complex chloride salts including sodium, magnesium, calcium, barium, and iron. In general, these tests demonstrated an

increasing difficulty in maintaining operation in the presence of these complex salts. Test X is a special case using a clean-in-place pulsed pole reversal to mitigate the effects of the multivalent cations.

Table 9 is a summary of tests performed with water from field sites. Tests labeled TD (Taylor Dooley #3) and MS (Maggie Spain) are from the Barnett shale formation. Sample MSD is the Maggie Spain sample diluted with tap water. Samples MUL (Marcellus unlabeled) and Mca (received labeled Mcadoo) are from the Marcellus shale formation. These samples presented problems, to varying degree, from the complex cation content. The response to the problem was the development of the clean-in-place pulsed pole reversal method (CIP). Tests performed with the CIP are designated with an asterisk (*).

Supplemental data were collected as volt-amp profiles. These were conducted by recording the current generated at set voltages of 2-15 volts. These data are presented throughout the results section, as needed to emphasize particular concepts.

Table 7: Summary of 15 Electrodialysis Runs with Sodium and Calcium Chloride

Test	TDS mg/l			Hours	Amps			kWh/ lb	NaCl %	Ca ⁺⁺ mg/l	Electrolyte g/L			Cathode Membrane
	Start	End	End		Start	Finish	Avg.				Na ₂ SO ₄	NaOH	Na ₂ HPO ₄	
A	31,000	3,000	64,400	6.8	2.30	1.80	1.66	0.099	3	0	90	1		CMX
B	28,500	3,100	46,200	7.3	1.75	1.07	1.46	0.107	3	0	30			CMX
C	31,500	2,000	48,800	6.6	2.15	1.08	1.67	0.104	3	0	90			CMX
D	31,000	4,750	49,300	6.0	2.32	1.79	2.09	0.1077	3	0	90	1		CMX
E	29,600	4,750	50,000	7.5	2.33	1.10	1.59	0.1048	3	0	60	2.2	30	CMX
F	43,500	23,500	65,000	7.6	1.93	1.13	1.50	0.1111	3	4,000	90	1		CMX
G	33,000	6,000	56,600	7.5	2.09	1.24	1.64	0.1064	3	1,000	90	1		CMX
H	67,500	50,500	93,000	7.5	2.76	1.43	1.74	0.132	6	4,000	120	1		CMX
I	58,000	10,000	83,200	9.3	2.84	1.83	2.50	0.134	6	0	120	1		CMX
J	31,500	3,200	52,600	6.0	2.24	1.26	1.88	0.111	3	0	90	1		CMX-S
K	41,500	9,500	52,600	8.0	2.24	1.60	2.03	0.12	3	4,000	90	1		CMX-S
L	64,000	36,400	88,300	8.5	2.5	2.28	2.44	0.137	6	4,000	120	1		CMX-S
M	30,100	3,000	49,700	6	2.47	1.09	1.93	0.109	3	0	90			CMX-S
N	39,800	7,000	68,000	8.5	2.13	1.56	1.98	0.118	3	4,000	90			CMX-S
O	39,800	6,200	76,000	8.0	2.07	1.98	1.67	0.119	3	4,000	90			CMX-S

Table 8: Summary of 7 Electrodialysis Runs with Complex Chloride Salts in 3% NaCl

Test	TDS mg/l			Hours	Amps			kWh/ lb	NaCl %	Ca ⁺⁺ mg/l	Mg ⁺⁺ mg/l	Ba ⁺⁺ mg/l	Fe ⁺⁺⁺ mg/l	Cathode Membrane
	Start	End	End		Start	Finish	Avg.							
Q	35,560	10,120	60,790	6.5	2.08	1.78	2.07	0.129	3	56	530	5	1	CMX-S
R	42,500	22,100	65,070	6.3	2.11	1.70	1.97	0.127	3	3,200	500	360	17	CMX-S
S	41,400	25,400	58,070	6.6	1.83	1.62	1.73	0.145	3	3,100	440	160	50***	CMX-S
T	40,800	21,000	57,100	7.8	2.16	1.10	1.69	0.136	3	2,500	550	370	64	CMX-S
U**	41,100	27,800	53,270	7.1	1.99	0.57	1.55	0.131	3	3,500	380	400	64	CMX-S
V	37,600	21,960	49,900	7.1	1.61	1.16	1.35	0.131	3	3,200	350	330	35	CMX-S
X*	38,300	19,300	53,000	5.5	1.71	1.24	1.50	0.129	3	2,600	470	260	36	CMX-S

All electrolyte solutions 90 g/l Na₂SO₄; * Clean-in-Place Pulsed Pole Reversal; **Reference for test X ***iron precipitated in feed tanks

Table 9: Summary of 11 Electrodialysis Runs with Field Samples from Barnett and Marcellus

Samples from the Barnett															
MS =Maggie Spain, MSD = Maggie Spain Diluted, TD = Taylor Dooley #3															
Test	TDS mg/l			Hrs	Amps			kWh/ lb	Na+ mg/l	Ca ⁺⁺ mg/l	Mg ⁺⁺ mg/l	Ba ⁺⁺ mg/l	Fe ⁺⁺⁺ mg/l	Cl- mg/l	SO ₄ ⁻² mg/l
	Start	End	End		Start	Finish	Avg.								
MS	44,600	34,500	56,500	6.0	1.85	0.51	1.01	0.131	15,000	2,100	270	22	24	29,000	216
MS*	43,600	26,960	51,900	6.0	1.77	0.93	1.22	0.131	13,000	2,000	350	16	32	31,000	147
MSD	25,000	9,500	38,000	7.5	1.45	0.94	1.17	0.111	7,600	1,100	150	3	12	15,000	78
MSD*	25,800	10,000	40,100	7.5	1.50	0.97	1.29	0.115	7,600	1,100	150	4	12	16,000	82
MSD*	28,000	9,270	47,100	7.5	1.56	1.14	1.41	0.127	7,900	1,100	160	4	13	16,000	70
TD	52,700	29,340	65,400	6.0	2.00	0.79	1.30	0.109	14,000	2,600	470	40	31	31,000	51
TD*	52,900	36,900	63,100	6.0	1.54	1.04	1.26	0.109	16,000	3,100	580	40	50	38,000	46
Samples from the Marcellus															
MUL = unlabeled site, Mca = labeled Mcadoo															
	TDS mg/l			Hrs	Amps			kWh/ lb	Na+ mg/l	Ca ⁺⁺ mg/l	Mg ⁺⁺ mg/l	Ba ⁺⁺ mg/l	Fe ⁺⁺⁺ mg/l	Cl- mg/l	SO ₄ ⁻² mg/l
	Start	End	End		Start	Finish	Avg.								
MUL	30,600	27,300	38,500	6.5	1.52	0.19	0.43	0.11	17,300	6,100	550	57	27	38,000	20
MUL*	30,200	25,100	39,700	6.5	1.53	0.60	0.60	0.122	16,500	5,400	500	52	25	39,000	21
Mca	43,000	32,100	55,250	6.5	2.01	0.48	1.28	0.148	11,000	3,600	310	19	23	26,000	50
Mca*	43,300	33,750	60,100	6.5	1.99	0.55	1.26	0.119	12,000	3,600	290	15	17	27,000	33
All testswith CMX-S cathode boundary membrane															
All electrolyte solutions 90 g/l Na ₂ SO ₄ ;															
* Clean-in-Place Pulsed Pole Reversal															

7.1 Range of Operation

The energy used to transfer a given mass of salt is an important economic consideration when dealing with high brine concentrations. For the present discussion, an arbitrary energy utilization rate of 0.1 - 0.15 kWh/lb NaCl transferred was established.

Figure 8 (see previous section) shows the predicted energy utilization generated from the computer simulations with 3% NaCl over a range of stack voltage. The following relation between energy utilization and applied voltage (for a 10 cell stack) and 3% NaCl is readily obtained for systems where ion transfer is >99% efficient, as typically occurs when operating well below the “limiting current”. The model predicts that a target voltage of 5.0 will produce the desired energy efficiency of 0.104 kWh/lb NaCl removed.

A series of six full runs (six hours or more duration at 5V stack potential) were performed starting at 3% NaCl and an additional three tests were performed with 3% NaCl plus additional TDS (total dissolved solids) as CaCl₂, achieving more than 90% NaCl transfer from the diluate to the concentrate. Energy efficiencies were calculated and presented in Table 10. The average energy utilization rate was 1.07 ± 0.07 kWhr/lb. This is in excellent agreement with the predicted value of 0.104 kWhr/lb, and is given as evidence that the current efficiency in this system approaches 100% under ideal conditions. Based on these observations, the target voltage for the pilot plant was established at 5.0 volts.

Run Number	Diluate Start TDS mg/l	Diluate End TDS mg/l	NaCl %	CaCl ₂ %	Duration Hours	Efficiency kWhr/lb
A	31,000	3,000	3		6.8	0.099
B	28,500	3,100	3		7.3	0.107
C	31,500	2,000	3		6.6	0.104
D	31,000	4,750	3		6.0	0.108
E	29,600	4,750	3	0.3	7.5	0.104
F	43,500	23,500	3	1.1	7.6	0.101
G	33,000	6,000	3		7.5	0.106
J	31,500	3,200	3		6.0	0.114
K	41,500	9,500	3	1.1	8.0	0.120
Average						0.107
Std. Dev.						0.007

7.2 Electrolyte Chemistry

Improvements to the chemistry of the electrolyte followed three topic areas:

- Effect of electrolyte concentration
- pH of electrolyte solution
- buffering the electrolyte

7.2.1 Effect of electrolyte concentration

The pilot plant manufacturer recommended that an electrolyte solution of about 30 g/L Na₂SO₄ should suffice for an adequate treatment rate for a 3% salt solution. Theoretical examples presented in Figures 9-12 suggest that significant resistance exists in the electrolyte cell. A series of tests with electrolyte chemistry ensued to reduce this resistance.

Figure 13 shows a Volt-Amp profile with different strengths of electrolyte. In performing a Volt-Amp profile the concentration of salt in the feed tank and in the concentrate tank were roughly equivalent (3% NaCl) and represented salt distributions similar to the the starting conditions for an ED run. The voltage of the power supply was systematically reduced from the maximum recommended 15 V (1.5 V per cell). The current was measured at each voltage increment until no current was detected. In this series, the pH of the electrolyte was about 7.3 units. The conventional solution for electrolyte was represented as a solution of 30 g/l Na_2SO_4 , as recommended by the pilot plant manufacturer. Increasing the electrolyte concentration to 60 g/l and again to 90 g/l had the effect of increasing the system amperage, indicating that there was significant resistance to ion transfer operating at high salt concentrations. Naturally, these same resistances also occur when treating water at low salt concentrations. However, they may have been previously overlooked at the low salt concentrations because they are not as strongly manifested as are other resistances. This significant discovery has direct impact on the predicted rate of ion transfer for a given stack area. Additionally, the improved amperage at a given voltage means that less surface area is needed to achieve the same ion transport flux.

A significant observation from Figure 13 is the position of the intercept on the voltage axis. No current was measured at a voltage of less than about 2.4 V. This represents the minimum voltage to initiate the reactions at the electrode and is presented as the electrode potentials plus “overvoltage”. Therefore, the minimum voltage for a neutral pH electrolyte, such as sodium sulfate, is about 2.4 V.

7.2.2 Electrolyte pH

The use of sodium hydroxide in electrolytes for complex brines with high concentrations of iron was ultimately abandoned due to the potential for precipitation of iron within the electrode cells. The results are presented, herein, for completeness. The information may have utility for waters not heavily concentrated with iron.

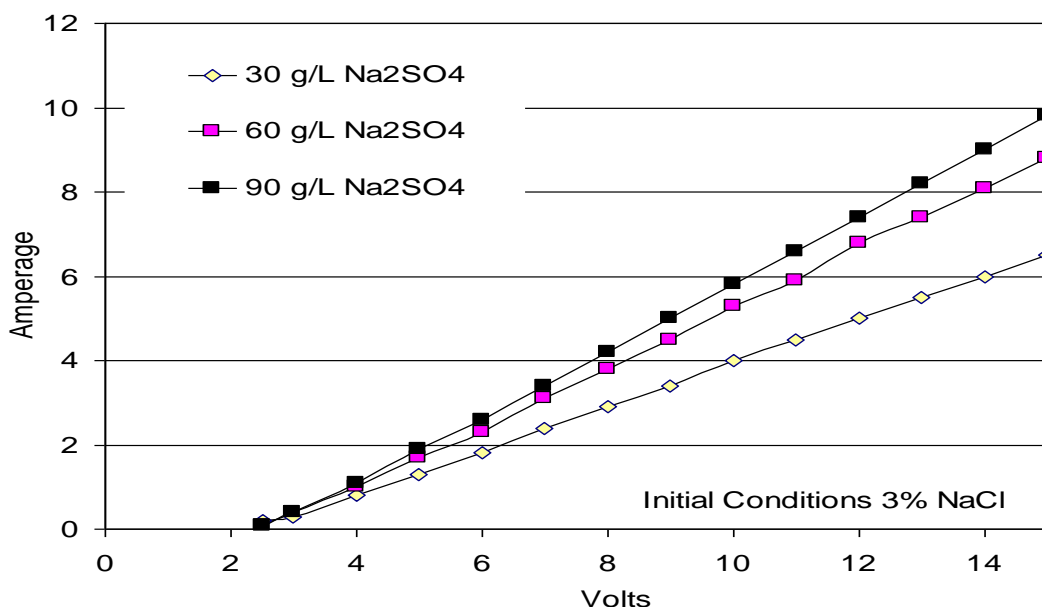


Figure 13: Effect of Electrolyte Concentration on Initial Current Density in 3% NaCl

Another series of experiments focused on the pH of the electrolyte solution. The specific tests performed were with 1) 30 g/l Na₂SO₄ with 0.5 g/l NaOH, 2) 30 g/l Na₂SO₄ + 1 g/l NaOH, 3) 60 g/l Na₂SO₄ + 1 g/l NaOH and 4) 90 g/l Na₂SO₄ + 1 g/l NaOH. The feed and concentrate tanks contained 3% NaCl solution. This provided sufficient hydroxide to increase the pH of the electrolyte from about 7.3 to between 11.5 and 12.4 pH units.

Figure 14 shows that even a small amount of sodium hydroxide added to the electrolyte (Na₂SO₄) caused improved amperage throughout the entire range of applied voltage potential. Furthermore, as the amperage nears zero, the minimum voltage required shifted downward from about 2.4 V range to about 2.0 V. This finding suggested that a fundamental mechanistic change in the reaction at the electrodes had occurred that was not seen at neutral pH.

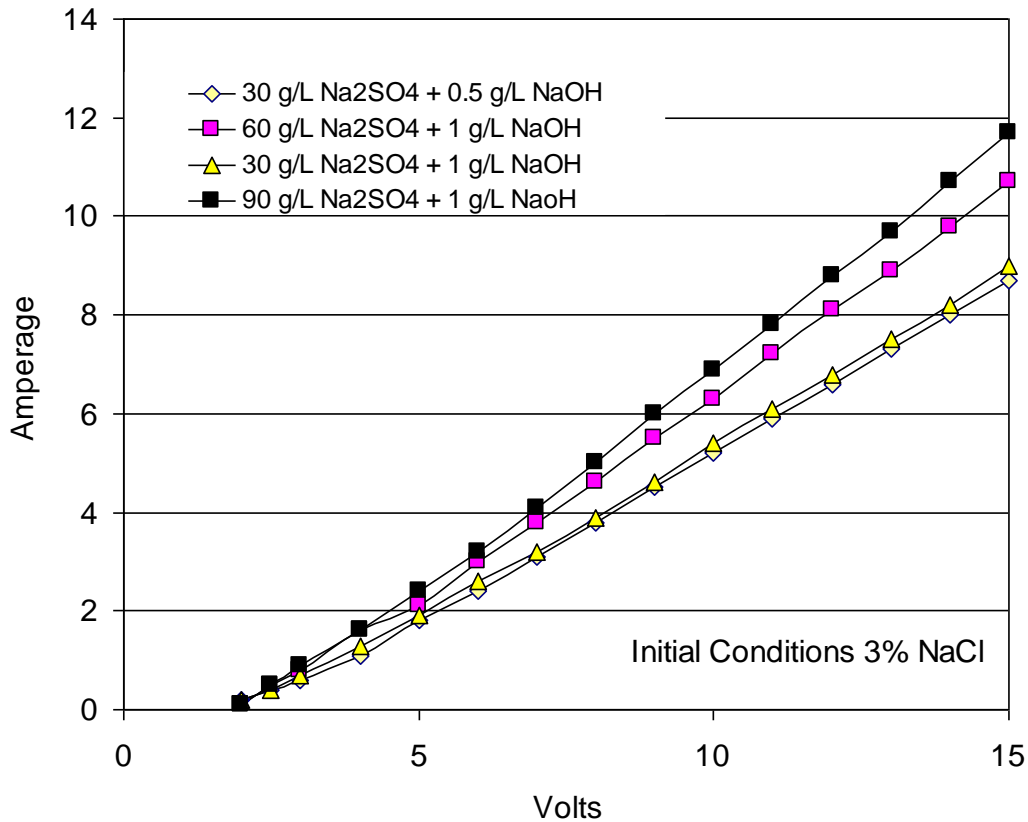
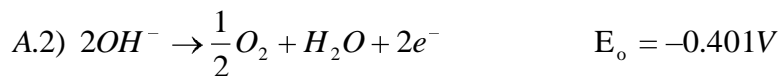


Figure 14: Effect of Sodium Hydroxide Addition on Electrolyte Performance

One potential mechanistic explanation for the shift in required overvoltage was that the high pH in the electrolyte had the effect of “feeding the anode” with hydroxide. Referring once again to Equation A2;



The free hydroxide needed to make the majority of oxygen at the anode from hydroxide (as opposed to water, see Equation A1) can be estimated. If the flow of electrolyte to the anode is Q(liters/sec), the amperage is i(amps), and F is the Faraday constant (96,500 coulomb/mole),

then the concentration change in free hydroxide between the influent and the effluent , ΔOH^- (mole/Liter), is expressed in Equation G1:

$$G1) \Delta\text{OH}^- \cong \frac{i}{FQ}$$

For an anolyte flow of 1 liter/minute (0.0167 L/sec) and a current of 2.5 amps, the destruction of free hydroxide is about 0.00155 mole/Liter. If the oxygen generation is to occur without significant water splitting, (Equation A2 predominates over A1) then the pH of the electrolyte entering the anode cell should exceed pH of about 11.2. However, the reaction occurs at the electrode surface, not in the bulk solution. It is therefore reasonable to require additional free hydroxide ion in the bulk solution to overcome diffusion resistance at the fluid boundary of the anode.

A series of three full runs was performed with 3% NaCl that further demonstrate the benefits of improved electrolyte chemistry. Figure 15 (Test B) shows treatment with the standard electrolyte consisting of 30 g/l Na_2SO_4 . Figure 16 (Test C) shows treatment with 90 g/l Na_2SO_4 electrolyte. Figure 17 (Test D) shows treatment with 90 g/l Na_2SO_4 plus 1 g/l NaOH.

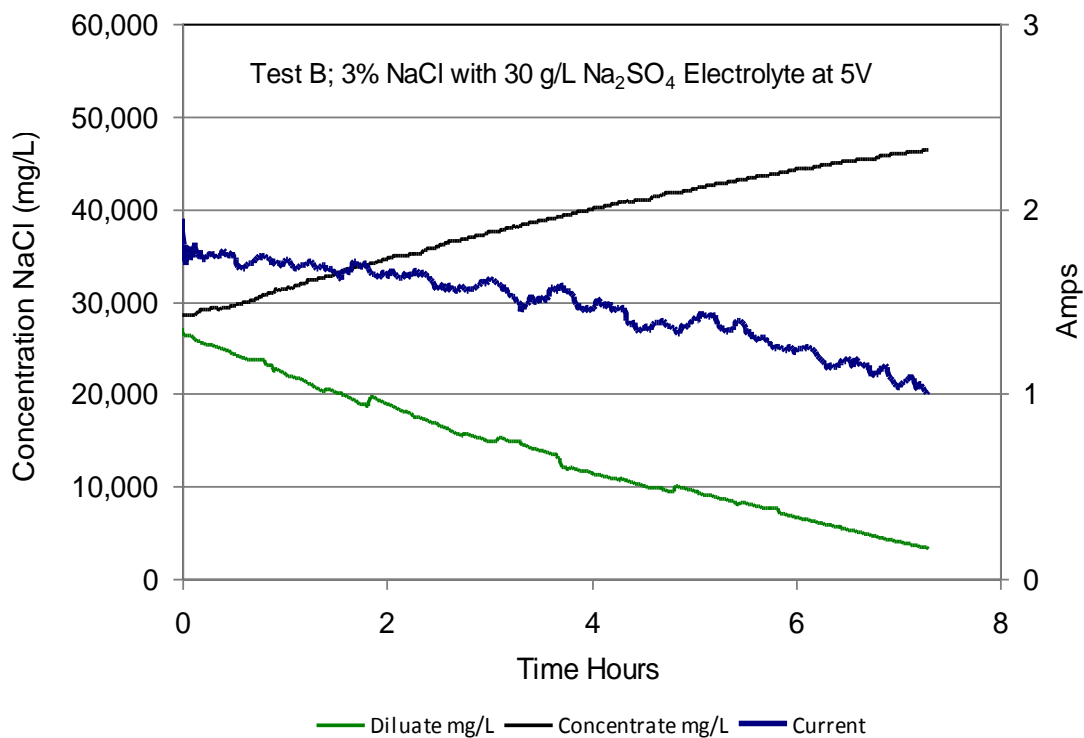


Figure 15: 3% NaCl with 30 g/l Disodium Sulfate Electrolyte

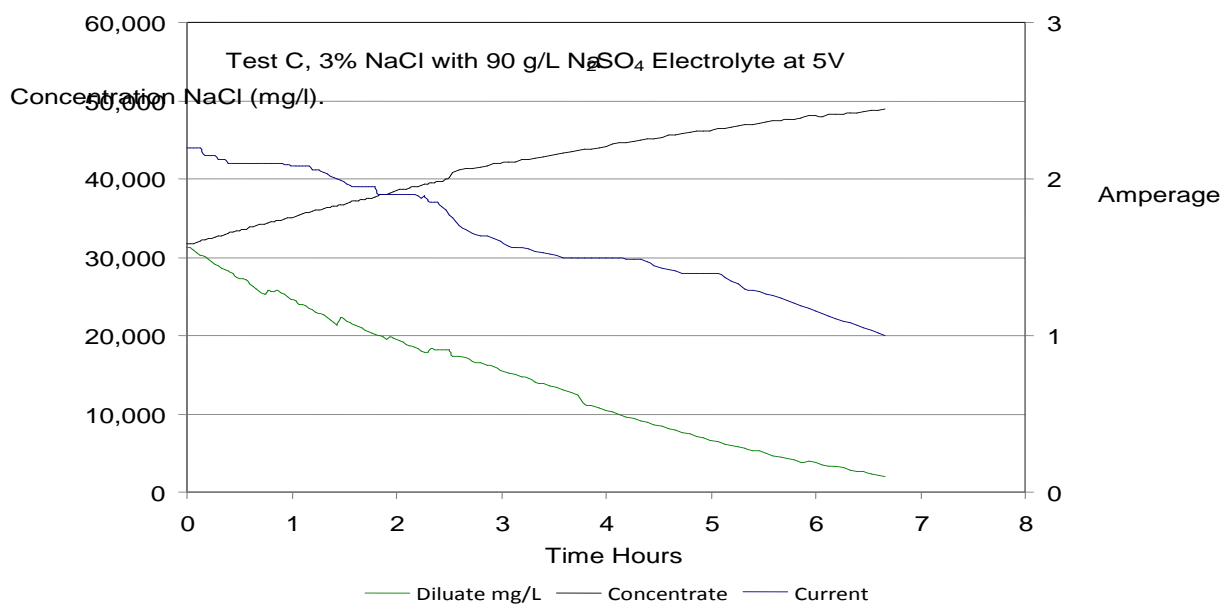


Figure 16: 3% NaCl with 90 g/l Disodium Sulfate Electrolyte

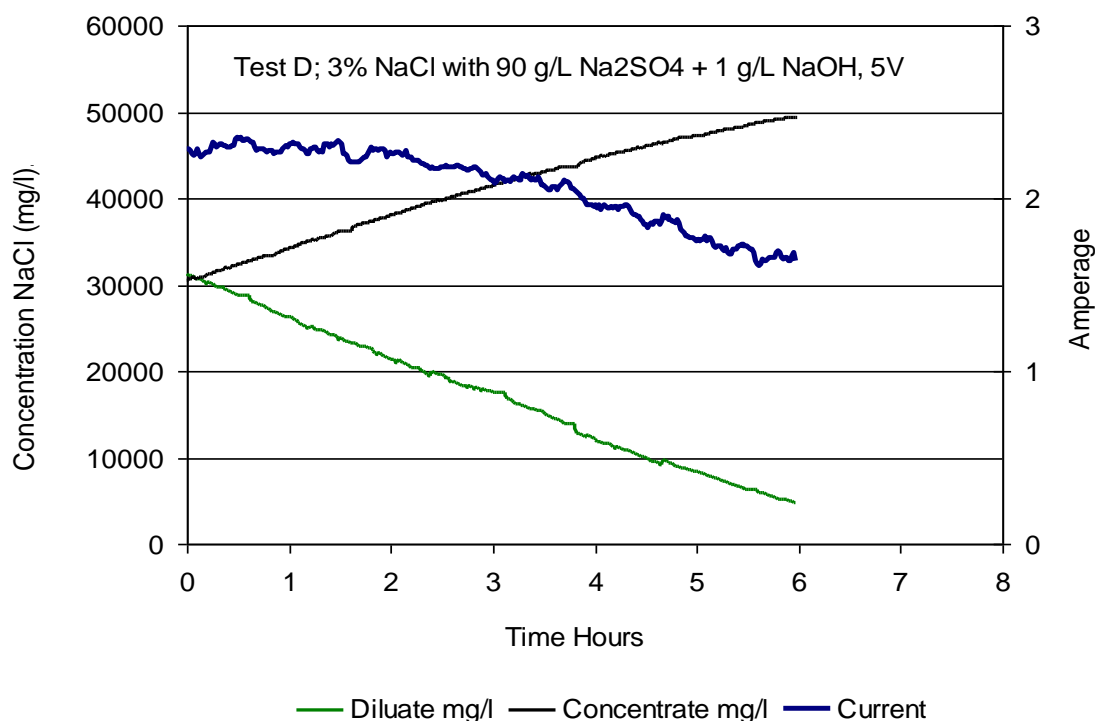


Figure 17: 3% NaCl with 90 g/l Disodium Sulfate + 1 g/l NaOH in the Electrolyte

Table 11 is a summary of results from Figures 15, 16, and 17. As described in Figure 8 and Table 10; a comparison of current is a useful and appropriate proxy for ion flux when the current efficiency approaches 100%. As seen in Table 11, the current at 5V stack potential improves with incremental improvement of the electrolyte chemistry. This trend is evident at the beginning of each run, at the end of each run, and as reflected by the average current throughout each run.

Test	Start NaCl mg/l	Finish NaCl mg/l	Hours	Amps Start	Amps Finish	Amps Avg.	kWh/lb	Na ₂ SO ₄ g/l	NaOH g/l
B	28,500	3,100	7.3	1.75	1.07	1.46	0.107	30	0
C	31,500	2,000	6.6	2.12	1.29	1.73	0.099	90	0
D	31,000	4,750	6.0	2.32	1.79	2.09	0.109	90	1

Figure 18 is a direct comparison of the average current in the three tests in this example. This figure depicts the conventional electrolyte as 100% ion flux. Increasing the electrolyte concentration improves the ion flux by 24% compared to standard electrolyte. Adding 1 g/l NaOH to the more concentrated electrolyte improves the ion flux by 43% compared to standard conditions. A summary of improvements is presented in Figure 23.

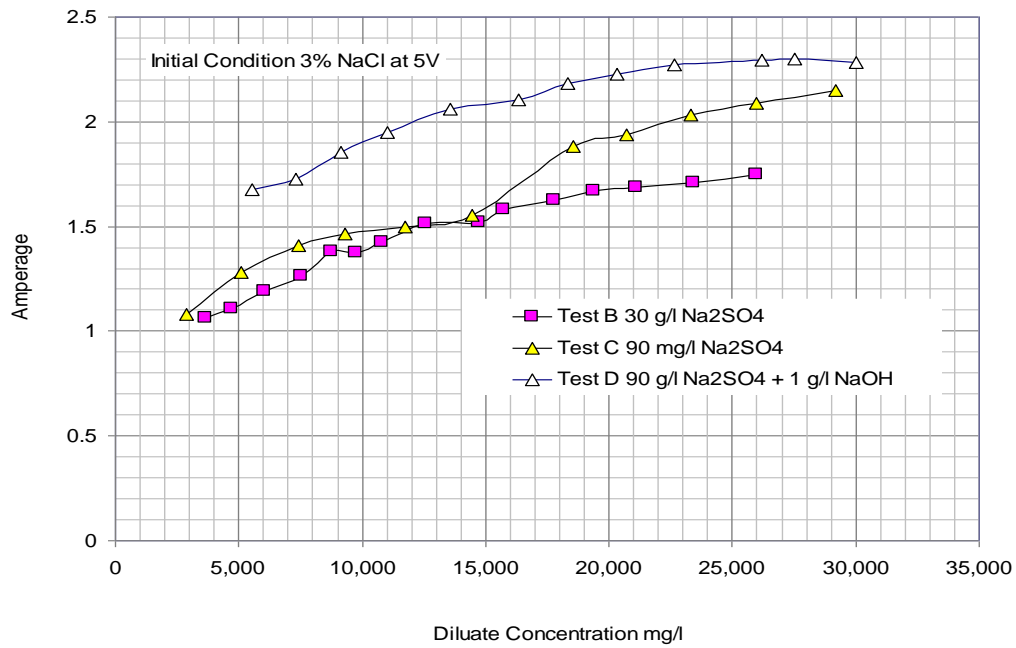


Figure 18: Amperage Profile for Electrolyte Chemistry Improvements

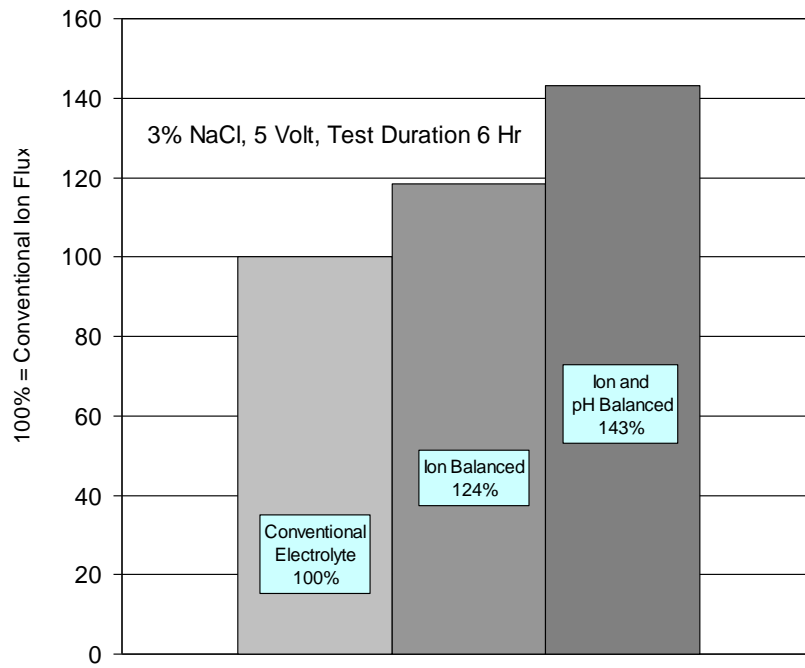


Figure 19: Performance Enhancements through Chemical Adjustment of the Electrolyte

7.2.3 Disodium Phosphate (Na_2HPO_4) as an Electrolyte

The use of phosphate in electrolytes for complex brines with high concentrations of calcium was ultimately abandoned due to the potential for precipitation of calcium phosphate within the electrode cells. The results are presented, herein, for completeness. The information may have utility for waters not heavily concentrated with calcium.

One disadvantage of the addition of sodium hydroxide to an electrolyte is that elevated and uncontrolled pH shifts may potentially occur, especially at the surface of the cathode. The pH of the electrolyte prepared with disodium sulfate alone was about 7.5. With added sodium hydroxide, the pH of the initial electrolyte was around pH 12.3. By natural extension of equations A1 and C2, the local pH in the anolyte is expected to decrease, and the pH of the catholyte is expected to increase. To avoid potential damage to the various components of the electrodialysis unit, it would be advantageous to control the pH of the electrolyte.

One natural choice for pH control is the phosphate buffer system, such as the chemical reaction of the third acid proton of Na_2HPO_4 and the conjugate base, Na_3PO_4 . As seen in Figure 20 with a series of Volt-Amp profiles, Na_2HPO_4 was not as effective a electrolyte as is sodium sulfate (Figures 13 and 14). However, with the addition of 2.8 g/l NaOH, the pH of the phosphate system stabilized around 10.5 units and an improved electrolyte was generated.

A full ED run was performed with the electrolyte prepared with 60 g/l disodium phosphate, 30 g/l disodium phosphate, and 2.2 g/l sodium hydroxide. The test water was 3 % NaCl. Results in

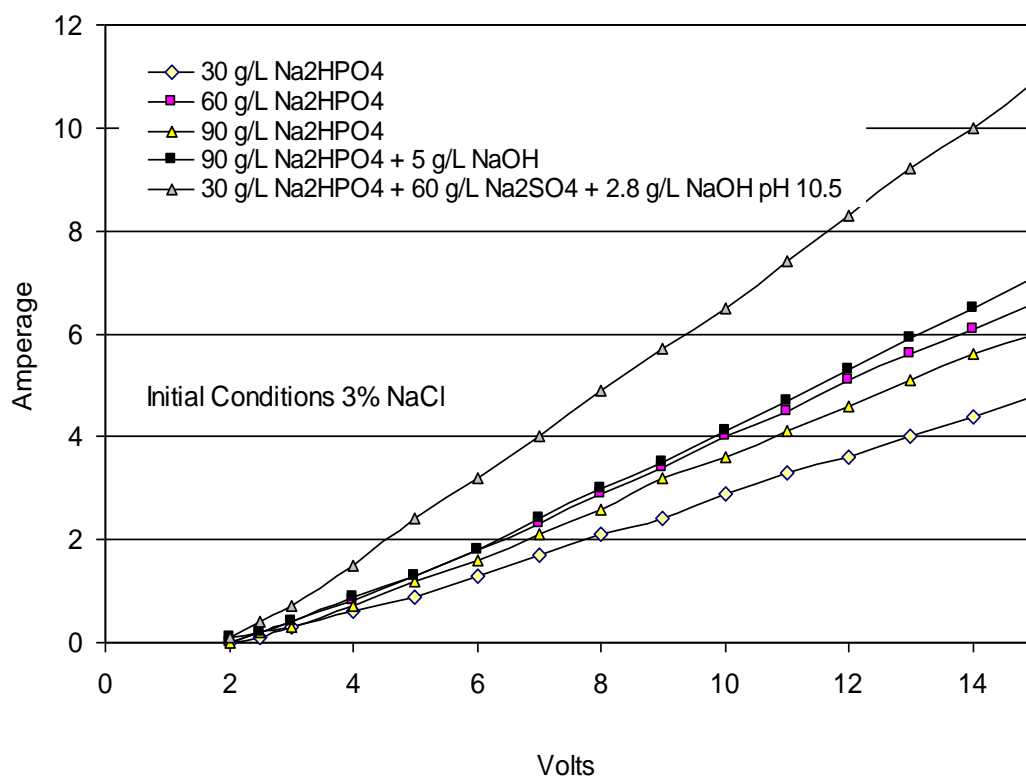


Figure 20: Disodium Phosphate as an Electrolyte

Figure 21 shows good performance could be achieved with this complex electrolyte.

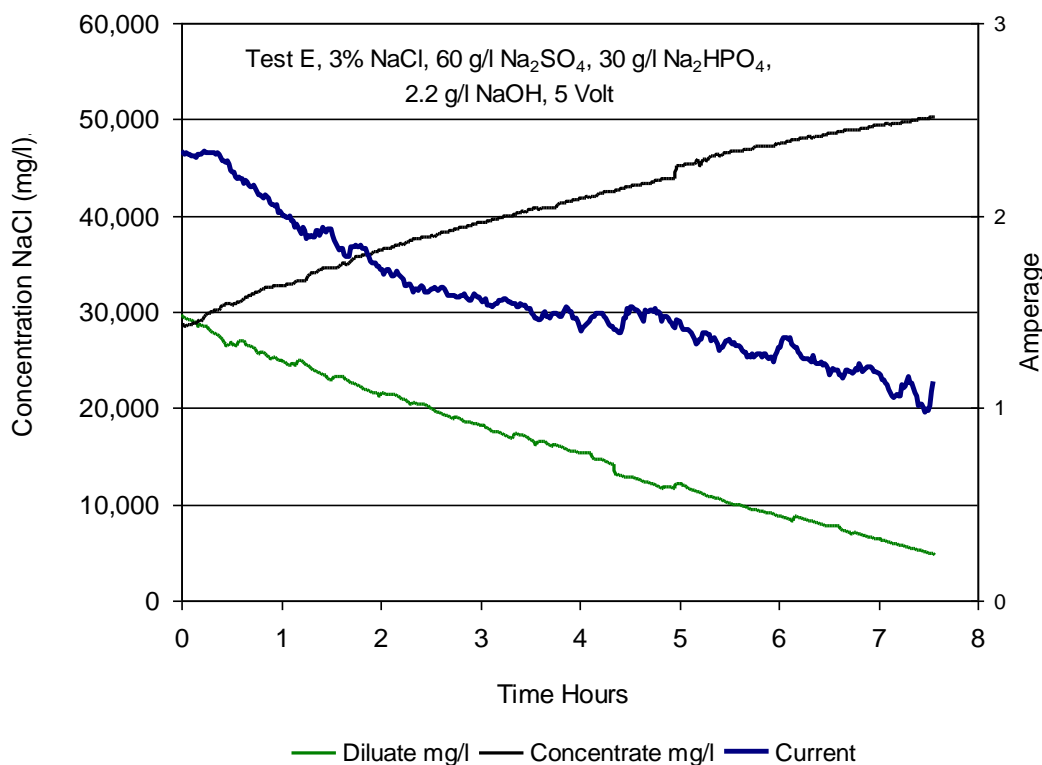


Figure 21: Disodium Phosphate as an electrolyte Test Run E

A natural outcome of the concept for buffering the anolyte at an elevated pH (see Equation A2) is the notion of providing sufficient buffering capacity. The buffering capacity (BC, equivalents/L) required to stabilize pH (while the majority of oxygen at the anode is being produced from hydroxide) can be estimated. If the flow of electrolyte to the anode is Q (liters/sec) and the amperage is i (amps), and F is the Faraday constant (96,500 coulomb/mole), then the concentration of buffer needed to have a (relatively) constant pH is expressed in Equation B1:

$$B1) \quad BC > \frac{i}{FQ}$$

For an anolyte flow of 1 Liter/minute and a current of 2.5 amps, the buffer capacity needed is approximately 0.00155 equivalents/liter. If this is to readily occur, then the pH of the anolyte must enter the electrolyte cell at a pH of about 11.2 or higher, and the buffer capacity must be greater than 0.0115 equivalents/l. If the chosen buffer couple is $\text{HPO}_4^{-2} \rightleftharpoons \text{PO}_4^{-3}$, then about 0.22 g/l Na_2HPO_4 (adjusted to pH 11.4) is minimally needed.

However, since the reaction occurs in the immediate vicinity of the electrode (within the diffusion boundary layer), a greater concentration of buffer may be desired in order to control the boundary condition.

This result leads to the natural experiment where the benefits of elevated pH in a buffered electrolyte are examined. Test E demonstrates a full desalting run at 5 Volts stack potential with

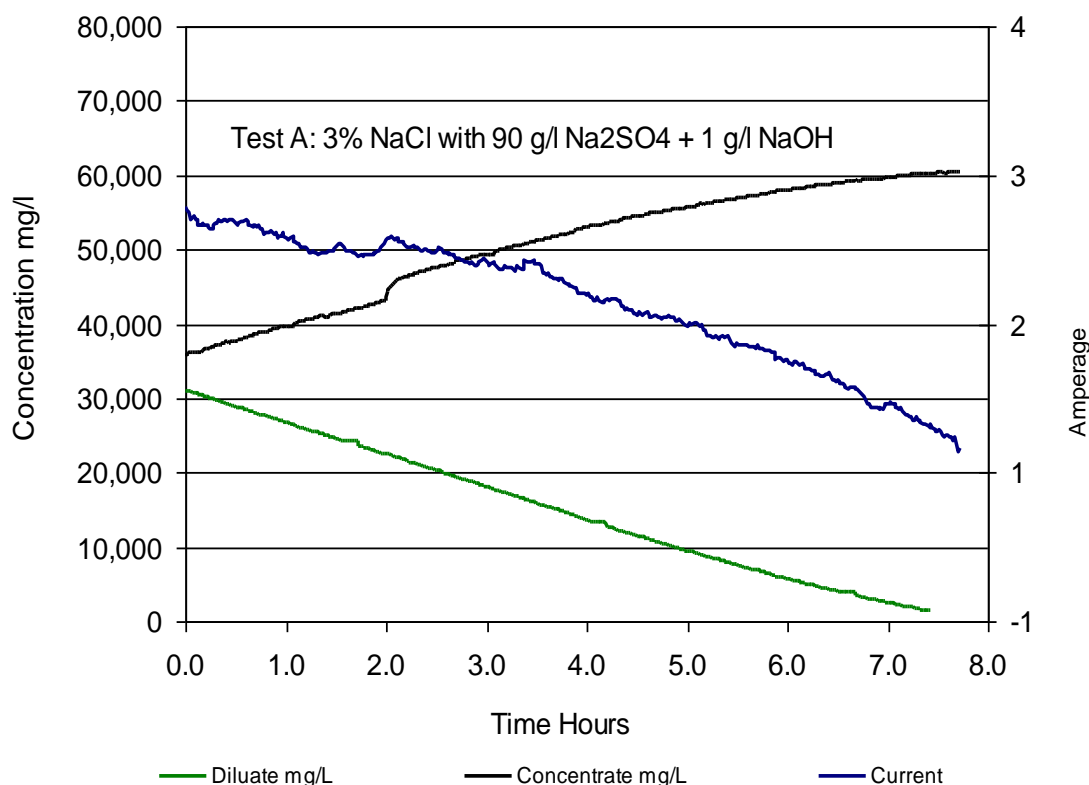


Figure 22: Test A, Reference Test for 3% NaCl

initial 3% NaCl as the test water. The electrolyte utilized was composed of 60 g/l Na₂SO₄, 30 g/l Na₂HPO₄ and 2.2 g/l NaOH. The pH of both the catholyte and the anolyte was around pH 12.2 to 12.5 the results of this run are presented in Figure 21 (Test E). This demonstrates that an effective electrolyte may be blended from a strong electrolyte and a weaker, buffering electrolyte.

In a later experiment, phosphate buffer was used with waters with complex mixtures of multivalent cations. This test was a failure due to precipitation in the electrolyte as cations crossed into the catholyte. It was assumed that the precipitate was calcium phosphate. Therefore, further tests with phosphate were abandoned for the purpose of treating hydraulic fracture flowback waters. There may be future value in the pursuit of phosphate based electrolytes in waters with minimal concentrations of calcium or other multivalent cations.

7.3 Effect of Calcium on Electrodialysis

The chemical nature of flowback water (Hayes, 2009) is summarized in the introduction of this document (Tables 1,2, and 3). These tables show the median chemical composition of Marcellus flowback water on day five from the fracture. The median total dissolved solids was about 67,300 mg/l. Importantly, the median calcium carbonate hardness is 17,700 mg/l as CaCO₃ is balanced against 122 mg/l alkalinity as CaCO₃, implying that the majority of the hardness is soluble. Major contributions to this hardness are Mg (559 mg/l), Ba (686), Sr (1,080 mg/l), and Ca (4,950 mg/l).

To put this into perspective, Kaakinen (1984) experienced difficulty in treating water from two sources. One source had a TDS range of 3,200-3,400 mg/l with calcium (7-18 mg/l) and magnesium (15-30 mg/l). The second source had a TDS range of 9,140-9,180 mg/l, with calcium (35-60 mg/l) and magnesium (52-55 mg/l). The author attributed membrane fouling in the concentrate stream to the hardness, and recommended that either the water be pretreated with chemical precipitation or treated in parallel with ion exchange.

To simulate the type of problems that might be encountered in flowback waters, calcium chloride was used to represent the unbalanced hardness that might be encountered. A series of three electrodialysis runs with initial sodium chloride concentrations of 3% and a pair of test with sodium chloride at 6% were performed.

The first of the 3% sodium chloride tests had no added calcium beyond that present in the tap water, such that the total dissolved solids in the test solution was around 30,000 mg/l (Test A, Figure 22). Test A and served as the baseline. The second test (Test G, Figure 23) was conducted with 3% sodium chloride plus 1000 mg/l Ca^{++} (from CaCl_2) such that the total dissolved solids was around 33,000 mg/l. The third test (Test F Figure 24) was with 3% NaCl plus 4000 mg/l Ca^{++} (from CaCl_2) with a total dissolved solids concentration around 41,000 mg/l. In all three tests, the electrolyte comprised of 90 g/L Na_2SO_4 plus 1 g/L NaOH and had a pH from 12.2-12.6 units. The volume of the electrolyte was about 10.5 L. All three tests were conducted at 5 V total stack potential (across 10 cell pairs plus electrode cells). The diluate tank and the concentrate tank both initially contained around 10.5 L feed stock. The ED system was operated for at least 6 hours for each test.

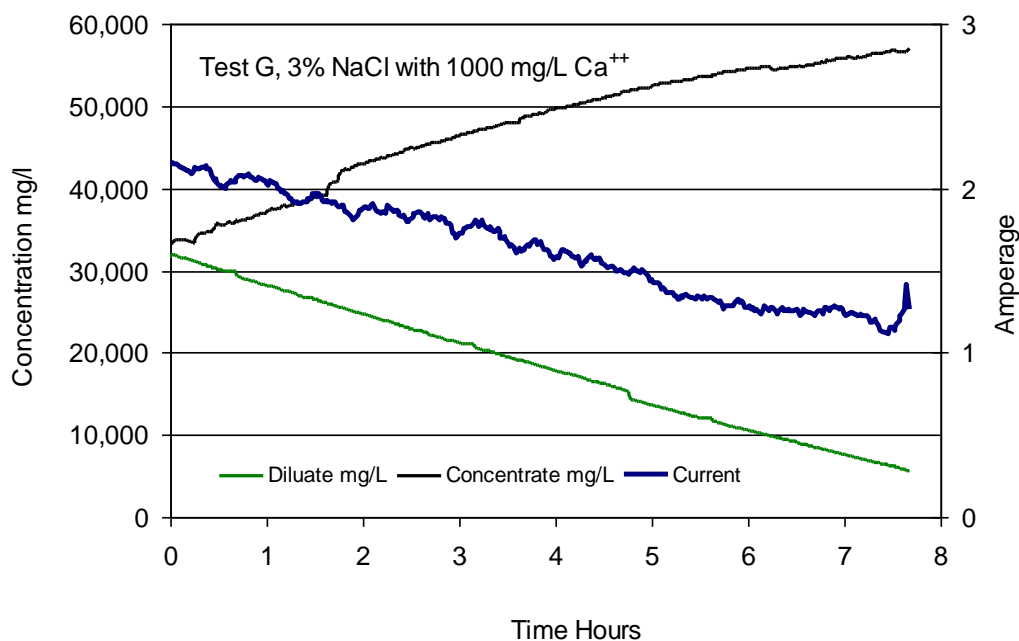


Figure 23: Test G with 3% NaCl + 1000 mg/l Ca^{++}

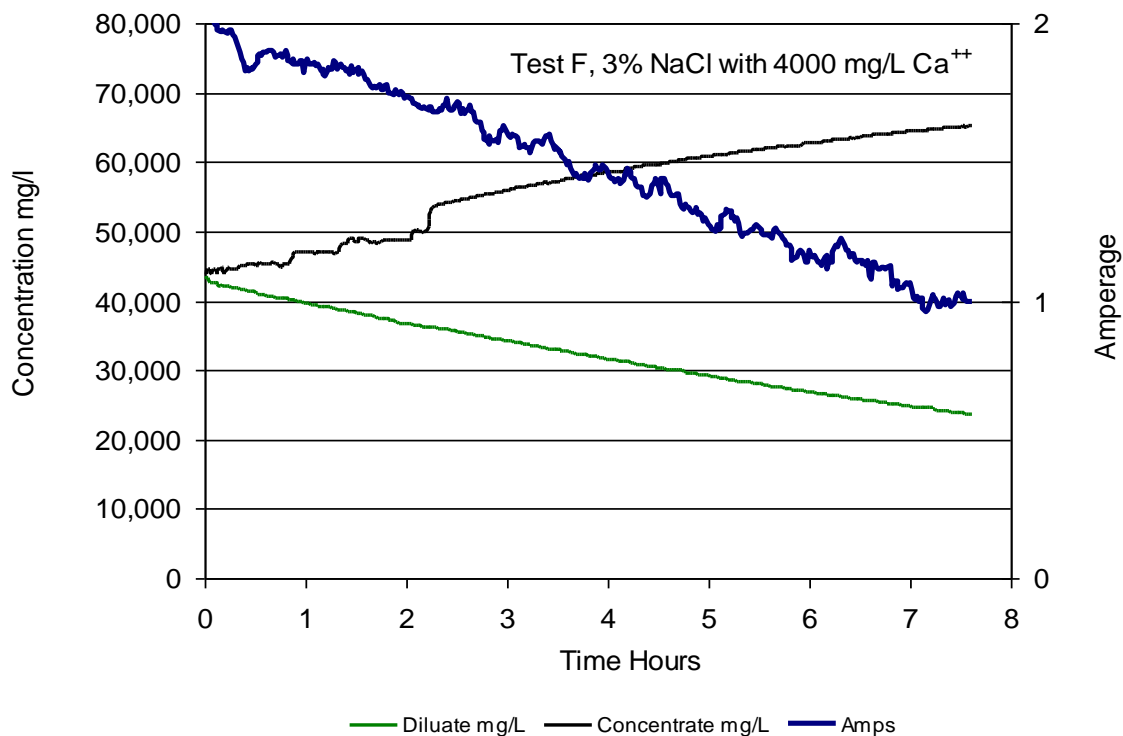


Figure 24: Test F, 3% NaCl with 4000 mg/l Ca^{++}

Figures 22, 23, and 24 are best compared by an analysis of the progression of the current during the treatment process. Current was averaged in $\frac{1}{2}$ hour intervals throughout each test and plotted versus the concentration in the diluate. In these tests, the current efficiency is nearly 100% such that amperage is a direct measure of ion flux. Figure 25 shows the $\frac{1}{2}$ hour average amperage data versus diluate concentration from the data from Figures 26, 27 and 28. As seen in this figure, there is a marked decrease in current caused by the addition of 1000 mg/l Ca^{++} . The amperage data at 30,000 mg/l diluate concentration indicate that 1000 mg/l Ca^{++} causes an 11% decrease in ion flux. A calcium concentration of 4000 mg/l causes a decrease of 40%. As a guide to further analysis, computer simulations are presented for 3% NaCl to simulate Test A, and for 4.2% NaCl to simulate Test F.

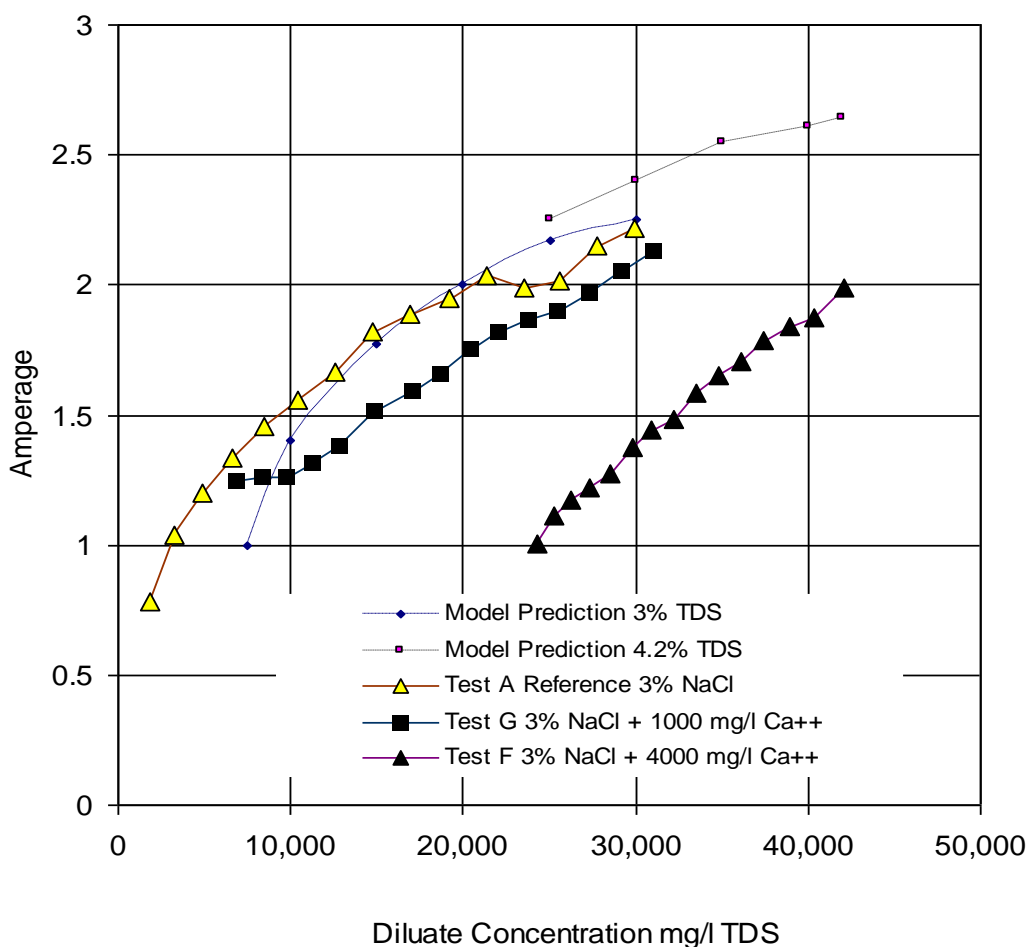


Figure 25: Summary of Current Density Profiles Showing Effect of Calcium Addition with Conventional Membrane at the Cathode.

To demonstrate that the loss of ion flux, as tracked by the current (amperage) was caused by a change in the electrolyte chemistry, a series of Volt-Amp profiles of current versus voltage were taken for Test F, with 3% NaCl and 4,000 mg/l Ca^{++} . The first profile in Figure 26 is an initial condition test at the start of the run. The current at 15 V exceeds 10 amps. By the time the run was terminated, the current at 15 V was about 5 amps. To test the origin of the fouling, the electrolyte was acidified. About 30 g HCl (0.35 wt/wt) was added to the electrolyte to shift the pH from about 12.5 to 3.8. After 15 minutes the VA profile showed an improvement in current at 15 V to more than 6 amps. The acidified electrolyte was cycled (at 0 volt stack potential) overnight for 10 hours. A final VA profile was performed and showed an increased current at 15 volt to greater than 7 amps. These data suggest that a calcium precipitate or other acid soluble precipitate was interfering with ion flux. These data also suggest that a majority of the resistance to ion flux caused may be reversed by acid treatment of the electrolyte solution.

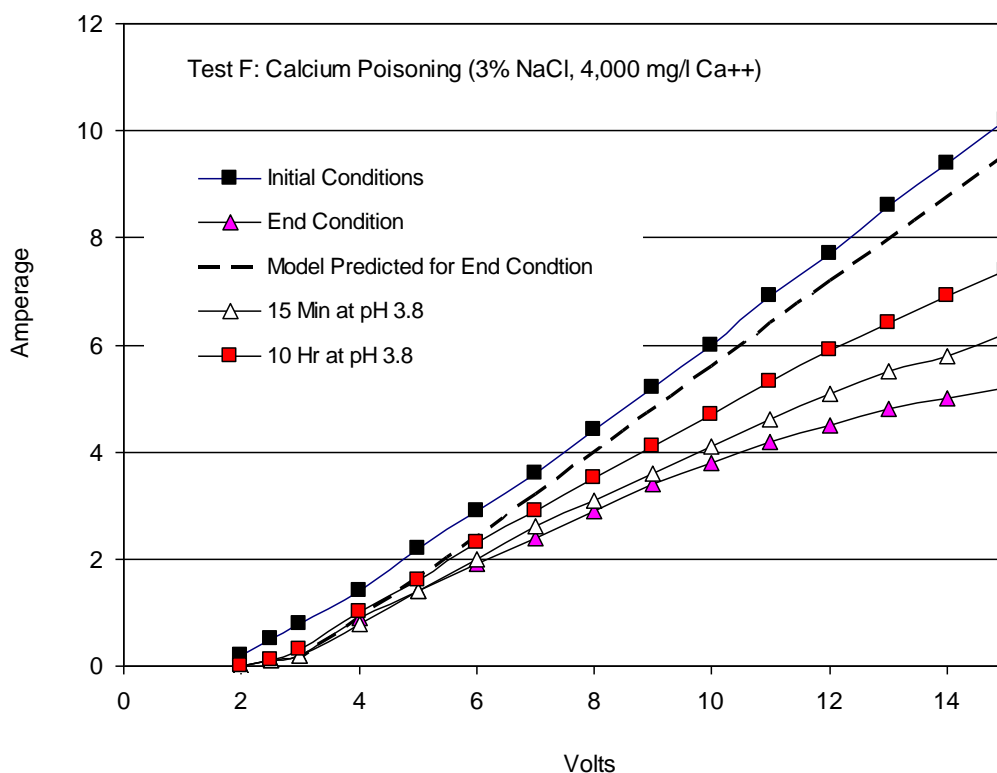


Figure 26: Recovery of Current Density by Acidification of the Electrolyte after Calcium Poisoning

A pair of electrodialysis runs with initial sodium chloride concentrations of 6% was also performed to determine the effect of calcium on electrodialysis. The first of these tests (Test I) had no added calcium beyond that present in the tap water, such that, the total dissolved solids concentration in the test solution was around 60,000 mg/l. This represented the baseline. The second test (Test H) had 6% NaCl plus 4,000 mg/l Ca^{++} (from CaCl_2) such that the total dissolved solids was around 71,000 mg/l. In both tests, the electrolyte comprised of 120 g/l Na_2SO_4 plus 1 g/L NaOH and had a pH from 12.2-12.6 units. The volume of the electrolyte was about 10.5 L. Both tests were conducted at 5 V total stack potential (across 10 cell pairs plus electrode cells). The diluate tank and the concentrate tank both initially contained around 10.5 L feed stock. The ED system was operated for at least 6 hours for each test. Results from the full runs are presented in Figures 27 and 28.

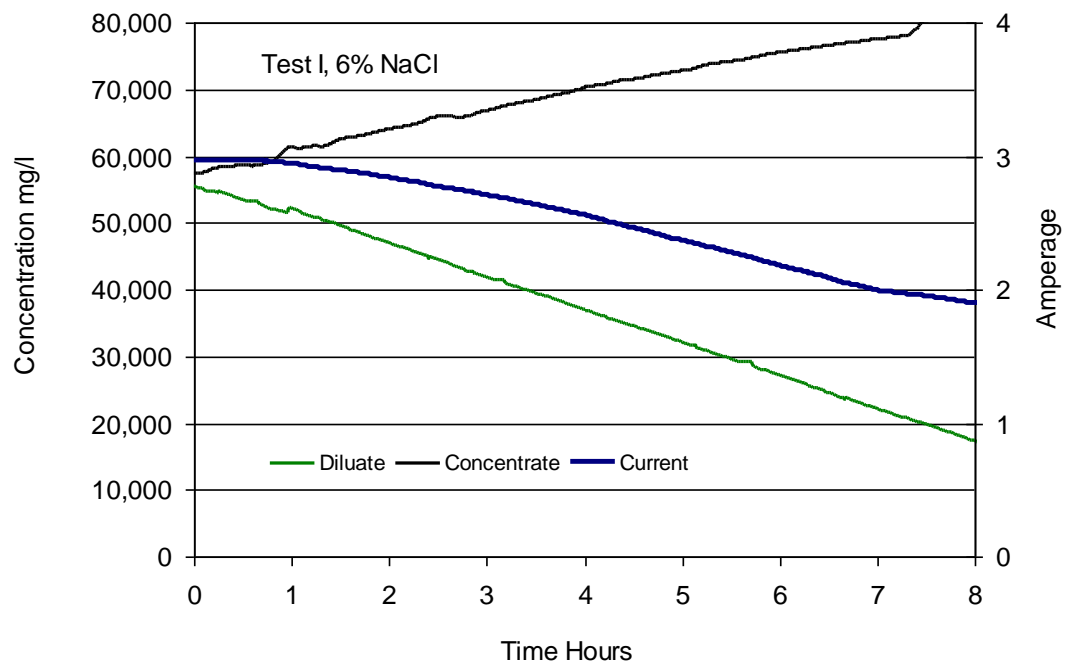


Figure 27: Test I; Baseline 6% NaCl

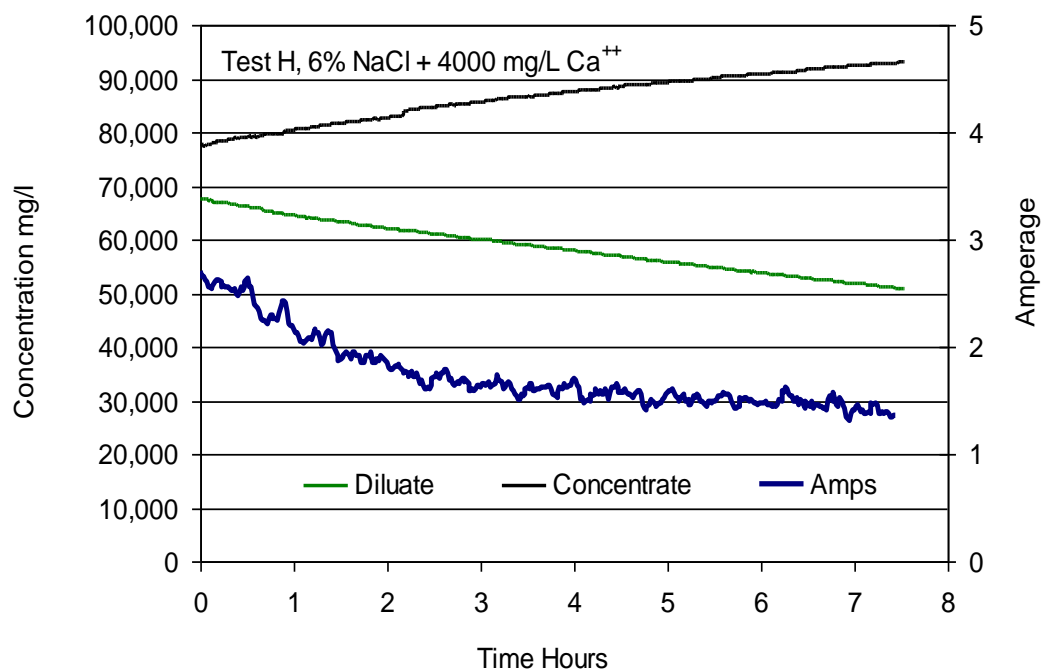


Figure 28: Test H, 6% NaCl with Calcium Poisoning

Figures 27 and 28 are best compared by an analysis of the progression of the current during the treatment process. Current was averaged in $\frac{1}{2}$ hour intervals throughout each test and plotted versus the concentration in the diluate. Figure 29 shows the $\frac{1}{2}$ hour moving average amperage data versus diluate concentration from the data from Figures 27 and 28. As seen in this figure, there is a marked decrease in current caused by the addition of 4,000 mg/l Ca^{++} . The amperage data at 55,000 mg/l diluate concentration indicate that 4,000 mg/l Ca^{++} caused a 50% decrease in ion flux. As a guide to further analysis, performance projections from the computer simulation are presented for 6% NaCl to simulate Test I, and for 7.2% NaCl to simulate Test H.

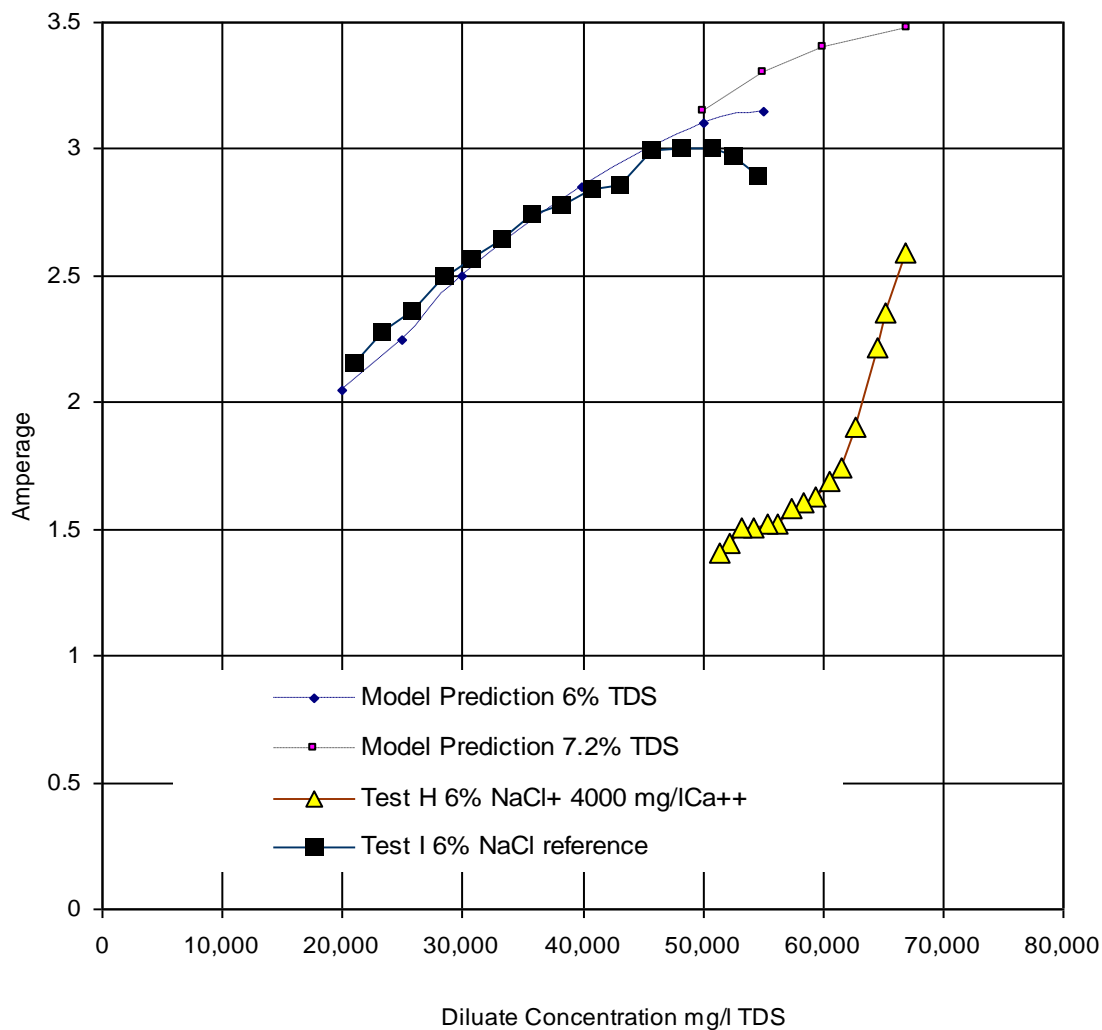


Figure 29; Comparison of Test H and I Showing poisoning of the Current Density with 4000 mg/l Ca++ in the Feed Stock

To demonstrate that the loss of ion flux (vis. Amperage) was caused by a change in the electrolyte chemistry, a series of Volt-Amp profiles of current versus voltage (Figure 30) were taken for the run (Test H) with 4,000 mg/l calcium. The first test is an initial condition test at the start of the run and shows that the current at 15 V is about 12 amps. By the time the run was terminated, the current at 15 V was about 7 amps. About 35 g HCl (0.35 wt/wt) was added to the electrolyte to shift the pH from about 12.5 to 2.9. After 5 minutes the VA profile showed an improvement in current at 15 V to more than 9.5 amps. The acidified electrolyte was cycled (at 0 volt stack potential) for 24 hours. The VA profile showed an increased current at 15 volt to greater than 12.5 amps. These data suggest again that a majority of the resistance to ion flux caused by calcium can be reversed by acid treatment of the electrolyte solution.

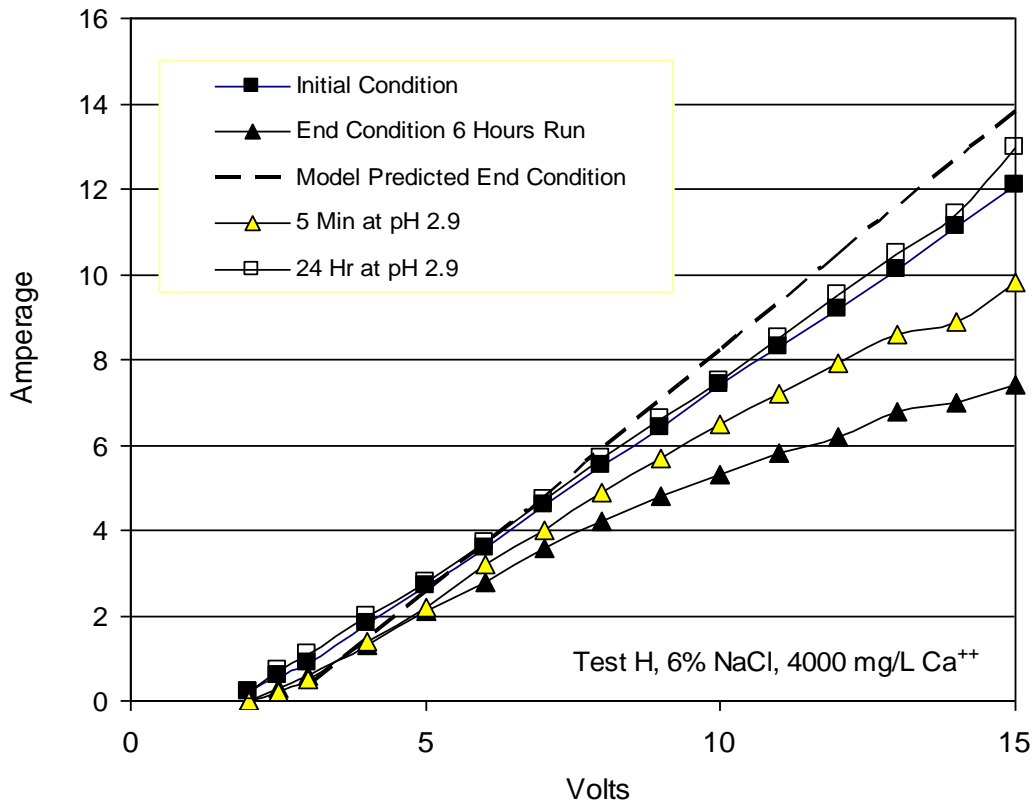


Figure 30: Recovery of Current Density by Electrolyte Acidification after Calcium Poisoning of the Electrolyte Test H.

7.4 Mitigation of the Calcium Problem with Cathode Protection

Figures 25 and 29 demonstrate that soluble calcium can be a serious problem for the treatment of highly concentrated brine solutions. Figures 26 and 30 suggest that the loss of ion flux can be reversed by acid treatment of the electrolyte. Since there was very little soluble calcium initially in the electrolyte, then calcium problems in the electrolyte are associated with the transport of calcium into the electrolyte.

The construction of the electrodialysis stack has only one point of contact between the electrolyte and mobile cations (Section 3, Figure 6) at the cation selective membrane at the boundary of the cathode. The membrane at this boundary in all previous tests was a non-exclusionary cation selective membrane. This membrane allows calcium to freely transport into the electrolyte.

One potential means of mitigating the effect of calcium transport into the electrolyte is, therefore, to replace the single cathode boundary membrane with a multivalent exclusionary, cation selective membrane. The following results show the effort to mitigate the transport of calcium into the electrolyte by protection of the cathode with a single multivalent exclusionary membrane. The electrodialysis stack was refurbished for this portion of testing by the replacement of the cathode cell boundary membrane with a multivalent exclusionary membrane.

Test J was a standard run (Figure 31) with 3% NaCl and no added calcium. These results are directly referenced to Test A (Figure 22); the difference is the type of membrane at the cathode boundary. Figure 32 is a summary of the ½ hour average amperage versus diluate concentration for Tests J and A. These results indicate that the replacement of the single membrane at the cathode had negligible effect on the process with sodium chloride as the only soluble salt. Computer simulated results for 3% NaCl are presented for comparison.

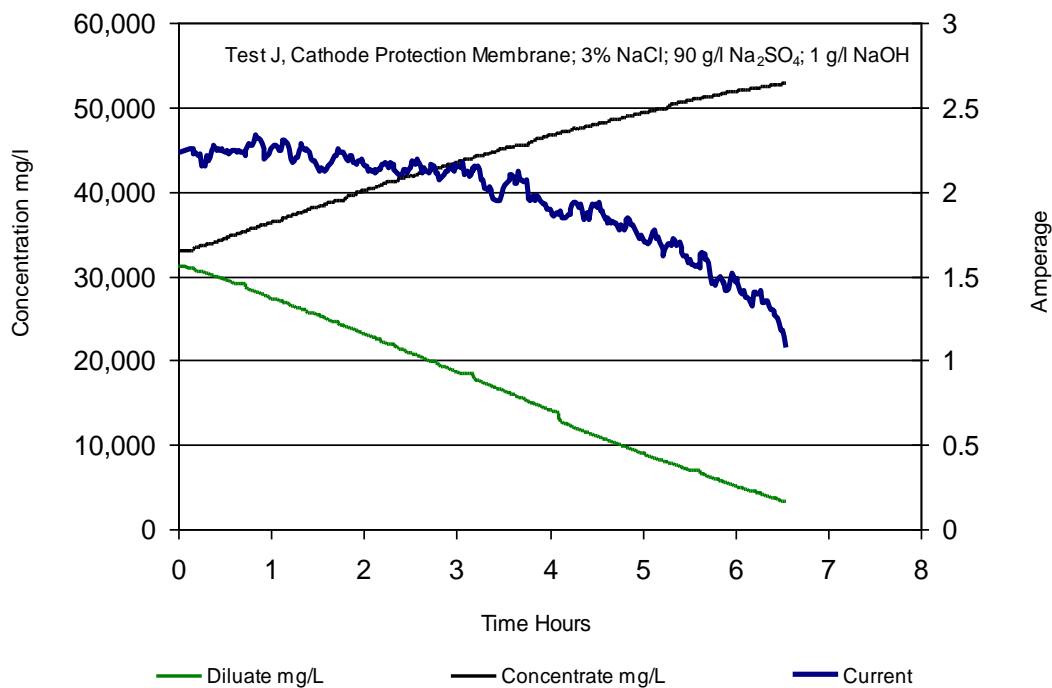


Figure 31: Test J, Standard 3% NaCl Test with the Multivalent Exclusionary Membrane at the Cathode Boundary.

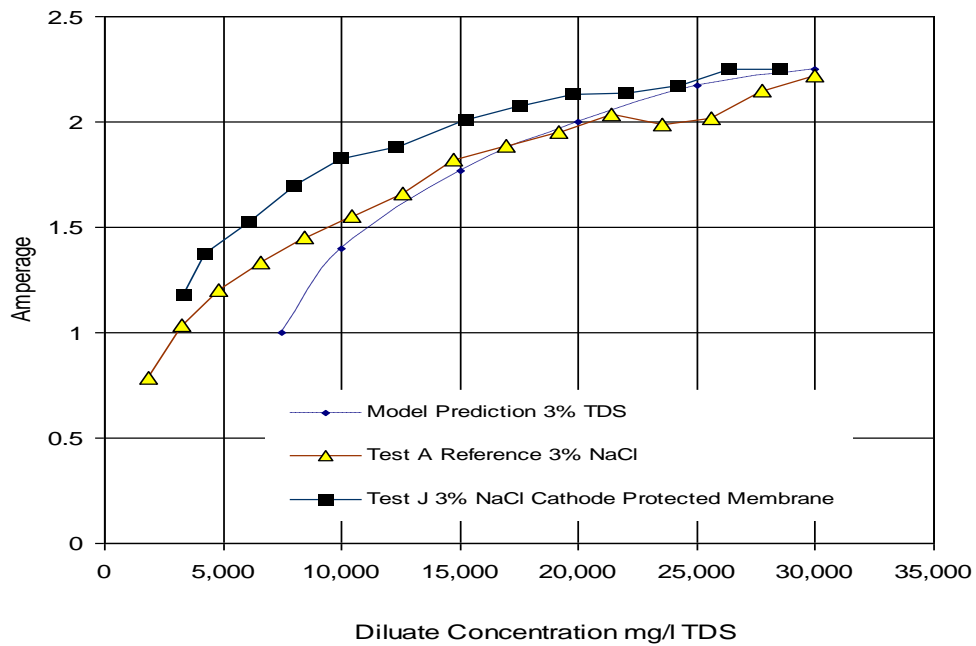


Figure 32: Comparison of Current Density with Cathode Protective Membrane (Test J) Compared to Standard Reference (Test A)

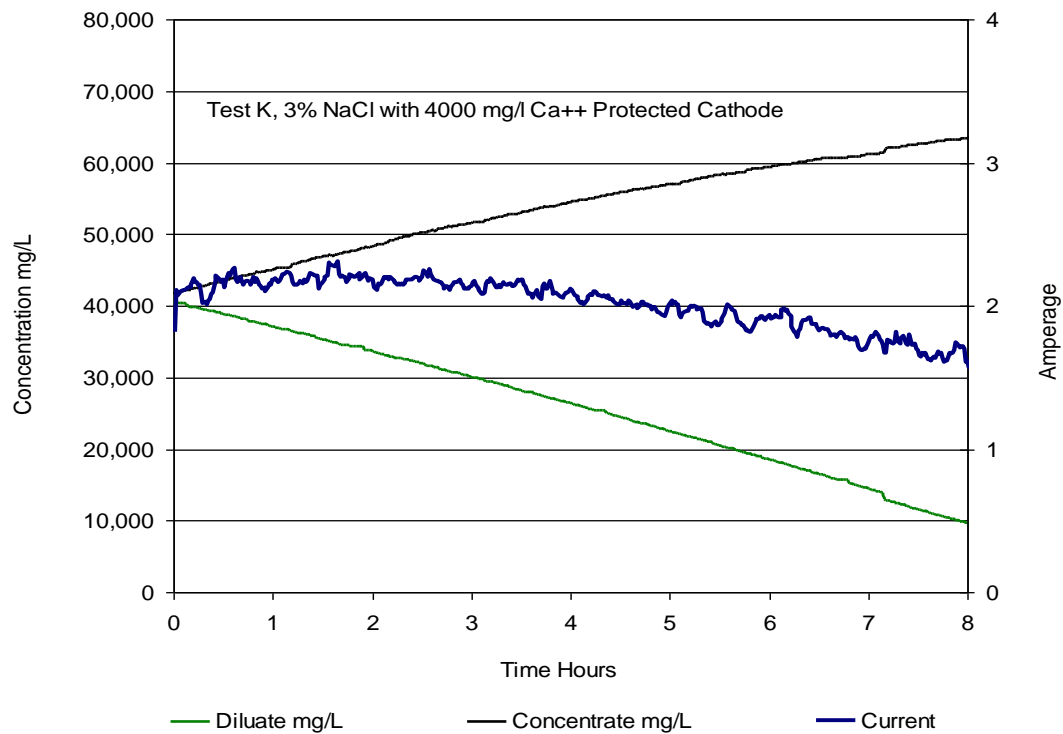


Figure 33: Test K, 3% NaCl Challenged with 4000 mg/l Ca++ with Protective Membrane at the Cathode Boundary

Test K (Figure 37) was performed using the protected cathode challenged with 3% NaCl plus 4,000 mg/l Ca^{++} added. This test is a direct comparison to Test F with the unprotected cathode (Figure 25). Compared to Test F, Test K with the protected catholyte showed improved amperage and ion flux throughout the entire run.

Figure 34 is a summary of the ½ hour average amperage versus diluate concentration for Tests K (challenged protected cathode) and J (unchallenged protected membrane). The results of test F (challenged, unprotected cathode) are reproduced for comparison. This figure shows little degradation of ion flux when the protected membrane system is challenged with 4000 mg/l Ca^{++} .

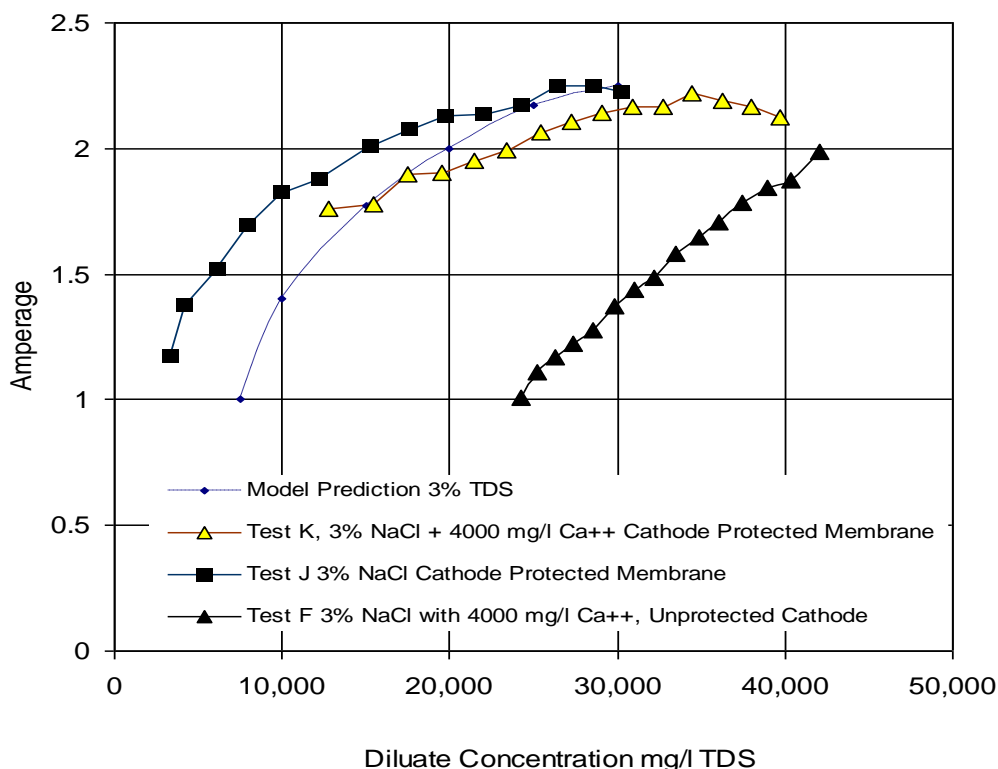


Figure 34: Effect of Cathode Protection by Multivalent Cation Exclusionary Membrane

Test L (Figure 35) was performed with 6% NaCl plus 4000 mg/l Ca^{++} and is the counterpart to Test H (Figure 28). Compared to Test H, Test L with the protected catholyte showed improved amperage and ion flux throughout the entire run. Figure 36 is a plot of the 1/2 hour average amperage versus diluate concentration for Test L compared to Test I (unprotected cathode, 6% salt and no calcium). The results from Test H are reproduced for comparison.

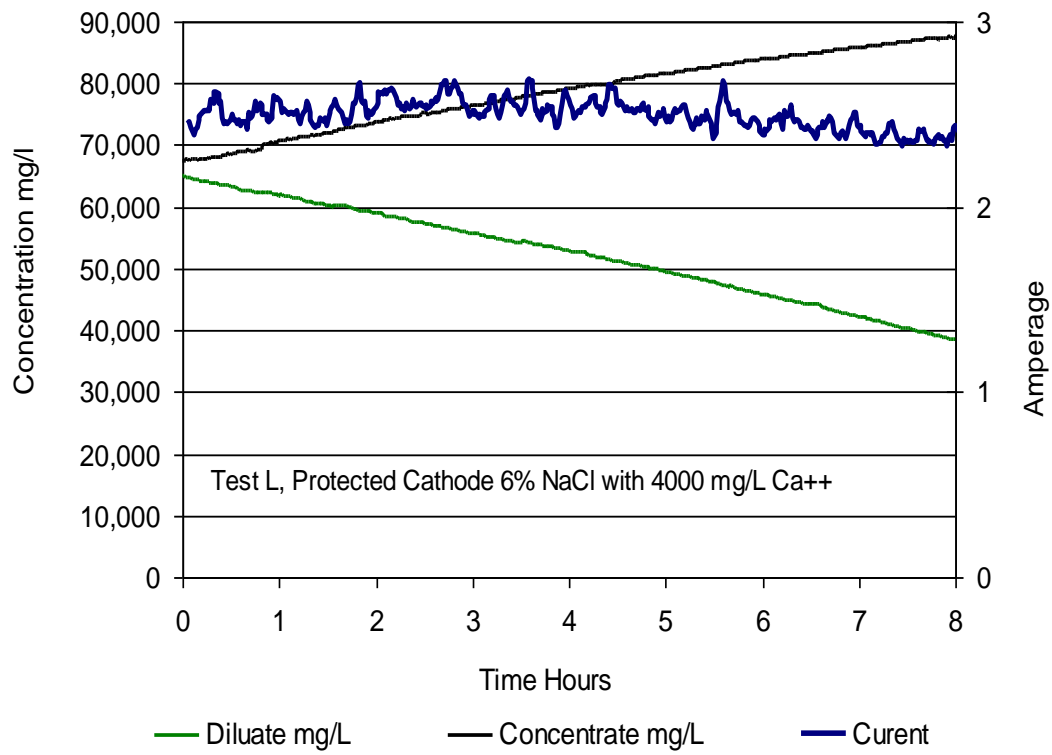


Figure 35: Test L with 6% NaCl with 4000 mg/l Ca⁺⁺

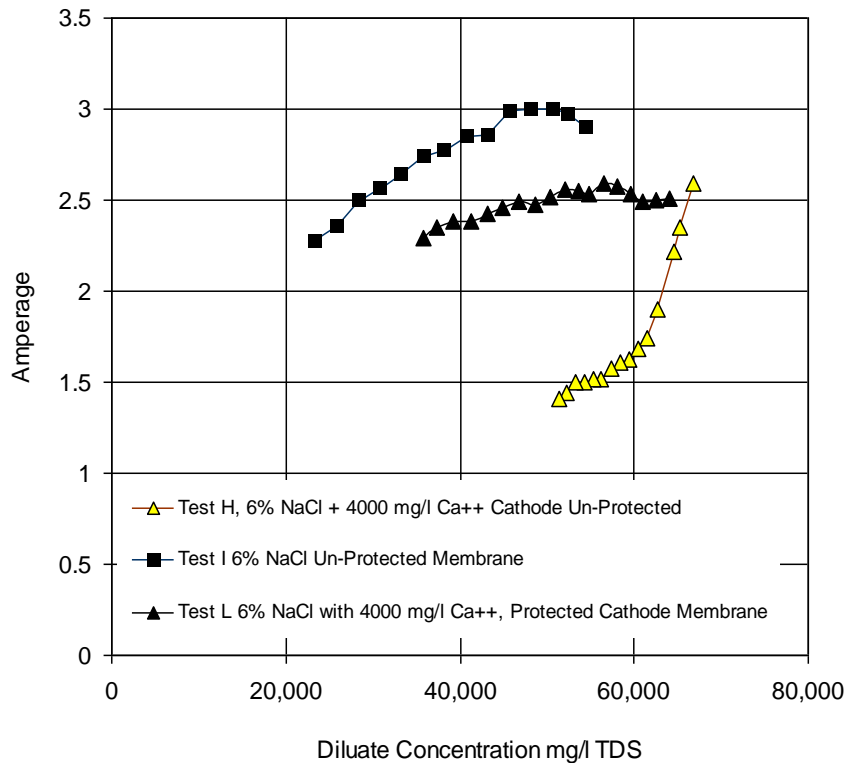


Figure 36: Effect of Calcium on Protected and Un-Protected Cathode with 6% NaCl

In order to better exemplify the relation of calcium transport across the cathode cell boundary to loss of ion flux, grab samples were taken for the Tests A,G,F (Table 12) and Tests J and K (Table 13). Data for sodium, calcium, chloride, total dissolved solids and pH were summarized. The Des Plaines, Illinois, tap water appears to have between 33 to 40 mg/l calcium, such that calcium is present in all samples. There appears to be one outlier in the tap water calcium data for Test L with calcium at 139 mg/l.

Table 12: Chemical Analyses: Tests with Unprotected Cathode					
Test A43, 3% NaCl	Na	Ca	Cl	TDS	pH
Tap	9	40	15	1,400	7.9
Feed	9,900	43	19,000	33,000	7.5
Diluate	920	0	1,400	500	7.9
Concentrate	18,000	140	31,000	57,000	7.9
Initial Electrolyte	22,000	73	73	92,000	12.3
Final Electrolyte	26,000	100	1,000	100,000	12.3
Test G39, 3% NaCl with 1000 mg/l Ca ⁺⁺	Na	Ca	Cl	TDS	pH
Tap	12	33	15	260	7.8
Feed	9,900	1,100	18,000	35,000	8.0
Diluate	2,500	1	3,700	6,600	8.2
Concentrate	18,000	2,200	30,000	59,000	8.2
Initial Electrolyte	not done	not done	not done	not done	not done
Final Electrolyte	33,000	180	49	98,000	12.4
Test F40, 3% NaCl with 4000 mg/l Ca ⁺⁺	Na	Ca	Cl	TDS	pH
Tap	26	37	15	ND	8.2
Feed	13,000	4,400	25,000	55,000	7.9
Diluate	6,700	750	12,000	25,000	8.4
Concentrate	14,000	6,100	35,000	63,000	7.8
Initial Electrolyte	31,000	38	27	110,000	12.4
Final Electrolyte	24,000	160	47	91,000	12.3
Test H45, 6% NaCl with 4000 mg/l Ca ⁺⁺	Na	Ca	Cl	TDS	pH
Tap	9	39	19	ND	7.9
Feed	21,000	3,500	45,000	84,000	8.0
Diluate	14,000	1,600	28,000	53,000	8.2
Concentrate	27,000	5,100	57,000	110,000	8.0
Initial Electrolyte	19,000	47	140	120,000	12.4
Final Electrolyte	34,000	130	200	110,000	12.3

Table 13: Chemical Analyses, Tests with Protected Cathode					
Test J48, 3% NaCl	Na	Ca	Cl	TDS	pH
Tap	7	35	15	540	7.6
Feed	10,000	32	18,000	37,000	7.5
Diluate	1,800	1	2,700	5,700	7.6
Concentrate	17,000	110	30,000	62,000	7.4
Initial Electrolyte	26,000	49	250	98,000	12.5
Final Electrolyte	24,000	63	220	96,000	12.5
Test K49, 3% NaCl with 4000 mg/l Ca ⁺⁺	Na	Ca	Cl	TDS	pH
Tap	11	45	81	640	7.7
Feed	10,000	3,500	25,000	76,000	8.0
Diluate	2,800	14	5,400	11,000	8.9
Concentrate	18,000	6,600	41,000	120,000	7.7
Initial Electrolyte	24,000	56	300	98,000	12.4
Final Electrolyte	23,000	97	250	98,000	12.3
Test L53, 6% NaCl with 4000 mg/l Ca ⁺⁺	Na	Ca	Cl	TDS	pH
Tap	320	130	27	740	7.9
Feed	25,000	3,800	42,000	110,000	7.9
Diluate	12,000	800	20,000	43,000	8.5
Concentrate	32,000	8,000	61,000	150,000	7.8
Initial Electrolyte	25,000	100	270	130,000	12.0
Final Electrolyte	36,000	190	350	130,000	12.0

It is expedient to define the relative flux of an ion, such as calcium, between the diluate and the concentrate, as compared to flux of the ion from the water to the electrolyte. The relative flux index (RFI) is defined as the change in electrolyte concentration compared to the change in concentration between the concentrate and the feed.

$$RFI_{Ca^{++}} = \frac{\Delta C_{electrolyte}}{C_{concentrate} - C_{diluate}}$$

Table 14 compares the values for four tests with direct comparison of protected versus unprotected cathodes; Test K vs Test F and Test L3 vs Test H. As seen with these calculations, much more calcium is introduced into the electrolyte (low CFR) with the unprotected cathode, as compared to the protected cathode (high CFR). The ability of the more exclusionary membrane to reject calcium is seen to be about 70%.

Table 14: Rejection of Calcium in Cathode Protected Membrane					
Test	Cathode Protected	NaCl % Feed	Ca ⁺⁺ Feed mg/l	RFI _{Ca⁺⁺}	% Ca Rejected
F	No	3	4,400	0.023	
K	Yes	3	3,500	0.062	73%
H	No	6	3,500	0.024	
L	Yes	6	3,800	0.083	66%

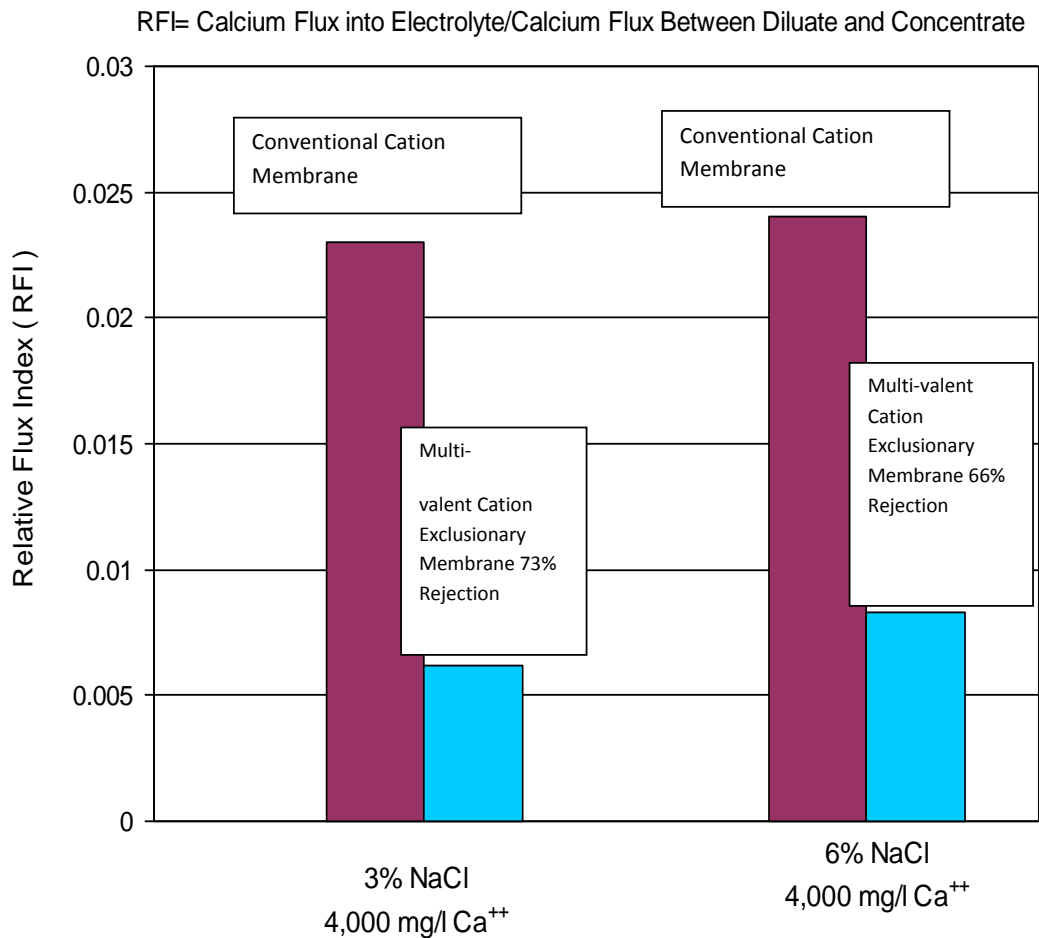


Figure 37: Cathode Protective Membrane Accounts for 66-73% Rejection of Calcium Flux to the

7.5 Mechanism of Calcium Interference

Figures 25 and 29 clearly demonstrate that a non-selective membrane at the boundary of the cathode electrolyte is highly sensitive to calcium entering the electrolyte cell. Figures 26 and 30 suggest that acid cleaning reverses the detrimental effects of calcium in the electrolyte cell.

It is evident from the tests evaluated in tables 12, 13, and 14, and from the summary plot, Figure 37, that the single exclusionary membrane installed at the cathode boundary is effective at reducing calcium flux into the cathode cell by about 70%. The corollary to this observation is that 30% of the potential flux of calcium still enters the catholyte.

Long term operation of an electrolyte bath, therefore, should still be impacted by incursion of multivalent cations. The following three tests (Tests M, N, and O) were performed to investigate the fate of calcium into and out of the electrolyte with the cathode protection membrane in place.

Test M (Figure 38 and Table 15) was performed based on the premise that the electrolyte could become fouled and, therefore, present impedance to ion flux. In this test, the preferred electrolyte, 90 g/l Na_2SO_4 with 1 g/l NaOH at pH 12.5 was used. The salt solution was 3% NaCl with no calcium, and presented no challenge to the electrolyte. At $\frac{1}{2}$ hour, the electrolyte was challenged with 400 mg/l Ca^{++} . A white precipitate immediately formed. The test continued for another hour when the pH of the electrolyte was dropped to pH 3.2 with 3 g/L HCl. The test continued for an additional $4\frac{1}{2}$ hour with no indication of flux inhibition (Figure 38). Therefore, the act of creating calcium precipitate within the electrolyte solution does not appear represent an operational problem. Furthermore, when the calcium precipitate was dissolved with acid, the soluble calcium caused no inhibition. In fact, quite an opposite effect was noted. Calcium was observed to leave the electrolyte and become concentrated in the concentrate stream.

Table 15: Test M, Effect of Precipitated and Soluble Calcium in Electrolyte: Test for Transport of Calcium from Electrolyte into Concentrate						
Time	Action				Response	
0-Hour	Initial Condition Electrolyte; vol. =10.5 L, 90 g/L Na_2SO_4 With 1 g/L NaOH pH 12.5 Salt Solution; 3% NaCl only				Represents Baseline Conditions	
$\frac{1}{2}$ -Hour	Added 1 g/L CaCl_2 (400 mg/l) into Electrolyte Tank				Immediate white ppt. in electrolyte	
1 $\frac{1}{2}$ Hour	Added 0.3 g/L HCl to Electrolyte Tank				pH 3.2 in electrolyte, ppt cleared	
1 $\frac{1}{2}$ - 6 Hour	Continued Test at 5V				Efficient operation recorded	
Sample	Time Hour	Na	Ca	Cl	TDS	pH
Feed	0	11,000	29	18,000	29,000	10.0
D4 Diluate	1.5	8,900	23	14,000	22,000	10.2
D5	2.5	7,200	10	11,000	18,000	10.2
D6	3.5	6,200	4	8,600	13,000	10.2
D7	4.5	3,000	<2.5	5,500	8,100	10.2
D8	6	1,500	<2.5	2,900	3,900	10.1
C4 Concentrate	1.5	15,000	110	22,000	37,000	9.6
C5	2.5	15,000	110	24,000	42,000	9.3
C6	3.5	18,000	130	26,000	44,000	9.3
C7	4.5	16,000	110	30,000	48,000	9.2
C8	6	19,000	120	30,000	54,000	9.3
E1 Electrolyte	0	34,000	<2.5	27	98,000	12.4
E2	0.5	25,000	15	47	96,000	12.5
E3	1	25,000	490	1,700	86,000	11.8
E4	1.5	29,000	610	1,500	87,000	11.4
E5	2.5	26,000	350	1,800	85,000	2.7
E6	3.5	31,000	380	1,700	86,000	2.7
E7	4.5	29,000	390	1,700	88,000	2.8
E8	6	29,000	390	1,800	90,000	2.8

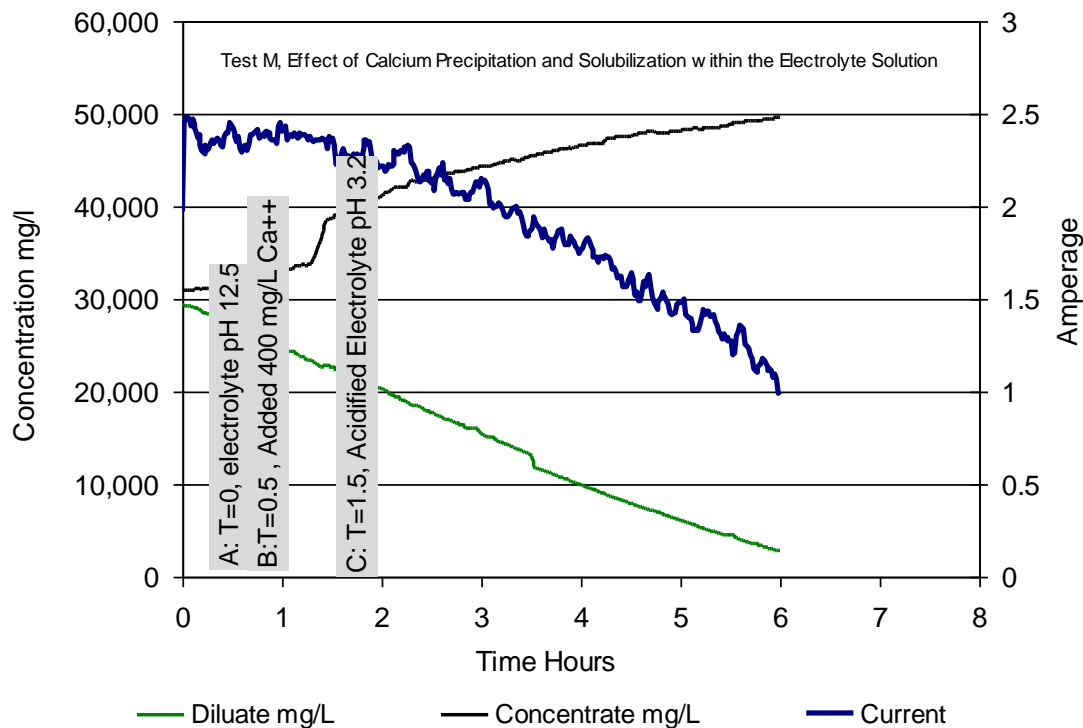


Figure 38: Test M; Effect of Adding Calcium (400 mg/l) to the Electrolyte, Followed by Acidification of the Electrolyte

Test N (Figure 39 and Table 16) was performed to determine if the transport of soluble calcium from the diluate to the electrolyte or the transport from the electrolyte to the concentrate could present an ion flux inhibition. In this test, a reduced volume (3.4 L instead of 10.5L) electrolyte was used in order better measure the rate of calcium change across the hydraulic boundaries. The salt solution treated was 3% NaCl with 4,000 mg/l Ca^{++} . The electrolyte was 90 g/L Na_2SO_4 at pH 6.8 with an initial concentration of 100 mg/l Ca^{++} . As seen in Table 16, the electrolyte slowly collected calcium from an initial concentration of 110 mg/l to a concentration of 400 mg/l at 7.5 hours in the small volume of electrolyte. This is consistent with the approximate rate of calcium incursion seen in Test K (initially 45 mg/l increased to 97 mg/l in 10.5 L electrolyte).

The entire run N (Figure 39) was efficient, indicating that soluble calcium in the treated water and soluble calcium in the electrolyte did not cause an ion flux inhibition. It should be noted that this test utilized electrolyte at pH 6.8 and the amperage was initially about 2.1. In previous tests, the preferred electrolyte was prepared at pH 12, in which cases, the initial amperage at 3% NaCl was about 2.3-2.4 amps. The lower overall amperage in Test N is attributed to the pH effect, as noted in the previous results with electrolyte improvements.

Table 16: Test N: Effect of Soluble Calcium in Electrolyte: Test for Transport of Soluble Calcium from Diluate to Electrolyte and from Electrolyte to Concentrate						
Time	Action			Response		
0-Hour	Initial Condition Electrolyte; vol. = 3.4 liter, 90 g/l Na ₂ SO ₄ ,pH 6.7 Plus 100 mg/l Ca ⁺⁺ Salt Solution; 3% NaCl plus 4000 mg/l Ca ⁺⁺			Represents Challenged Condition		
0-7 ½ Hour	Continued Test at 5 V			Appeared a normal run for neutral pH electrolyte		
(Note low electrolyte volume to increase rate of change in concentration)						
	Time Hour	Na	Ca	Cl	TDS	pH
Feed	0	12,000	3,600	25,000	68,000	3.8
D2 Diluate	3	8,400	1,700	17,000	42,000	6.6
D3	6	4,800	110	7,300	16,000	6.6
D4	7.5	3,300	12	5,300	8,500	6.7
C2 Concentrate	3	8,400	3,600	30,000	86,000	6.1
C3	6	14,000	6,100	38,000	100,000	6.3
C4	7.5	17,000	6,600	38,000	110,000	6.4
E1 Electrolyte	0	25,000	110	230	100,000	4.5
E2	3	24,000	180	250	100,000	3.7
E3	6	27,000	330	300	98,000	3.8
E4	7.5	22,000	400	340	98,000	3.8

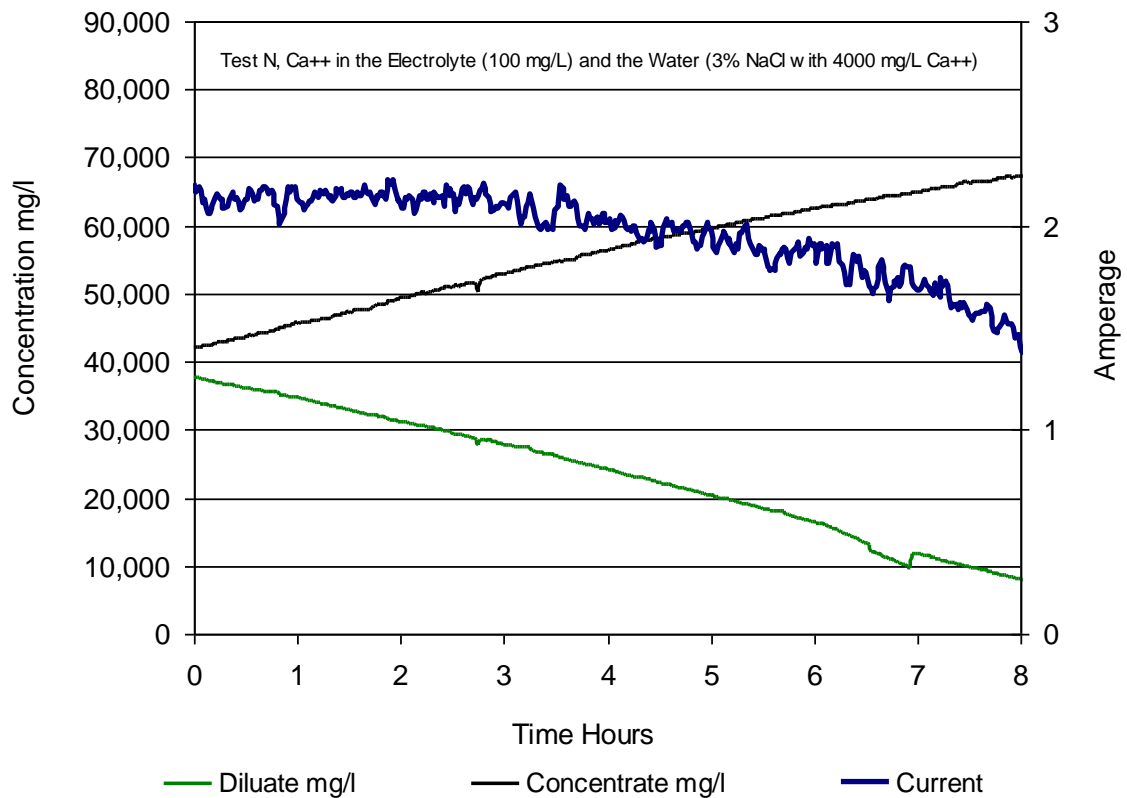


Figure 39: Test N, Effect of Soluble Calcium in Electrolyte

Test O (Figure 40 and Table 17) was performed to determine if bicarbonate or carbonate in the electrolyte, in the presence of calcium, could cause degradation of ion flux with a protected cathode. The electrolyte was initially at pH 6.8 and consisted of 90 g/L Na_2SO_4 with 100 mg/l Ca^{++} . The salt water to be treated was initially 3% NaCl with 4,000 mg/l Ca^{++} . At ½ hour into the run, 200 mg/l NaHCO_3 was added to electrolyte. No degradation of performance was noted. At 1 hour, 1 g/L NaOH was added to the electrolyte to precipitate the calcium carbonate. No degradation of performance was noted.

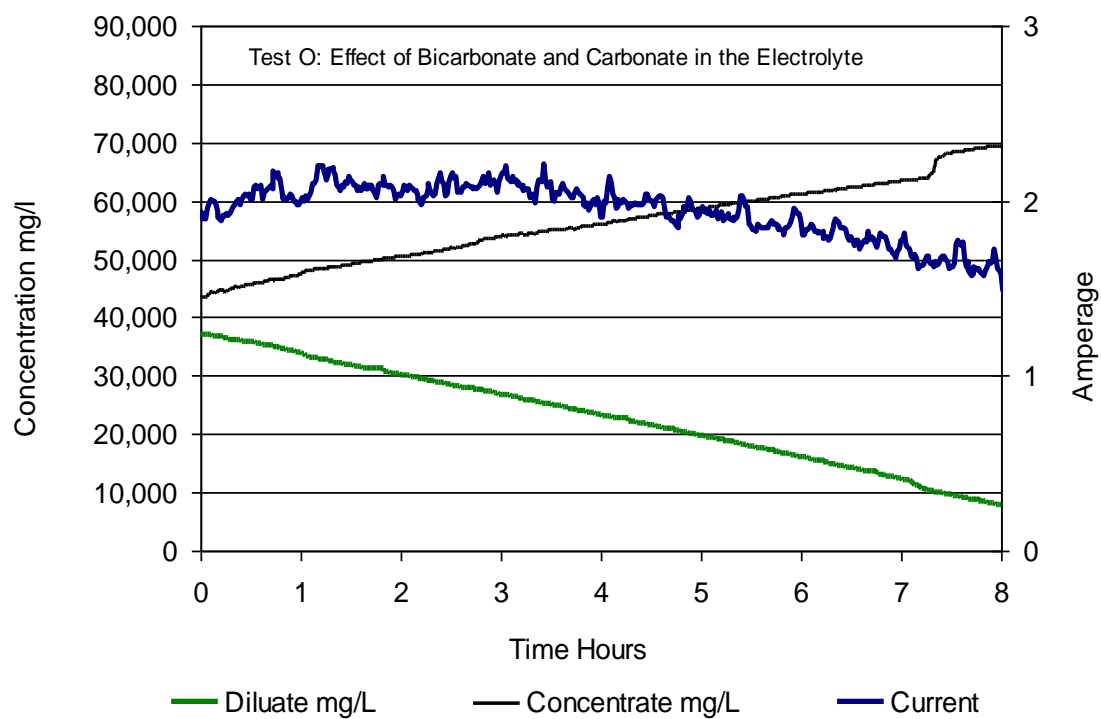


Figure 40: Test O: Effect of Adding Carbonate and Bicarbonate to Precipitate the Calcium in the Electrolyte

Table 17: Test O: Effect of Bicarbonate and Carbonate on the Electrolyte Solution						
Time		Action			Response	
0-Hour		Initial Condition Electrolyte; vol. = 10.5 Liter 90 g/l Na ₂ SO ₄ With 0 g/l NaOH pH 6.7 Plus 100 mg/l Ca ⁺⁺ Salt Solution; 3% NaCl plus 4000 mg/L Ca ⁺⁺			Represents Challenged Condition	
½- Hour		Added 220 mg/l NaHCO ₃ to electrolyte tank			No change	
1-Hour		Added 1 g/L NaOH to electrolyte tank			pH to 12.5, no change in performance	
1-7 ½ Hour		Continued at 5 V			Good performance	
	Time Hour	Na	Ca	Cl	TDS	pH
Feed	0	9,800	3,300	25,000	65,000	6.6
D4 Diluate		3,200	27	4,800	9,500	27.0
C4 Concentrate		16,000	5,900	41,000	110,000	6.7
E1 Electrolyte		26,000	110	200	99,000	7.5
E2		25,000	150	270	99,000	7.2
E3		26,000	190	290	100,000	12.2
E4		27,000	150	310	100,000	12.2

Tests M, N, and O, demonstrate that once the calcium exclusionary membrane is placed to protect calcium incursion into catholyte, there is very little that can be done to the electrolyte chemistry to further impede ion flux. This is illustrated in Figure 41. Test M can be compared to Test J; the difference being that Test M had calcium added to the electrolyte. Test N can be compared to Test K, the difference being, again, the addition of calcium to the electrolyte in Test N. Test O can be compared to Tests K and N, with the difference that the calcium added to the electrolyte was deliberately precipitated with bicarbonate and sodium hydroxide.

This suggests that the weak link in the electrolyte system is precipitation of calcium on the internal surface of an unprotected cathode membrane. Therefore, the placement of a more selective membrane at the cathode boundary creates a very robust electrolyte system that is virtually undisturbed by calcium. Since soluble calcium does cross the exclusionary membrane, it is interesting that process degradation does not occur. This may indicate that the exclusionary membrane additionally acts to discourage the precipitation of calcium on the internal cathode cell boundary.

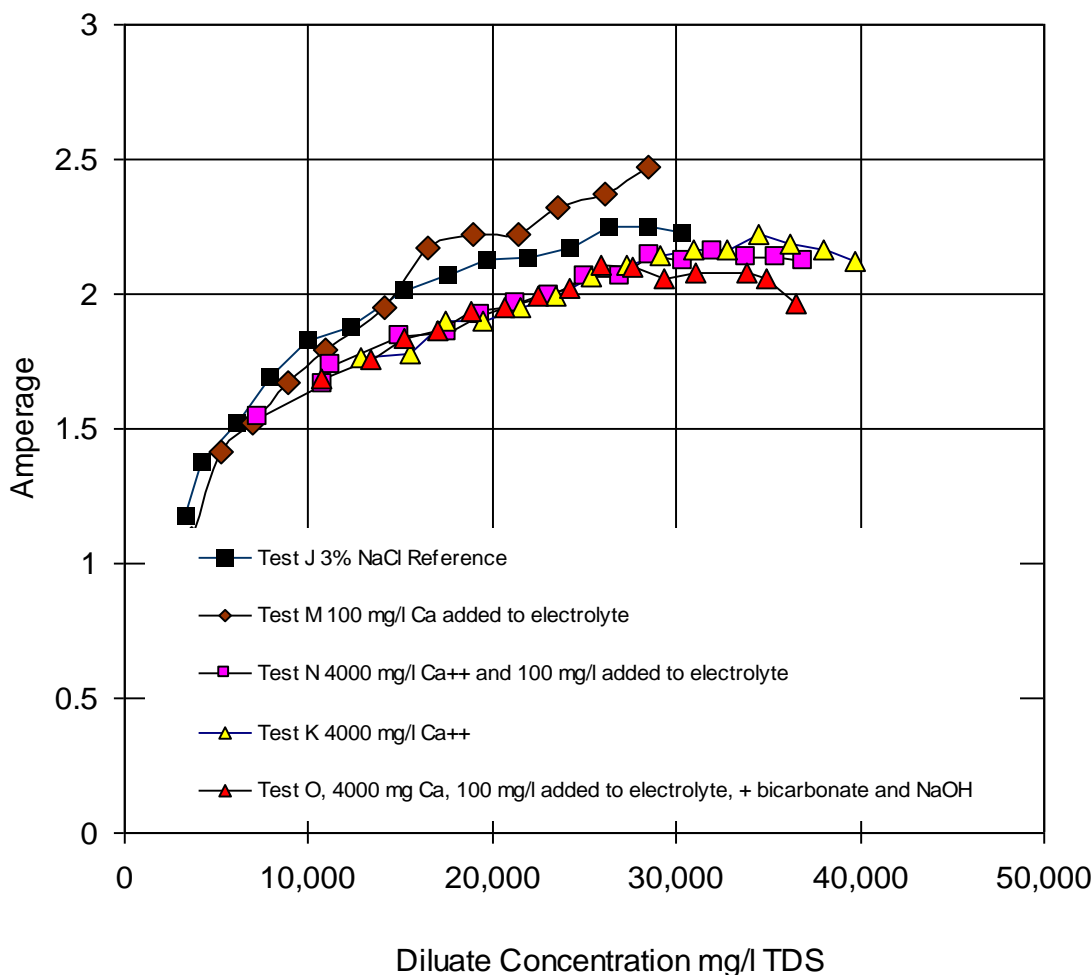


Figure 41: Unexpected Benefits of Cathode Protection from Calcium

7.6 Effect of Multivalent Cations

The previous section was an investigation into the effects of calcium on electrodialysis. A change of the single cathode barrier membrane to the CMX-S material appeared to reduce the detrimental effects of calcium on ED performance. Other cations are prevalent in the flowback water from shale gas hydraulic fracture operations. In particular, the other cations are magnesium, barium and iron. This section focuses on identifying the extent of the problems expected with these other cations with the CMX-S barrier membrane in place.

A series of four full electrodialysis runs, Test Q, R, S, and T were performed.

Test Q (Figure 42) used test water composed of 3% NaCl with 600 mg/l magnesium added as the chloride salt. Performance appeared very to be very similar to runs with pure sodium chloride. Chemical data are presented in Table 18. The relative transfer rate of magnesium between the diluate and the concentrate was about 50% higher than sodium.

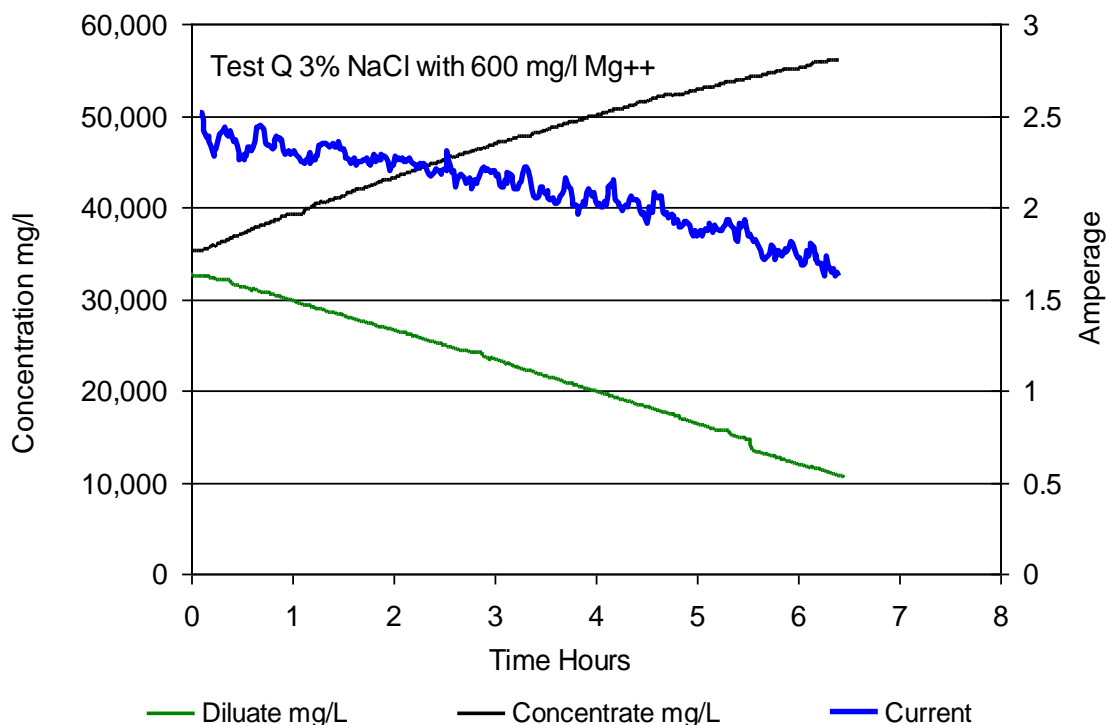


Figure 42: Test Q: Effect of Magnesium on ED performance

Table 18: Chemical Analyses, Tests with Protected Cathode Test Q Magnesium				
	Na mg/l	Ca mg/l	Mg mg/l	TDS mg/l
Feed	11,000	56	530	34,195
Concentrate	18,000	60	970	56,271
Diluate	4,000	0.51	29	10,546
Initial Electrolyte	24,000	27	4.9	
Final Electrolyte	24,000	33	27	

Test R was performed with 3% sodium chloride plus 400 mg/l barium, 3,200 mg/l calcium, 500 mg/l magnesium with no additional iron added. The full run results are shown in Figure 43. The rate of salt concentration was greatly diminished as compared to Test Q. Chemical data are presented in Table 19. Calcium, Magnesium, and barium readily cross the membrane stack from the diluate to the concentrate. Magnesium appears to cross to the concentrate at a relative rate slightly higher to the flux of sodium. Calcium and Barium are transported to the concentrate relatively faster than sodium. Calcium and magnesium collect in the electrolyte. Barium is either not easily transported in to the electrolyte, or it is immediately precipitated (barium sulfate) and is not collectable in the electrolyte samples.

Table 19: Test R with Protected Cathode ; Magnesium, Barium and Calcium					
	Na mg/l	Ca mg/l	Mg mg/l	Ba mg/l	TDS mg/l
Feed	11,000	3,200	500	360	41,200
Concentrate	17,000	6,300	650	770	60,090
Diluate	6,300	930	230	25	22,080
Initial Electrolyte	26,000	7.1	8.3	0.18	
Final Electrolyte	26,000	470	45	0.18	

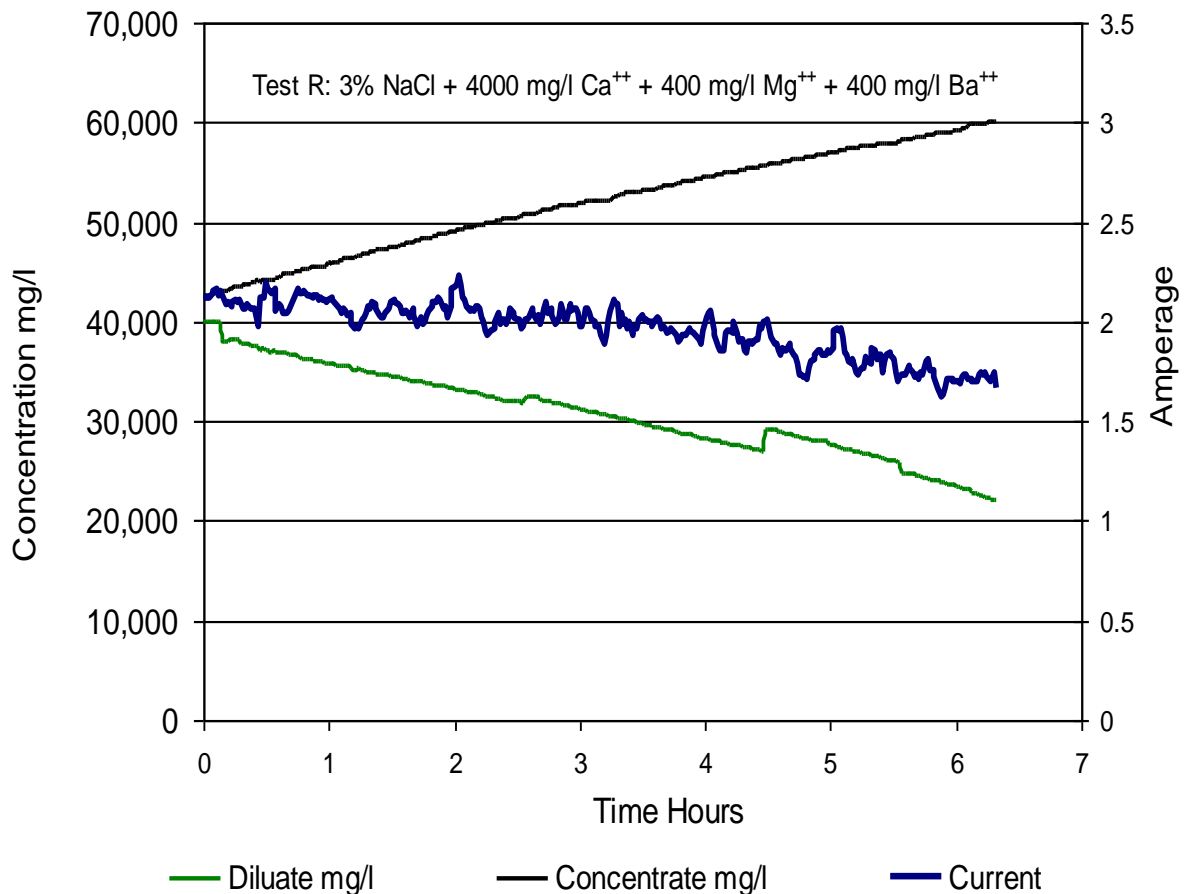


Figure 43: Test R, Effect of Calcium, Barium, and Magnesium

Test S was initiated with the re-blended water from Test R (3% sodium chloride plus 400 mg/l barium, 3,200 mg/l calcium, 500 mg/l magnesium with no additional iron added). An initial volt-amp profile was conducted. About 40 g/l iron as ferric chloride was then added to the test water and a second volt-amp profile was recorded. The iron was sufficient to cause immediate precipitation in the concentrate and diluate tanks. The volt-amp profiles are presented in Figure 44 and show an immediate loss of 20% of the current by the addition of the iron.

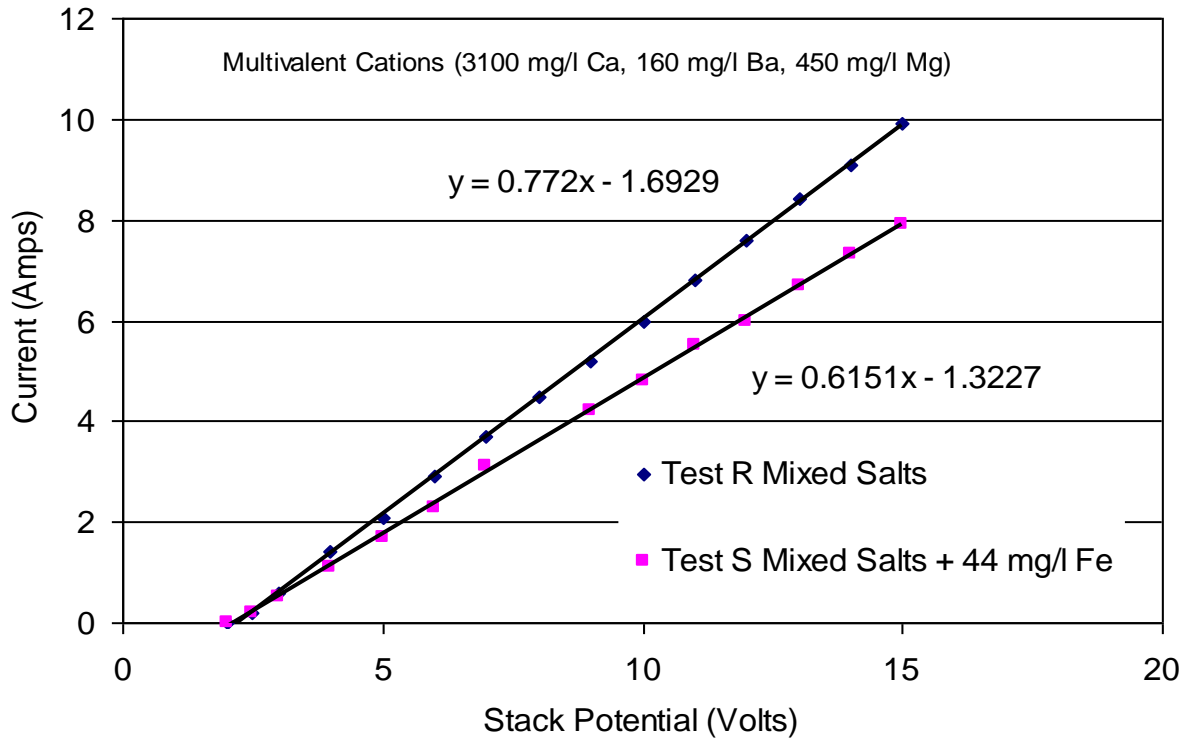


Figure 44: Test S, Immediate Loss of Current Density by Addition of 44 mg/l Fe

Test S resumed with a full ED run (Figure 45). The iron addition was enough to cause immediate precipitation within the feed tanks. The rate of salt concentration was greatly diminished as compared to either Test Q or R. Chemical data are presented in Table 20. Calcium, magnesium, and barium readily cross the membrane stack from the diluate to the concentrate. Calcium and Barium are transported to the concentrate relatively faster than sodium. In this test, the iron transport to the concentrate was about an equivalent relative rate as sodium. Barium was either not easily transported in to the electrolyte, or it was immediately precipitated (barium sulfate) and not collected in the electrolyte samples. Iron did not appear to cross into the electrolyte. Surprisingly, magnesium did not further concentrate in the electrolyte.

Table 20: Test S with Protected Cathode ; Magnesium, Barium, Calcium and Iron						
	Na mg/l	Ca mg/l	Mg mg/l	Ba mg/l	Fe mg/l	TDS mg/l
Feed	11000	3100	440	160	44	41400
Concentrate	17000	5700	650	360	50	58070
Diluate	7800	840	290	57	22	25400
Initial Electrolyte	27000	350	54	0.29	1.7	
Final Electrolyte	28000	420	55	0.29	1.7	

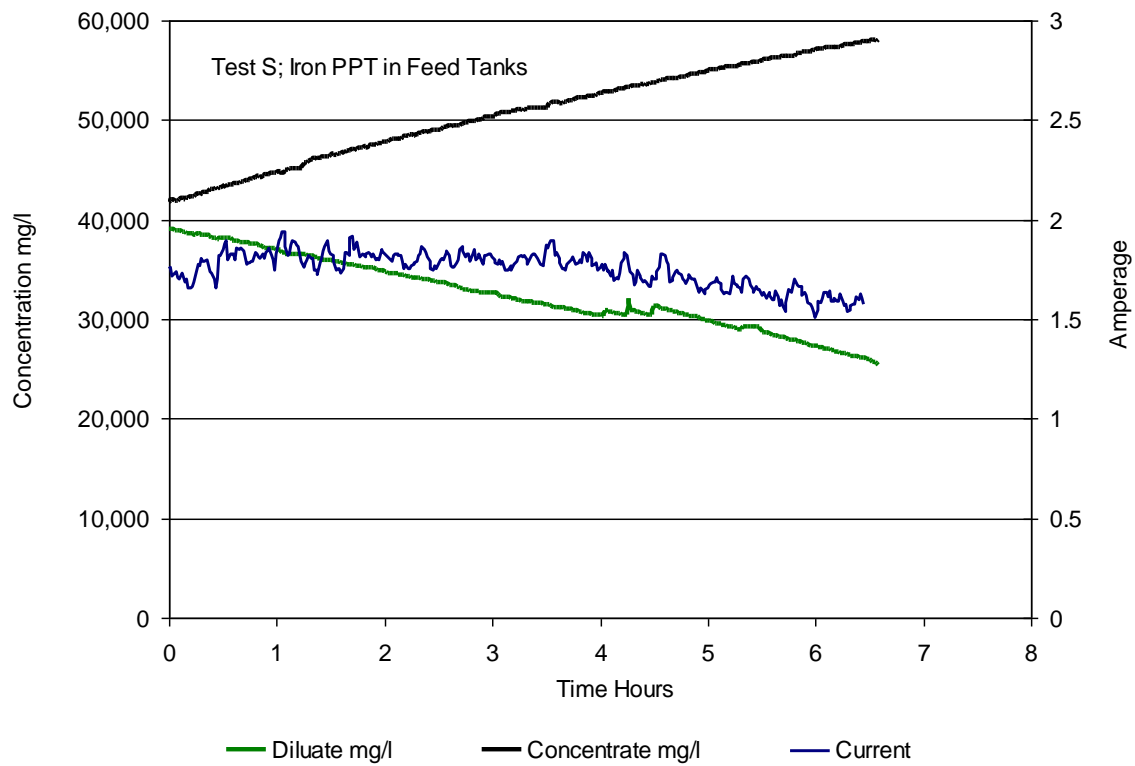


Figure 45 Test S with Precipitated Iron in Test Water

A final Test T was performed in this series as a repeat of Test S with fresh electrolyte and test water. The results are presented in Figure 46. The overall rate of salt transfer was equivalent to Test S. Calcium, magnesium, and barium readily cross the membrane stack from the diluate to the concentrate. Calcium and Barium are transported to the concentrate relatively faster than sodium. In this test, the iron concentration in the concentrate is lower than the feed stock, possibly indicating that iron is not soluble. Barium is either not easily transported in to the electrolyte, or it is immediately precipitated (barium sulfate) and is not collectable in the electrolyte samples. Iron does not appear to cross into the electrolyte. Surprisingly, magnesium did not further concentrate in the electrolyte.

Table 21: Test T with Protected Cathode ; Magnesium, Barium, Calcium and Iron						
	Na mg/l	Ca mg/l	Mg mg/l	Ba mg/l	Fe mg/l	TDS mg/l
Feed	9600	2500	570	370	64	40800
Concentrate	21000	6000	820	620	45	57046
Diluate	7500	510	180	61	28	21100
Initial Electrolyte	23000	52	1.3	0.17	< 0.83	
Final Electrolyte	23000	180	2	0.16	0.86	

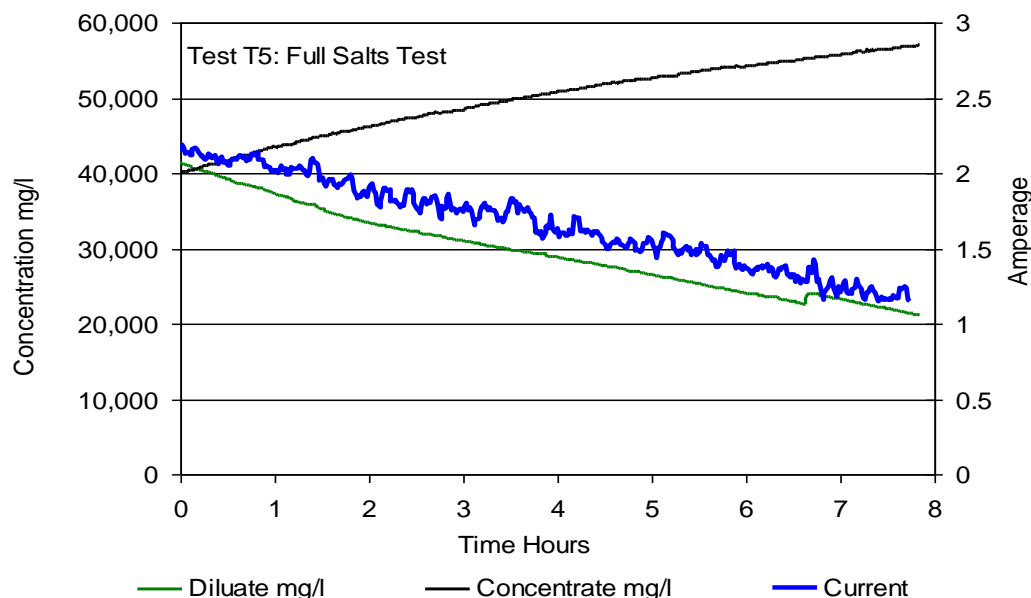


Figure 46: Test T, Full Salt Test Repeat of Test S

Figure 47 is a summary of current density data for the test series Q,R,S, and T. Test Q with magnesium only compares favorably with Test J with pure sodium chloride. Test R with calcium, barium, and magnesium shows a loss of efficiency compared to reference Test K, with 4000 mg/l calcium. Addition of iron in tests T and S is seen to cause large decrease in current density.

7.7 Clean-in-Place Pulsed Pole Reversal

In highly concentrated brines containing significant concentrations of multivalent cations, such as magnesium, calcium, barium, and iron, the cations can cause immediate and long term loss of overall ion flux (amps) for a given voltage. In conventional electrodialysis, the presence of these multivalent cations ions would cause frequent cleaning of the electrodes. Conventional cleaning usually involves alternating flushes of both the electrode cells and the treatment cells with a strong acid (e.g. 1% HCl) followed by strong base (e.g., 1% NaOH). Conventional washing also requires significant down time. An additional disadvantage of conventional cleaning is the need for handling and storage of strong chemical cleaning agents.

Pole reversal is routinely performed in modified conventional electrodialysis systems. In these modified conventional systems, the electrode polarity is switched for extended periods of time, up to several hours per switch. In order to accommodate this reversal, there must also be a hydraulic shift that changes the concentrate stream to become the diluate stream, and vice-versa.

This section describes the development of a means of cleaning the electrode cells by pulsed pole reversal. Periodic pulsed pole reversal was used to provide a rapid partial disruption of the fouling of the electrode cell by divalent cations. The pole reversal was performed in these tests by simply switching the anode and cathode wires at the electrodes. Arbitrary pulse times of several seconds up to one minute and potentials of 5 to 15 volts were applied, as described for each test.

As performed in the following tests, pole reversal has an inherent inefficiency. During the pole reversal, the normal ion flow from the diluate to the concentrate is temporarily reversed, causing a back-flow of ions from the concentrate to the diluate. The magnitude of this inefficiency may be calculated by comparing the electricity use, as measured by amp-seconds in the overall forward reaction (normal operation) process compared to the amp-seconds applied during the pole reversal.

The Forward Reaction (ions flowing from the diluate to the concentrate) is the product of the average current throughout the run and the time in the normal operating mode (amp-seconds). The time expended in the normal operating mode is the total time of the run minus the time in CIP-pole reversal mode.

When in the CIP-pole reversal mode, the ion flux throughout the ED unit is reversed, with ions flowing from the concentrate to the diluate, causing a Reverse Reaction. The Reverse Reaction (amp-seconds) is estimated as sum of the products of the time expended in the individual

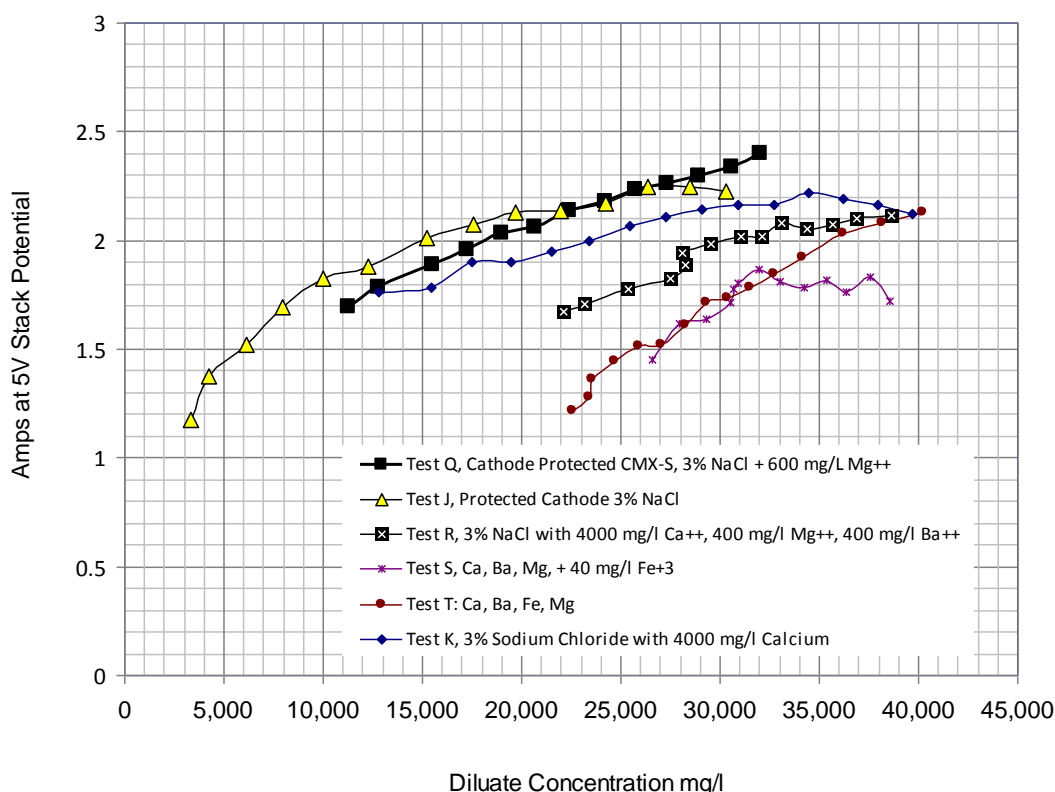


Figure 47: Summary Effects of Various Cation Blends on Current Density

reversals and the observed current during the reversal. In the various examples in this report the imposed reverse flux is from 4 to 14 percent of the forward flux.

The relative flux efficiency between a normal ED run (without CIP) and an ED run with CIP is estimated from the final concentrate and diluate concentrations. The difference between the final concentrate concentration and the final diluate concentration in any test is an estimate of the ion flux. The relative flux efficiency is calculated as the ratio of the ion flux estimate of the run with CIP divided by the estimate without CIP. The value of the relative flux efficiency is reported as a percentage improvement which is calculated as $100 \times (1 - \text{relative flux efficiency})$.

Test U was similar to test conditions previously described for tests S and T and represents the baseline for the CIP procedures. This test was conducted in the normal operating mode without pulsed pole reversal. The test solution in this example was prepared with of 30 g/l NaCl, 3,500 mg/l Ca⁺⁺ from calcium chloride, 400 mg/l Mg⁺⁺ from magnesium chloride, 400 mg/l Ba⁺⁺ from barium chloride, and 60 mg/l Fe⁺⁺⁺ from ferric chloride added to deionized water. Figure 48 shows the concentration of salts in the diluate and concentrate streams and the amperage as a function of elapsed time. The figure also shows the average amperage draw throughout the test run. After six hours, the diluate concentration had dropped from about 40,000 mg/l to about 27,000 mg/l. The current had dropped to less than 0.5 amps with an average current of about 1.25 amps. The total electrical use was (1.25 amps x 6 hours x 60 x 60 = 27,000) amp-seconds. Chemical analyses are presented in Table 22.

	Na mg/l	Ca mg/l	Mg mg/l	Ba mg/l	Fe mg/l	TDS mg/l
Feed	11000	3500	380	400	64	41,100
Concentrate	16000	6300	580	760	63	52,650
Diluate	8200	1600	290	80	21	28,050
Initial Electrolyte	26000	46	3.4	0.081	0.67	
Final Electrolyte	25000	160	6.9	1.5	1.7	

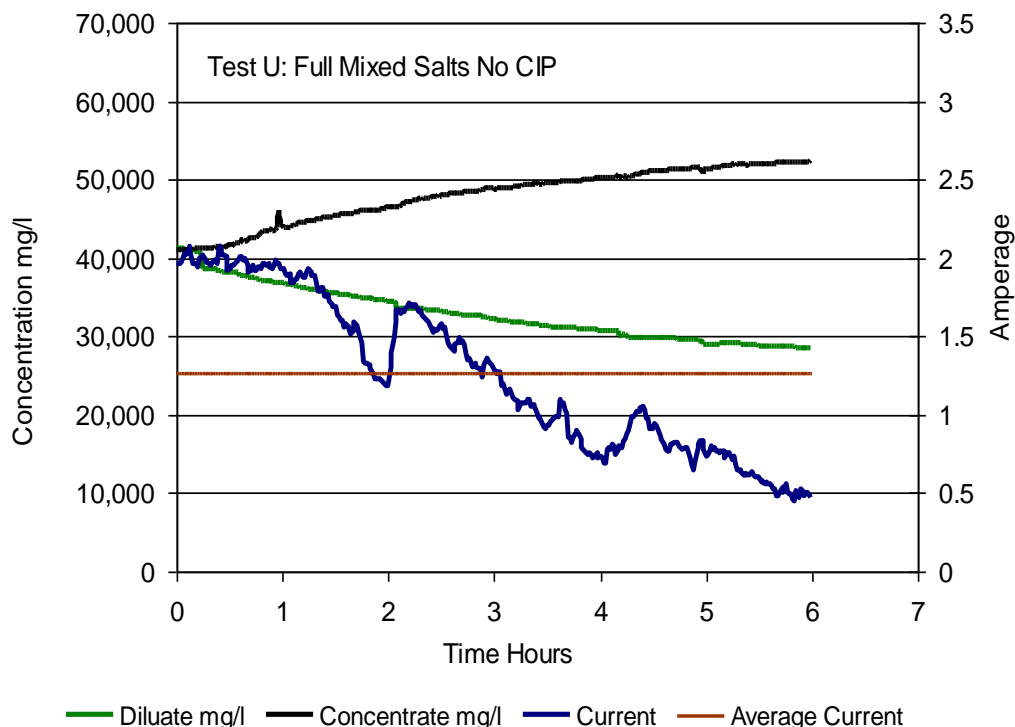


Figure 48: Mixed Salt Test U, Baseline without Clean-in-Place Pole Reversal

Test X was conducted in two parts. The feed stock was first made with 3% NaCl in deionized water. A volt-amp profile was conducted to be sure that the ED stack was sufficiently clean and operating up to initial standards. A mixture of concentrated brine was added to make up the initial feed water to 4000 mg/l Ca^{++} from calcium chloride, 400 mg/l Mg^{++} from magnesium chloride, 400 mg/l Ba^{++} from barium chloride, and 40 mg/l Fe^{+++} from ferric chloride. A second volt-amp profile was then conducted. The results from this pair of VA profiles are presented in Figure 49. The loss of performance by the addition of complex cations was immediate and significant, amounting to about 20% loss of current.

Test X then proceeded with full operation including an arbitrary pole reversal regime (15V reverse pulse applied for one minute every hour). Figure 50 shows the concentration of the diluate and concentrate streams and the amperage as a function of elapsed time. The figure also shows the average amperage draw throughout the test run. After six hours, the diluate concentration had dropped from about 38000 mg/l to about 20,000 mg/l. The current had dropped to less than 1.2 amps with an average current of about 1.5 amps.

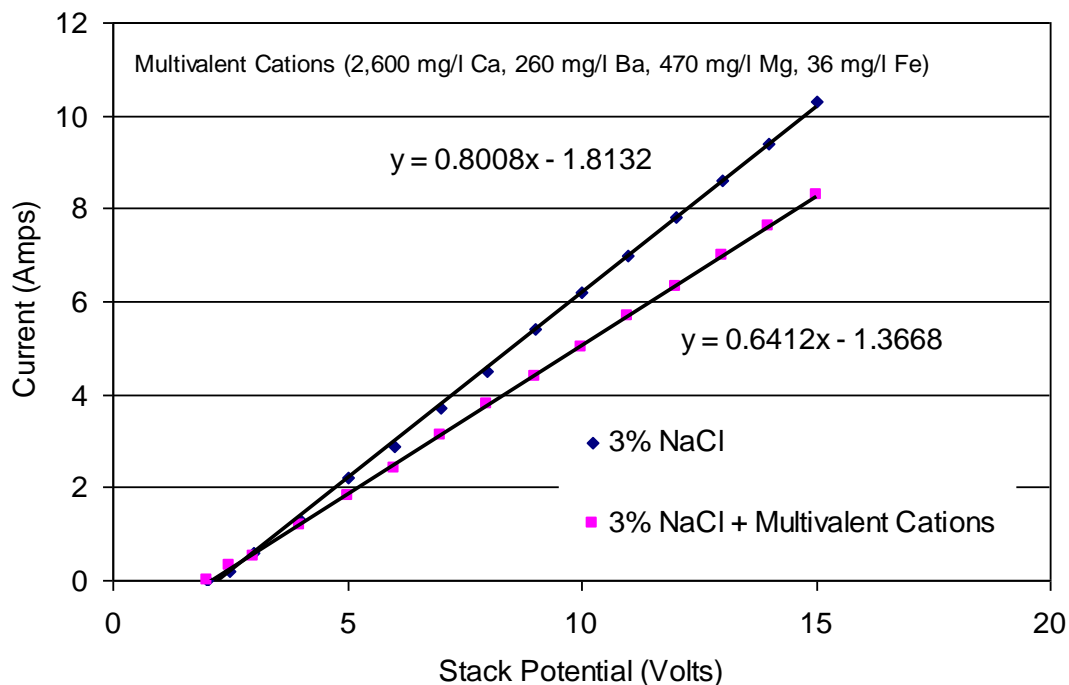


Figure 49: Immediate Loss of Current by Addition of Complex Salts to NaCl, Test X

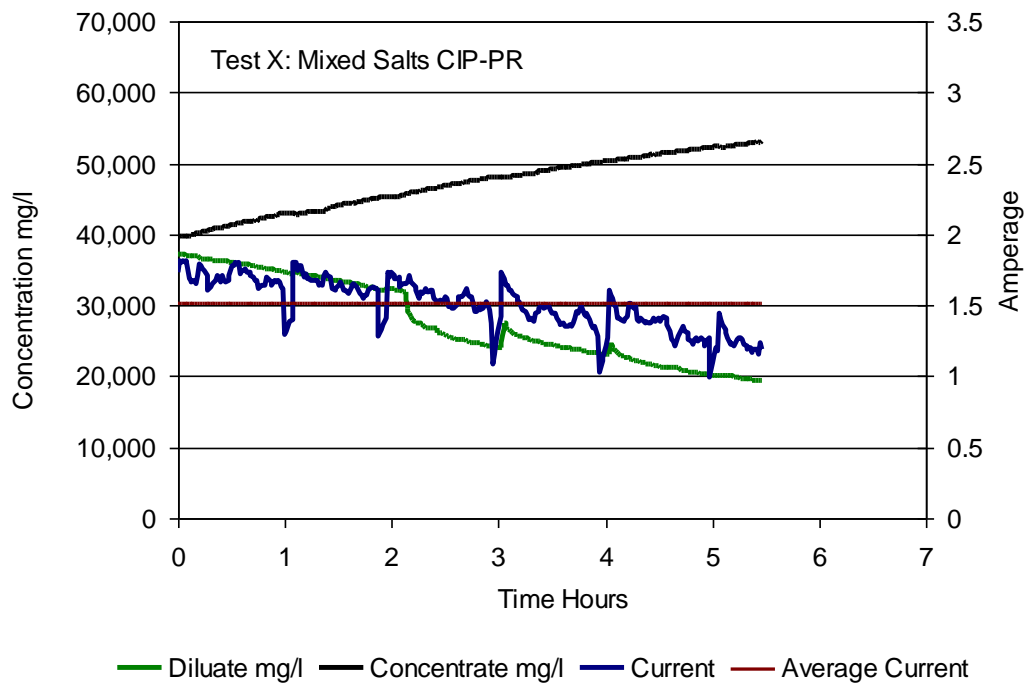


Figure 50: Test X: Mixed Salt Test with Clean-in-Place Pole Reversal

The total electrical use for the forward reaction was about 1.5 amps x (6 hours x 60 x 60 - 5 minutes x 60) = 32,355 amp-seconds. The pulsed pattern in the amperage data reflects the imposition of the pole reversal. The total reverse reaction electrical use was 2,814 amp-seconds (Table 23). The total electrical use was 32,355 + 2,814 = 35,169 amp-seconds. The reverse reaction represented about 8 percent of the total electrical use.

Table 23: CIP Regime for Test X: Mixed Salts Test				
Hours	Volts	Amps	Seconds	Amp-Seconds
1	15	9.3	60	558
2	15	9.3	60	558
3	15	9.7	60	582
4	15	9.3	60	558
5	15	9.3	60	558
Total Amp-Seconds Expended				2,814

Table 24: Test X with CIP-PR ; Magnesium, Barium, Calcium and Iron						
	Na mg/l	Ca mg/l	Mg mg/l	Ba mg/l	Fe mg/l	TDS mg/l
Feed	11,000	2,600	470	260	36	38,500
Concentrate	16,000	5,100	750	500	63	53,058
Diluate	8,200	290	160	14	3.9	19,294
Initial Electrolyte	26,000	55	3.6	< 0.2	0.74	
Final Electrolyte	25,000	94	5.6	0.17	1.1	

Figures 51 and 53 indicate that the pole reversal can even out the current throughout the ED stack run. Table 25 is a summary of operations from the two example tests. Test X (with CIP-PR) had a slightly higher average current (1.5 amps) compared to Test U (no CIP-PR) with a current of 1.25 amps. The flux of TDS salts between the diluate and the concentrate was improved by about 37% by the expenditure of 2,800 amp-seconds in pole reversal.

Table 25: Summary of CIP-PR Improvements with Lab Examples U and X								
	Initial TDS	Diluate TDS	Conc. TDS	Avg. Amps @ 5V	Forward Reaction Amp-sec	Reverse CIP-Amp-Sec	Ion Flux Increase CIP-PR	kWh/lb
Test U No CIP	41,100	28,050	52,650	1.25	27,000	0	NA	0.131
Test X CIP-PR	38,500	19,200	53,050	1.50	32,355	2,800	37%	0.129

7.8 Samples from the Barnett and the Marcellus

Two test waters were received from sites in the Barnett, Taylor Dooley Site #3 and Maggie Spain. Two test waters were received from sites in the Marcellus, labeled Marcellus Unlabeled, and Mcadoo.

The Taylor Dooley sample was initially red with iron, with a pH of 5.6, a conductivity of 128 mS/cm, and a TDS of 150,000 mg/l. About 0.2 g NaOH was added to 18 liters of sample to achieve a pH of 6.2 units. The sample was then aerated 10 minutes at 1 l/min air flow. The aerated material was settled for 3 hours. The decanted liquor was filtered on an Ace Hardware 5 µ household filter. Chemical analyses of samples from raw material, decanted water, and filtered water are presented in Table 26. Barium, calcium, and magnesium seemed unaffected by the pretreatment regime. About 25% of the iron was removed. The sample was extremely conductive, and beyond the expected capacity of the ED stack. The sample was therefore diluted about 1 volume of sample to 1 volume of tap water to make the working samples in the following section.

The Maggie Spain sample was initially black with an organic sulfide odor. The initial pH was 6.5 units with a conductivity of about 69 mS/cm, and a TDS of about 68,000 mg/l. About 9.9 g NaOH was added to 20 liters of sample to achieve a pH of 9.9 units. The sample was then aerated 15 minutes at 1 l/min air flow. The aerated material was settled for about 16 hours. The decanted liquor was filtered on an Ace Hardware 5 µ household filter. Chemical analyses of samples from raw material, decanted water, and filtered water are presented in Table 267. Barium, calcium, and magnesium seemed unaffected by the pretreatment regime. About 50% of the iron was removed. The sample was extremely conductive, however it was at the upper range

of expected treatment with the ED. The sample was therefore used, as described, in the first pair of tests. A second series of three tests was performed using about a 1:1 volume dilution with tap water.

The Mcadoo sample was initially red with iron, with a pH of 5.6, a conductivity of 140 mS/cm, and a TDS of 180,000 mg/l. Precipitated iron was evident on the bottom of the sample bottle prior to initial mixing. NaOH was added to achieve a pH of 8.9 to aide in precipitation of iron. The sample was then aerated 10 minutes at 1 l/min air flow. The aerated material was settled for 14 hours. The decanted liquor was filtered on an Ace Hardware 5 μ household filter. Chemical analyses of samples from raw material, decanted water, and filtered water are presented in Table 27. Barium, calcium, and magnesium seemed unaffected by the pretreatment regime. About 30% of the iron was removed. The sample was extremely conductive, and beyond the expected capacity of the ED stack. The sample was therefore diluted about 1 volume of sample to 2 volumes of tap water to make the working samples in the following section.

Table 26: Initial Treatment of Samples from the Barnett						
	Taylor Dooley			Maggie Spain		
	Raw	Decant	Filtered	Raw	Decant	Filtered
Barium (mg/l)	66	110	99	25	28	22
Calcium (mg/l)	6000	6500	6300	2600	2100	2100
Iron (mg/l)	110	100	74	52	23	24
Magnesium (mg/l)	810	870	860	340	320	270
Sodium (mg/l)	31000	33000	33000	14000	14000	15000
Chloride (mg/l)	70000	70000	68000	27000	29000	29000
Sulfate	< 20	< 20	< 20	105	183	216
Hardness (As CaCO ₃)	18000	20000	17000	8000	6400	6400
Acidity (As CaCO ₃)	240	100	100	190	12	12
Alkalinity, Bicarbonate (CaCO ₃)	180	110	100	440	ND	160
Alkalinity, Carbonate (CaCO ₃)	< 10	< 10	< 10	< 10	120	< 10
Alkalinity, Hydroxide (CaCO ₃)	NA	NA	NA	NA	220	ND
Alkalinity, Total (CaCO ₃)	180	110	100	440	340	160
Total Dissolved Solids (mg/l)	150000	160000	150000	68000	62000	62000
Total Suspended Solids (mg/l)	880	310	< 160	220	< 64	ND
Total Organic Carbon (mg/l)	ND	ND	ND	ND	10	ND
pH	5.6	6.2	ND	6.5	9.9	ND
Conductivity (mS/cm)	128	ND	ND	69	ND	ND
	Raw sample red with iron. Added 0.2 g NaOH to 18 liters to ph 6.2. Aerated 10 minutes at 1 l/min. Settled 3 hr, decanted, Filtered on Ace Hardware 5 μ household filter.			Raw sample black with strong sulfide/organic odor. Added 18 g NaOH to 20 liters to pH 9.9. Aerated 15 minutes at 1 l/min. Settled 15 hr, decanted. Filtered on Ace Hardware 5 μ household filter.		

The unlabeled Marcellus sample was initially red with iron, with a pH of 4, a conductivity of 163 mS/cm, and a TDS of 220,000 mg/l. Precipitated iron was evident on the bottom of the sample bottle prior to initial mixing. NaOH was added to achieve a pH of 8.6 to aide in precipitation of iron. The sample was then aerated 10 minutes at 1 l/min air flow. The aerated material was settled for 14 hours. The decanted liquor was filtered on an Ace Hardware 5 μ household filter. After an additional 24 hours, the sample was again filled with precipitated iron. The sample was filtered a second time. Chemical analyses of samples from raw material, decanted water, and filtered water (second filtration) are presented in Table 27. Barium, calcium, and magnesium seemed unaffected by the pretreatment regime. About 20% of the iron was removed. The sample was extremely conductive, and beyond the expected capacity of the ED stack. The sample was therefore diluted about 1 volumes of sample to 4 volumes of tap water to make the working samples in the following section.

Table 27: Initial Treatment of Samples from the Marcellus						
	Mcadoo			Marcellus Unlabeled		
	Raw	Decant	Filtered	Raw	Decant	Filtered
Barium (mg/l)	76	44	46	190	160	180
Calcium (mg/l)	13000	12000	11000	17000	16000	17000
Iron (mg/l)	93	67	61	340	290	290
Magnesium (mg/l)	990	900	910	1800	1900	1600
Sodium (mg/l)	42000	39000	35000	43000	35000	44000
Chloride (mg/l)	84000	88000	87000	110000	100000	110000
Sulfate	45.8	51.3	39.8	< 20	< 20	< 20
Hardness (As CaCO ₃)	37000	34000	31000	50000	48000	49000
Acidity (As CaCO ₃)	< 11	< 11	< 11	< 11	20	20
Alkalinity, Bicarbonate (CaCO ₃)	< 10	68	300	< 10	60	24
Alkalinity, Carbonate (CaCO ₃)	160	390	< 10	150	< 10	< 10
Alkalinity, Hydroxide (CaCO ₃)	200			190		
Alkalinity, Total (CaCO ₃)	370	460	300	340	60	24
Total Dissolved Solids (mg/l)	180000	180000	190000	220000	260000	270000
Total Suspended Solids (mg/l)	ND	ND	ND	ND	ND	ND
Total Organic Carbon (mg/l)	ND	ND	ND	ND	ND	ND
pH	5.6	6.2	ND	4.0	9.9	ND
Conductivity (mS/cm)	140	ND	ND	163	ND	ND
	Raw sample red with iron, slight organic odor. Added NaOH to pH 8.9. Aerated 10 minutes at 1 l/min. Settled 14 hr, decanted, Filtered on Ace Hardware 5 μ household filter.			Raw sample red with iron, slight organic odor. Added NaOH to pH 8.6. Aerated 15 minutes at 1 l/min. Settled 14 hr, decanted. Filtered on Ace Hardware 5 μ filter. Filtered again after 24 hours.		

7.9 Treatment of Field Samples; with and without CIP-PR

The results in this section were designed to 1) demonstrate electrodialysis on pretreated field samples and 2) continue the development of the clean-in-place concept. The results are reported

by field sample, first the treatment without in-place cleaning, followed by results with a CIP regime.

7.9.1 Taylor Dooley from the Barnett

Field brine from Taylor Dooley Natural Gas Hydrofracture was treated with normal operation without pulsed pole reversal. The clarified water used in the test contained about 14,000 mg/l Na^+ , 2,600 mg/l Ca^{++} , 31 mg/l Fe^{+++} , 470 mg/l Mg^{++} , 40 mg/l Ba^{++} , and 31,000 mg/l Cl^- . Figure 51 shows the concentration of the diluate and concentrate streams and the amperage as a function of elapsed time. The figure also highlights the average amperage draw throughout the test run. This test was conducted without pulsed pole reversal. After six hours, the diluate concentration had dropped from about 52,700 mg/l to about 39,060 mg/l. The current had dropped to less than 0.5-1.0 amps with an average current of less than 1.3 amps. The overall electrical usage was 28,080 amp-seconds. Chemical data are reported in Table 28. The trends are similar to previously reported, with transport of the multivalent cations freely into the concentrate, and limited recovery (or transport) of barium and iron into the electrolyte.

Table 28: Test TD without CIP-PR ; Magnesium, Barium, Calcium and Iron, Taylor Dooley						
	Na mg/l	Ca mg/l	Mg mg/l	Ba mg/l	Fe mg/l	TDS mg/l
Feed	14000	2600	470	40	31	52,700
Concentrate	19000	4200	510	69	44	65,400
Diluate	9600	890	250	4.7	8.4	39,050
Initial Electrolyte	34000	< 2	< 1	0.078	< 1	
Final Electrolyte	27000	55	< 20	0.078	< 1	
TDS data reflect conductivity probe reading at 6 hours						

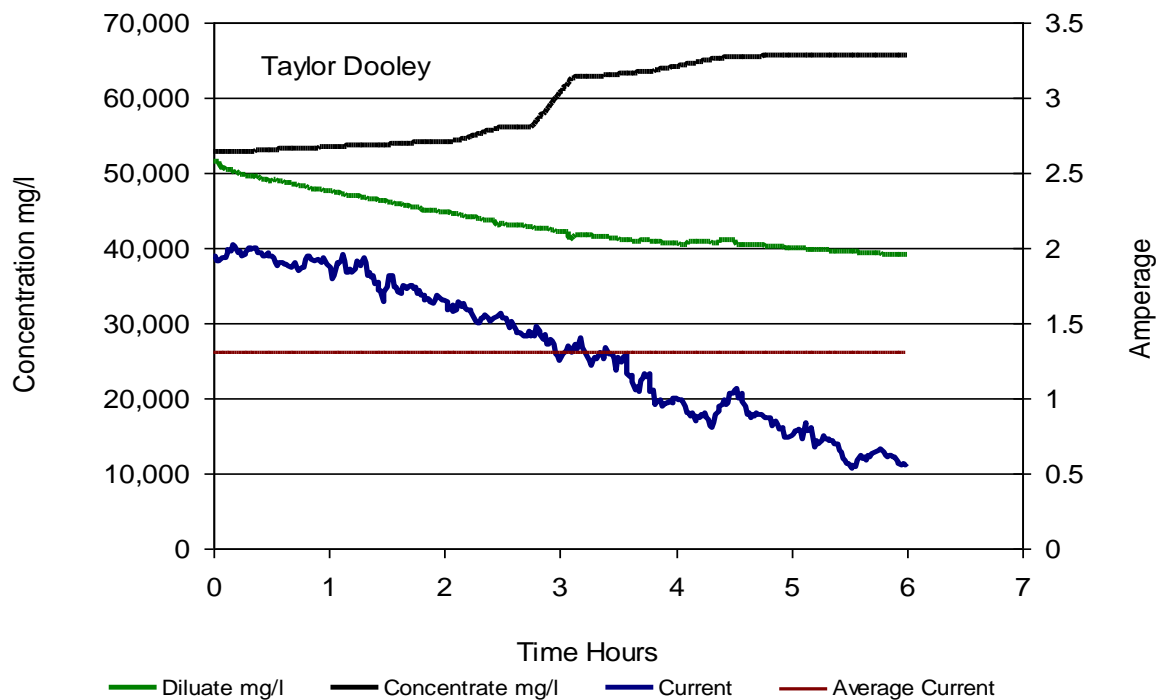


Figure 51: Taylor Dooley Barnett Shale Sample, no CIP

The Taylor Dooley water from the previous test was re-blended for retesting with a clean-in-place regime. The arbitrary pole reversal was one minute every hour at 15 V. Figure 52 shows the concentration of salts as mg/l sodium chloride in the diluate and concentrate streams and the amperage as a function of elapsed time. The sequence of reversals is presented in Table 29. The current dropped from an initial value of about 1.9 amps to less than 1.2 amps after 1 hour. The pole reversals are shown to boost the amperage periodically up to about 2 amps. After 6 hours, the diluate concentration had dropped from about 52,700 mg/l to about 36,900 mg/l. The average current was about 1.26 amps. The total forward reaction electrical usage was about 1.26 amps x (6 hours x 60 x 60 – 5 minutes x 60) = 26,838 amp-seconds. The reverse reaction electrical use was about 3030 amp-seconds. The total electrical use was 26,838 + 3030 = 29,868 amp seconds. The reversal represented about 10 % of the total. Chemical data are presented in Table 30.

Hours	Volts	Amps	Seconds	Amp-Seconds
1	15	10.2	60	612
2	15	9.9	60	594
3	15	10	60	600
4	15	10.1	60	606
5	15	10.3	60	618
Total Expended Amp-Seconds				3030

Table 30: Test TD with CIP-PR ; Magnesium, Barium, Calcium and Iron, Taylor Dooley						
	Na mg/l	Ca mg/l	Mg mg/l	Ba mg/l	Fe mg/l	TDS mg/l
Feed	16000	3100	580	40	50	52700
Concentrate	20000	4200	640	52	63	63050
Diluate	14000	3100	340	8.7	22	36300
Initial Electrolyte	27000	120	7.5	0.33	1.4	
Final Electrolyte	26000	130	7	0.18	1.3	
TDS data reflect conductivity probe reading at 6 hours						

The summary of ion transport during the 6 hour tests is summarized in Table 31. Apparently the CIP regime used for this test water was not sufficient to create an increased efficiency. However, the reverse flux of ions during the pole reversals did not appear to hamper efficiency.

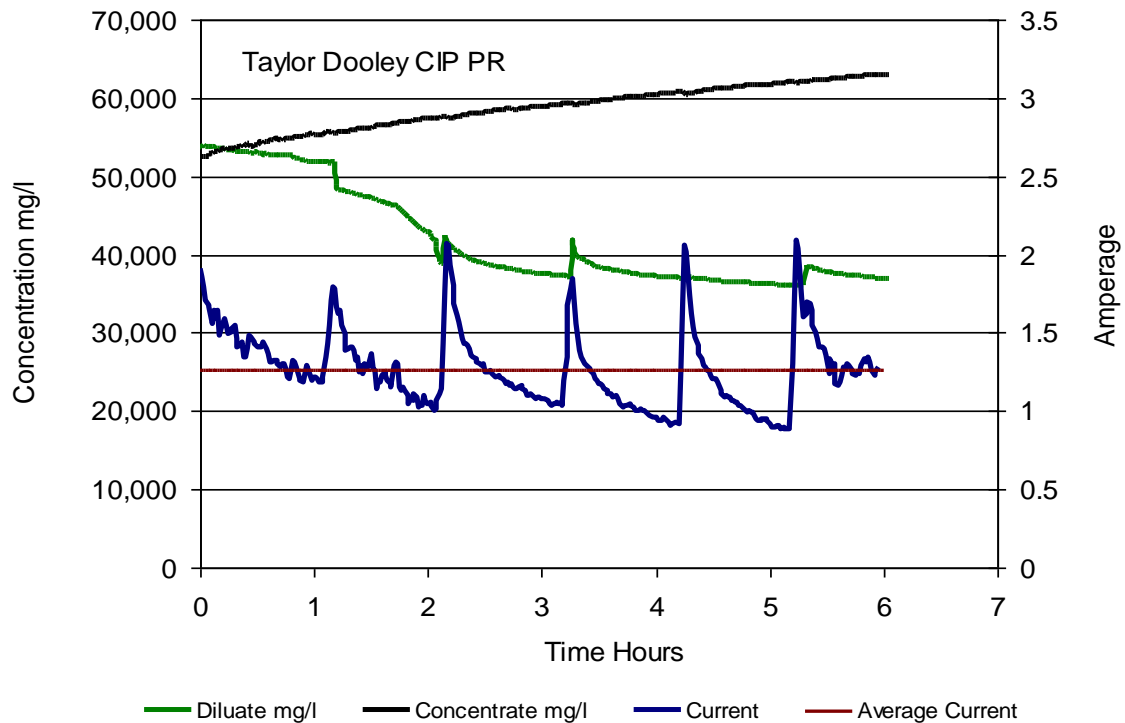


Figure 52: Taylor Dooley Barnett Shale Sample, with CIP

Table 31: Summary of CIP-PR with Taylor Dooley Samples								
	Initial TDS	Diluate TDS	Conc. TDS	Avg. Amps @ 5V	Forward Reaction Amp-sec	Reverse CIP- Amp-Sec	Ion Flux Increase CIP-PR	kWh/lb
TD No CIP	52700	39050	65400	1.30	28,080	0	NA	0.121
TD* CIP-PR	53100	36300	63050	1.26	24,200	3,030	1%	0.118

7.9.2 Maggie Spain from the Barnett

Field brine from Maggie Spain was treated in a normal operation without pulsed pole reversal. The test water contained about 15,000 mg/l Na^+ , 2,100 mg/l Ca^{++} , 24 mg/l Fe^{+++} , 270 mg/l Mg^{++} , 22 mg/l Ba^{++} , and 29,000 mg/l Cl^- . Figure 53 shows the concentration of salts as in the diluate and concentrate streams and the amperage as a function of elapsed time. The figure also highlights the average amperage draw throughout the test run. After six hours, the diluate concentration had dropped from about 45,000 mg/l to about 34,000 mg/l. The current had dropped to less than 0.5-1.0 amps with an average current of less than 1 amp. The overall electrical usage was 20,500 amp-seconds. Chemical analysis of the cations is presented in Table 32.

	Na mg/l	Ca mg/l	Mg mg/l	Ba mg/l	Fe mg/l	TDS mg/l
Feed	15000	2100	270	22	24	44,600
Concentrate	20000	3700	460	37	38	56,500
Diluate	8800	350	110	1.1	3.4	34,500
Initial Electrolyte	26000	72	< 20	0.13	1.3	
Final Electrolyte	27000	130	< 20	0.051	1.8	

TDS data reflect conductivity probe reading at 6 hours

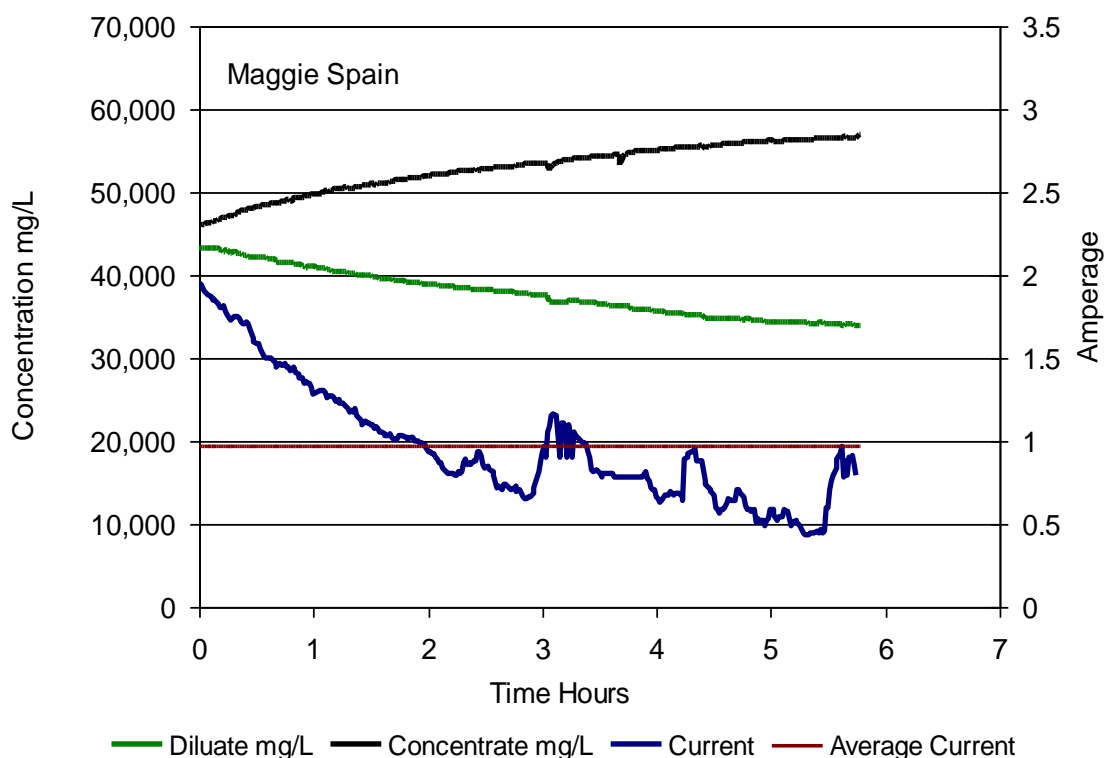


Figure 53: Maggie Spain Field Sample Test without Pulsed Pole Reversal

A companion test with Maggie Spain water was performed with pole reversal. The test solution in this example was the same water from the previous example. The water was re-blended to start the test at the average concentration. The water contained about 15,000 mg/l

Na⁺, 2100 mg/l Ca⁺⁺, 24 mg/l Fe⁺⁺⁺, 270 mg/l Mg⁺⁺, 22 mg/l Ba⁺⁺, and 29,000 mg/l Cl⁻. Chemical analyses are presented in Table 35. An arbitrary pole reversal regime was implemented with a 15V reverse pulse applied for one minute every hour (Table 33). Figure 54 shows the concentration of salts in the diluate and concentrate streams and the amperage as a function of elapsed time. After six hours, the diluate concentration had dropped from about 45,000 mg/l to less than 30,000 mg/l. The current had dropped to less than 0.5-1.0 amps with an average current of about 1.2 amps. The total electrical use for the forward reaction was about 1.2 amps x (6 hours x 60 x 60 - 6 minutes x 60) = 25,488 amp-seconds. The total reverse reaction electrical use was about 3738 amp-seconds. The total electrical use was 25,488 + 3,738 = 29,226 amp-seconds. The reverse reaction represented about 12.8 percent of the total electrical use (Table 36).

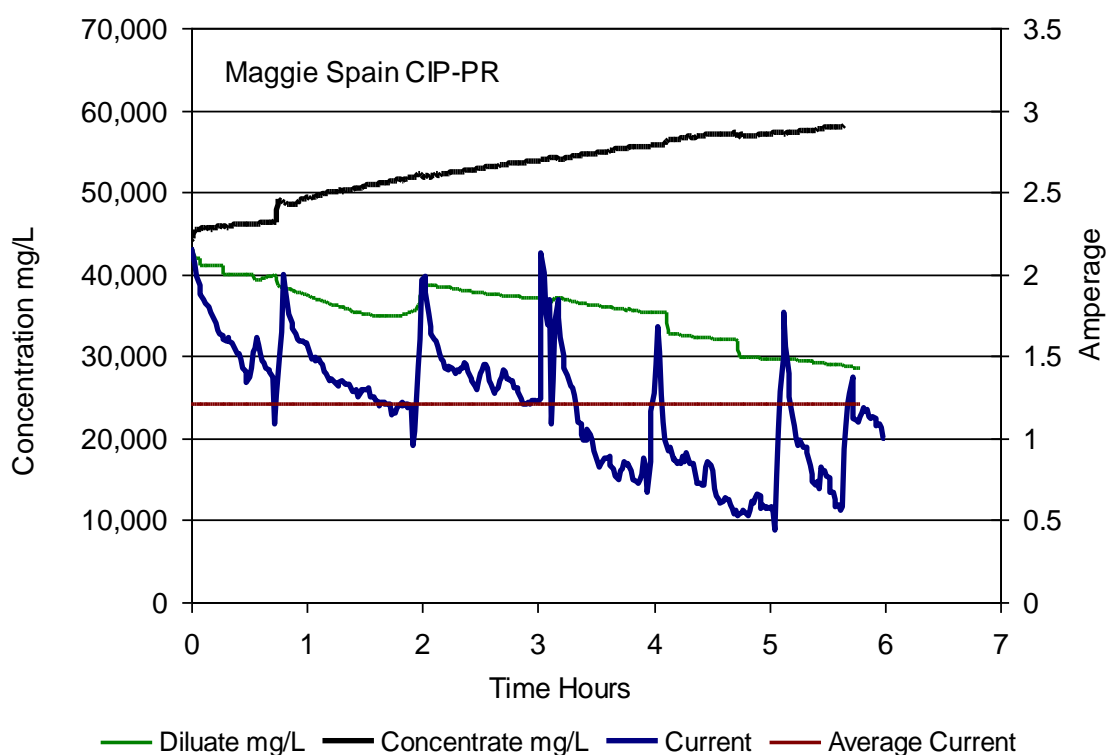


Figure 54: Field Sample Test with Pulsed Pole Reversal, Maggie Spain

Table 33: CIP Regime for the Maggie Spain				
Hours	Volts	Amps	Seconds	Amp-Seconds
1	15	9.5	60	570
2	15	10.5	60	630
3	15	10.4	60	624
4	15	10.7	60	642
5	15	10.6	60	636
6	15	10.6	60	636
Total Amp-Seconds Expended in CIP				3,738

Table 34: Test MS with CIP-PR ; Magnesium, Barium, Calcium and Iron, Maggie Spain						
	Na mg/l	Ca mg/l	Mg mg/l	Ba mg/l	Fe mg/l	TDS mg/l
Feed	10,000	2,600	470	260	36	43,600
Concentrate	13,000	5,100	750	500	63	58,100
Diluate	5,600	290	160	14	3.9	26,960
Initial Electrolyte	18,000	55	3.6	< 0.2	0.74	
Final Electrolyte	31,000	94	5.6	0.17	1.1	
TDS data reflect conductivity probe reading at 6 hours						

Table 35: Summary of CIP-PR Improvements with Maggie Spain Water								
	Initial TDS	Diluate TDS	Conc. TDS	Avg. Amps @ 5V	Forward Reaction Amp-sec	Reverse CIP- Amp-Sec	Ion Flux Increase CIP-PR	kWh/lb
Maggie Spain	44,600	34,500	56,500	1.02	20,500	0	NA	0.131
MS* CIP-PR	43,600	28,500	58,100	1.21	25,488	3,738	37%	0.133

A second series of test was performed with Maggie Spain water. Water from the previous test was recovered from the diluate and concentrate tanks, and re-blended with an equal volume of tap water. The series of tests consists of four parts, an initial run (Run 1) in normal mode; a second run (Run 2) with a CIP-PR regime 10V for 30 seconds every hour; a third run, (Run 3) with a CIP-PR regime 10 V for 15 sec every ½ hour, and a fourth example with an extensive cleaning regime that included acid washing of the electrodes.

Run 1 in the series was performed with the diluted water containing about 7,600 mg/l Na⁺, 1,100 mg/l Ca⁺⁺, 12 mg/l Fe⁺⁺⁺, 150 mg/l Mg⁺⁺, 3.6 mg/l Ba⁺⁺, and 15,600 mg/l Cl⁻. Fresh electrolyte was prepared with 90 g/l disodium sulfate at neutral pH. Run 1 was conducted in normal operating mode without CIP. Figure 55 shows the concentration of salts in the diluate and concentrate streams and the amperage as a function of elapsed time. The figure also shows the average amperage draw throughout the test run. After 7.5 hours, the diluate concentration had dropped from about 24,600 mg/l to about 7,070 mg/l. The current had dropped to less than 0.75 amps with an average current of less than 1.17 amps. The overall electrical usage was 31,590 amp-seconds. Chemical analyses are presented in Table 36.

Table 36: Test Maggie Spain Diluted, without CIP; Mg, Ba, Ca and Fe						
	Na mg/l	Ca mg/l	Mg mg/l	Ba mg/l	Fe mg/l	TDS mg/l
Feed	7600	1100	150	2.8	12	24,500
Concentrate	12000	2100	290	5.7	23	39,700
Diluate	2900	7	4.1	0.79	< 2.5	7,700
Initial Electrolyte	27000	< 5	< 2.5	< 0.1	< 2.5	
Final Electrolyte	24000	27	< 2.5	0.2	< 2.5	
TDS data reflect conductivity probe reading at 6 hours						

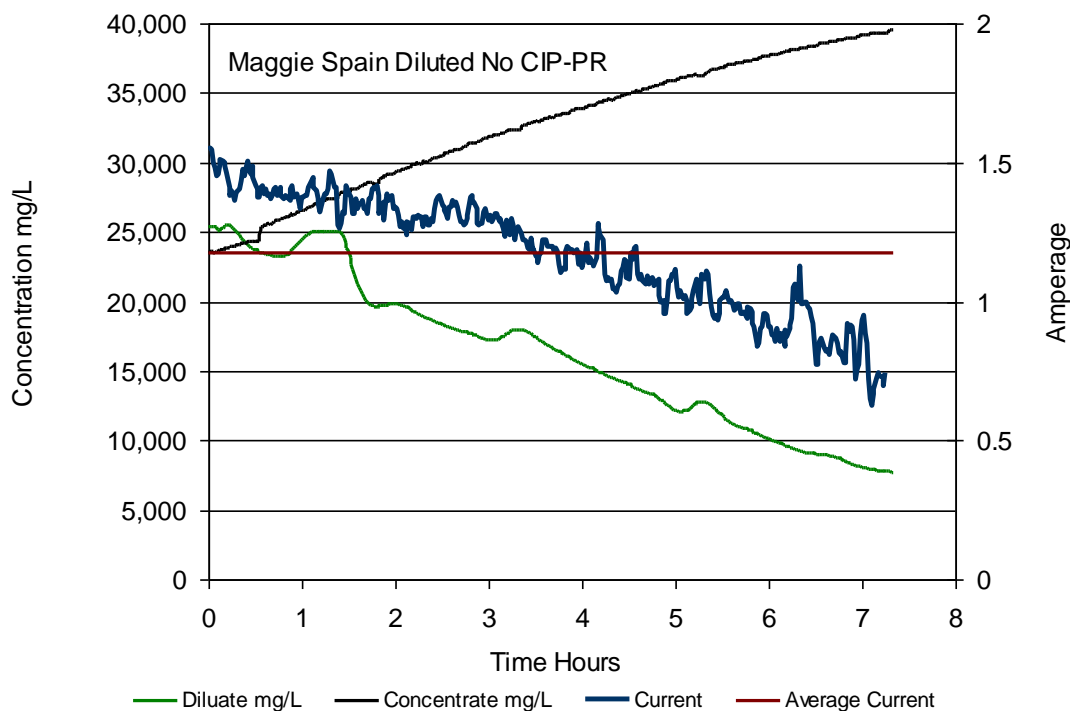


Figure 55: Maggie Spain Field Sample (diluted 1:1) without CIP Pole Reversal

The second test (Run 2) with diluted Maggie Spain water included a CIP pole reversal regime. Water from the previous test was recovered and re-blended to initiate Run 2. Electrolyte was recovered from the previous test, Run 1. An arbitrary CIP pole reversal of 10 V was implemented for 30 seconds once per hour. The pole reversal regime is summarized in Table 37. Figure 56 shows the concentration of salts in the diluate and concentrate streams and the amperage as a function of elapsed time. After 7.5 hours, the diluate concentration had dropped from about 25,000 mg/l to about 9,400 mg/l. The current had dropped to just over 1.0 amps with an average current of about 1.26 amps. The total electrical usage was 34,677 amp-seconds. The reverse polarity accounted for 657 amp-seconds. Overall, the efficiency of the run and total ion flux was nearly identical to Run 1 without CIP. Chemical results for this test are in Table 38.

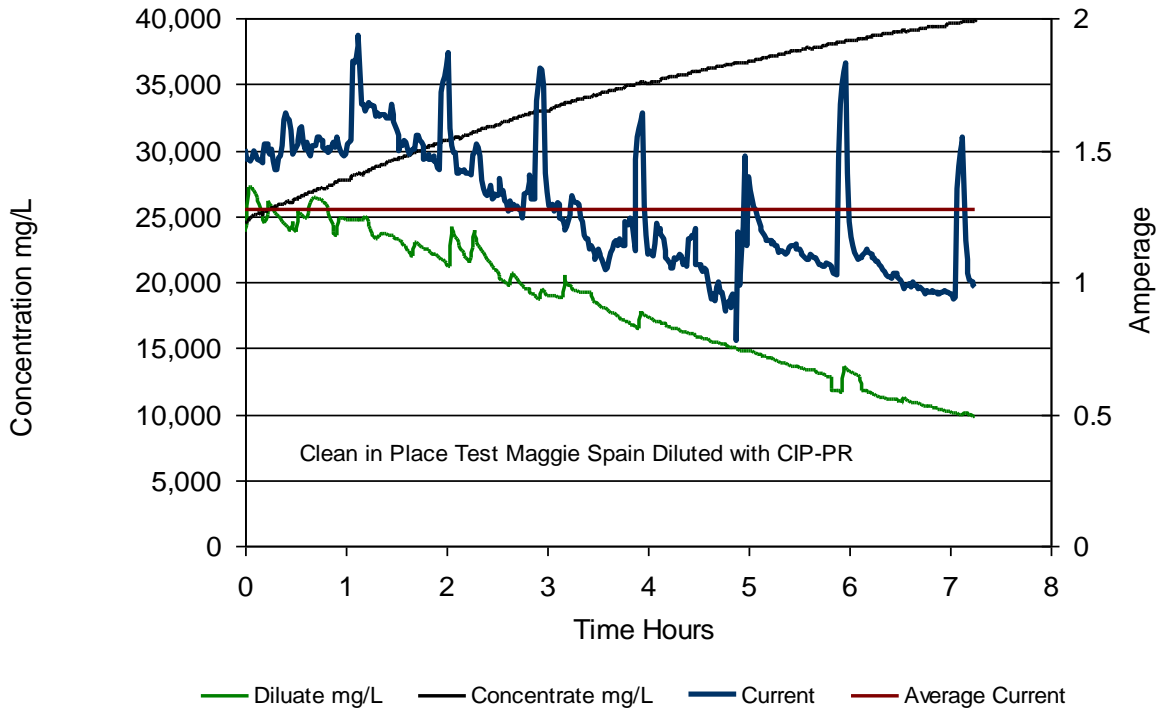


Figure 56: Maggie Spain Field Sample (diluted) with CIP Pole Reversal

Table 37: CIP Regime for the Maggie Spain Diluted Regime 1				
Hours	Volts	Amps	Seconds	Amp-Seconds
1	10	3.2	30	96
2	10	3.5	30	105
3	10	3	30	90
4	10	3	30	90
5	10	3	30	90
6	10	3	30	90
7	10	3.2	30	96
Total Amp-Seconds Expended in CIP				657

Table 38: Test Maggie Spain Diluted, with CIP Regime 1; Mg, Ba, Ca and Fe						
	Na mg/l	Ca mg/l	Mg mg/l	Ba mg/l	Fe mg/l	TDS mg/l
Feed	7,900	1100	160	4	13	25,800
Concentrate	12,000	2200	300	7.6	24	40,100
Diluate	3,500	18	14	0.64	< 2.5	9,360
Initial Electrolyte	25,000	42	3.1	< 0.1	< 2.5	
Final Electrolyte	24,000	67	3.9	< 0.1	< 2.5	
TDS data reflect conductivity probe reading at 7.5 hours						

Water from Example 4B, Maggie Spain Barnett Field sample, was recovered and re-blended to initiate Run 3 of this series. Electrolyte was reused from the previous Run 2. An arbitrary CIP pole reversal of 10 V was implemented for 15 seconds once every ½ hour. Figure 57 shows the concentration of salts in the diluate and concentrate streams and the amperage as a function of elapsed time. The figure also shows the average amperage draw throughout the test run. After 7.5 hours, the diluate concentration had dropped from about 28,000 mg/l to about 9,300 mg/l. The current had dropped to just over 1.2 amps with an average current of about 1.43 amps. The total electrical usage was 38,994 amp-seconds. Overall, the efficiency extent of the treatment was much improved over the initial Run 1 and initial Run 2. The more timely utilization of the reversal (every 30 minutes versus every hour, see Table 39) may account, in part for the improved ion flux. The reverse polarity accounted for 657 amp-seconds, or about 1.6% of the overall electrical use. Chemical data are in Table 40.

Table 39: CIP Regime for Maggie Spain Run 3				
Hours	Volts	Amps	Seconds	Amp-Seconds
0.5	10	3	15	45
1	10	3.2	15	48
1.5	10	3	15	45
2	10	3	15	45
2.5	10	3	15	45
3	10	3	15	45
3.5	10	3.5	15	52.5
4	10	3	15	45
4.5	10	3	15	45
5	10	3	15	45
5.5	10	3.2	15	48
6	10	3	15	45
6.5	10	3.7	15	55.5
7	10	3	15	45
Amp-seconds Total		654		

Table 40: Test Maggie Spain Diluted, with CIP Regime 1; Mg, Ba, Ca and Fe						
	Na mg/l	Ca mg/l	Mg mg/l	Ba mg/l	Fe mg/l	TDS mg/l
Feed	7600	1100	150	3.6	12	28,000
Concentrate	13000	2200	300	7.5	24	47,100
Diluate	3200	7.5	7.1	0.48	< 2.5	9,270
Initial Electrolyte	25000	99	8.5	< 0.1	< 2.5	
Final Electrolyte	25000	130	8.6	< 0.1	< 2.5	
TDS data reflect conductivity probe reading at 7.5 hours						

A summary of results for the diluted Maggie Spain samples (Runs 1,2,3) are presented in Table 41. These data suggest that the first CIP regime (Run 2) did not improve overall results. (ie., Run 1 versus Run 2). However, selection of a less than fully aggressive CIP does not harm the process. Selection of a more suitable regime, such as in Run 3, shows distinct ion flux improvement over the process without CIP.

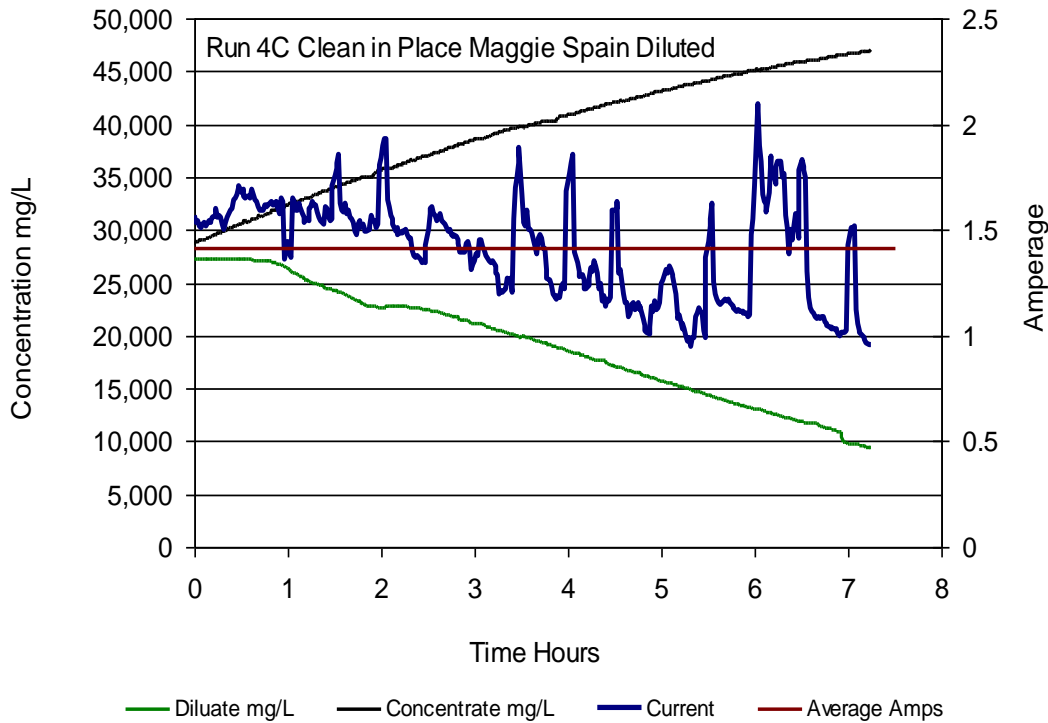


Figure 57: Maggie Spain CIP Regime 2; 10 V for 15 seconds every ½ hour

	Initial TDS	Diluate TDS	Conc. TDS	Avg. Amps @ 5V	Forward Reaction Amp-sec	Reverse CIP- Amp-Sec	Ion Flux Increase CIP-PR	kWh/lb
MSD 1 No CIP	24,500	7,700	39,700	1.17	31,590	NA	NA	0.111
MSD 2 CIP 1	25,800	9,360	40,100	1.27	34,020	657	-1%	0.115
MSD 3 CIP 2	28,000	9,270	47,100	1.43	38,340	654	18%	0.127

In this series, fresh electrolyte was prepared for Run 1. Following tests utilized used electrolyte from the previous runs. Table 42 is a summary of the multivalent cation content in the electrolyte after each of the Maggie Spain Diluted Runs 1, 2, and 3. Calcium readily increased from less than 5 mg/l (detection limit) to 130 mg/l. Magnesium slowly increased from less than 2.5 mg/l (detection limits) to about 8.6 mg/l. On a mass basis, the rate of magnesium increase is somewhat faster than calcium considering that calcium is seven times more concentrated than magnesium in the feed stock. Iron and barium did not appear to enter the electrolyte.

Table 42: Accumulation of Multivalent Cations in the Electrolyte During MSD Runs 1-3				
	Fresh Electrolyte	End Run 1 (4A)	End Run 2 (4B)	End Run 3 (4C)
Barium	<0.1	0.2	<0.1	<0.1
Calcium	<5	27	67	130
Iron	<2.5	<2.5	<2.5	<2.5
Magnesium	<2.5	<2.5	3.9	8.6

The relative cleanliness of the ED system was monitored at various points throughout the test series (Runs 1-3) and during an extensive cleaning process at the end of Run 3. Volt-amp profiles (VA profile) were used to monitor the condition of the electrodialysis process at an instant in time, for comparison to various reference profiles

An initial reference profile was established at the beginning of Run 1, and labeled as Start Run 1 in Figure 58. After Run 1, the unit was cleaned by a 5 minute pole reversal at 15 V. No other cleaning technique was used prior to Run 2.

The reference profile at the beginning of Run 2 was established and labeled Start Run 2 in Figure 58. After 4B, the unit was cleaned by a 5 minute pole reversal at 15 V. No other cleaning technique was used prior to Run 3.

The reference profile at the beginning of run 4C was established and labeled Start Run 3 in Figure 58. The data from these initial profiles are indistinguishable, indicating that the cleaning before the start of Run 2 and before the Run 3 was sufficiently aggressive. This established that the initially clean system at the start of Run 1 was similar to the starting condition of Run 2 and Run 3.

Immediately at the end of Run 3, representing about 1/2 hour after the final reversal performed in Run 3, the diluate and concentrate tanks were re-blended. A VA profile, labeled End Run 3 in Figure 58 indicated that the current was about 10% lower than the initial reference tests. A 1 minute pole reversal at 15V was then performed. The data (labeled 1 minute pole reversal) in Figure 58 show that the current returned to about 95% of initial capacity.

An additional 9 minute 15V reversal then performed. The data (labeled 10 minute reversal) in Figure 58 show that the current returned to full capacity. The electrodialysis system was then drained, and the used electrolyte and the feed stock (diluted Maggie Spain water) were retained.

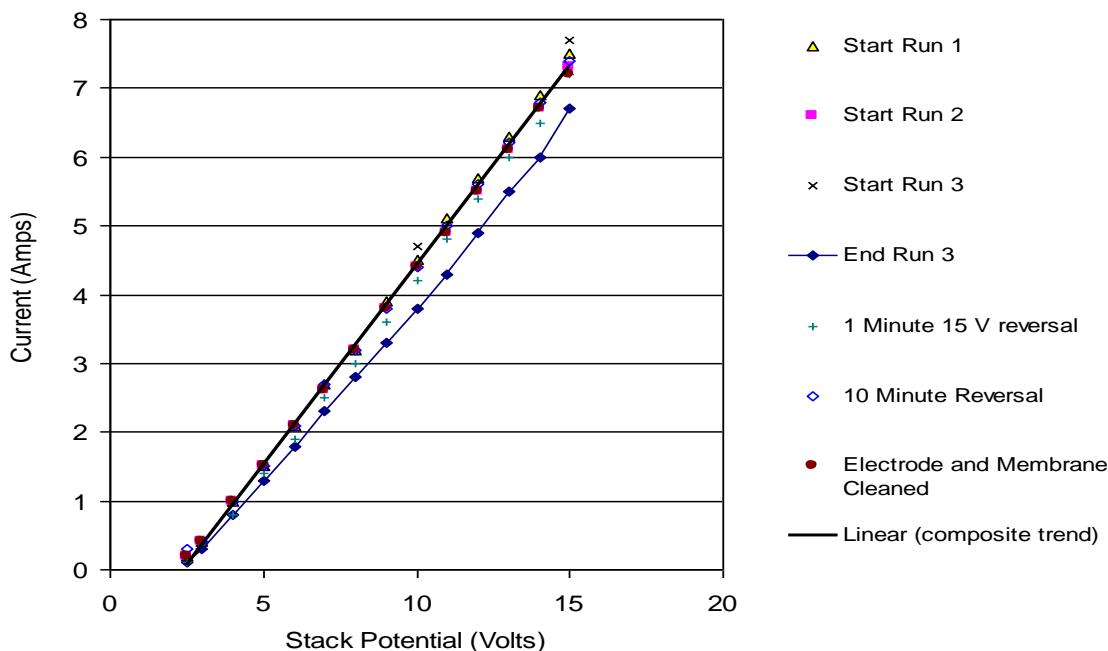


Figure 58: Example 3D, Ability of Proposed CIP-PR to Restore Electrodes to an Initial Condition.

The electrodes and the membrane stack were then extensively cleaned. The extensive cleaning involved a 10 minute flush with 0.1% HCL followed with a 10 minute flush with 0.1% NaOH, followed with a 10 minutes with fresh 0.1% HCl. The system was then rinsed 3 times with tap water.

The retained electrolyte and feed stock were returned to the electrodialysis unit. The VA profile (labeled Electrode and Membrane Cleaned) in Figure 58 shows that extensive cleaning did not improve the performance over the initial reference, indicating that the stack was clean. This further demonstrates that the pole reversal technique, as used between Runs 1, 2, and immediately after Run 3 may be sufficient to replace the more aggressive and time consuming acid and caustic washing procedures.

Table 42 shows that there was an increase in calcium present in the electrolyte as the test series progressed from fresh electrolyte to the end of Run 3. The CIP-PR method was sufficient to maintain the electrolyte throughout the entire series with diluted Maggie Spain water. Extensive cleaning was not needed.

7.9.3 Unlabeled Sample from the Marcellus

An unlabeled field brine sample from the Marcellus Shale Formation, was tested in normal operating mode without pulsed pole reversal. The clarified water contained about 8,400 mg/l Na^+ , 3,000 mg/l Ca^{++} , 14 mg/l Fe^{+++} , 280 mg/l Mg^{++} , 28 mg/l Ba^{++} , and 19,000 mg/l Cl^- . Figure 59 shows the concentration of salts in the diluate and concentrate streams and the amperage as a function of elapsed time. The current dropped very rapidly from an initial value of about 1.8 amps to less than 0.5 amps after only 1.5 hours. After 6.5 hours, the diluate concentration had dropped from about 30,700 mg/l to about 27,400 mg/l. The average current had dropped to less than 0.46 amps. The overall electrical usage was 0.46 amps x 6.5 hours x 60 x 60 = 10,764

amp-seconds. Chemical data are presented in Table 43. It is not surprising that this was a difficult sample to treat based on the ratio of calcium to sodium, which exceeded 35%.

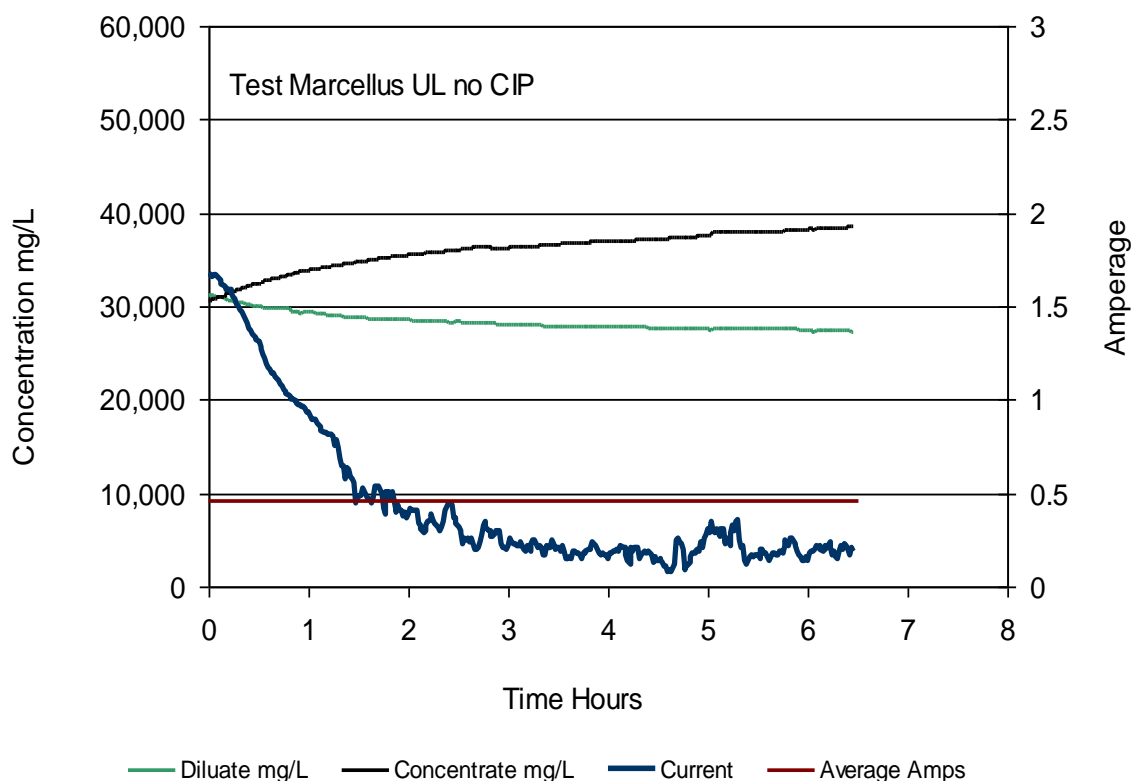


Figure 59: Marcellus UL Field Test Sample with no CIP

Table 43: Marcellus Unlabeled without CIP, Mg, Ba, Ca and Fe						
	Na mg/l	Ca mg/l	Mg mg/l	Ba mg/l	Fe mg/l	TDS mg/l
Feed	8400	3000	280	28	14	30,000
Concentrate	10000	3800	310	40	18	38,500
Diluate	7300	2300	240	17	9.5	27,300
Initial Electrolyte	32000	190	7.6	0.14	< 1	
Final Electrolyte	31000	240	8.2	< 0.04	1.3	
TDS data reflect conductivity probe reading at 6.5 hours						

The test water from the previous example with the unlabeled Marcellus sample was re-blended and treated again using a CIP pole reversal regime. The pole reversal regime was complex, and involved reversals of 15, 10, and 5 volts for a variety of times. The sequence of reversals is presented in Table 44. Figure 60 shows the concentration of salts in the diluate and concentrate streams and the amperage as a function of elapsed time. The current dropped very rapidly from an initial value of about 1.8 amps to less than 1 amp after only 1 hour. The pole reversals are shown to boost the amperage periodically. After 6.5 hours, the diluate concentration had dropped from about 30,700 mg/l to about 25,500 mg/l. The average current had dropped to less than 0.74 amps. The total forward reaction electrical usage was about 0.74

amps x (6.5 hours x 60 x 60 - 350) = 17,057 amp-seconds. The reverse reaction electrical use was about 2129 amp-seconds. The total electrical use was 17,057 + 2129 = 19,186 amp seconds. The reversal represented about 11 % of the total. Results from the chemical analyses are presented in Table 45.

Table 46 summarizes the results from the unlabelled Marcellus tests. The TDS data show that the CIP for this test water resulted in a 30% ion flux improvement for an expenditure of 14% of the energy in pole reversal.

Table 44: Marcellus UL CIP Regime				
Hour	Volt	Amps	Seconds	Amp-Seconds
0.5	10	6	20	120
1	10	5.5	20	110
1.5	10	4.5	20	90
2	15	8.3	30	249
2.5	10	5	20	100
3	15	8.3	30	249
3.5	10	5	20	100
4	15	8.3	30	249
4.5	10	5	20	100
4.75	5	3	15	45
5	15	8.2	30	246
5.25	5	3	15	45
5.5	10	4.5	20	90
5.75	5	3	15	45
6	15	8.2	30	246
6.25	5	3	15	45
Total Amp-Seconds Expended in CIP				2,129

Table 45: Marcellus Unlabeled with CIP-PR, Mg, Ba, Ca and Fe						
	Na mg/l	Ca mg/l	Mg mg/l	Ba mg/l	Fe mg/l	TDS mg/l
Feed*	8250	2700	25	26	12	30,200
Concentrate	9600	3800	300	40	16	39,700
Diluate	6900	1600	200	12	7.9	25,100
Initial Electrolyte	26000	230	9.4	< 0.04	1.1	
Final Electrolyte	28000	290	12	< 0.04	1.6	
TDS data reflect conductivity probe reading at 6.5 hours						
*False sample results suspected for the feed sample, reported as average of diluate and concentrate concentrations						

Table 46 Summary of CIP-PR Improvements with Marcellus Unlabeled Sample								
	Initial TDS	Diluate TDS	Conc. TDS	Avg. Amps @ 5V	Forward Reaction Amp-sec	Reverse CIP- Amp-Sec	Ion Flux Increase CIP-PR	kWh/lb
MSD 1 No CIP	30,000	27,300	38,500	0.45	10,764	NA	NA	0.115
MSD 2 CIP 1	30,200	25,100	39,700	0.74	17,057	2,129	30%	0.127

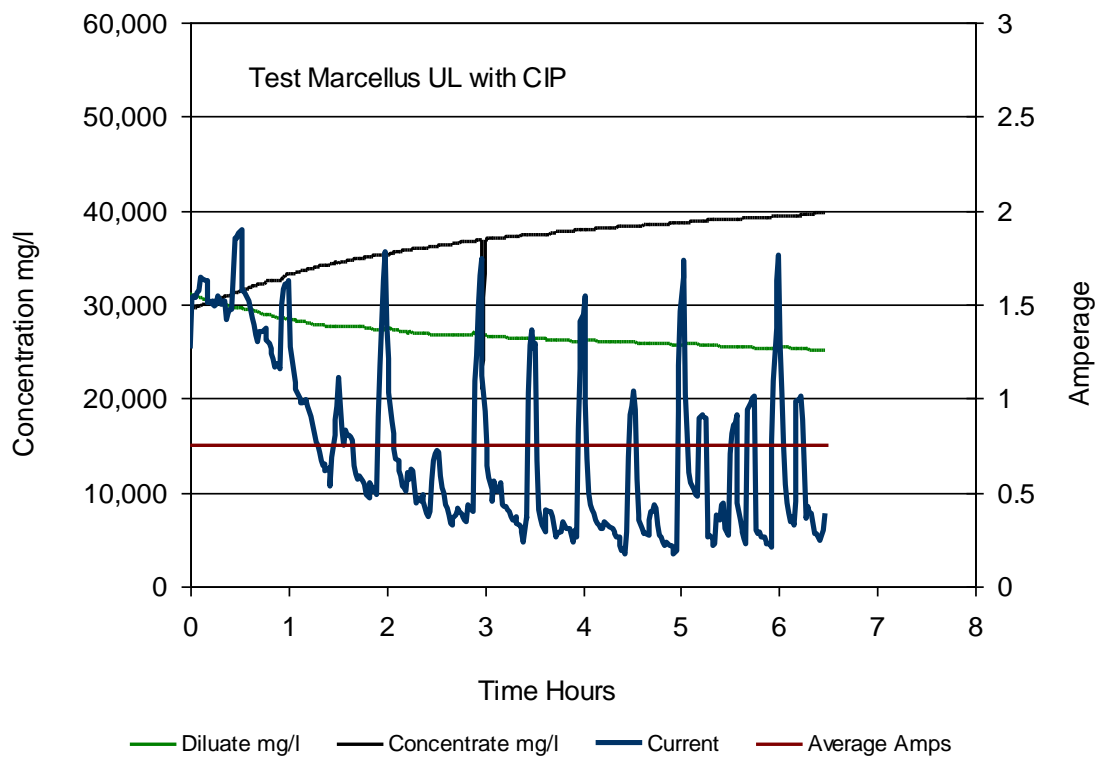


Figure 60: Marcellus UL Field Test Water with Complex CIP Pole Reversal

7.9.4 Mcadoo Labeled Sample from the Marcellus

A field brine sample, labeled Mcadoo, from the Marcellus Shale Formation, was tested in normal operating mode without pulsed pole reversal. The clarified water contained about 11,000 mg/l Na^+ , 3,600 mg/l Ca^{++} , 23 mg/l Fe^{+++} , 310 mg/l Mg^{++} , 26 mg/l Ba^{++} , and 26,000 mg/l Cl^- . Figure 61 shows the concentration of salts in the diluate and concentrate streams and the amperage as a function of elapsed time. The current dropped very slowly from an initial value of about 2 amps to less than 0.5 amps after 5.5 hours. After 6.5 hours, the diluate concentration had dropped from about 43,000 mg/l to about 32,100 mg/l. The average current had dropped to less than 1.29 amps. The overall electrical usage was 1.29 amps x 6.5 hours x 60 x 60 = 31,900 amp-seconds. Chemical data are presented in Table 47.

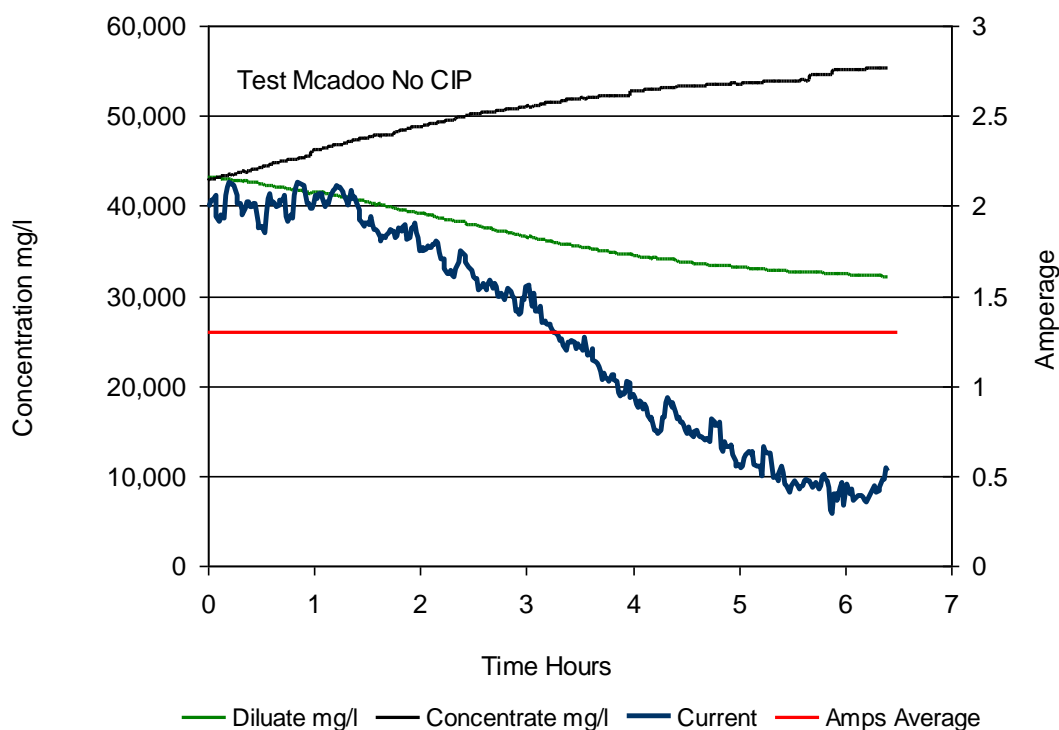


Figure 61: Mcadoo Sample from the Marcellus, No-CIP

Table 47: Mcadoo Sample from Marcellus without CIP-PR, Mg, Ba, Ca and Fe						
	Na mg/l	Ca mg/l	Mg mg/l	Ba mg/l	Fe mg/l	TDS mg/l
Feed*	11000	3600	310	26	23	43,000
Concentrate	13000	4800	380	40	28	55,200
Diluate	8600	1600	220	12	7.9	32,100
Initial Electrolyte	30000	2.2	< 1	< 0.04	< 1	
Final Electrolyte	26000	89	2.8	< 0.04	< 1	
TDS data reflect conductivity probe reading at 6.5 hours						

The test water from the previous example with the Mcadoo labeled sample was re-blended and treated again using a CIP pole reversal regime. The pole reversal regime was 15 volts for 20 seconds every hour. The sequence of reversals is presented in Table 48. Figure 62 shows the concentration of salts in the diluate and concentrate streams and the amperage as a function of elapsed time. The current dropped relatively rapidly from an initial value of about 2 amps to less than 1 amp after about 3 hours. The pole reversals are shown to boost the amperage periodically. After 6.5 hours, the diluate concentration had dropped from about 43,300 mg/l to about 33,700 mg/l. The average current had dropped to less than 1.26 amps. The total forward reaction electrical usage was about 1.26 amps x (6.5 hours x 60 x 60 - 120) = 29,330 amp-seconds. The reverse reaction electrical use was about 960 amp-seconds. The total electrical use was 24,240 amp seconds. The reversal represented about 3 % of the total. Results from the chemical analyses are presented in Table 49.

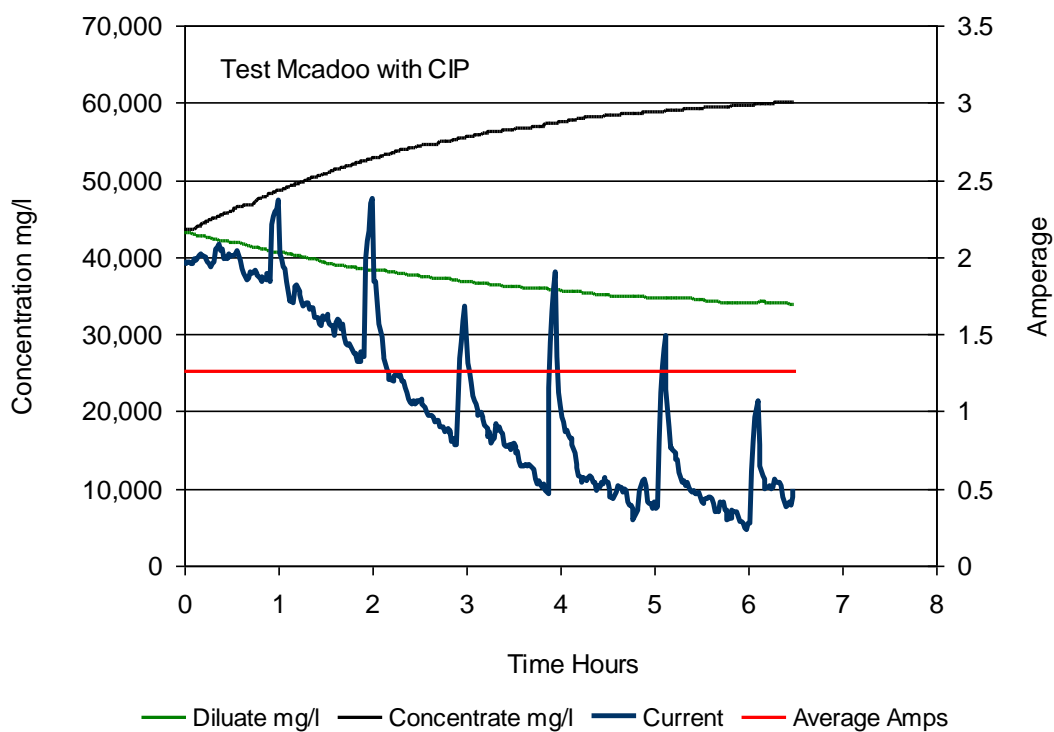


Figure 62: Sample Mcadoo from the Marcellus, with CIP-PR

Table 48: Sample Mcadoo CIP Regime				
Hour	Volt	Amps	Seconds	Amp-Seconds
1	15	8	20	160
2	15	8	20	160
3	15	8	20	160
4	15	8	30	160
5	15	8	20	160
6	15	8	30	160
Total Amp-Seconds Expended in CIP				960

Table 49: Mcadoo Sample from Marcellus with CIP-PR, Mg, Ba, Ca and Fe						
	Na mg/l	Ca mg/l	Mg mg/l	Ba mg/l	Fe mg/l	TDS mg/l
Feed*	12000	3600	290	15	17	43,300
Concentrate	15000	4900	370	24	22	60,100
Diluate	9700	2000	260	5.2	10	33,700
Initial Electrolyte	27000	200	6.9	0.045	1	
Final Electrolyte	27000	140	5.7	0.081	< 1	
TDS data reflect conductivity probe reading at 6.5 hours						

Table 50 summarizes the results from the Mcadoo site sample. The TDS transfer data suggest that the CIP for this test water resulted in a 14% ion flux improvement for an expenditure of 3% reverse polarity.

Table 50: Summary of CIP-PR Improvements with Sample Mcadoo								
	Initial TDS	Diluate TDS	Conc. TDS	Avg. Amps @ 5V	Forward Reaction Amp-sec	Reverse CIP- Amp-Sec	Ion Flux Increase CIP-PR	kWh/lb
MSD 1 No CIP	43,000	32,100	55,200	1.29	31,900	NA	NA	0.148
MSD 2 CIP 1	43,300	33,700	60,100	1.26	29,330	960	14%	0.119

7.10 Effect of Temperature

Electrodialysis presents a unique process control problem. Both the ion flux across the treatment membranes and the reactions at the electrodes are temperature sensitive. The Arrhenius temperature dependency equation was manipulated to include the effects of both temperatures on the process (Section V.3). Test water was prepared with 30 g NaCl per liter water. The electrolyte solution was prepared from 90 g Na₂SO₄ per liter water. Ice was occasionally substituted for water at a rate of 1000 g ice per liter water. A 100 W fish tank heater was occasionally used to obtain data at temperatures exceeding 300 °K.

The ED pilot plant was placed in recycle mode, with the diluate tank and concentrate tanks cross-connected to assure constant feed of 3% NaCl water throughout the test series.

The data in this section consisted of a series of VA amp profiles generated by quickly ramping the power source down, in one volt increments, from 16 to 2 volts. The amperage was recorded at each increment and provided a snap shot view of the ED process under the extant conditions. Each VA profile was fairly linear throughout the entire range of volts, with small deviations below 4 volts. Data in this section are presented as the linear interpolation for the amperage at 15 V, as determined from linear least squares regressions of each data set from 5 and 15 volts.

The reported amperages in this section are representative of 15 Volt stack potential. This is a deviation of most other data presented in this report, which was mostly at 5 volt stack potential. The higher voltage data are used, herein, because of a greater sensitivity of the response of the amperage at the various temperatures. Data were collected in two series, Series 1 and Series 2.

7.10.1 Series 1

The first series was performed to provide three distinct subsets, 1A, 1B, and 1C. Series 1A (Table 51) tested water at a constant temperature (281 ± 1 °K) with the electrolyte temperature varied. Series 1B (Series 1B) tested electrolyte at a constant elevated temperature (303 ± 2 °K) with the water temperature varied (Table 52). The temperature of the electrolyte and test water naturally (and equilibrated) drifted with time. These data (Table 53) were collected over a range of temperatures as opportunity dictated, making the third subset, Series 1C.

Table 51: Data Series 1A, Cool Water; Varied Electrolyte Temperature			
Test	c	c	d
Electrolyte (°C)	11.5	14.6	16.3
Water (°C)	8.1	8.2	8.7
Slope (amp/volt)	0.5	0.5	0.5
Intercept (amp)	-1.4	-1.4	-1.3
Amps @15 V	6.3	6.4	6.6

Table 52: Series 1B; Warm Electrolyte; Varied Water Temperature							
Test	h	i	j	k	l	m	n
Electrolyte (°C)	31.1	30.7	29.8	29.0	31.9	31.7	30.6
Water (°C)	30.6	23.4	24.2	27.5	32.8	12.5	15.2
Slope (amp/volt)	0.9	0.8	0.8	0.8	0.9	0.7	0.7
Intercept (amp)	-2.2	-1.8	-2.0	-2.1	-2.2	-1.6	-1.7
Amps @15 V	11.0	9.8	10.1	10.5	11.5	8.7	9.1

Table 53: Data Series 1C; Varied Electrolyte and Varied Water Temperatures											
Test	a	e	f	g	o	p	q	r	s	t	u
Electrolyte (°C)	10.7	16.9	17.4	18.9	29.0	28.2	27.5	27.7	26.1	24.7	20.3
Water (°C)	6.6	11.9	12.3	10.0	18.5	20.0	21.4	28.1	25.5	24.0	19.7
Slope (amp/volt)	0.5	0.6	0.7	0.7	0.8	0.8	0.8	0.9	0.9	0.8	0.8
Intercept (amp)	-1.3	-1.7	-1.7	-1.8	-1.8	-1.9	-2.0	-2.2	-2.1	-2.0	-1.9
Amps @15 V	5.9	8.0	8.2	8.2	9.6	9.9	10.1	10.9	10.8	10.5	9.6

Figure 63 shows volt-amp profiles for a range of results from Series 1 data. Test-a was the coldest overall conditions with the water at 6.6 °C and electrolyte at 10 °C. When the water temperature was elevated to 32.8 °C and the electrolyte was elevated to 31.2 °C in Test-l, the current nearly doubled, indicating a doubling of ion flux between the diluate and the concentrate streams. The amperage was intermediate in Test-g when the water temperature was 10°C and the electrolyte temperature was 18.9 °C.

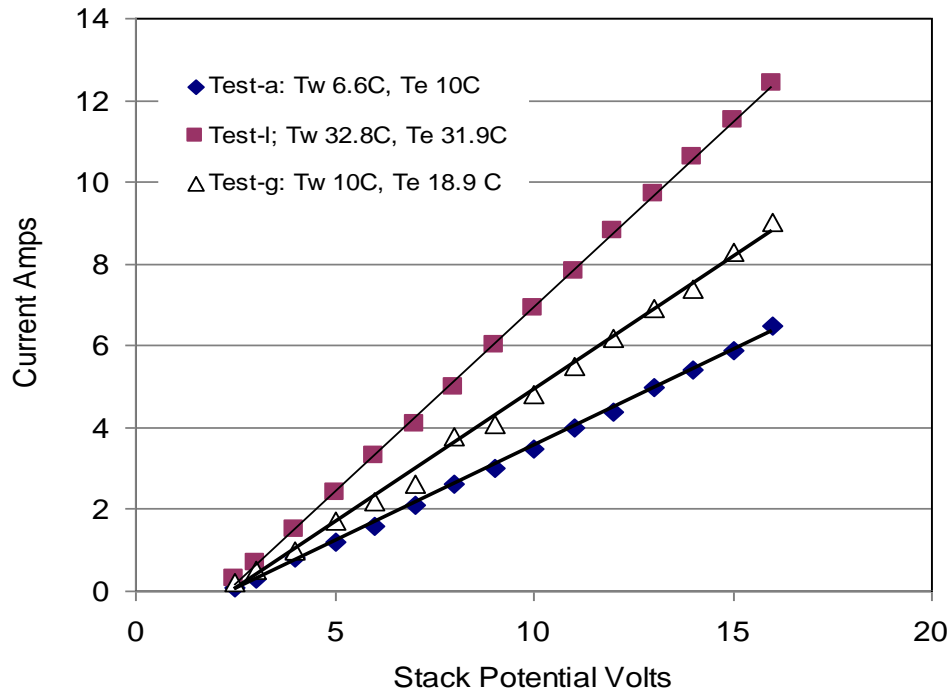


Figure 63: Example Volt-Amp Profiles with 3% NaCl and 90 g/l Disodium Sulfate Electrolyte over a Range of Temperature Conditions.

The discussion of the Arrhenius equation in the Background predicts that results for water at constant temperature with varied electrolyte temperature (Table 51) will differ from results when the electrolyte is constant temperature and the water temperature is varied (Table 52). Figure 64 shows a typical Arrhenius plot of the natural logarithm of the rate (amps) versus inverse temperature ($1/^{\circ}\text{K}$). As expected, two separate relations are developed, as in Equations 5 and 6 from Section 6.3. Nomenclature is repeated for ease of presentation.

T_w = temperature of the salt water, $^{\circ}\text{K}$

T_e = temperature of the electrolyte, $^{\circ}\text{K}$

i_{Tw} = amperage when water temperature varies, electrolyte temperature constant

i_{Te} = amperage when electrolyte temperature varies, water temperature varies

i = amperage when electrolyte and water temperature have any temperature

E_w = Activation energy for the salt diffusion in the water solution

E_e = Activation energy for the electrolyte reaction

E = Activation energy for the overall reaction

R = universal gas law constant

C_{303} = Arrhenius coefficient, electrolyte held constant $T_e = 303^{\circ}\text{K}$ (amps)

B_{281} = Arrhenius coefficient, water held constant $T_w = 281^{\circ}\text{K}$ (amps)

A = Arrhenius coefficient (amps)

$$5) \ln(i_{T_w=281}) = \ln(B_{281}) - \frac{E_{T_e}}{RT_e}$$

$$\ln(B_{281}) = 5.16$$

$$B_{281} = 174$$

$$\frac{E_{T_e}}{R} = 948$$

$$6) \ln(i_{T_e=303}) = \ln(C_{303}) - \frac{E_{T_w}}{RT_w}$$

$$\ln(C_{303}) = 6.16$$

$$C_{303} = 473$$

$$\frac{E_{T_w}}{R} = 1143$$

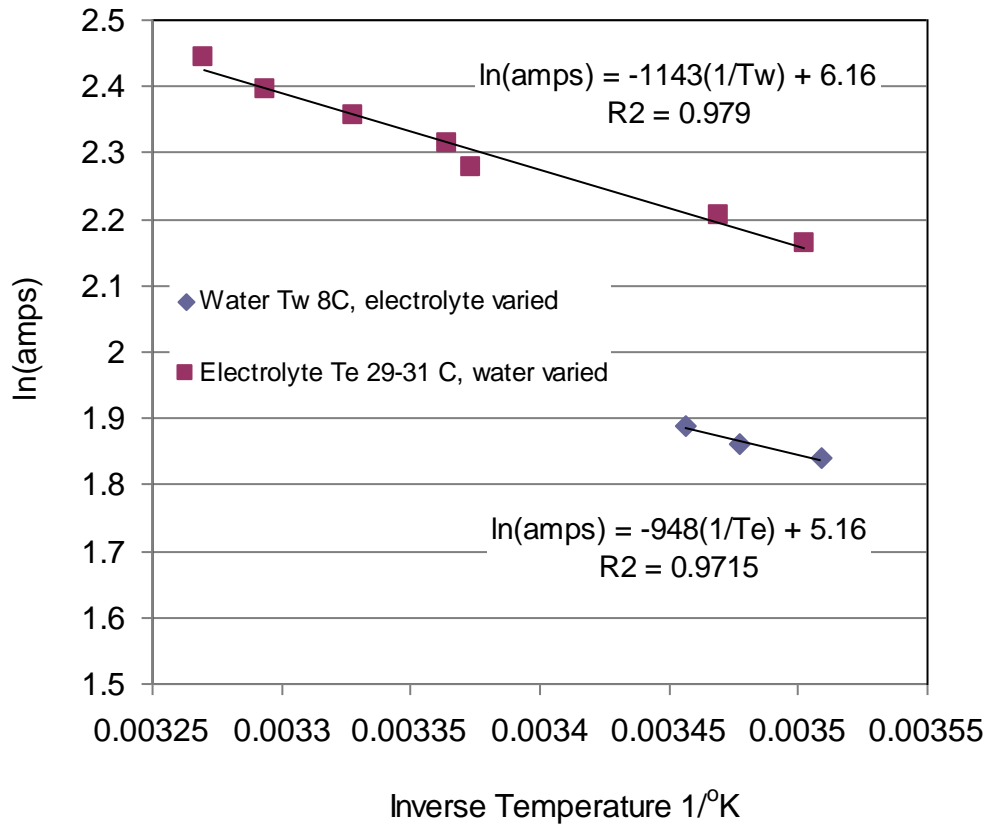


Figure 64: Arrhenius Plot of Data from Tables 49 and 50

The generalized coefficients C* and B* are developed from Equations 9 and 10, Section V.3. This analysis leads to the conclusion that B* = C* to within a few percentage points, as defined previously.

$$9) C_{T_e} = C^* e^{-E_e / RT_e}$$

$$C^* = 473e^{948/303} = 10805$$

$$10) B_{T_w} = B^* e^{-E_w / RT_w}$$

$$B^* = 174e^{1143/281} = 10164$$

The average of B* and C* (=10485) was used in the generalized equation for a reaction governed by two temperatures. The general temperature model is given by Equation 11 (Section V.3).

$$11) i_{(T_w, T_e)} = B^* e^{-E_w / RT_w} e^{-E_e / RT_e}$$

$$11a) i_{(T_w, T_e)} = 10485 e^{-1143/T_w - 948/T_e}$$

Data with a varied range of electrolyte and water temperatures (Series 1C, Table 53) were analyzed with Equation 11a. Figure 65 shows the observed current versus the predicted current for the data in Table 53. This demonstrates a reasonable agreement, indicating in principle, that the dual effect of temperature may be modeled in this pilot unit, as in Equation 11a.

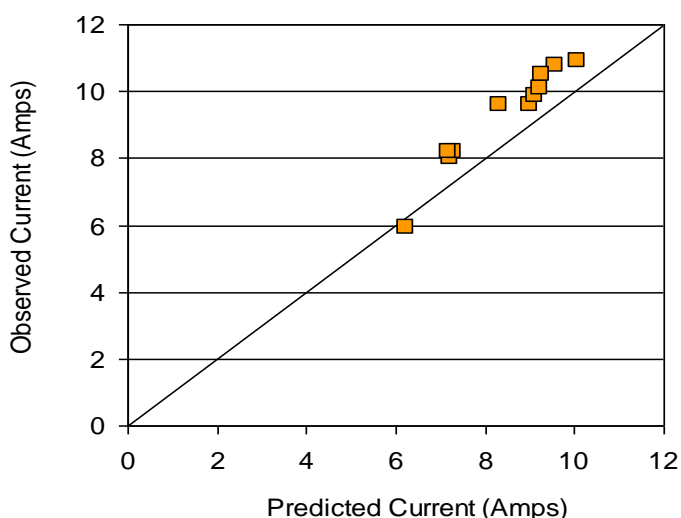


Figure 65: Data from Table 3 with Varied Water and Electrolyte Temperatures versus Prediction from Equation 11a.

7.10.2 Series 2

A second series was performed to provide tests where the electrolyte temperatures were equal to the water temperatures. In this case, cool electrolyte and cool water were initially used. Data were collected throughout the run as the temperature of the equilibrated system slowly rose. The electrolyte and water temperatures were within about 1 °K of each other and reported as the average temperature. A special case for Equation 11 (Section V.3) occurs when the two temperatures, T_e and T_w are equal. The special case becomes Equation 11B (or Equation 1).

Data in Table 54 represent a second series of data collected when the two temperatures were equivalent. The data points in Figure 66 represent a plot of the logarithm of the observed amps versus the inverse temperature. The line in Figure 66 was generated from the predictive Equation 11b. The close fit again indicates that the temperature response in the pilot unit is predictable.

Table 54: Series 2, Electrolyte and Water Temperature $\pm 1^\circ\text{C}$					
Test	Electrolyte and Water Temperature $^\circ\text{C}$	Amps @ 15 Volt	Test	Electrolyte and Water Temperature $^\circ\text{C}$	Amps @ 15 Volt
a2	8.8	7	h2	22.8	9
b2	10	7.6	i2	26.2	10
c2	14.1	7.6	j2	30.7	11.6
d2	20	8.1	k2	32.2	12
e3	21	8.4	l2	32.8	12.2
f2	22	8.7	m2	33.3	12.6
g2	22.7	8.9			

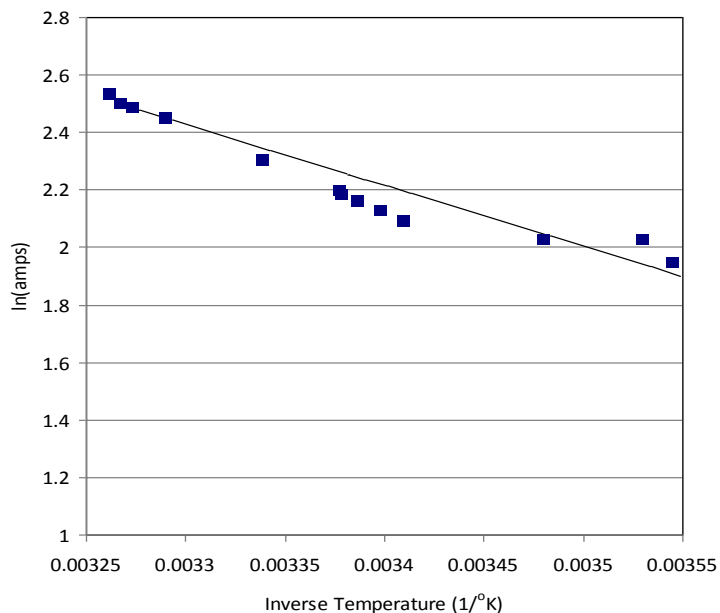


Figure 66: Arrhenius Plot of Data from Table 52 (Points) and Prediction (Line) from Equation 11b.

7.11 Estimated Capital and Operational Costs

Eurodia provided a set of capital and operational costs for specific examples provided by GTI. These examples represented range of conditions expected in the field. The economic data were reanalyzed for this report. The guiding parameter that linearized the economic data was found to be the pounds of salt removed per day. Figure 67 is a simplified conversion chart to convert the volume of water treated (BBL/day) to the mass of salt treated (Lb TDS removed/day) as a function of the parts per million removed from the influent water. Test conditions presented for analysis are in Table 55. The original economic data presented by Eurodia are presented in Table 56. Capital costs includes stacks, rectifiers, pumps, circulation tanks, piping and valves, Instruments, automation, engineering, and start-up assistance. Capital costs do not include pre-treatment, storage tanks, buildings, site work, or utility connections.

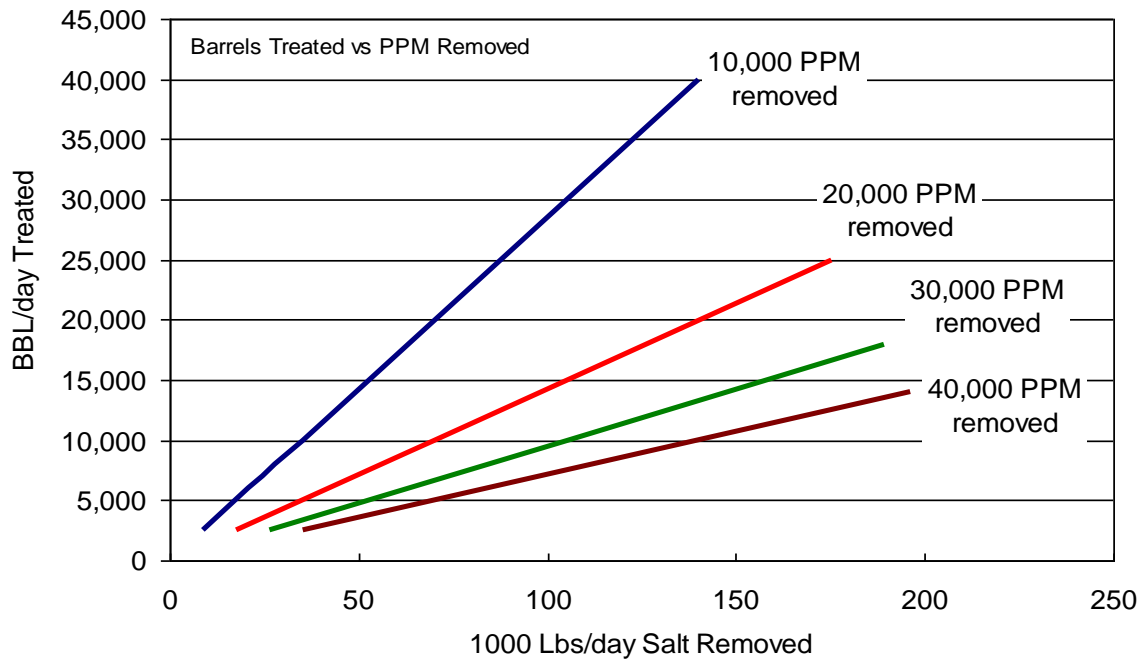


Figure 67: Conversion Chart, BBL/day Treated Water vs Pounds Salt Removed/day as a Function of the PPM Salt Removed.

Table 55: Test Cases for Economic Analysis							
Test Case	A3	A4	A5	A6	B1	B2	B3
Inlet TDS	70,000	40,000	20,000	10,000	40,000	40,000	40,000
Effluent TDS	40,000	10,000	10,000	1,000	10,000	10,000	10,000
BBL/d treated	10,000	10,000	10,000	10,000	50,000	20,000	2,000
1000 Lb Salt/Day removed	117	117	40	34	586	234	23

Table 56: Economic Data Provided by Eurodia							
Test Case	A3	A4	A5	A6	B1	B2	B3
Number of Stacks	15	15	6	6	64	32	3
Number of Cells/stack	736	736	620	620	860	690	732
Replace Membranes \$/1000 gallon	0.87	0.87	0.29	0.29	0.74	0.78	0.87
Cleaning lb HCL/1000 gallons	0.05	0.05	0.033	0.033	0.05	0.05	0.05
Stack Power kWh/1000 gallon	7.2	8	2.7	2.3	8	8	8
Pumping Power kWh/1000	0.017	0.017	0.006	0.006	0.017	0.017	0.017
Capital* (\$ million)	6.9	6.9	2.9	2.9	32.6	13.9	1.6
*Capital Costs Includes: Stacks, Rectifiers, Pumps, Circulation tanks, Piping and valves, Instruments, Automation, Engineering, and Start-up Assistance							

Data in Table 56 require conversion to cost terms. Power is estimated at \$0.10/kWh. Cleaning acid is assumed to be \$0.50/lb. Additionally, specific placeholders are assumed to present a more complete economic forecast. Placeholder values for labor and maintenance, building capital, and utilities are presented in Table 57. Amortization of capital is based on the annual cost of a present worth over 7 years at 7% interest.

Table 57: Additional Economic Assumptions			
Assumptions	Cost	Unit	Incremental
Power	\$0.10	kWh	
HCl	\$0.50	Lb	
Labor*	\$200	Day	+\$20/stack-day
Building*	\$150,000	Base	+\$10,000/stack
Utilities*	\$150,000	Base	+\$10,000/stack
Amortization of Capital	Annual cost	Present Worth	7 years at 7% interest
*Placeholder values for estimate only			

Estimates of capital cost are presented on a case-by-case basis in Table 58. Daily costs are presented in Table 59. When normalized on a basis of 'pounds salt removed per day', these cases are linearized. Normalized operational data are presented in Tables 60.

Total capital, as a function of salt removal, is presented in Figure 68. Case B1 appears out of range of any expected design project, and is excluded from this figure. Daily operations costs are presented in Figure 69. Case B1 is also excluded from this plot.

Table 58: Capital Costs on a Case-by-Case Basis							
	A3	A4	A5	A6	B1	B2	B3
Stacks	6.9	6.9	2.9	2.9	32.6	13.9	1.6
Building	0.3	0.3	0.2	0.2	0.8	0.5	0.2
UTILITIES	0.3	0.3	0.2	0.2	0.8	0.5	0.2
Total (\$ Million)	7.5	7.5	3.3	3.3	34.2	14.8	2.0

Table 59: Daily Operating Costs on a Case-by-Case Basis							
	A3	A4	A5	A6	B1	B2	B3
Stack Power	3,024	3,360	1,134	966	16,800	6,720	672
Replace membranes	365	365	122	122	1,554	655	73
Labor	300	300	240	240	520	360	220
Pumping	7	7	2	2	35	14	1
Cleaning Chemical	11	11	7	7	53	21	2
Total (\$/day)	3,707	4,043	1,505	1,337	18,962	7,770	969

Table 60: Operating Costs Cost Basis \$/Thousand Pounds Salt Removed							
	A3	A4	A5	A6	B1	B2	B3
1000 lb Salt removed/day	117	117	39	33.6	585.0	234.0	23.4
Stack Power	25.8	28.7	28.6	28.7	28.7	28.7	28.7
Membrane Replacement	3.1	3.1	3.1	3.6	2.7	2.8	3.1
Labor	2.6	2.6	6.1	7.1	0.9	1.5	9.4
Pumping	0.1	0.1	0.1	0.1	0.1	0.1	0.1
Cleaning Chemical	0.1	0.1	0.2	0.2	0.1	0.1	0.1
Total (\$/thousand lb salt)	31.7	34.5	38.0	39.7	32.4	33.2	41.4

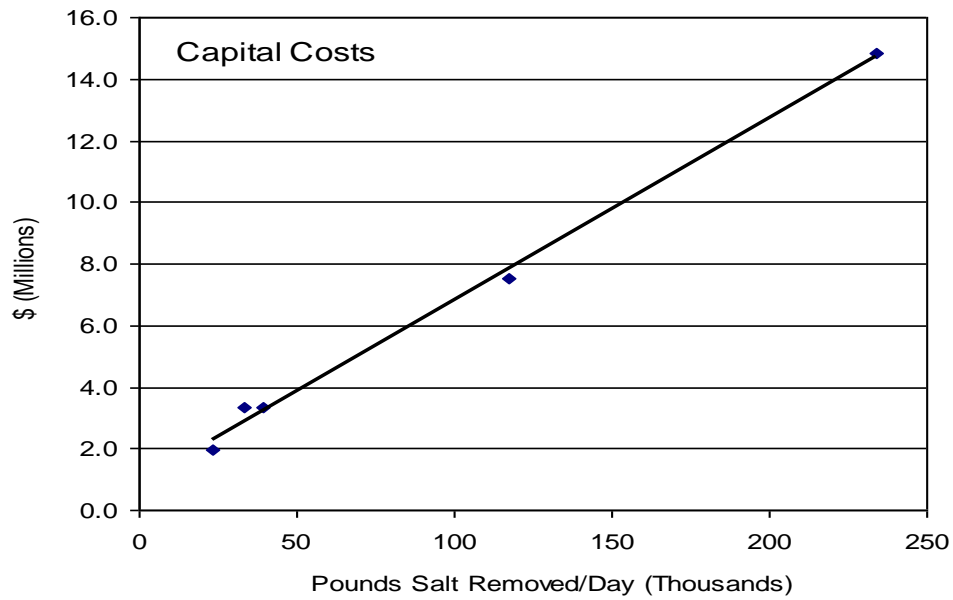


Figure 68: Capital Costs as a Function of Daily Salt Removal

Operating costs are shown in Figure 70. In both figures, cases A3 and A4 were combined as being nearly redundant. Case B1 was neglected as being out of range. Pumping and cleaning chemical costs were combined, being minimal compared to the other costs. When presented in this manner, it can be seen that the stack power and membrane replacement costs are nearly constant on a basis of \$/lb salt treated. The economy of scale appears to be in labor. The reader should be reminded that labor is a placeholder value for this evaluation.

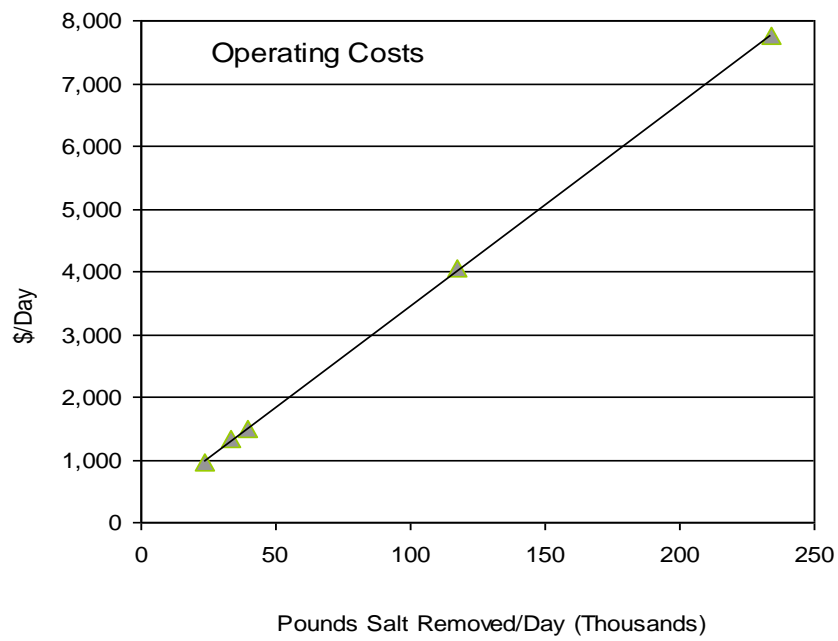


Figure 69: Operating Costs as a Function of Salt Removal

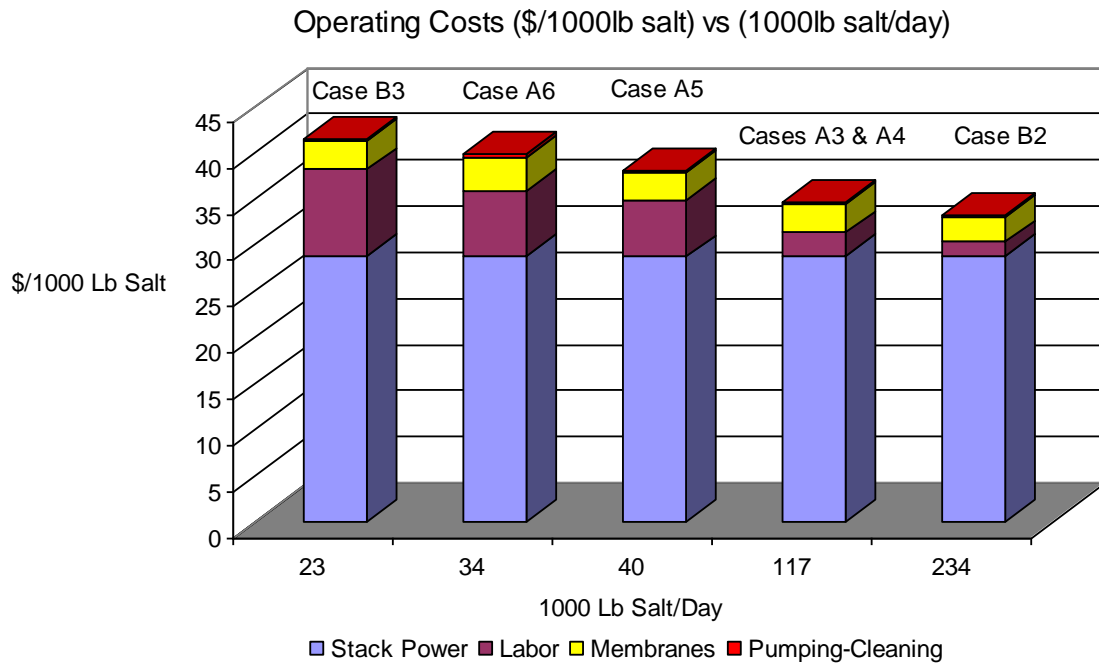


Figure 70: Breakdown of Operating Costs (\$/1000 lb salt) as a Function of Daily Salt Removal

Capital costs are shown on a case-by-case basis as a function of salt removal in Figure 71. Recall that these values are based on amortized capital (7 years, 7%). Economy of scale appears to stabilize between Cases A3 and A4 and Case B3, indicating that the most efficient capital use appears to be for cases that exceed 117,000 pounds of salt per day. This range of treatment can be converted to barrels per day by consulting Figure 67.

{

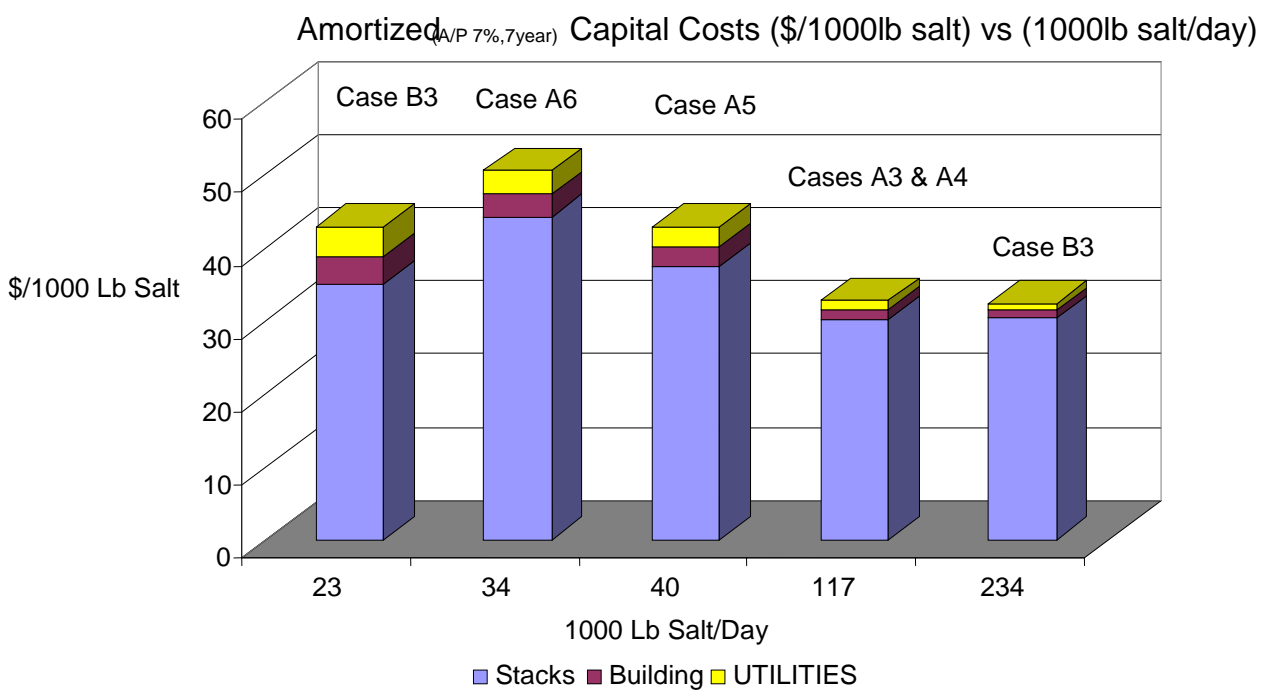


Figure 71: Amortized Capital Normalized (\$/1000 Lb Salt Treated) versus Daily Treatment

8. DISCUSSION

Electrodialysis is conventionally limited to waters containing several thousand mg/l TDS and not more than several hundred mg/l calcium and magnesium. Flowback waters contain tens of thousands of mg/l TDS and thousands of mg/l calcium, magnesium and other multivalent cations. Technical guidance for treatment of these types of brines was not available in the open literature. A number of problems were systematically addressed as the project proceeded from the treatment of water containing pure sodium chloride (30,000-60,000 mg/l) to the treatment of solutions with sodium, calcium (up to 4,000 mg/l), barium (up to 400 mg/l), iron (up to 50 mg/l), and magnesium (up to 600 mg/l), and finally to the treatment of field samples from the Barnett and the Marcellus. This discussion focuses on the practical aspects of discoveries in the topic areas pertaining specifically to treating these types of heavy brine.

During the test period, a number of problems were encountered. Literature suggests that these problems historically impeded development of electrodialysis for complex solutions of concentrated divalent cations. As these problems were encountered in this project, they were addressed by making a number of improvements to the electrodialysis process specific to this laboratory unit. Some of these improvements represent potentially scalable means for cost savings. Others of these improvements represent critical changes needed to keep the electrodialysis unit operational.

8.1 Defining a Range of Operation

An arbitrary energy utilization limit (0.1 to 0.15 kWh/lb TDS) was established to keep the electrical costs of electrodialysis at \$0.18 per barrel of flowback water treated. This limit was based on the projected recovery of 67% of the volume from each barrel (42 gallon/barrel) and taking the diluate stream from 50,000 mg/l TDS to 10,000 mg/l TDS. The cost of electricity was assumed to be \$0.10/kWh. Theoretical calculations for this pilot plant suggested that the goal could be achieved by maintaining a low stack potential of 5 volts (nominally 0.5 volts/membrane pair). Energy utilization was calculated for 33 electrodialysis runs. Figure 72 is a summary of 33 tests conducted under different conditions (See Tables 7, 8 and 9) including waters from four field sites. These data suggest a weak correlation between the initial concentration and the work required per pound of salts transferred. It is significant that the field waters performed within the range of results expected from laboratory tests.

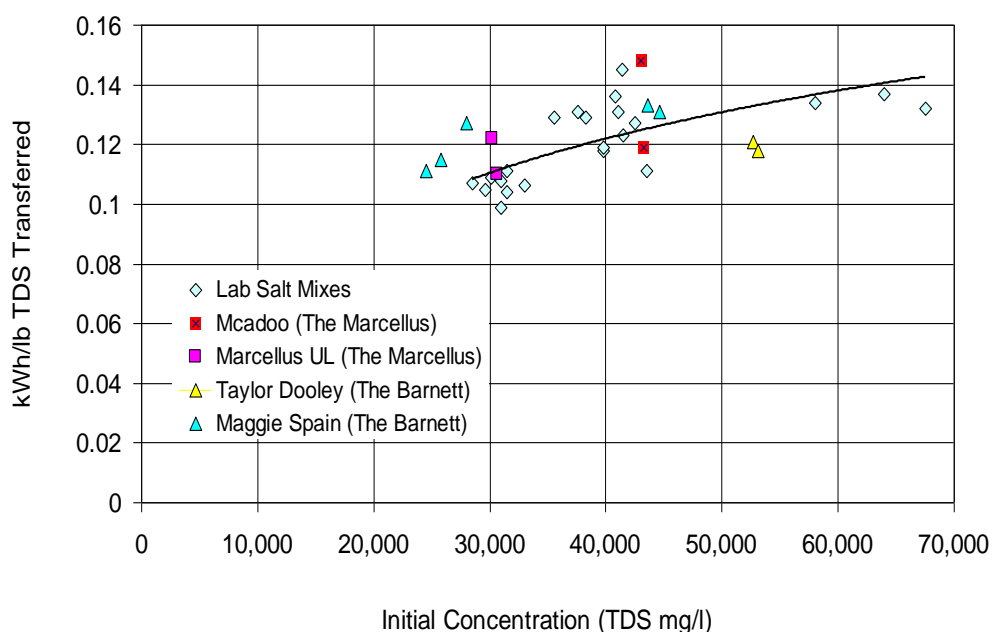


Figure 72: Summary of All ED Runs, Energy Utilization (Work) Required Per Pound of TDS Transferred

8.2 Electrolyte Chemistry

The chemistry of the electrolyte solution was investigated as a means of improving the rate of salt transfer at the desired energy limit. Theoretical calculations indicated that there would be significant resistance to ion flux within the electrode cells at high concentrations of brine (See Figures 9-12, Section 6.2). Increasing the electrolyte concentration to an ionic strength similar to the water being treated increased ion flux. Figure 18 (Repeated from Section 7) shows the current as a function of diluate concentration in three tests with 3% NaCl. Increasing the electrolyte from 30 to 90 g/l disodium sulfate at neutral pH produced a clear improvement in current (as proxy for ion flux).

Improvements were also observed by elevating the pH of electrolyte to a pH greater than 11. This apparently lowered the overvoltage by about 0.4 volts by providing hydroxide for the oxidative reaction at the anode. Figure 18 (repeated from Section 7) shows that 1 g/l sodium hydroxide added to an electrolyte solution containing 90 g/l disodium sulfate improved ion flux. This observation may have utility for waters with low concentrations of multivalent cations. However, pH control of the electrolyte at elevated may be problematic if there is incursion of calcium into the electrolyte.

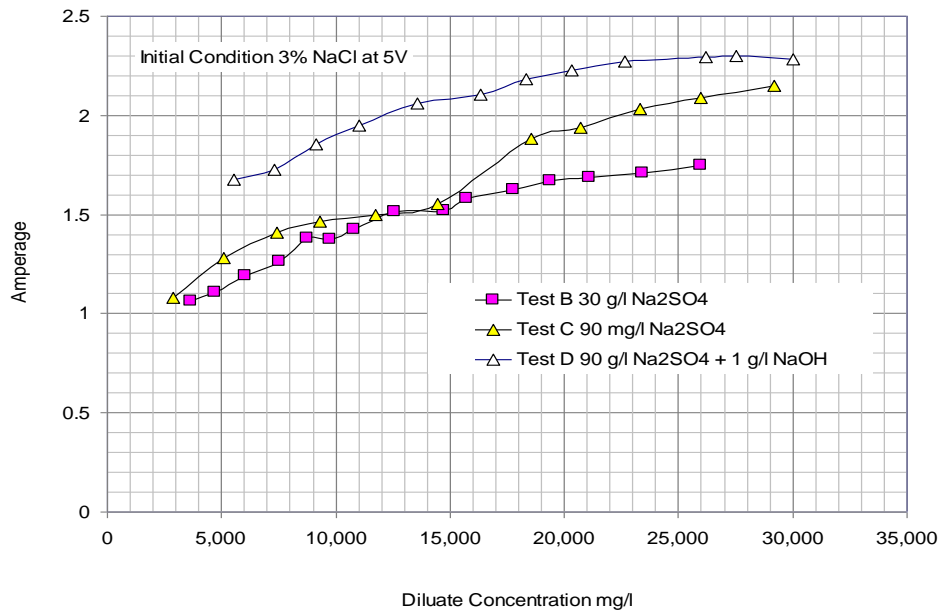


Figure 18 (repeated): Amperage Profile for Electrolyte Chemistry Improvements

8.3 Mitigation of the Effects of Calcium with Cathode Protection

A generic cation selective membrane was installed at the boundary to the cathode cell. High rates of calcium incursion into the electrolyte were encountered causing calcium fouling of the electrode cell. Figure 73 shows the loss of current (ion flux) in 3% sodium chloride as 1,000 mg/l and 4,000 mg/l Ca^{++} was added to the test water. Similar results were obtained with 6% sodium calcium and 4,000 mg/l Ca^{++} .

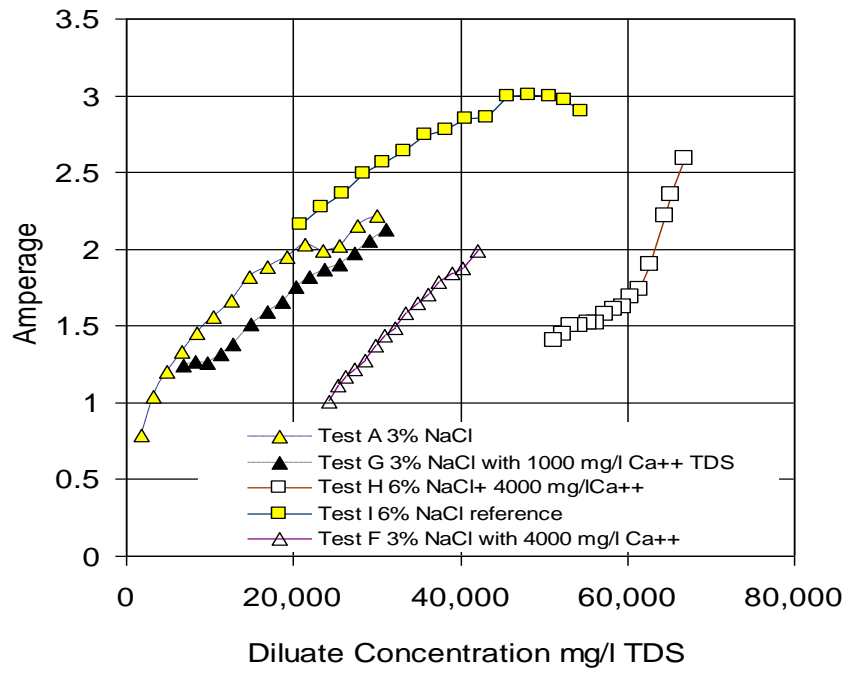


Figure 73: Effect of Calcium Addition to Test Waters with Unprotected Cathode Barrier

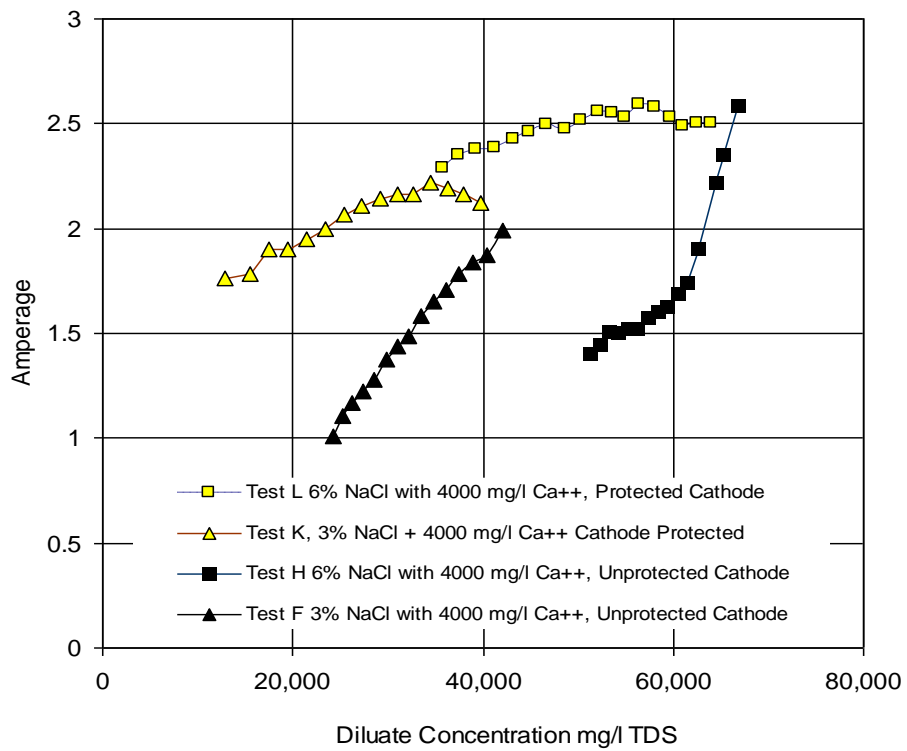


Figure 74: Improved Performance in Solutions of Calcium with Cathode Protective Membrane Installed at the Cathode Boundary

The cathode boundary membrane was replaced with a membrane that selected against multivalent cations. This single change in the stack configuration caused immediate improvement in performance in the presence of calcium. Above Figure 74 shows the dramatic improvement in ion flux with tests with sodium chloride and calcium when the improved membrane was installed.

The chemistry of the electrolyte and test waters was analyzed to determine the extent of the calcium exclusion to the electrolyte. A relative flux index (RFI) was defined as the ratio of the flux of calcium into the electrolyte and the flux of calcium from the diluate to the concentrate. A low RF index indicates a higher rate of rejection at the cathode barrier membrane. Figure 37 (repeated from Section 7) shows that there was substantial rejection (around 70%) of calcium by the more selective cathode barrier membrane.

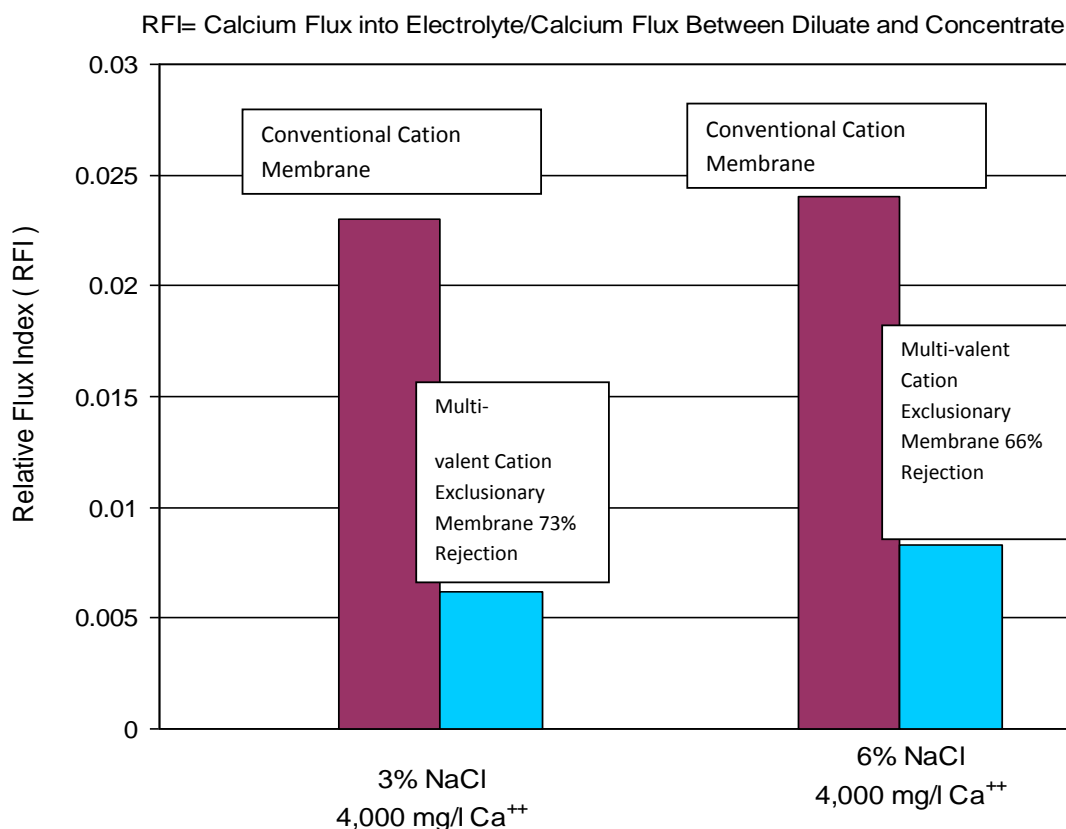


Figure 37: Cathode Protective Membrane Accounts for 66-73% Rejection of Calcium Flux to the Electrolyte

In further tests with the multivalent exclusionary membrane, calcium was deliberately introduced into the electrolyte to achieve an electrolyte concentration of >1000 mg/l calcium, both as free ions or as a precipitate. These additions of calcium, surprisingly, did not interfere with the ED performance. This indicates that the initial poisoning was at the surfaces of the cathode boundary and that the protective membrane has a surprising added benefit.

8.4 Interference from Multivalent Cations

Mitigation of the transport of calcium by the use of the more exclusionary CMX-S membrane represented a major improvement by rejection of about 70% of the calcium incursion. Unfortunately, this means that 30 % of the potential calcium still enters the electrolyte. Additionally, flowback waters contain numerous other multivalent cations that present potential problems. Six laboratory tests were performed with complex salt solutions. Eleven tests were performed with samples from the field containing complex salts. These tests will be presented as they pertain to understanding the degree of interference and possible mechanisms of interference caused by multivalent ions.

It is convenient to introduce the computation of the relative stack flux (RSF_{ion}) of the various ions from the diluate to the concentrate normalized to the concentration of the initial feedstock. The relative stack flux (RSF_{ion}) may be further normalized to the value obtained for sodium.

$$RSF_{ion} = \frac{C_{Concentrate} - C_{Diluate}}{C_{Feed}}$$

$$Normalized_{Na^+} = \frac{RSF_{ion}}{RSF_{Na^+}}$$

Table 61 is a summary of the initial conditions for six lab tests and eleven field tests. Calculated values for the relative stack flux for sodium (RSF_{Na}) are also presented. Figure 75 shows is a strong relation between the relative stack flux for sodium and the total concentration of the multivalent cations. The concentrations are presented as the total molecular charge equivalents of the cations in milliequivalents per liter (meq/l). The greater the total concentration of multivalent cations, the poorer the overall performance, as represented by the relative sodium flux.

Test	Initial TDS	Hours	Na mg/l	Ca mg/l	Mg mg/l	Ba mg/l	Fe mg/l	RSF_{Na}
Q	35,560	6.5	11,000	56	530	5	1	1.27
R	42,500	6.3	11,000	3,200	500	360	17	0.92
S	41,400	6.6	11,000	3,100	440	160	50	0.74
T	40,800	7.8	9,600	2,500	550	370	64	0.95
U**	41,100	7.1	11,000	3,500	380	400	64	0.64
V	37,600	7.1	11,000	3,200	350	330	35	0.80
X*	38,300	5.5	11,000	2,600	470	260	36	0.78
MS	44,600	6.0	15,000	2,100	270	22	24	0.80
MS*	43,600	6.0	13,000	2,000	350	16	32	1.22
MSD	25,000	7.5	7,600	1,100	150	3	12	1.10
MSD*	25,800	7.5	7,600	1,100	150	4	12	1.21
MSD*	28,000	7.5	7,900	1,100	160	4	13	0.66
TD	52,700	6.0	14,000	2,600	470	40	31	0.35
TD*	52,900	6.0	16,000	3,100	580	40	50	0.31

MUL	30,600	6.5	17,300	6,100	550	57	27	0.33
MUL*	30,200	6.5	16,500	5,400	500	52	25	0.41
Mca	43,000	6.5	11,000	3,600	310	19	23	0.43
Mca*	43,300	6.5	12,000	3,600	290	15	17	0.76

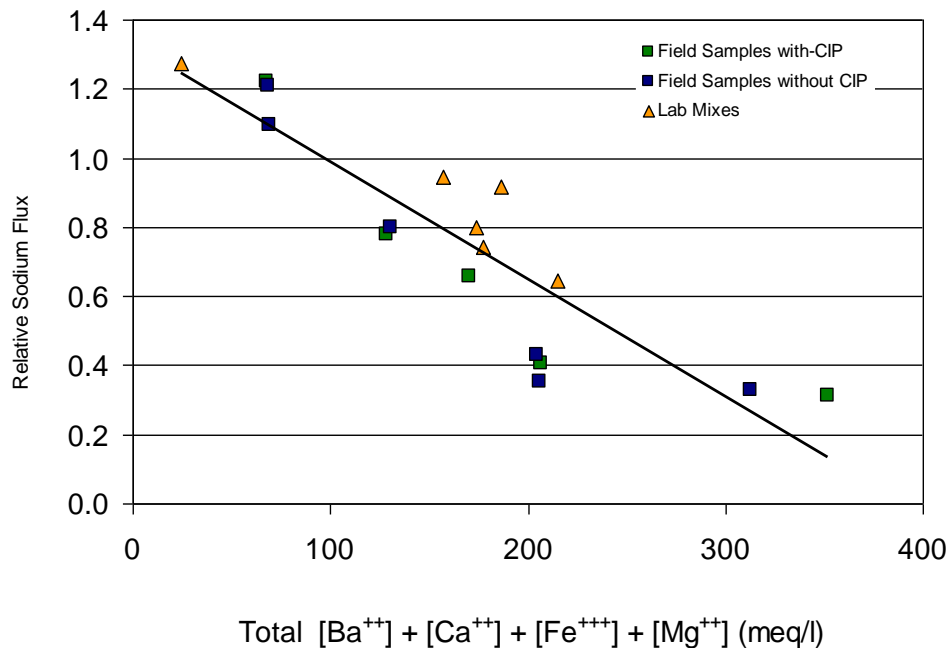


Figure 75: Loss of Sodium Transport Capacity as a Function of the Concentration of the Multivalent Cations

A series of tests with complex mixtures of cations was performed to investigate the fate of calcium, barium, magnesium, and iron in the electrodialysis process. Results from six tests with complex salts are summarized in Figure 47 (Repeated from Section 7). Test J represents a baseline with 3% sodium chloride with the protective membrane. Addition of 600 mg/l magnesium (Test M) had little effect on the process. Addition of calcium (4,000 mg/l, Test K) caused a slight decrease (10%) in the rate of the process. Addition of 400 mg/l barium with 4000 mg/l calcium and 400 mg/l magnesium (Test R) decreased amperage by about 30%. Addition of 40 mg/l iron to the mix (Tests S and T) resulted in further decrease (40-50%) in ion flux.

Volt-Amp profiles were routinely performed to reference performance of the electrodialysis process at various times during the process. These tests are the record of amperage at increments of 1 volt from 2 to 15 volts and represent a snapshot of performance at an instant in time. A reference profile was taken at the start of Test X with 3% NaCl. The complex salt mixture (2,600 mg/l calcium, 260 mg/l barium, 470 mg/l magnesium, and 36 mg/l iron) was then blended into the test water. An immediate decrease in amperage was recorded (Figure 49, repeat from Section 7).

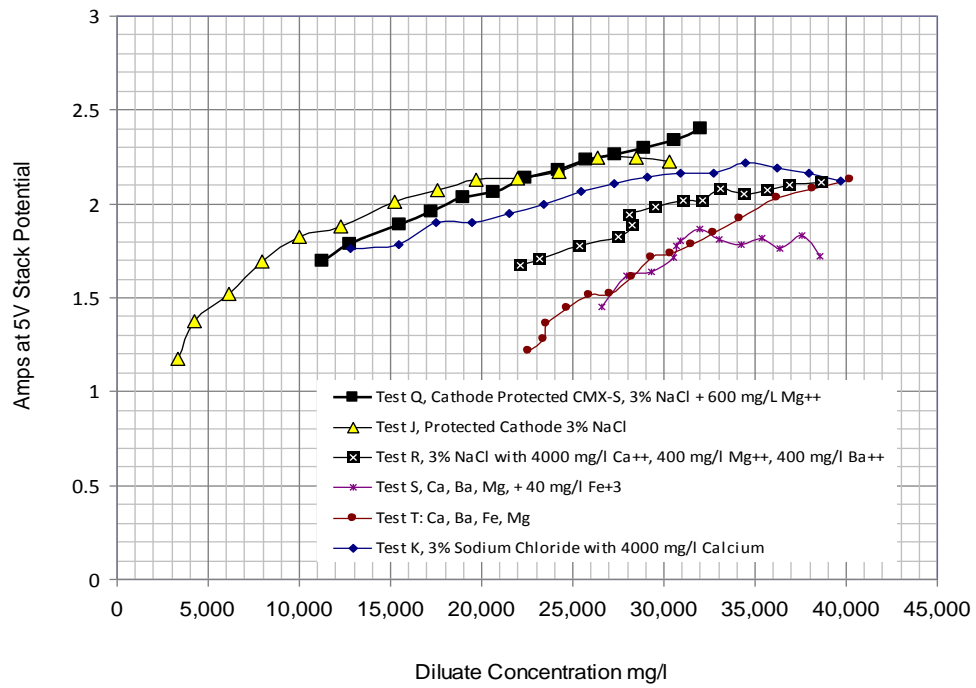


Figure 47 (repeat): Summary Effects of Various Cation Blends on Current Density

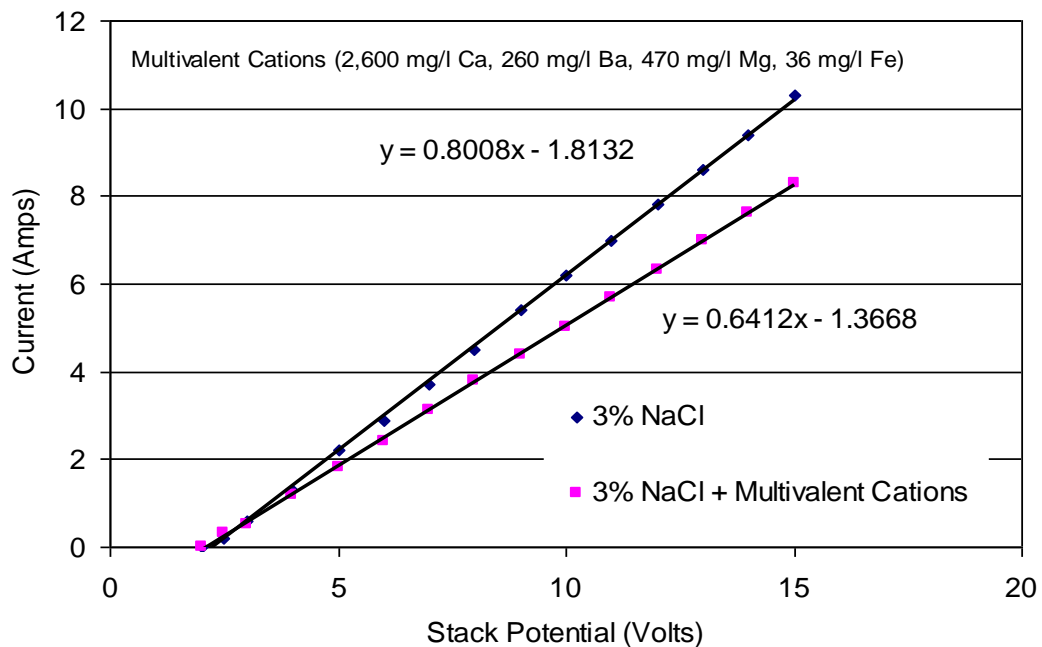


Figure 48 (repeat): Immediate Loss of
Current by Addition of Complex Salts, Test X

A similar test was performed at the start of Test S. In this case, (Figure 44) the reference profile was taken with a complex salt mixture (3,100 mg/l calcium, 160 mg/l barium, 450 mg/l magnesium) and showed a high level of potential performance. A dose of iron (44 mg/l) was then added feedstock. There was an immediate loss of current (20%).

The previous four figures indicate a difference in the relative interference caused by the different multivalent cations. Iron caused an immediate and severe loss of ion flux. Magnesium seem to cause little problem. Barium and calcium yield long term interference.

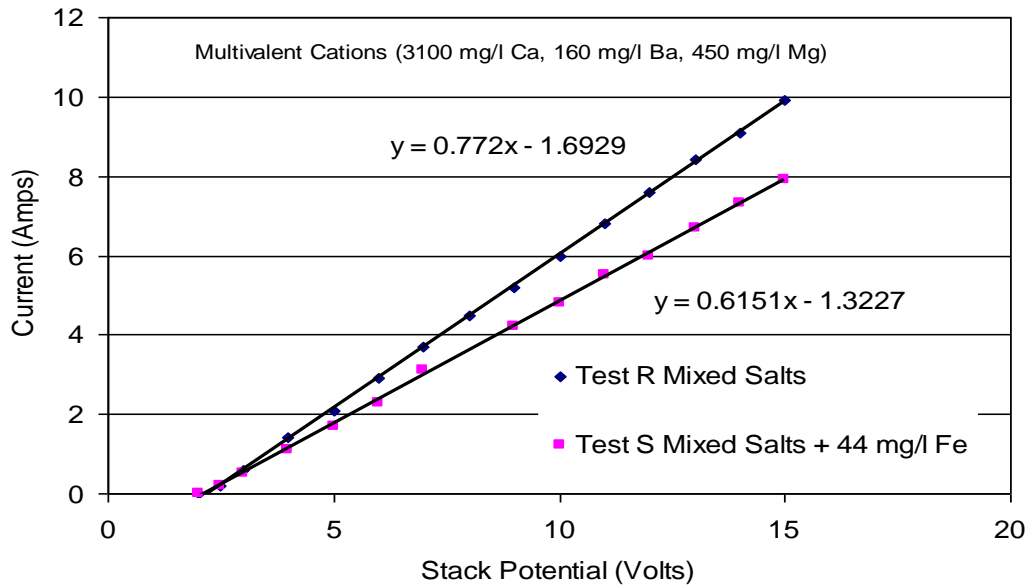


Figure 44(repeat): Loss of Current Density by Addition of 44 mg/l Fe Test X

8.5 Fate of Multivalent Cations

Further understanding of the mechanism of interference and the fate of the multivalent cations was gained from the chemical data from six tests with complex salts and eleven tests with waters from field sites. Data were analyzed by calculating the relative flux of each ion into the concentrate or into the electrolyte. The relative stack flux (RSF_{ion}) is the difference between the concentrate concentration and the diluate concentration divided by the initial feedstock concentration. The relative stack flux normalized to sodium is the ratio of RSF_{ion} to RSF_{Na^+} . The relative electrolyte flux (REF_{ion}) is the change in electrolyte concentration divided by the difference in the concentration of the concentrate and the diluate. The majority of the current in the ED stack is carried by sodium transport. The relative electrode flux of sodium is approximately equal to the reciprocal number of membrane pairs ($REF_{Na^+} \approx 1/10$). The relative electrolyte flux normalized to sodium is approximately $10 \times REF_{ion}$.

$$REF_{ion} = \frac{\Delta C_{electrolyte}}{C_{Concentrat} - C_{Feed}}$$

$$REF_{Na^+} \cong \frac{1}{10} \frac{C_{Concentrat} - C_{Feed}}{C_{Concentrat} - C_{Feed}}$$

$$Normalized_{Na^+} = \frac{REF_{ion}}{REF_{Na^+}}$$

The calculated values of the relative stack flux of the various cations are presented in Table 62. In all cases, it is seen that the relative flux of the multivalent cations exceeds the relative flux of sodium, indicating that there is preferential transport of the multivalent cations from the diluate

to the concentrate. This relation is seen in Figure 76. This figure is a plot of the average relative membrane fluxes (of all tests) normalized to sodium.

Table 62: Fate of the Cations; Transport From the Diluate to the Concentrate					
	Relative Membrane Flux (RMF _{ion}) Dimensionless				
Test	Ba	Ca	Fe	Mg	Na
Q	1.71	1.97	1.43	1.88	1.27
R	1.87	1.49	1.80	0.95	0.92
S	1.45	1.49	0.78	0.77	0.74
T	1.64	1.69	0.47	1.28	0.95
U	1.62	1.19	1.00	0.67	0.64
X*	1.89	1.78	1.76	1.26	0.80
MS	1.88	1.65	1.67	1.23	0.78
MS*	0.83	1.51	1.43	0.85	0.80
MSD	1.51	1.99	1.61	1.94	1.22
MSD*	1.69	1.97	1.62	1.82	1.10
MSD**	1.76	1.99	1.62	1.91	1.21
TD	1.74	1.30	1.36	0.68	0.66
TD*	1.43	0.30	0.96	0.61	0.35
MUL	0.81	0.49	0.62	0.25	0.31
MUL*	1.08	0.81	0.68	0.40	0.33
Mca	1.61	1.00	1.12	0.53	0.41
Mca*	1.29	0.84	0.75	0.35	0.43
Average	1.52	1.38	1.22	1.02	0.76
Relative to Na	2.00	1.82	1.60	1.35	1.00

See Tables 8 and 9 for Test Conditions

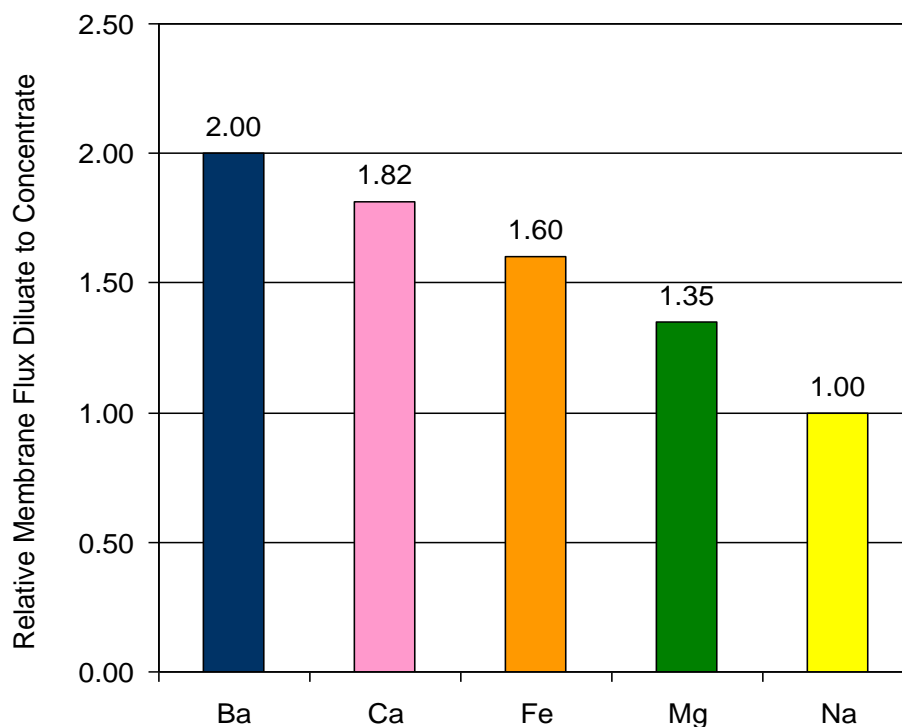


Figure 76: Fate of the Cations; Relative Flux from the Diluate to the Concentrate; Normalized to Sodium

The calculated values of the relative electrode flux of the various cations are presented in Table 62. Some tests results could not be calculated because one or more test results were reported as below detection limits (DL). In all cases, it is seen that the relative flux of the multivalent cations is less than the relative flux of sodium, indicating that there is selection against transport of the multivalent cations from the diluate to the electrolyte. This is expected due to the placement of the multivalent exclusionary membrane at the cathode barrier. Some of the barium results were calculated to be negative. Most likely some barium precipitated as barium sulfate and became unrecoverable in the test sample. However, it would appear as if very little barium crosses the cathode cell barrier. Figure 77 is a plot of the average relative electrolyte fluxes (of all tests) normalized to sodium.

Table 62: Fate of the Cations; Transport From the Diluate to the Electrolyte					
	Relative Electrolyte Flux (REF _{ion}) Dimensionless				
Test	Ba	Ca	Fe	Mg	Na
Q	-0.005	0.101	DL	0.023	≈0.1
R	0.000	0.056	0.012	0.085	≈0.1
S	0.000	0.014	0.000	0.003	≈0.1
T	0.000	0.023	DL	0.001	≈0.1
U	0.002	0.024	0.025	0.012	≈0.1
X*	0.000	0.008	0.006	0.003	≈0.1
MS	-0.002	0.017	0.014	DL	≈0.1
MS*	-0.017	0.012	0.011	0.006	≈0.1
MSD	DL	DL	DL	DL	≈0.1
MSD*	0.000	0.011	DL	0.003	≈0.1
MSD**	0.000	0.014	DL	0.000	≈0.1

TD	0.000	DL	DL	DL	≈0.1
TD*	-0.003	0.009	-0.002	-0.002	≈0.1
MUL	-0.004	0.033	DL	0.009	≈0.1
MUL*	DL	0.027	0.062	0.026	≈0.1
Mca	-0.004	0.027	DL	0.011	≈0.1
Mca*	0.003	0.017	0.000	0.017	≈0.1
Average	-0.002	0.026	0.014	0.014	≈0.1
Relative to Na+	-0.021	0.264	0.142	0.142	1.0
DL= not calculated, one or more values < detection limit					

See Tables 8 and 9 for Test Conditions

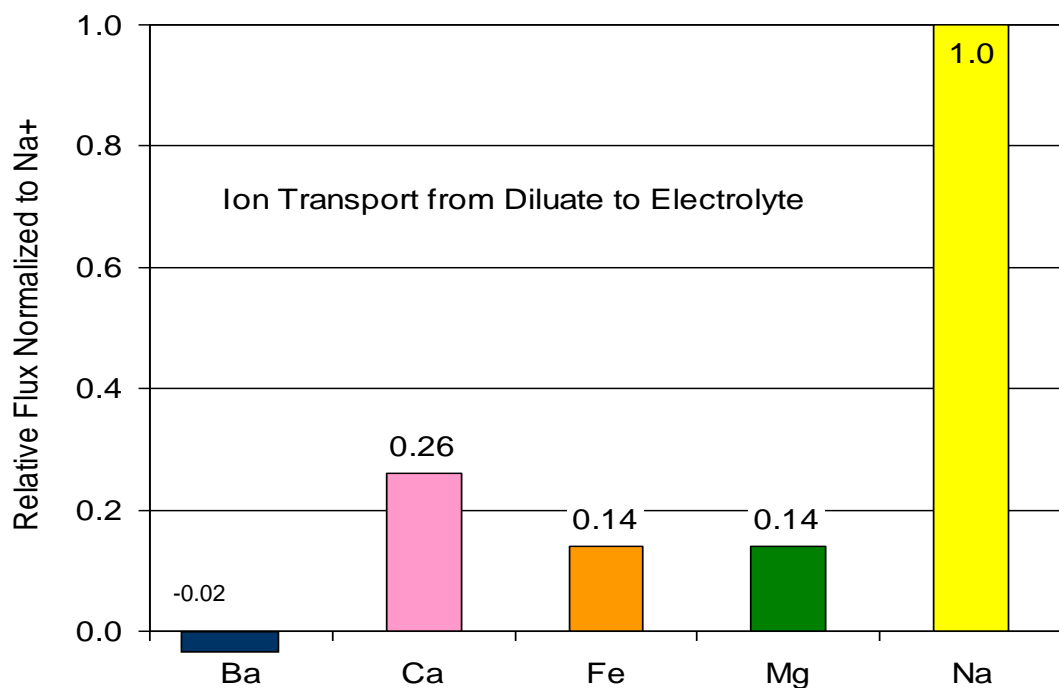


Figure 77: Fate of the Cations; Relative Flux from the Diluate to the Concentrate; Normalized to Sodium

8.6 Mechanism of Interference by Multivalent Cations

The data presented above suggest that each cation affects the electrodialysis process in a slightly different way. The following discussion introduces concepts on how these various ions cause interference with the improved ED system using the multivalent cation exclusionary membrane at the cathode boundary. It is convenient to introduce terms to describe the types (Type I, Type II and Type III fouling).

8.6.1 Type I Fouling

This occurs within the electrolyte cell as either precipitation on the electrodes or on the interior wall of cathode barrier membrane. This is a long term fouling that would require a fair amount of time to develop. This would need to be cleaned with a strong acid rinse.

8.6.2 Type II Fouling

This occurs as a direct consequence of using a cathode barrier membrane that selects against multivalent cations. When the multivalent cations are attracted to the cathode, their passage is rejected. A stagnant charge barrier builds on the diluate side of the cathode barrier membrane. This would be a rapid type of fouling. It would be first noticed as a loss of amperage in proportion to the ratio of the equivalents of multivalent cations compared to that of sodium. The fouling would build with time as a stagnant charge barrier presents increasingly more resistance.

8.6.3 Type III Fouling

This occurs at all stack membranes and is a consequence of either very large ions unable to readily cross any membrane, or precipitation on the membrane surface. This can be either a slow process, or can be immediate if the precipitation is rapid.

Each cation would have a different propensity to enter into one or more of these types of fouling. Table 63 is a conceptual rating of the perceived potential for each of the cations to create a problem with electrodialysis.

Table 63: Perceived Mechanism of Fouling Presented by the Various Multivalent Cations*			
Cation	Type I Electrode Cell	Type II Cathode Membrane	Type III All Membranes
Calcium	1	2	1
Magnesium	0	1	0
Barium	0	3	0
Iron	1	3	3
0 = not likely	1 = possible	2 = likely	3 = definite

*Assuming the multivalent cation exclusionary membrane is installed at the cathode boundary

Calcium: With an unprotected cathode, calcium presented an immediate loss of efficiency, and likely had a strong tendency to enter into both Type 1 and Type 2 fouling. With a protective exclusionary membrane at the cathode barrier, it was very difficult to create fouling conditions within the electrode cells. Calcium is therefore downgraded to a cautionary status in Type I fouling. The effects of calcium in the electrolyte may be further minimized by operating at neutral pH and minimizing exposure of the electrolyte to carbonate intrusion. It is believed that calcium presented a fairly strong potential for Type II fouling. In waters without carbonate hardness, calcium should not present a strong Type III fouling potential if pH is neutral. Caution is advised if the pH of the water is high, especially if carbonates are present.

Magnesium: Magnesium is present in much lower concentration than calcium, therefore, the rate of accumulation of magnesium in the electrolyte will be fairly low. Magnesium is fairly insoluble in the presence of sulfate, therefore, this cation is not likely to be a problem in Type I fouling. Magnesium will compete with sodium at the cathode barrier, and will be a possible problem in Type II fouling. Magnesium will not likely precipitate within the stack membranes, and is therefore discounted as a potential problem with Type III fouling.

Barium: Barium is a large and heavy ion. With the exclusionary membrane placed at the cathode boundary, there is little evidence that barium crosses into the electrolyte. Any barium that does cross into the electrolyte will immediately precipitate as barium sulfate. This can be removed by continuous filtration of the electrolyte. Therefore, barium is thought to be unimportant

in Type I fouling. Barium, however, would be a strong candidate for Type II fouling by virtue of its potential to block passage of sodium through the cathode barrier membrane. Barium readily passes from the diluate to the concentrate. If the treated water is low in sulfate, then barium should not pose a problem with Type III fouling. If the water is highly concentrated in sulfate, then barium could present a problem in the membrane stack. However, waters high in sulfate concentration would not produce soluble barium; most of the barium would remain in the subsurface.

Iron: Iron slowly crosses from the diluate to the electrolyte and can precipitate at even low pH. Therefore, iron is a candidate for Type I fouling. A likely remedy for Type I fouling would be periodic pH swings in the electrolyte followed by filtration. There is evidence that iron may act in Type II fouling. However, iron precipitate was observed to be present in stack membrane wash water. There is clear evidence that an addition of 40 mg/l iron to a complex salt causes immediate disruption of process. This can only be attributed to Type III fouling. The best remedy for handling iron is robust pretreatment.

8.7 Development of Clean-in-Place Pole Reversal

A concept for maintaining consistent operation was investigated on a preliminary basis. Long term loss of process efficiency was observed when calcium, iron, and barium were present in the test water. A possible mechanism is the establishment of a stagnant charge layer at the cathode boundary membrane (Type II fouling). Short pulses (15 seconds to one minute duration at intervals of 15 minutes to one hour) of pole reversal (cathode to anode) at elevated voltages (5-15 V) appeared to improve total ion flux. Tests were conducted with mixed salt solutions and field waters from the Barnett and Marcellus.

Table 64 is a summary of comparisons of all the CIP-PR tests and the reference baseline tests. Flux improvements of up to 37% were measured for waters treated using a CIP regime. Two tests, however, showed little or no improvement with CIP. Either the water was not amenable to the CIP, or the CIP protocol was insufficient. It is noteworthy that Sample MSD 1 (Maggie Spain Diluted, CIP regime 1) did not show an improvement. However, Sample MSD 2 (Maggie Spain Diluted, CIP regime 2) showed an 18% improvement over the base case. The difference in the regimes was only a timing issue. Regime 2 was ½ the pulse time, but twice as often as Regime 1.

	Initial TDS	Diluate TDS	Conc. TDS	Avg. Amps @ 5V	Forward Reaction Amp-sec	Reverse CIP- Amp-Sec	Ion Flux Increase CIP-PR	kWh/lb
Test U No CIP	41,100	28,050	52,650	1.25	27,000	0	NA	0.131
Test X CIP-PR	38,500	19,200	53,050	1.50	32,355	2,800	37%	0.129
TD No CIP	52700	39050	65400	1.30	28,080	0	NA	0.121
TD* CIP-PR	53100	36300	63050	1.26	24,200	3,030	1%	0.118
Maggie Spain	44,600	34,500	56,500	1.02	20,500	0	NA	0.131
MS* CIP-PR	43,600	28,500	58,100	1.21	25,488	3,738	37%	0.133
MSD 1 No CIP	24,500	7,700	39,700	1.17	31,590	NA	NA	0.111
MSD 2	25,800	9,360	40,100	1.27	34,020	657	-1%	0.115

CIP 1								
MSD 3 CIP 2	28,000	9,270	47,100	1.43	38,340	654	18%	0.127
MUL No CIP	30,000	27,300	38,500	0.45	10,764	NA	NA	0.115
MUL CIP	30,200	25,100	39,700	0.74	17,057	2,129	30%	0.127
Mac No CIP	43,000	32,100	55,200	1.29	31,900	NA	NA	0.148
Mac CIP 1	43,300	33,700	60,100	1.26	29,330	960	14%	0.119

The CIP-PR method is amenable to automation. The control cycle may be on a pre-timed basis, or on-demand based on a process variable such as amperage. The control point could be based on empirical data, or could be set based on process deviation from a computer simulation. Figure 82 is a computer generated example of operational conditions for this batch pilot plant with sodium chloride at 5 volts stack potential. Selection of any diluate concentration and any concentrate concentration yields the expected process amperage. For example, a diluate concentration of 15,000 mg/l and a concentrate concentration of 60,000 mg/l should operate at 1.5 amps. Any deviation from this current could be programmed to automatically generate a pole reversal.

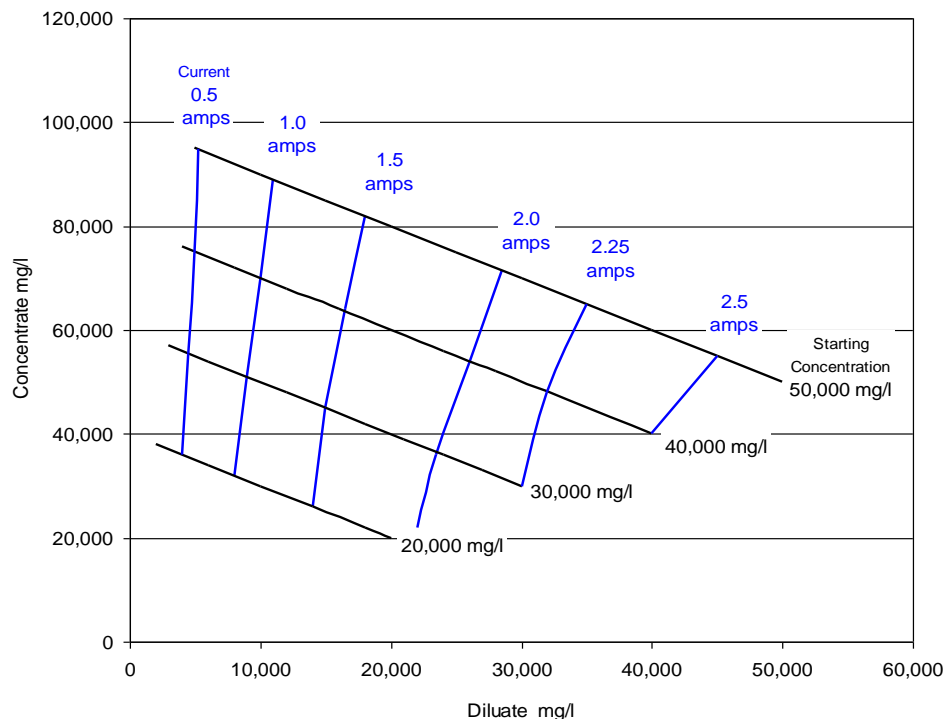


Figure 78: Control Chart for Operation of the Pilot ED Unit (at 5 Volts) as a Basis for Implementation of a CIP-Pole Reversal.

8.8 Field Waters from the Barnett and the Marcellus

Four samples were received from two field sites in each the Barnett and the Marcellus. Simple pretreatment consisting of pH adjustment to neutrality, aeration, and filtration with a 5 μ cartridge filter was sufficient to create treatable waters. In three of four cases, the water was deemed beyond the concentration suitable for effective electrodialysis (150,000 – 270,000 mg/l TDS), and likely represented water collected from late in the flowback periods at these sites. These waters were diluted with tap water for the tests with ED.

Overall rates of treatment with ED were slow compared to previous tests with laboratory generated water, as expected from the high levels of multivalent cations in the samples. Iron seemed to be the worst component in these samples. Pretreatment only removed about 30% of the available iron. However, state of the art pretreatment with aeration and flocculation/sedimentation can achieve reliable iron removals of greater than 90%, as observed in the field at the Maggie Spain Water Recovery Facility (Hayes and Severin, 2012). This pretreatment step is very low in cost, amounting to less than 10 cents per barrel. In view of the ease with which iron can be controlled, fastidious iron removal is recommended prior to processing shale gas waters with ED.

One example test with Marcellus Unlabeled Water (Figure 50 repeat from Section 7) is presented as an example of treatment without pole reversal clean-in-place. The counter-part to this run, with the same water, but including a clean-in-place pole reversal regime is shown in Figure 60 (repeat from Section 7).

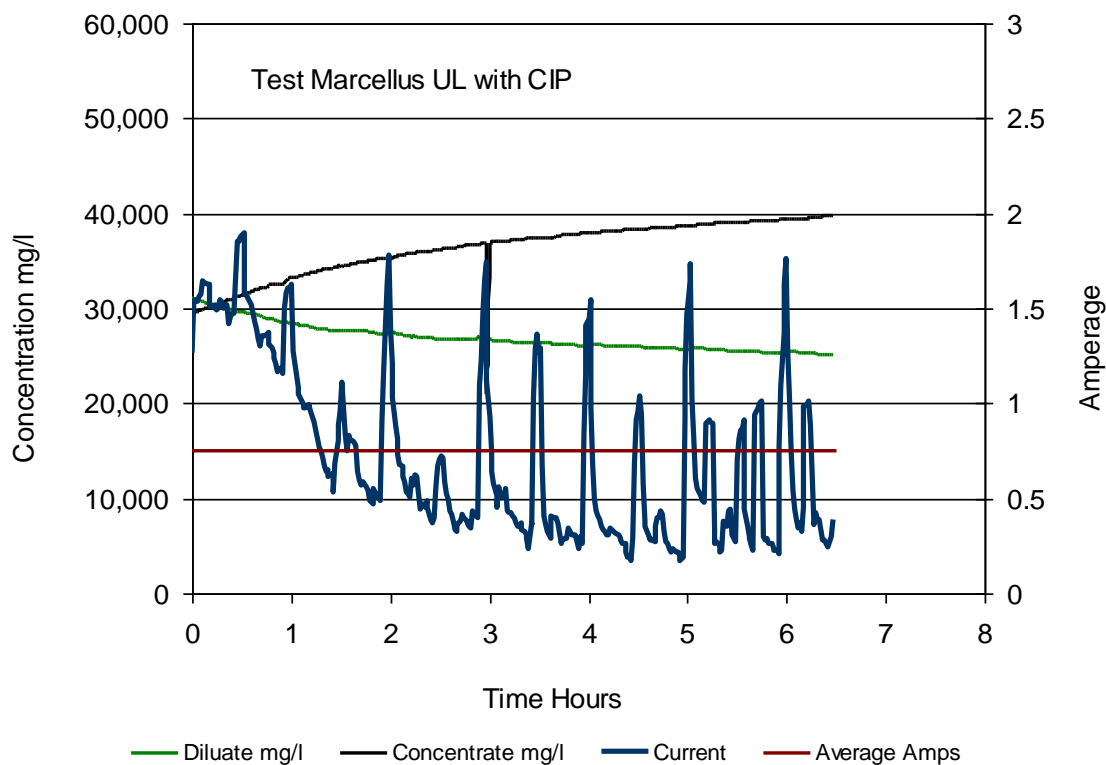


Figure 60 repeat: Marcellus UL Field Test Water with Complex CIP Pole Reversal

8.8.1 Effect of Temperature

The electrodialysis process poses a unique opportunity to take advantage of improved current capacity with increased operating temperature. The design of the electrodialysis process creates two co-dependent, rate limiting reaction sites; the electrode cell reactions, and the transport of ions within the membrane stack. The Arrhenius equation for temperature dependency was modified for two co-dependent rates over a temperature range of 8°C to 33°C. Independent temperature coefficients for the electrode cells and the stack were obtained. These relations faithfully predicted operation over range of other temperatures. These tests predict that field operation can be improved with increased operating temperature. Partial, yet significant improvements may be made by increasing only the electrolyte bath temperature. As such, the full water stream does not need to be temperature controlled. Waste heat added to the electrolyte should improve performance even with cold influent water.

Table 65 shows predictions for this pilot unit at various temperatures. This table shows that significant rate increases can be made if waste heat were to be used to heat either the electrolyte or the water. If water and electrolyte are both at a temperature of 5°C, then increasing the electrolyte to 35°C, then a 39% improvement in process rate is potentially achievable.

Table 65: Potential Improvements with Operation at Elevated Temperatures			
Water Temperature °C	Electrolyte Temperature °C	Current (amps) 5 volt	Percent Improvement Over Baseline
5	5	1.3	0
5	15	1.5	13
5	25	1.6	26
5	35	1.8	39
5	45	2.0	54
10	15	1.6	21
10	25	1.8	35
10	35	2.0	50
10	45	2.2	65
15	15	1.7	30
15	25	1.9	45
15	35	2.1	61
15	45	2.3	77
25	25	2.2	66
25	35	2.4	84
25	45	2.6	102

8.9 Process Improvements for the Field

The discussion presented above describes the challenges overcome and opportunities identified for the treatment of heavily concentrated brines with electrodialysis. In summary, these are:

Increase the concentration of electrolyte to reduce resistance at the electrodes. This can improve rate of the ED process by around 24%, depending on the relative resistance at the electrodes. The relative resistance at the electrodes decreases as the number of cells per ED stack increases. With 700 cells per unit, the improvement is around 3%.

If the level of calcium and iron is fairly low, then the pH of the electrolyte can be increased to pH 11. This reduces the overvoltage applied to the anode and can account for an additional 15% improvement in the rate of the process depending on the total voltage at the electrodes. The relative improvement decreases as the total stack voltage increases.

With high concentrations of calcium, protection of the cathode barrier membrane with a multivalent cation exclusionary membrane is imperative. Improvements of 40% are possible. More specifically, this improvement allows for the utilization of the ED under normally impossible conditions.

Clean-in-place technology will be needed to keep the ED unit operational for very little expenditure, 35% process improvement can be realized using a simple pulsed pole reversal. Once again, it is difficult to fully recognize the value of this improvement. This improvement allows for the utilization of the ED process under normally impossible conditions.

The use of waste heat to increase the temperature of the electrolyte, the water, or both, can improve the rate of the process by 15%.

Figure 79 is a summary of potential process improvements to electrodialysis for the treatment of steams, such as shale gas hydrofracture flowback waters. This figure suggests that rates could be improved by 2.5 to 3 times that of a base case.

The corollary is also true; conditions in flowback waters are so difficult for conventional ED that there is no means of adequately defining a baseline. To put this into perspective, Kaakinen (1984) experienced difficulty in treating water from two sources. One source had a TDS range of 3200-3400 mg/l with calcium (7-18 mg/l) and magnesium (15-30) mg/l. The second source had a TDS range 9140-9180 mg/l, with calcium (35-60 mg/l) and magnesium (52-55 mg/l). The author attributed membrane fouling in the concentrate stream to the hardness, and recommended that either the water be pretreated with chemical precipitation or treated in parallel with ion exchange. Basically, ED would be inoperable without these improvements recommended in this project. Tests performed in this project represent the new baseline for the electrodialysis of heavy brines.

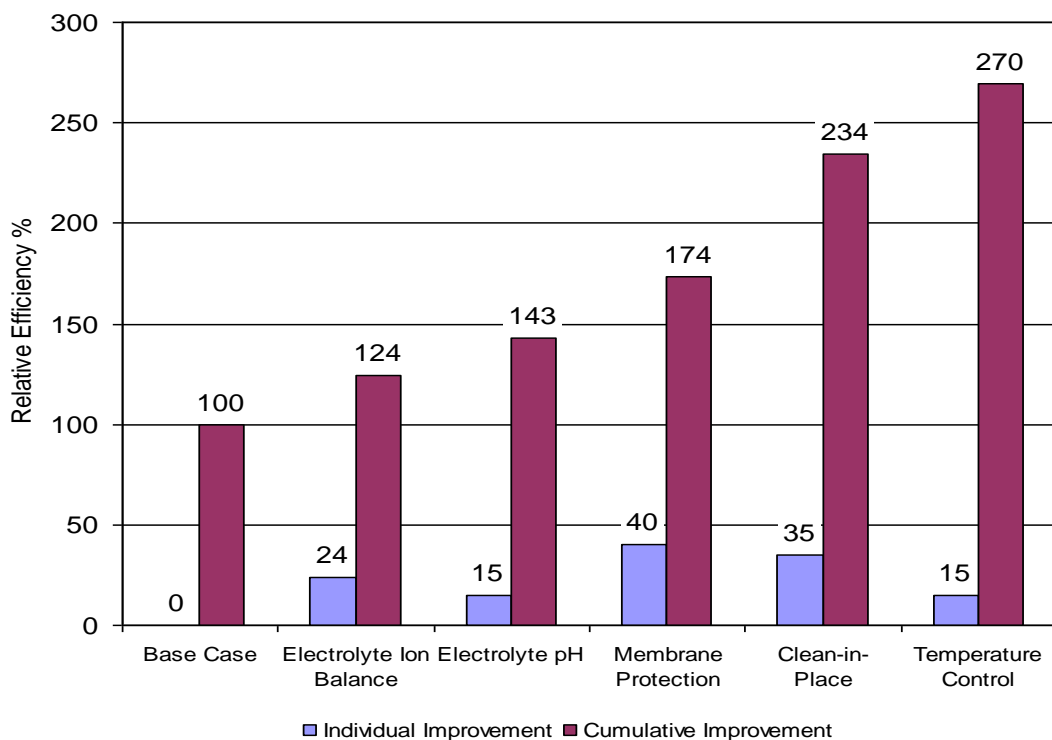


Figure 79: Summary of Potential Process Improvements

8.10 Economic and Design Considerations

Economic data presented by Eurodia (see Results 7.11) provide a wealth of design data from an independent source. It is important to put these data into perspective with the information developed in this laboratory study.

Eurodia presented process data consistent with summary data in Tables 8, 9, and 10 in the Results section without regard to any process changes indicated throughout this study. As such, the economic data in Section 7.11 represent a conventional process design, as presented by Eurodia. A Stepwise breakdown of the Eurodia data to establish conventional design parameters is presented in Table 66. The power required to generate one pound of salt in the economic

example (row 10) was about 0.26 kWh/lb. The key calculation occurs in row 27; volts per cell; which is about 1.33 volts in most of the test cases.

The tests in this pilot study were performed at 5.0 volts over ten cells, or about 0.5 volts per cell. This was a deliberate attempt to demonstrate a reduction in potential operating costs. The average power requirement in the pilot study was about 1.2 kWh/lb salt.

Table 66: Reverse Engineering of the Economic Data to Conventional Design parameters								
Row	Case Conditions	A3	A4	A5	A6	B1	B2	B3
1	Inlet TDS	70,000	40,000	20,000	10,000	40,000	40,000	40,000
2	Effluent TDS	40,000	10,000	10,000	1,000	10,000	10,000	10,000
3	BBL/d treated	10,000	10,000	10,000	10,000	50,000	20,000	2,000
4	1000 Lb Salt/Day	117	117	40	34	586	234	23
	Engineering Analysis	A3	A4	A5	A6	B1	B2	B3
5	kWh/1000 gallon	72	80	27	23	80	80	80
6	gallon/day	420,000	420,000	420,000	420,000	2,100,000	840,000	84,000
7	kWh/day	30,240	33,600	11,340	9,660	168,000	67,200	6,720
8	kW	1,260	1,400	473	403	7,000	2,800	280
9	kW/stack	84	93	79	67	109	88	70
10	lb salt/day	117107	117107	39585	33649	585530	234213	23422
11	kWh/lb salt	0.26	0.29	0.29	0.29	0.29	0.29	0.29
12	lines	5	5	2	2	16	8	1
13	stacks/line	3	3	3	3	4	4	4
14	cells/stack	736	736	620	620	860	690	732
15	m ² /cell	0.8	0.8	0.8	0.8	0.8	0.8	0.8
16	Area/stack m ²	588.8	588.8	496	496	688	552	585.6
17	Total Area m ²	8832	8832	2976	2976	44032	17664	2342
18	Equivalents/hr Total	39,139	39,139	13,230	11,246	195,694	78,278	7,828
19	Equivalents/sec Total	10.9	10.9	3.7	3.1	54.4	21.7	2.2
20	Equiv./sec per stack	0.725	0.725	0.613	0.521	0.849	0.679	0.544
21	Equiv./sec per cell	0.000985	0.000985	0.000988	0.00084	0.000988	0.000985	0.000743
22	Amps per stack	95	95	95	81	95	95	72
23	Amps per cell	95	95	95	81	95	95	72
24	Amps/m ² membrane	238	238	238	203	238	238	179
25	Total amps	1425	1425	572	486	6100	3041	287
26	Stack voltage	884	982	826	828	1148	921	977
27	Cell voltage	1.20	1.33	1.33	1.34	1.33	1.33	1.33

The expectation is that the design criteria used for the economic data represent cases with an ion flux about $(1.33/0.5) = 2.6$ times greater than attempted in the pilot study. This is borne out by the stepwise calculations (Table 67) comparing the pilot conditions with the conditions generated in the cost section. The pilot unit was operated at about 210 g/m²-hr; whereas, the economic data were developed for a flux of 450 g/m²-hr.

The relation between voltage and amperage was investigated in many of the pilot runs; indicating a linear relationship. The criteria of ion flux per volt indicates that the pilot unit operated at 420 g/m²-volt while the economic data were defined for about 337 g/m²-volt. By this metric, the pilot data and economic projections are normalized; with a slightly conservative (25%) bias in the economic data.

The linear relationship between the voltage and the amperage, at these ultra-high salt concentrations, indicates that there is an economic trade-off between surface area (vis. capital costs) versus operating costs (watts = volts x amps). From this standpoint, the economic data

provided represent a relatively high operating cost and low capital costs. The pilot data represent conditions representative of high capital costs and low operating costs.

These two design parameters, surface area and voltage, can be used to advantage. Given a locally high power cost, there would be an advantage to designing with a higher surface area. Given a locally low power cost, there would be a potential for cost savings by designing with a lower surface area.

Table 67: Comparison of Typical Pilot Run vs Typical Economic Case (by Eurodia)			
Pilot Unit Typical Case		Example Economic Case A4	
30	g/l removed	30	g/l removed
10.5	liters	420,000	gallons
315	grams removed	3.784	liter/gallon
7.5	hours	24	hours
42	grams per hour removed	1,986,600	grams per hour removed
1	stack	15	stacks
10	cells/stack	736	cells/stack
4.2	grams per hour per cell	180	grams per hour per cell
0.02	m ² /cell	0.4	m ² /cell
210	g/m ² - hour	450	g/m ² - hour
5	volts	982	volts
0.5	volts/cell	1.33	volts/cell
420	g/m ² -volt	337	g/m ² -volt

It is interesting that the economic data, as presented by Eurodia, were considered to be within normal design conditions. This entire report, however, is replete with process work-arounds and improvements deemed necessary to make these waters behave like normal water. This puts Figure 79 in perspective. Most of the process improvements developed in this report, as indicated in this figure, are necessary in order to treat this water with any degree of normalcy.

9 CONCLUSIONS

The treatment of flowback waters from shale gas hydrofracture with electrodialysis represented a dual technical challenge. Normal operation of electrodialysis is in the range of several thousand mg/l TDS and limited to several hundred mg/l calcium and magnesium. Technical guidance was not available in the open literature for these types of brines. This project centered on 1) keeping the operating costs under a controlled limit and 2) finding opportunities to maximize process output. A number of problems were encountered that were systematically addressed as the project proceeded from the treatment of water containing pure sodium chloride (30,000-60,000 mg/l) to the treatment of solutions with sodium, calcium (up to 4,000 mg/l), barium (up to 400 mg/l), iron (up to 50 mg/l), and magnesium (up to 600 mg/l), and finally to the treatment of field samples from the Barnett and the Marcellus. The conclusion focuses on the practical aspects of discoveries in the topic areas pertaining specifically to treating these types of heavy brine.

Defining a Range of Operation: An arbitrary objective range of 0.1 to 0.15 kWh per lb total dissolved solids removed was established based on theoretical calculations. Summary data suggest that this goal is achievable in all the waters tested. The energy goal is achieved by maintaining a low stack potential. For this pilot plant, the target potential was 5 volts (nominally 0.5 volts/membrane pair).

Chemistry of the Electrolyte: The chemistry of the electrolyte solution was investigated as a means of improving the rate of salt transfer at the desired energy limit. Theoretical calculations

showed that at high concentrations of brine, there would be significant resistance to ion flux within the electrode cells. Increasing the electrolyte concentration to an ionic strength similar to the water being treated increases ion flux for a given stack potential. Improvements may also be made by lowering the overvoltage of the electrodes by operation of the electrolyte at a pH greater than about pH 11. However, pH control of the electrolyte becomes problematic if there is incursion of multivalent cations into the electrolyte.

Mitigating the Effects of Calcium: At the start of testing, a generic cation selective membrane was used at the boundary to the cathode cell. High rates of calcium incursion were encountered causing calcium fouling of the electrodes. The cathode boundary membrane was replaced with a membrane that selected against multivalent cations. Calcium flux into the electrolyte was reduced by more than 75%. An apparent added benefit was that calcium deliberately introduced into the electrolyte, both as free ions or as a precipitate, no longer interfered with ion flux. This indicates that the initial poisoning was at the surfaces of the cathode boundary.

Interference and Fate of Multivalent Cations: The adverse role of calcium (eg. multivalent cations) on duration of a process run were expected, and demonstrated. The effect of multivalent cation incursion into the electrolyte was mitigated with a more optimum cathode boundary membrane. Iron causes an immediate loss of process efficiency, likely by precipitation at all membrane surfaces. Calcium, barium, and magnesium caused a slower degradation of ion flux. The fate of the multivalent cations was investigated. Barium, iron, magnesium, and calcium readily transport from the diluate to the concentrate. The ability of the transport of these ions exceeds that of sodium between the diluate and the concentrate. Calcium and magnesium transport slowly into the electrolyte. Barium and iron were either not readily transported, or not readily measured in the electrolyte.

9.1 Preliminary Clean-in-Place

A concept for maintaining consistent operation was investigated on a preliminary basis. Long term loss of process efficiency was observed when calcium, iron, and barium were present in the test water. A possible mechanism is the establishment of a stagnant charge layer at the cathode boundary membrane. Short pulses (15 seconds to one minute duration at intervals of 15 minutes to one hour) of pole reversal (cathode to anode) at elevated voltages (5-15 V) appeared to improve total ion flux. Tests were conducted with mixed salt solutions and field waters from the Barnett and Marcellus. Flux improvements of up to 37% were measured for waters treated using a CIP regime.

9.2 Field waters from the Barnett and the Marcellus

Four samples were received from two field sites in each the Barnett and the Marcellus. Simple pretreatment consisting of pH adjustment to neutrality, aeration, and filtration with a 5 μ cartridge filter was sufficient to create treatable waters. In three of four cases, the water was deemed beyond the concentration suitable for effective electrodialysis (150,000 – 270,000 mg/l TDS), and likely represented water collected from late in the flowback periods at these sites. These waters were diluted with tap water for the tests with ED. Overall rates of treatment with ED were slow, as expected from the high levels of multivalent cations in the samples. Iron seemed to be the worst component in these samples. Pretreatment only removed about 30% of the available iron: however, a previous GTI report observed measurement taken for a commercial scale oxidation followed by flocculation/sedimentation achieved > 90% removal of iron from shale gas water over an 8-week sampling period (Hayes and Severin 2012 C).

9.2.1 Effect of Temperature

The electrodialysis process poses a unique opportunity to take advantage of improved current capacity with increased operating temperature. The design of the electrodialysis process creates two co-dependent, rate limiting reaction sites; the electrode cell reactions, and the transport of ions within the membrane stack. The Arrhenius equation for temperature dependency was modified for two co-dependent rates over a temperature range of 8°C to 33°C. Independent temperature coefficients for the electrode cells and the stack were obtained. These relations reliably predicted operation over range of other temperatures. These tests predict that field operation can be improved with increased operating temperature. Partial, yet significant improvements may be made by increasing only the electrolyte bath temperature. As such, the full water stream does not need to be temperature controlled. Waste heat added to the electrolyte should improve performance even with cold influent water.

9.2.2 Process Recommendations:

- Iron appears to be the most likely cation to cause fouling of the ED process. Iron should be aggressively removed in pre-treatment.
- Increase the concentration of electrolyte to reduce resistance at the electrodes. This can improve rate of the ED process by around 24%.
- If the level of calcium and iron is fairly low, then the pH of the electrolyte can be increased to pH 11. This reduces the overvoltage applied to the anode and can account for an additional 15% improvement in the rate of the process.
- With high concentrations of calcium, protection of the cathode barrier membrane with a multivalent cation exclusionary membrane is imperative. Improvements of 40% are possible.
- Clean-in-place technology will be needed to keep the ED unit operational for very little expenditure, 35% process improvement can be realized using a simple pulsed pole reversal.
- The use of waste heat to increase the temperature of the electrolyte, the water, or both, can improve the rate of the process by at least 15%.

10 REFERENCES

- Galusky, L. Peter, Jr. and Hayes, Thomas D. (2011A), RPSEA Topical Report, Contract 08122-05, Feasibility and Design Approach for Automated Classification and Segregation of Early flowback Water for Reuse in Shale Gas Hydrofracture, Report No, 08122-05.06
- Galusky, L. Peter, Jr., and Hayes, Thomas D. (2011B), RPSEA Topical Report, Contract 08122-05, Feasibility and Design Approach for Automated Classification and Segregation of Early flowback Water for Reuse in Shale Gas Hydrofracture, Report No. 08122-05.07
- Hayes, T.D. (2009), Sampling and Analysis of Water Streams Associated with the Development of Marcellus Shale Gas, Final Report to the Marcellus Shale Coalition. Gas Technology Institute, Des Plaines, IL.
- Hayes, T. D., and Severin, B.F., (2012 A) Characterization of Flowback Waters from the Marcellus and the Barnett Shale Regions. RPSEA Report No. 08122-05.09. March 2012.
- Hayes, T.D., and Severin, B.F., (2012 B) Engineering Decision Tool for the Evaluation of Mechanical Vapor Recompression for the Treatment of Shale Gas Flowback Water. RPSEA Report No. 08122-05.11. February 2012.
- Hayes, T. D., and Severin, B.F., (2012 C) Preliminary Engineering Systems Analysis of Shale Gas Water Management. RPSEA Report No. 08122-05.10. February 2012.
- Hayes, T.D.. and Severin, B.F. (2010), Electrolyte Chemistry Improvements for Electrodialysis of Heavy Brine, Gas Technology Institute, Des Plaines, Ill, Patent Disclosure.
- Huang, X., Agnihotri, D.,Freeman, B.D., Hayes, R.,Kasemset, S., Lee, A., Li, H., Sharma, M., and Shine, S., (2011), Field Assessment and Anti-Fouling Polymeric Membrane Coatings for Treatment of Barnett Shale Flowback Produced Water. RPSEA Report No. 08122-05.05. March 2011.
- Kaakinen, J., (December 1984), High Recovery Desalting of Brackish Water by Electrodialysis, Field Tests at Yuma Desalting Test Facility & at La Verkin Springs, Report REC-ERC-84-24, Bureau of Reclamation Energy and Research Center, Denver Colorado.
- Li, A., Kasemset, S., Miller, D.j., Freeman,B.D., and Sharma, M. , (2010), Innovative UF / NF / RO Membrane Performance Through the Use of Innovative Coatings: Selection of Membrane Supports and Coatings for Barnett Well Flowback Water Separations. RPSEA Report No. 08122-05.03. November 2010.
- Severin, B.F., and Hayes, T.D., (2010), Development of Electrodialysis for Shale Gas Water Reuse. RPSEA Report No. 08122-05.01. November 2010.
- Xu, T., and Huang, C. (2008), Electrodialysis-Based Technologies, a Critical Review, AIChE J., 54, pp. 3147-3159.

11 ACKNOWLEDGEMENTS

The authors express their appreciation for the contributions of Jennifer Yang, Development Engineer, GTI, for developing the data acquisition system using LabVIEW® software and Excel interface. The authors also acknowledge Lloyd Wilkiel for facilitating logistical support required for electrodialysis process operation and component modification. Commercial electrodialysis prototype modifications, modeling support for conceptual ED scaleup, and cost estimates for examples of full-scale ED applications were provided by Ameridia of Somerset, NJ. The authors also wish to thank Devon Energy and Range Resources for providing aliquots of water that were used in the testing and development of ED at GTI.